

In presenting this thesis in partial fulfillment of the requirements for an advanced degree at Idaho State University, I agree that the Library shall make it freely available for inspection. I further state that permission to download and/or print my thesis for scholarly purposes may be granted by the Dean of the Graduate School, Dean of my academic division, or by the University Librarian. It is understood that any copying or publication of this thesis for financial gain shall not be allowed without my written permission.

Signature _____

Date _____

SPATIAL AND TEMPORAL PATTERNS OF LATE PLEISTOCENE GLACIATION
IN THE LEMHI RANGE, EAST-CENTRAL IDAHO

By

Harrison Adam Colandrea

A thesis

submitted in partial fulfillment

of the requirements for the degree of

Master of Science in the Department of Geosciences

Idaho State University

Summer 2016

Committee Approval

To the Graduate Faculty:

The members of the committee appointed to examine the thesis of HARRISON ADAM COLANDREA find it satisfactory and recommend that it be accepted.

Glenn D. Thackray
Major Advisor

Benjamin T. Crosby
Committee Member

Keith Reinhardt
Graduate Faculty Representative

Acknowledgements

I would first like to thank my advisor, Glenn Thackray, for taking me on as a graduate student and giving me the opportunity of a lifetime. You put together a fantastic research project and managed to gather a great deal of funding, allowing the project to flourish and achieve our scientific aspirations. I have learned so much from you about the field of Quaternary Geology and Geomorphology. You have taught me field techniques that I will carry with me in my professional career, and you have developed my “eye” for glacial geomorphology. You also taught me how to be a successful scientist, in terms of conducting and presenting research. Having you as a mentor has allowed me to grow as a person and a scientist. I learned how to successfully and confidently convey science to an audience through speaking and writing under your tutelage. You are like a father figure to me, as you were there for me through the good times and the bad times, making the daily struggles of graduate school and the feelings of being homesick more manageable. I could not have asked for a better graduate advisor and I am very grateful for you as a person. You have inspired me and you will continue to inspire others in your life and in the realm of geology. Thank you from the bottom of my heart.

I would like to thank my advising committee for their insightful comments and questions, and for challenging me and pushing my knowledge of geology to the limit. Ben Crosby, for not only playing an integral role in the development of my knowledge of geomorphology and progressing this project to reach its potential, but also for being an excellent mentor. I learned a great deal about how to be an influential and affective teacher from assisting you with multiple classes. I cannot thank you enough for what you have done for me. Keith Reinhardt, for pushing me to learn more about biology in our reading group, and for providing a unique external prospective to this project.

Thank you to the researchers that have shared published, unpublished, and updated data with me, including Bruce Finney, John Gosse, Joe Licciardi, Grant Meyer, and Amie Staley. Also, thank you to Paul Bierman and the University of Vermont, as well as the Lawrence Livermore National Laboratory Center for Accelerator Mass Spectrometry, for processing my samples for cosmogenic radionuclide dating.

Thank you to my field assistant Ashley Reibel. You made a huge sacrifice for me and did a great job helping me with this project. I could never repay you for that. A very special thank you to the camp ground host and hostess at Meadow Lake Campground. They took Ashley and I in and treated us like part of their family, from checking in on us every morning and evening to see how the research was going and making sure we were doing well, to making hobo dinners and s’mores. You made the days that much more enjoyable.

I would also like to thank those at ISU who have made this a seamless transition and a life changing journey. Melissa Neiers, for her financial assistance, but more importantly being my geology mom and providing unconditional love and support. You made me feel at home from the moment I arrived at ISU. You are never underappreciated or undervalued in my eyes. Kate Zajanc for always being there when I needed any assistance whatsoever. You helped with travel, policies, procedures, and my daily graduate school life. Lori Tapanila, for being an excellent Teaching Assistant Coordinator. You make all of the TAs look good by doing all of the hard work. You

supported me when teaching became difficult and you were there for me during hard times. Diana Boyack, for all of her support in the DML and for helping me construct the final version of my surficial geologic map. Dave Pearson, for letting me utilize the ISU grinding lab to get my samples prepped during a time of absolute chaos. Sarah Godsey, for sharing her knowledge of kriging and supporting me inside and outside of the classroom. Bruce Finney, for sharing your Meadow Lake data with me, supporting me, and taking a genuine interest in my research project. Shannon Kobs-Nawotniak, for progressing my speaking in front of audiences, always including me in the student outreach programs, and for teaching me about “Trash-Cano.” Paul Link, for showing tough love during the time that I was TA. I did not realize it then, but you were only helping me grow. Also, thank you for all the tireless work you put into field camp. You are the epitome of ISU.

Lastly, I would like to thank all of my friends and family who have rooted me on and supported me my entire life, and especially during my time in Idaho. Amie Staley, for being a great friend and mentor. We became much closer during our time in Idaho and I cannot thank you enough for how much you have helped me. All of my Idaho friends, especially Nakul, Jimmy, and Ryan. You guys provided stress and comic relief and taught me how to climb. You made this my second home. All of my friends in New York who checked up on me and kept up with me during this chapter of my life, I cannot thank you enough. You all were in my heart every day. My mother Barbara, my father Bernie, and my step-father Ray, for providing unconditional love every single day, financial support, making me call them at least every Sunday, and for supporting my decisions in life. It was hard for everyone when I moved away from home, but I believe it only brought us closer together. My brother Jay for his constant love and support. Although we are on different paths in life, we are the same and we are inseparable. My dog Abby, for sticking with me through this time apart. The most difficult part of this journey was missing out on two years of your life. You are my inspiration for everything I do in life. This accomplishment is for all of you.

Table of Contents	
List of Figures.....	xi
List of Tables	xiii
Abstract.....	xiv
Chapter 1. Motivation, Methods, and Hypothesis	1
1.1 Introduction	1
1.1.1 Importance	2
1.2 Previous Work.....	5
1.2.1 Marine Oxygen Isotope Record.....	5
1.2.2 Regional Mountain Glaciation.....	6
1.2.3 Lemhi Range, Idaho.....	10
1.2.4 Geology of the Lemhi Range, Idaho.....	15
1.2.5 Equilibrium-Line Altitudes.....	17
1.3 Hypothesis and Objectives	20
Hypothesis A.....	20
Hypothesis B.....	20
1.3.1 Surficial Geologic Map of the Gilmore 7.5-Minute Quadrangle and the Northeastern Quarter of the Big Windy Peak 7.5-Minute Quadrangle	20
1.4 Organization of Thesis	21
References	22
Chapter 2. Surficial Geologic Map of the Gilmore 7.5-Minute Quadrangle and the Northeastern Quarter of the Big Windy Peak 7.5-Minute Quadrangle, Lemhi Range, East-Central Idaho	27
Abstract	27
2.1 Introduction	28
2.2 Geologic Overview	33
2.2.1 Description of Bedrock Units	35
Tertiary Volcanic Rocks	36
Paleozoic Sedimentary Rocks.....	36
Proterozoic Sedimentary Rocks.....	38
2.3 Quaternary Geology Nomenclature and Regional Glacial Overview	39
2.3.1 Terminology.....	39
2.3.2 Western Wyoming and Central Idaho Glaciation.....	42

2.4 Methods	45
2.4.1 Mapping Glacial and Outwash Landforms	45
2.5 Results	46
2.5.1 Surficial Geologic Map of the Gilmore 7.5-Minute Quadrangle and the Northeastern Quarter of the Big Windy Peak 7.5-Minute Quadrangle, Lemhi Range, East-Central Idaho	46
2.5.2 Description of Map Units.....	49
Holocene Non-Glacial Landforms	49
Postglacial Alluvial Deposits and Landforms.....	49
Mass Movement Deposits and Landforms	50
Periglacial Landforms	51
Mid-Late Pleistocene Glacial Landforms	52
End Moraines	52
Dead Ice Features.....	57
Mid-Late Pleistocene Outwash Landforms	58
Outwash Fans.....	58
Alluvial Terraces.....	59
2.6 Interpretation of Map Units.....	61
2.6.1 Timing of Glacial Events	63
Lemhi Advance 1	64
Lemhi Advance 2.....	65
Lemhi Advance 2 – Spatial Comparison of Landforms Between Valleys	70
Lemhi Advance 2 – Morphological Comparisons of Moraines Between Valleys	71
Lemhi Advance 2 – Regional Comparison.....	72
Lemhi Advance 3.....	73
Lemhi Advance 3 – Spatial Comparison of Landforms Between Valleys	74
Lemhi Advance 3 – Morphological Comparisons of Moraines Between Valleys	76
Lemhi Advance 3 – Regional Comparison.....	77
Lemhi Advance 4.....	78
Western Flank Glacial Extent	79

Glacial Recession.....	79
Recession of Lemhi Advance 1-4.....	79
2.6.2 Timing of Post-Glacial Events.....	81
2.7 Conclusion.....	82
References.....	83
Chapter 3. Late Pleistocene Glacial Geomorphology and Paleoclimatology in the East-Central Lemhi Range, Idaho, U.S.A.	87
Abstract.....	87
3.1 Introduction.....	88
3.2 Setting.....	92
3.3 Previous Work.....	95
3.3.1 Previous Work Suggesting Variability in Glaciation across Northwestern Inland Mountain Glacier Systems.....	95
Modern ELAs.....	99
3.4 Methods.....	101
3.4.1 Surficial Mapping of the Gilmore 7.5-Minute Quadrangle and the Northeastern Quarter of the Big Windy Peak 7.5-Minute Quadrangle, Lemhi Range, East-Central Idaho.....	101
3.4.2 Cosmogenic Radionuclide Dating.....	103
3.4.3 Glacier and Paleoclimate Modeling.....	104
3.4.3.1 Glacier Longitudinal Profiles.....	105
3.4.3.2 Glacier Surface and Equilibrium-Line Altitude Reconstructions	107
Glacier Surface Reconstruction.....	107
Equilibrium-Line Altitude Reconstruction.....	109
Accumulation-Area Ratio.....	109
Toe-to-Headwall-Altitude Ratio.....	110
3.5 Results.....	111
3.5.1 Surficial Mapping.....	111
3.5.2 Glacier Modeling and Equilibrium-Line Altitudes.....	114
3.6 Discussion.....	121
3.6.1 Glacial Advance Sequences.....	121
Lemhi Advance 1.....	121
Lemhi Advance 2.....	122

Lemhi Advance 2 – Spatial Comparison of Landforms Between Valleys	123
Lemhi Advance 2 – Morphological Comparisons of Moraines Between Valleys	126
Lemhi Advance 2 – Regional Comparison	127
Lemhi Advance 3	128
Lemhi Advance 3 – Spatial Comparison of Landforms Between Valleys	129
Lemhi Advance 3 – Morphological Comparisons of Moraines Between Valleys	131
Lemhi Advance 3 – Regional Comparison	132
Lemhi Advance 4	133
Western Flank Glacial Extent	133
3.6.2 Inferences from Insolation	135
3.6.3 Regional Glacial Recession	137
3.6.4 Equilibrium-Line Altitudes	140
3.6.4.1 Equilibrium-Line Altitude Comparisons for Paleoclimate Inferences	140
3.6.4.2 MIS 4-3 Paleoclimatic Inferences	148
3.7 Conclusions	148
References	151
Chapter 4. Conclusion	157
4.1 Lemhi Range Glaciation and Climatic Conditions	157
4.1.1 Surficial Mapping of the Gilmore 7.5-Minute Quadrangle and the Northeastern Quarter of the Big Windy Peak 7.5-Minute Quadrangle: Evidence for Multiple Glacial Advances	157
4.1.2 Cosmogenic Radionuclide Dating: Quantitative Evidence of Glaciation...158	
4.1.3 Equilibrium-Line Altitudes: Inferences of Climatic Conditions	159
4.2 Suggestions for Future Work	161
References	165
Appendices.....	166

Appendix A: Terrestrial Cosmogenic Radionuclide Dating – Background, Sampling Methods, Preparation, and Status of Collected Samples Not Included in Text	166
References	175
Appendix B: Paleo-Glacier Reconstructions – Paleo-Glacier Longitudinal Profiles and Individual Paleo-Glacier Surfaces.....	177
Appendix C: Equilibrium-Line Altitudes and Temperature Depression – Accumulation-Area Ratio Method ELAs, Toe-to-Headwall-Altitude Ratio Method ELAs, Temperature Depression, and Regional Comparisons.....	194
References	202

List of Figures

1.1 Location Map of Lemhi Range	3
1.2 Precipitation Maps of Western United States and Idaho	4
1.3 Marine Oxygen Isotope Curve.....	6
1.4 Location Map of Maritime and Inland Mountain Glacier Systems	8
1.5 Inland Mountain Glacier System Chronology Map.....	9
1.6 Location Map of Gilmore and Middle Ridge	13
1.7A Trend of Glaciation in the Lemhi Range and Hypsometric Profile of the Lemhi Range	14
1.7B Hypsometric Profile of the Lemhi Range	14
2.1 Location Map of the Gilmore and Big Windy Peak Quadrangles	29
2.2 Younger and Older Moraine Example.....	30
2.3 Bedrock Units Exposed in the Gilmore and Big Windy Peak Quadrangles.....	31
2.4A, B, C, D Lemhi Range Moraine Delineation.....	47
2.5 Hummocky Dead Ice Landform at Spring Mountain Canyon.....	48
2.6A Surficial Geologic Map of the Gilmore and Northeast Quadrant of the Big Windy Peak Quadrangles.....	62
2.6B Correlation of Surficial Map Units.....	63
2.7 Deer Creek Glacial Sequence	66
2.8A Deer Creek Qm3, Qm2, Qm1 Longitudinal Profile.....	67
2.8B Meadow Lake Creek Qm3, Qm2, Longitudinal Profile.....	67
2.8C Long Canyon Qm3, Qm2, Longitudinal Profile	67
2.9 Meadow Lake Creek Glacial Sequence	68
2.10 Long Canyon Glacial Sequence.....	69
2.11 Spring Mountain Canyon Glacial Sequence	70
2.12 Solar Insolation Duration Map of the Lemhi Range.....	75
2.13 Central Lemhi Range Glacial Advance Sequence	81
3.1 Inland Mountain Glacier System Chronology Map.....	90
3.2 Location Map of Lemhi Range	93
3.3 Hillshade of Glacially Sculpted Valleys in the Lemhi Range	94
3.4 Geologic Map of Rock Creek and Otto Glacier.....	100
3.5 Location Map of the Gilmore and Big Windy Peak Quadrangles	103
3.6A, B, C, D Lemhi Range Moraine Delineation.....	112
3.7 Hummocky Dead Ice Landform at Spring Mountain Canyon.....	113
3.8 Meadow Lake Creek Glacier Surface Longitudinal Profile	115

3.9 Lemhi Range Paleo-Glacier Surface and ELA Reconstructions	116
3.10 Lemhi Range AAR and THAR ELAs	118
3.11 Lemhi Range AAR and THAR ELAs vs. Modern ELAs	120
3.12A Deer Creek Qm3, Qm2, Qm1 Longitudinal Profile.....	124
3.12B Meadow Lake Creek Qm3, Qm2, Longitudinal Profile	124
3.12C Long Canyon Qm3, Qm2, Longitudinal Profile	124
3.13A Deer Creek Glacial Advance Sequences.....	125
3.13B Meadow Lake Creek Glacial Advance Sequences.....	125
3.13C Long Canyon Glacial Advance Sequences	125
3.13D Spring Mountain Canyon Glacial Advance Sequences	125
3.14 Solar Insolation Duration Map of the Lemhi Range.....	130
3.15 Central Lemhi Range Glacial Advance Sequence	134
3.16 Insolation Time Series	136
3.17 Assumed LGM ELAs across Lemhi Range (THAR and AABR Methods)	141
3.18 ELA Contour Map of the Western United States	142
3.19 Inland Mountain Glacier AAR ELAs	147

List of Tables

2-1 Glacial Terminology Correlation.....42
3-1 AAR ELAs for Reconstructed Lemhi Range Glaciers117
3-2 THAR ELAs for Reconstructed Lemhi Range Glaciers117
3-3 Regional AAR ELAs for Inland Mountain Glacier Systems143

Abstract

The spatial extent of glaciation varied across the eastern range-front of the Lemhi Range, east-central Idaho, indicating multiple episodes of glaciation during the last two glacial cycles. This study utilized extensive field mapping, in conjunction with satellite imagery and digital elevation models (DEMs) to document the glacial and alluvial deposits that represent distinct ice advance and retreat events from marine isotope stage (MIS) 6-2. Surficial mapping of glacial and alluvial features delineates four distinct glacial advances evidenced by mapped Qm1-Qm4 end moraines and coeval Qf1-Qf4 outwash fans. The geomorphic characteristics of the mapped end moraines, including moraine crest angularity, moraine relief, and distal moraine slope steepness, were analyzed semi-quantitatively from transverse profiles. These comparisons concluded that slope angle, crest angularity, and relief decrease as moraine age increases, and permit broad correlation of the glacial advances with widespread climatic events. The glacial advance sequences and estimated timings include Lemhi Advance 1 (MIS 6), Lemhi Advance 2 (MIS 4-3), Lemhi Advance 3 (MIS 2) and Lemhi Advance 4 (late MIS 2). Glacial recession in the Lemhi Range was completed by 14 ± 0.5 cal ka BP, as determined from radiocarbon dating of organic sediment from a Meadow Lake sediment core. Paleo-glacier ice surfaces were reconstructed for seven glaciated valleys across the eastern flank of the range from inferred MIS 2 age, Qm3 end moraines and weakly identifiable trimlines. Equilibrium-line altitudes (ELAs) were calculated using the accumulation-area ratio (AAR) and the toe-to-headwall-altitude ratio (THAR). The two methods of calculation are broadly consistent with one another, revealing average AAR-

and THAR-derived ELAs of 2650 m and 2690 m, respectively, across the Lemhi Range, with an overall ELA depression of ca. 600 m.

The calculated AAR ELAs in this study show similarities to MIS 2 and LGM/Pinedale age AAR-derived ELAs in the Lemhi Range (2720 m), Sawtooth Mountains, Idaho (2640 m) and Beaverhead Mountains, Montana (2650 m) (Meyer et al., 2004; Locke, 1990). This ELA similarity likely results from decreases in precipitation from rain shadowing by the Sawtooths, moisture diversion around these high ELA ranges to the north and south into the Snake River Plain, and weakening of westerly flow from glacial anticyclone easterly winds from the Cordilleran and Laurentide ice sheets. It is likely that cold easterly winds migrated over low portions of the Beaverhead Mountains (e.g., Railroad Canyon), directly east of the Lemhi Range, causing a cold and dry climate. Thus MIS 2 climate in the central Lemhi Range may have been influenced by the continental interior and its ice sheets, resulting in depressed ELAs. Similar ELA patterns of the Lemhi Range, Beaverhead Mountains, and Sawtooth Mountains may result from uniform cooling and consistent precipitation contrasts across the ranges, or greater temperature depression in the Lemhi Range and Beaverhead Mountains from cold easterly winds, coupled with reduced precipitation from decreased westerly winds in the Sawtooth Mountains during the last glacial cycle.

The character and relative position of Lemhi Advance 2 end moraines, which lie a short distance down-valley of or merge with Lemhi Advance 3 moraines, indicate glaciation of similar magnitude during MIS 4/3 (Lemhi Advance 2) and MIS 2 (Lemhi Advance 3). These relationships suggest that similar climatic conditions affected the

Lemhi during MIS 4/3, or that wetter and milder conditions drove glaciers to similar positions.

Chapter 1. Motivation, Methods, and Hypotheses

1.1 Introduction

The Last Glacial Maximum (LGM) has been widely defined as the most recent interval when global ice sheets reached their maximum integrated volume during the last glaciation, occurring ca. 18-25 ka (Mix et al., 2001). However, this pattern, seen in Northern Hemisphere ice sheets, engenders ambiguity regarding the spatial and temporal patterns of mountain glacier systems during the last glacial cycle (120-10 ka). The patterns of Late Pleistocene mountain glaciation across the western United States have long been a point of contention. Mountain glacier systems across the western United States have experienced variable maximum ice extent before, during, and after the LGM (e.g., Thackray, 2001 and 2008, Wyshnytzky et al., 2015, and Staley, 2015, in Pacific North America; Thackray et al., 2004, Kenworthy et al., 2014; Licciardi and Pierce, 2008), as well as on other continents (e.g., Rother et al., 2014, in Mongolia; Putnam et al., 2013, and Shulmeister et al., 2010, in New Zealand; Darvill et al., 2015, in southern South America). In many cases, it has been concluded that mountain glacier maximum ice extent was coeval with the maximum continental ice sheet extents during marine isotope stages (MIS) 2 and 6.

Mountain glacier systems are particularly sensitive to small-magnitude, short-term fluctuations in regional climate. These climatic fluctuations, however, are typically not recorded in continental-scale ice sheet records. This poses asynchrony in the timing of maximum ice extent across mountain glacier systems. This asynchrony has also been documented globally (Hughes et al., 2013), with the assertion that many mountain glaciers systems were asynchronous with the global LGM period. As new chronologic tools have been implemented widely, the perception of synchrony has changed. Detailed

field mapping, in concordance with glacial chronologies, can further constrain the timing and intensity of glaciation before, during, and after the LGM, thus improving the understanding of the climatic drivers of regional glaciation in space and time.

This study elucidates the patterns of extensive mountain glaciers and the paleoclimatic conditions that produced them in the central portion of the Lemhi Range, east-central Idaho (Figure 1.1). This study develops an original surficial geologic map of Late Pleistocene glacial and alluvial deposits in the Lemhi Range. Mapping of glacial and alluvial deposits establishes spatial relationships between landforms and defines ice limits for specific glacial events. Semi-quantitative moraine morphology establishes relative ages of glacial advances based on moraine crest angularity, distal slope steepness, and relief. This map provides the basis for glacier reconstructions and the calculation of Pleistocene equilibrium-line altitudes (ELA), which in turn yield possible precipitation-temperature relationships during the glacial events.

1.1.1 Importance

It is possible that climatic events during MIS 4 and 3, which strongly influenced Pacific Northwest mountain glacier systems (e.g., Olympic and Cascade Mountains, Thackray, 2001, Porter and Swanson, 2008), penetrated mountain ranges further inland and influenced the timing and intensity of glaciation in semi-arid mountain ranges, such as the Lemhi Range. Glaciers in the Olympic Mountains advanced repeatedly into the Pacific coastal lowlands due to strong influences of onshore Pacific moisture delivery coupled with modest cooling, leaving behind a detailed geomorphic and stratigraphic record with abundant datable organic material (Thackray, 2001, Marshall, 2013, Staley, 2015). Unfortunately, many inland mountain glacier records are hindered by a lack of

datable material, poor stratigraphic exposure, erosion or burial by later glacial advances, and intense research focus on the global Last Glacial Maximum advances (18-25 ka) with lesser focus on earlier events.

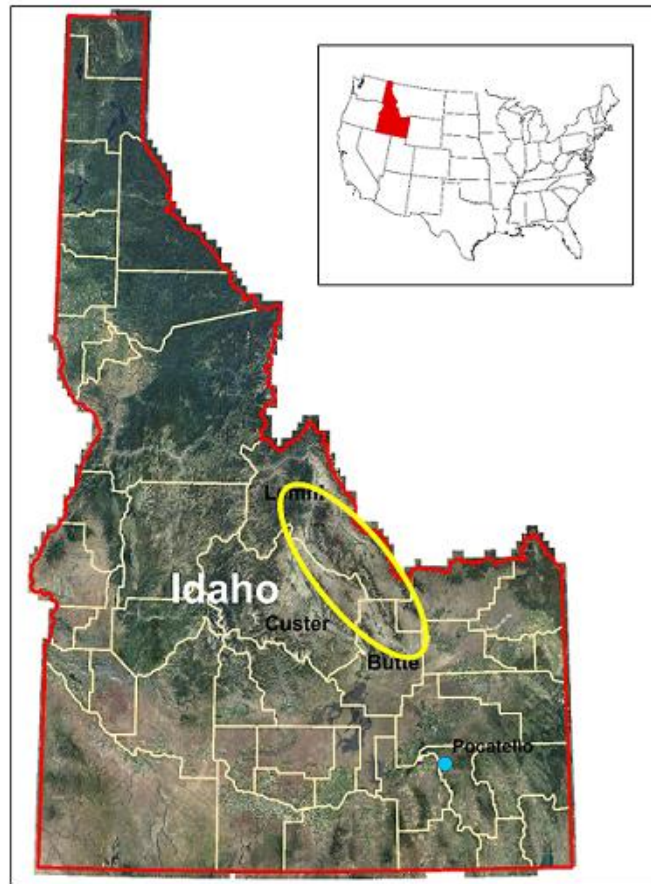


Figure 1.1 Location map of the Lemhi Range, east-central Idaho, identified by yellow bounding oval. The state of Idaho is segmented by counties, with counties of close proximity to the Lemhi Range labeled.

The Lemhi Range, east-central Idaho, offers significant information regarding the glacial history of western North America (Butler, 1981). The eastern flank of the central Lemhi Range exposes beautifully preserved, glacially derived deposits and landforms. This area was chosen for in-depth analysis due to the exquisite glacial moraine and fan sequences in a region with little glacial-chronologic data, and accessibility via dirt roads and former mining tracks, which meander up many of the valleys. Surficial deposits in

the central part of the Lemhi Range reflect the repeated occurrence of Pleistocene glacial or near-glacial climatic conditions (Dort, 1962). The eastern front of the Lemhi Range receives about 500-1000 mm/yr of precipitation (Figure 1.2). Precipitation at higher elevations accumulates approximately 750 mm/yr, mostly in the form of snow (Gallup, 1962). This semi-arid nature of the Lemhi Range suggests that the extent and erosional capacity of glaciers was limited between episodes of glaciation. Therefore, the range should preserve detailed records of regional climatic and geologic fluctuations through the Late Pleistocene because landforms of earlier episodes of glaciation have not been removed during later advances (Dort, 1962). Past glaciations also provide the opportunity to reconstruct paleoclimate indicators, such as ELAs.

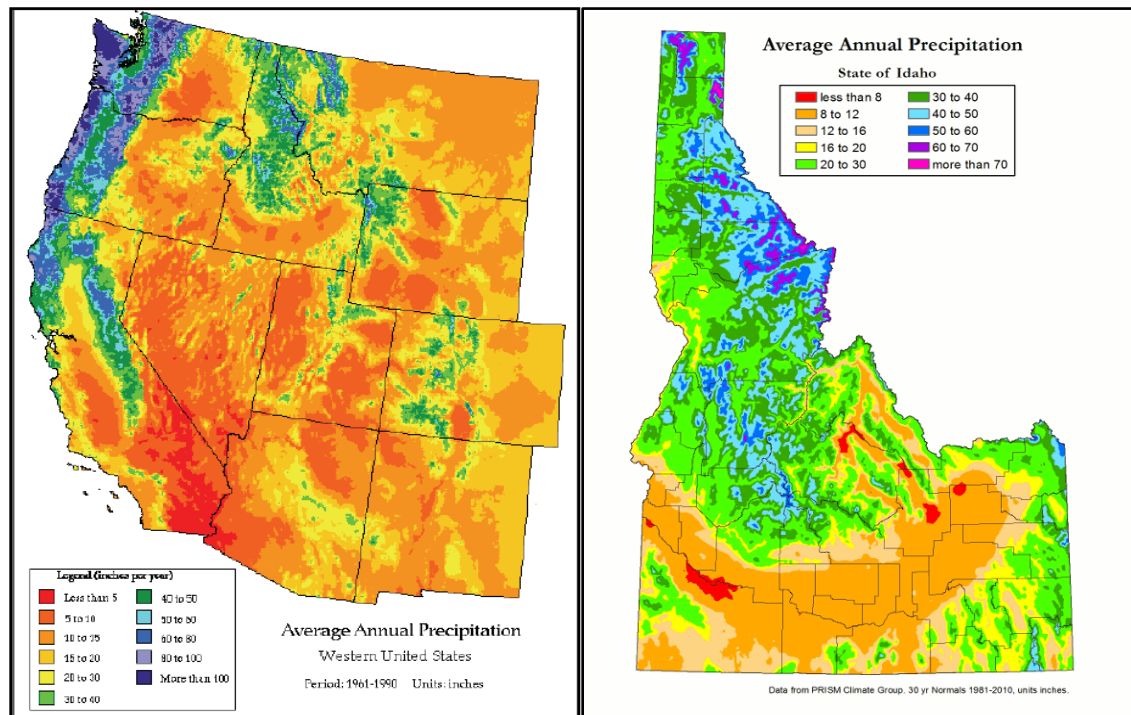


Figure 1.2 Precipitation maps showing the average annual precipitation across the western United States from 1961-1990 (left) (Western Regional Climate Center, 2015) and the average annual precipitation of Idaho from 1981-2010 (right) (Prism Climate Group, 2015).

1.2 Previous Work

This thesis emphasizes and expands upon previous studies of the extent of MIS 4-3 glaciation across the northwestern United States. This section discusses the few studies conducted in, and the geomorphic characteristics of the Lemhi Range, and provides a synthesis of previous publications that provide evidence suggesting that MIS 4-3 glaciation may have been more extensive than the LGM in the northwestern United States.

1.2.1 Marine Oxygen Isotope Record

Pleistocene climatic fluctuations can be correlated to the MIS record (detailed in Martinson et al., 1987), which reflects global ice volume inferred from the oxygen isotope ($\delta^{18}\text{O}$) record from benthic foraminifera and provides a framework for Quaternary chronostratigraphy. This record (Figure 1.3) depicts alternations between glacial and interglacial periods, with the ice volume record dominated by continental-scale ice sheets in the Northern Hemisphere. Martinson et al. (1987) used orbital tuning to construct a high-resolution deep-sea chronostratigraphy spanning the last 300,000 years, based on the high-resolution oxygen-isotope stratigraphy of Pisias et al. (1984). This thesis discusses the timing of mountain glacier maximum ice extent in reference to this record. The marine oxygen isotope stage boundaries are: MIS 1-2—14 ka, MIS 2-3—29 ka, MIS 3-4—57 ka, MIS 4-5—71ka, MIS 5-6—130 ka, MIS 6-7—191 ka. MIS 5 includes inferred global ice volume minima at 82 ka (MIS 5a), 96 ka (MIS 5c), and 123 ka (MIS 5e), and inferred ice volume peaks at 87 ka (MIS 5b), and 109 ka (MIS 5d) (Lisiecki and Raymo, 2005) (Figure 1.3).

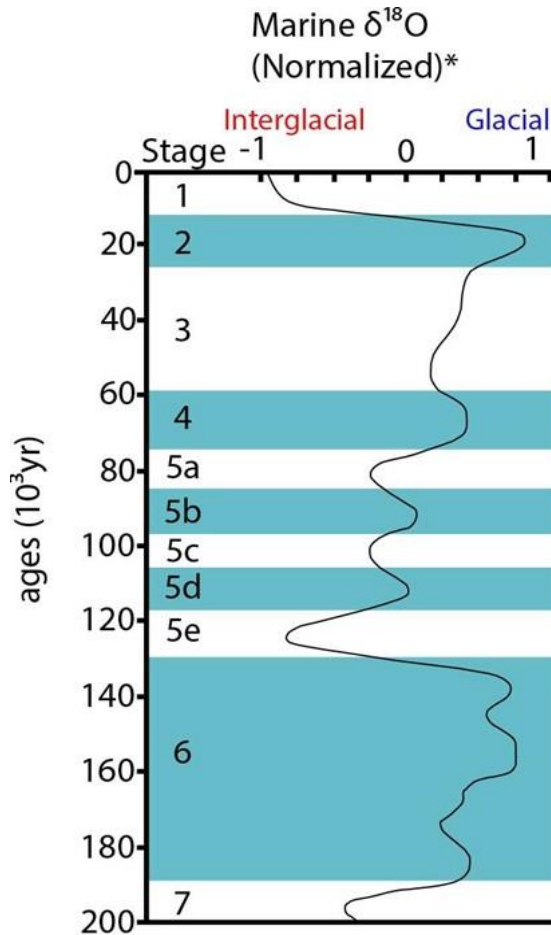


Figure 1.3 Marine Oxygen Isotope curve depicting the correlation between glacial/interglacial cycles and marine isotope stages (from Staley et al. (2015) modified from Kaufman et al. (2003), based on original data from Martinson et al. (1987)).

1.2.2 Regional Mountain Glaciation

Researchers have for many years debated the temporal patterns of Late Pleistocene glaciation in mountainous regions across the western United States (e.g., Licciardi, 2004; Licciardi and Pierce, 2008; Thackray, 2008; Laabs, 2009; Balco, 2009). The debates are rooted in an unjustified assumption that the maximum ice extent of western United States mountain glacier systems occurred coeval with the ice-sheet LGM and immediately post-LGM climatic events. This assumption fails to consider the variability in moisture availability and cooling driven by orographic and maritime

influences during pre-LGM and LGM climatic events (Thackray, 2008). High-precipitation maritime mountain glacier systems (Figure 1.4), such as the Olympic and Cascade Mountains in Washington, reached local maxima 90-60 ka and 34-31 ka, and were much less extensive during the LGM (Thackray, 1996, 2001, 2008; Marshall, 2013; Wyshnytzky et al., 2015; Staley, 2015). This Cascade/Olympic pattern contrasts with most of the published radiometric chronologies further inland, where MIS 2 advances are generally thought to have been more extensive than MIS 3 and MIS 4 advances (e.g., Gosse et al., 1995; Licciardi and Pierce, 2004; Licciardi and Pierce, 2008; Refsnider et al., 2008).

Inland mountain glacier systems, subject to lower precipitation and temperature, also achieved local maxima asynchronous to the LGM. Radiometric glacial chronologies obtained in the Uinta Mountains, Wallowa Mountains, and Wind River Range suggest maximum ice extent during the LGM (MIS 2) (Refsnider et al., 2008; Licciardi and Pierce, 2004; Gosse et al., 1995). Luminescence and fault offset glacial age estimates obtained in Lost River Range, which neighbors the Lemhi Range to the west, suggest pre-LGM maximum ice extent (MIS 4-3) (Kenworthy et al., 2014; Staley, 2015). Age estimates obtained through fault scarp offset and weathering/erosional indicators, in the Teton Range and Sawtooth Mountains, respectively, also suggest pre-LGM maximum ice extent (MIS 4-3) (Thackray and Staley, in review; Colman and Pierce, 1992; Thackray, 2004). Cosmogenic radionuclide (CRN) surface exposure ages from boulders in the greater Yellowstone glacial system and Teton Range suggest LGM or shortly post-LGM maximum ice extent (late MIS 2) (Licciardi and Pierce, 2008;). Figure 1.5 focuses on the above mentioned inland mountain glacier systems and the associated glacial

chronologies. Radiometric, fault offset, and erosional/weathering dating techniques suggest an asynchrony in the timing of maximum ice extent of inland mountain glacier systems across the northwestern United States.



Figure 1.4 Regional topographic image showing the locations of maritime (blue circle) and inland (red circle) mountain glacier systems across the northwestern United States. Figure modified from Thackray (2008).

Existing Late Pleistocene Geochronology of Mountain Glacier Systems

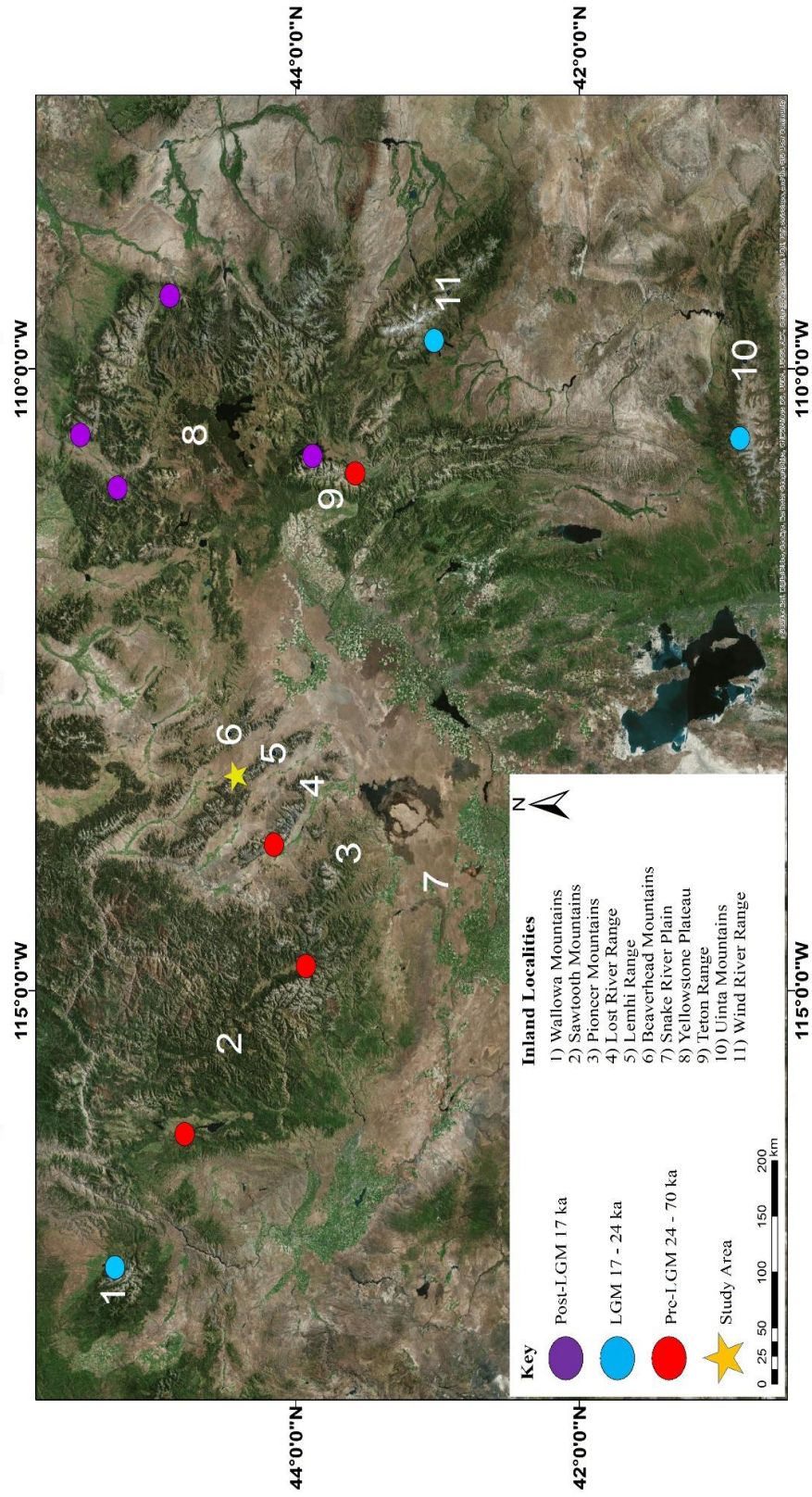


Figure 1.5 Regional topographic image of east-central Idaho, Wyoming, and southwestern Montana showing locations of inland mountain glacier systems and Late Pleistocene geochronologies of maximum ice extent. Ages were determined through cosmogenic radionuclide, optically stimulated luminescence, fault offset, and erosional LGM. See text for discussion of geochronology and references.

1.2.3 Lemhi Range, Idaho

The Lemhi Range is a northwest trending, 150 km-long, normal-faulted mountain range located north of the eastern Snake River Plain in east-central Idaho (Foster et al., 2008). The range crest has a mean altitude of 3,050 m (Butler, 1986). The east side of the Lemhi Range is incised by a system of glacially-scoured valleys which are oriented nearly perpendicular to the range. Most major east-facing valley heads were occupied by glaciers in late Pinedale time (30-14 ka) (Dort, 2003; Colman and Pierce, 1986) and previous glacial events. Glacial advance, recession, and deposition have produced intricate patterns of moraine and kettle topography in many valleys (Knoll, 1977; Butler, 1984).

This relatively arid portion of central Idaho lies between the Sawtooth Mountains, Idaho, and the Teton Range, Wyoming, where glacial chronologies are reasonably well understood. This is a key area to improve knowledge of spatial and temporal patterns of glaciation in the interior Western United States. However, Late Pleistocene Lemhi Range glaciation has been previously documented in insufficient detail by Dort (1962, 2003, 2004), Knoll (1977), Butler (1984, 1986), and at a broad-scale by Foster et al. (2008), and published chronologies are sparse. This dearth of chronologies has left many questions unanswered, especially regarding the spatial patterns and paleoclimatic conditions of Late Pleistocene glaciation. However, a minimum limiting radiocarbon age on final glacial retreat of 14 ± 0.5 cal ka BP is known from a Meadow Lake sediment core sample (B. Finney, personal communication, 2015).

Previous work on glacial sequences in the Lemhi Range was conducted mainly by W. Dort and K.M. Knoll, but published only in a series of conference abstracts and

regional publications. Dort (1962) first mapped and delineated Neoglacial moraines and mass wasting deposits in the central Lemhi Range, which he separated into Temple Lake (3000-5000 ka) and Little Ice age (1300-1850) sequences. Dort mapped Temple Lake deposits in Meadow Lake Creek, Long Canyon, Deer Creek, and Bruce Canyon. Little Ice Age deposits were mapped in these same valleys, as well as Spring Mountain Canyon.

Knoll (1977) documented Holocene and Pleistocene glacial landforms in Meadow Lake Creek (termed Meadow Lake Canyon by Knoll) and Long Canyon in the central Lemhi Range. He describes eighteen moraines in the lower half of Meadow Lake Canyon composed of till and stratified drift and ranging from 100 m to greater than 2.4 km in length. Knoll additionally describes five outwash fans derived from Meadow Lake Canyon that vary in size and slope, and formed at different times, representing at least three separate glaciations. In Long Canyon, Knoll (1977) describes nine moraines in the upper reaches, representing recessional glacier stillstands, and twenty-two moraines in the lower reaches ranging in length from 100 m to 2.3 km. He additionally describes outwash distributed in three major fans associated with different groups of end moraines around the mouth of Long Canyon, Knoll associates the identified glacial features in these canyons with individual glaciations, and their inferred ages, in a series of sketch maps as: Glaciation I (Pre-Bull Lake), Glaciation II (Bull Lake), Glaciation III (Pinedale), and Glaciation IV (Neoglaciation), with Glaciations II and III having multiple defined stadial events.

Dort (2003) describes fresh end moraines showing that Pinedale ice reached mountain-front canyon mouths at about 7200-7400 feet, and terminated up-valley in most

canyons. Dort also correlated subdued landforms that lie close in front of fresh end moraines with Bull Lake (180-130 ka) glaciation, and elsewhere where evidence of Bull Lake moraines is absent, Pinedale ice extended beyond the local Bull Lake ice limits. However, these age estimates were made without numerical dating, and the details of data and interpretations remain unpublished. Dort (2003) additionally described a fault block complex of Middle Ridge, located just beyond the 2-mile wide graben valley, east of the Lemhi Range (Figure 1.6). Dort describes 6-foot quartzite erratics, derived from Lemhi sources that lie on the highest summits of middle ridge, suggesting a glacier advance that predated the uplift of Middle Ridge. Dort sampled boulders of Jurassic quartzite from Middle Ridge. The analyses of the samples returned CRN age estimates of 500-350 ka, uncorrected for boulder erosion, suggesting a very extensive pre-Bull Lake ice advance (John Gosse, personal communication, 2015). The details of that study also have not been published and the attribution to glaciation is questionable. The depositional record of the episodic retreat phases of Pinedale ice conveys the greatest detail. Lateral and terminal moraines of Pinedale age were formed and preserved because of minimal postglacial runoff erosion (Dort, 2004).

Knoll (1977) and Butler (1984, 1986) described Holocene Neoglacial moraines, rock glaciers, protalus, and talus deposits within Long Canyon, Meadow Lake Creek, and Hilltop Valley, with age estimates based on dendrochronology and relative-age and dating techniques. In addition, Johnson et al. (2007) identified 48 rock glaciers in the Lemhi Range, analyzing them for lichen cover, ice presence, and signs of movement to determine their development and preservation. Johnson et al. (2007) concluded that

annual sun hours and lithology correlated most strongly with rock glacier presence and absence.



Figure 1.6 Google Earth image showing the location of Middle Ridge, Idaho, relative to Gilmore, Idaho, separated by the graben valley.

Foster et al., (2008) examined the effectiveness of small glaciers in limiting topography (i.e., the glacial buzzsaw hypothesis) by comparing the distribution of glacial erosion and fault slip rate with along-strike maximum elevation, hypsometry, and slope elevation profiles in the northern Basin and Range. In the Lemhi Range, glacial extent was limited in the southern portions, with LGM glacial extents increasing northwestward along-strike (Figure 1.7A). The Lemhi Range exhibits abnormally high LGM ELAs, when compared to other interior northwestern LGM ELAs, because of low precipitation

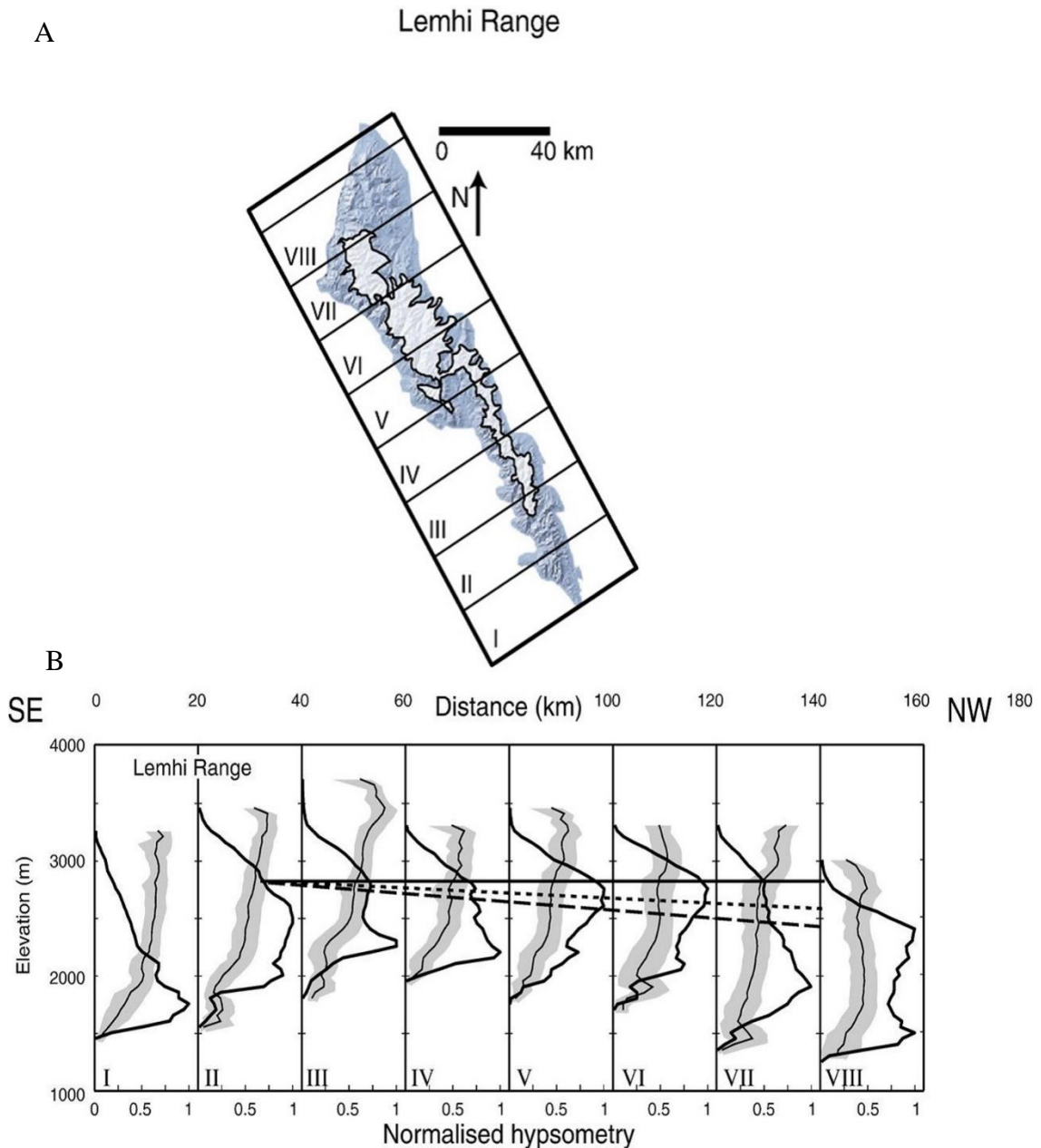


Figure 1.7 A) Trend of increased LGM glaciation northwestward along swath profiles in the Lemhi Range, Idaho. Roman numerals refer to the swaths in which hypsometry and slope elevation profiles were generated. The central Lemhi Range study area lies in swaths V and IV. B) Hypsometry profile for 20 km sections of the Lemhi Range, Idaho. The bold vertical profiles show the normalized hypsometry. The fine black (median slope) and shaded (inter-quartile range) vertical profiles represent slope angles. Sub-horizontal lines represent the regression lines from cirque floor (solid black line), AABR LGM (dotted/fine dashed) and THAR LGM (dashed/thick dashed) ELA data. Figures modified from Foster et al. (2008).

rates (Meyer et al., 2004). LGM glacier ELAs (Foster et al., 2008) were reconstructed for 20 relatively simple valleys with few tributaries in the Lemhi Range using the toe-to-headwall-altitude ratio (THAR) and the accumulation-area-balance ratio (AABR) methods (Chapter 3). In the southern portion of the range, ELA estimates from cirque floors and LGM reconstructions occur at similar altitudes. The hypsometric data (Figure 1.7B), from Foster et al., (2008), depict a greater concentration of lower elevations in the southern Lemhi Range. Farther north, the hypsometry is skewed towards higher elevations, where glaciation was more widespread, yielding a diversion of LGM trends, as LGM ELAs are estimated from basins containing larger glaciers.

1.2.4 Geology of the Lemhi Range, Idaho

The Lemhi Range is a northwest trending, normal-faulted mountain range located north of the eastern Snake River Plain in east-central Idaho, located within the Cordilleran fold and thrust belt, and in the Basin and Range province. The range is bounded by the Pahsimeroi and Lost River valleys to the west, and the Lemhi and Birch Creek valleys to the east (Link and Janecke, 1999; Johnson et al., 2007).

The strata exposed in the Lemhi Range were deposited in the Mesoproterozoic Belt intracratonic rift basin, and episodically during the late Neoproterozoic and Paleozoic Cordilleran miogeocline (Link and Janecke, 1999). The oldest rocks in the Lemhi Range are included in the Middle Proterozoic Yellowjacket Formation, comprised of predominantly feldspathic quartzite and siltite. Strata within the Lemhi Range were altered in the Late Cretaceous when the Medicine Lodge thrust moved eastward. (Ruppel and Lopez, 1981, 1988). Extension along numerous normal faults began prior to Middle Eocene Challis volcanism, which generated Tertiary half graben systems (Link and

Janecke, 1999). Strata were then intruded during the Eocene by small stocks of monzogranite, granodiorite, quartz monzodiorite, and quartz monzonite (Ruppel and Lopez, 1988). The coarse topography of the Lemhi Range seen today is mainly a result of uplift and erosional processes correlating to normal faulting. These processes allow for the exposure of Proterozoic to upper Paleozoic sedimentary and meta-sedimentary rocks that were folded and thrust-faulted during the Sevier Orogeny (Lund et al., 2003). The ice-sculpted central part of the Lemhi Range allows for exposure of an underlying geologic framework (Ruppel and Lopez, 1981, 1988).

The Gilmore and Big Windy Peak 7.5-minute quadrangles are located in the east-central portion of the Lemhi Range. Extensive geologic bedrock mapping has been previously conducted in these quadrangles, and the bedrock geology is relatively well understood. The mapping patterns reveal the structural, tectonic, and mineral deposition history (Ruppel and Lopez, 1981, 1988). Ruppel and Lopez (1981) constructed a 1:62,500 scale bedrock geologic map titled “Geologic Map of the Gilmore quadrangle, Lemhi and Custer Counties, Idaho”, published by the Department of the Interior, United States Geological Survey. Their mapping details Proterozoic to upper Paleozoic sedimentary and meta-sedimentary rocks and Eocene intrusive rocks, as well as detailed fault mapping and numerous cross-sections.

The previous geologic mapping however, provides minimal detail regarding Pleistocene glacial and alluvial deposits, as well as modern Holocene deposits, such as talus and landslides. Surficial mapping has been limited to areas along and adjacent to the Lemhi Fault, which bounds the western flank of the Lemhi Range. Janecke (1992) mapped the portion of the Big Windy Peak quadrangle in the vicinity of the active fault,

leading to the conclusion that the Lemhi Fault cuts Latest Pleistocene alluvial fan deposits. Glaciation and surficial mapping in the central Lemhi Range have therefore received scant attention.

Of the bedrock units exposed in the range, this study emphasizes the Middle Ordovician Kinnikinic Quartzite and Tertiary granitic rocks. Samples from these lithologies were extracted from boulders on moraine crests for CRN analysis. The Middle Ordovician Kinnikinic Quartzite is widely and predominantly exposed throughout the central portion of the Lemhi Range. The Kinnikinic Quartzite is 300-400 m thick in the central Lemhi Range and is characterized by light-gray to white, subangular to subrounded, well sorted, fine to medium grains of quartz, vitreous luster, and massive bedding structure. In the study area, the Kinnikinic Quartzite is exposed primarily in the upper portions of the valleys, providing a marker of glacial transport. The Tertiary granitic rocks are older than the Challis volcanics and are not exposed in the southern portion of the Lemhi Range (Ruppel and Lopez, 1988).

1.2.5 Equilibrium-Line Altitudes

The equilibrium line joins points on a glacier where annual accumulation exactly balances annual ablation, marking a net budget of zero (Porter, 1975). The altitude of the equilibrium line is rarely constant across a glacier, as it is a function of local climate, including the distribution of precipitation, snow accumulation, ablation, and shading (Meier and Post, 1962). In reality, it infrequently runs smoothly across the glacier and may form closed loops in places. Glacial ELAs have been widely used to infer past climatic conditions through the use of relationships derived from measurements of modern analogues. Previous studies in arctic and alpine areas (Porter, 1964, 1975;

Meierding, 1982) reveal that modern and Pleistocene ELAs reflect modern precipitation patterns, which are influenced by proximity to water sources, orography, and atmospheric circulation (Meierding, 1982).

The most rigorous methods of reconstructing paleo-ELAs are derived from a three-dimensional form of the former glacier surface, and all require assumption and interpolation. The accumulation-area ratio (AAR) method is the most widely applied technique for ELA estimation. The AAR refers to the amount of area above the equilibrium line (accumulation area) divided by the total area, and is based on the assumption that under steady-state conditions, the accumulation area of the glacier occupies a fixed proportion of the total glacier area (Meier and Post, 1962; Porter, 1975). Meier and Post (1962) empirically derived a series of accumulation area ratios by observing the transient snowlines, the percentage of the total area which was snow covered, and the character of snow for 475 glaciers across North America. Most mid- and high-latitude glaciers have balanced net budgets at AAR's between 0.5 and 0.8, with typical values of 0.55-0.65 (Meier and Post, 1962; Porter, 1975). For cirque, valley, and mid- and high-latitude glaciers, an AAR of 0.6 ± 0.05 can be applied to reconstruct paleo-ELAs by assuming that past glaciers had similar relationships between glacier mass balance and climate (Meier and Post, 1962; Porter, 1975; Bakke and Nesje, 2011).

In this study, the AAR and THAR methods are used to calculate paleo-ELAs from inferred MIS 2-correlative moraines in the central Lemhi Range, Idaho, to elucidate paleoclimatic conditions. Valleys that housed singular glacier systems (containing one cirque headwall) were preferentially chosen for reconstruction, although valleys chosen are not limited to this guideline. This study applies an AAR of 0.6 ± 0.05 to calculate

ELAs, coinciding with other studies that have previously applied the AAR method (Porter, 1975; Lundeen, 2001; Benn, 2005). The application of the AAR method begins with the inference of glacier extent from moraine mapping on a topographic map. In this study, bed elevation data from valley floors is extracted and used in conjunction with the *Profiler* Excel program (Benn and Hulton, 2010) to construct glacier surface profiles. This ice surface data, combined with elevation data from lateral moraines, terminal moraines, and trimlines, are used to reconstruct a digital elevation model (DEM) of the glacier surface. This DEM is used as an input into an ArcGIS based tool (Pellitero, 2015) that calculates the ELA of paleoglaciers, using the AAR method. Contours of the glacier surface are generated from the interpolated glacier surface through the Contour tool in ArcGIS. The contours are constructed at a user specified contour interval that is consistent with the interpolated surface, and happens to coincide with glacier flow patterns (being concave in the accumulation area and convex in the ablation area).

Glacier reconstruction and ELA calculations require a series of specifications, assumptions and interpolations. Steady-state conditions are assumed for glacier and ELA construction. This entails that the glacier is in a fixed position, representative of an equilibrium stage at maximum extent. This allows for the assumption that the ELA remains at a fixed position, with the accumulation area occupying 60 percent of the total glacier area. Intact terminal moraines are necessary to determine the ice marginal extent down-valley. Interpolation of trimlines constrains the lateral and up-valley extent of glaciers. Further detail regarding the reconstruction of paleo-glaciers and paleo-ELAs is provided in Chapter 3.

1.3 Hypothesis and Objectives

The following are the main hypotheses of this thesis:

Hypothesis A

Generation of a surficial geologic map of Late Pleistocene and Holocene glacial and alluvial deposits of the Gilmore 7.5' and the northeastern quarter of the Big Windy Peak 7.5' quadrangles, along with relative age dating and assessment derived from semi-quantitative analysis of moraine morphology, will reveal that pre-LGM (MIS 4-3; 25-75 ka) climatic events produced extensive mountain glaciers in east-central Idaho.

Hypothesis B

Calculation of equilibrium-line altitudes in the central portion of the Lemhi Range will reveal MIS 2 climatic drivers, similar to those in nearby inland mountain glacier systems (e.g., Lost River Range).

1.3.1 Surficial Geologic Map of the Gilmore 7.5-Minute Quadrangle and the Northeastern Quarter of the Big Windy Peak 7.5-Minute Quadrangle

This study has produced a surficial geologic map of the Gilmore 7.5' and the northeastern quarter of the Big Windy Peak 7.5' quadrangles. It builds on generalized surficial mapping of a published, bedrock-focused geologic map by Ruppel and Lopez (1981). This map displays details of Middle to Late Pleistocene and Holocene surficial deposits and landforms, further delineating glacial moraine and alluvial fan sequences, associated terraces, talus slopes and lobes, and landslide deposits. Glacial landform assemblages and modern surficial features are mapped on the basis of topographic, morphometric, and lithologic characteristics, as well as spatial and geomorphic relationships. Field mapping is combined with the use of USGS 10 m digital elevation

maps (DEM), aerial photographs of the Lemhi Range, and satellite/Google Earth imagery to determine landform distribution and relative age relationships between glacial landforms.

1.4 Organization of Thesis

This thesis is henceforth divided into three chapters. Chapter 2 is a standalone chapter that discusses the details of the surficial map, landform interpretations, and relative ages of glacial landforms for the Gilmore and Big Windy Peak 7.5' quadrangles, and is intended for publication as a report accompanying the surficial geologic map. Chapter 3 is a standalone manuscript intended for journal publication with intentional repetition. The manuscript follows a typical journal article format and details mapping strategies, ELA reconstruction, and interpreted paleoclimatic conditions. Chapter 4 is a conclusion chapter that summarizes the geomorphic mapping, ELA correlation, MIS 6-2 glaciation and relative ages of glacial features, and the climatic conditions driving spatial and temporal variability.

References

- Bakke, J., Nesje, A., 2011, Equilibrium-Line Altitude (ELA), *Encyclopedia of Snow, Ice and Glaciers*, 268-277.
- Balco, G., Briner, J., Finkel, R.C., Rayburn, J.A., Ridge, J.C., Schaefer, J.M., 2009, Regional beryllium-10 production rate calibration for late-glacial northeastern North America, *Quaternary Geochronology*, 4, 93-107.
- Benn, D.I., Owen, L.A., Osmaston, H.A., Seltzer, G.O., Porter, S.C., Mark, B., 2005, Reconstruction of equilibrium-line altitudes for tropical and sub-tropical glaciers, *Quaternary International*, 138, 8-21.
- Benn, D.I., Hulton, N., 2010, An Excel™ spreadsheet program for reconstructing the surface profile of former mountain glaciers and ice caps, *Computers & Geosciences*, 605-610.
- Butler, D.R., Sorenson, C.J., Wakefield, D., 1981, Differentiation of morainic deposits based on geomorphic, stratigraphic, palynologic, and pedologic evidence, Lemhi Mountains, Idaho, USA, *INQUA Symposia on the Genesis and Lithology of Quaternary Deposits*, 373-380.
- Butler, D.R., 1984, A late Quaternary chronology of mass wasting for a small valley in the Lemhi Mountains of Idaho, *Northwest Science*, 58.1, 1-13.
- Butler, D.R., 1986, Pinedale deglaciation and subsequent Holocene environmental changes and geomorphic responses in the central Lemhi Mountains, Idaho, USA, *Géographie physique et Quaternaire*, 40.1, 39-46.
- Colman, S.M., Pierce, K.L., 1986, Glacial sequence near McCall, Idaho: Weathering rinds, soil development, morphology, and other relative-age criteria, *Quaternary Research*, 25, 25-42.
- Colman, S.M., Pierce, K.L., 1992, Varied records of early Wisconsinan alpine glaciations in the western United States derived from weathering-rind thicknesses, in Clark, P.U., and Lea, P.D., eds., *The Last Interglacial-Glacial Transition in North America: Boulder, Colorado*, Geological Society of America Special Paper 270, 269-278.
- Darvill, C.M., Bentley, M.J., Stokes, C.R., Hein, A.S., 2015, Extensive MIS 3 glaciation in southernmost Patagonia revealed by cosmogenic nuclide dating of outwash sediments, *Earth and Planetary Science Letters*, 429, 157-169.
- Dort, W., 1962, Multiple glaciation of southern Lemhi Mountains, Idaho: preliminary reconnaissance report, *Tebiwa*, 5.2, 2-17.

- Dort, W., 2003, Multiple Pre-Bull Lake glaciations, eastern side of Lemhi Range, east-central Idaho, *Geological Society of America Abstracts with Programs*, 35.5.
- Dort, W., 2004, Records of multiple Pinedale glacier retreat/readvance pulses, Lemhi Mountains, east-central Idaho, *Geological Society of America Abstracts with Programs*, 36.4.
- Foster, D., Brocklehurst, S.H., Gawthorpe, R.L., 2008, Small valley glaciers and the effectiveness of the glacial buzzsaw in the northern Basin and Range, *Geomorphology*, 624-639.
- Gallup, D. L., 1962, Soil development related to glacial outwash near Gilmore, Idaho, *Tebiwa*, 5.2, 18-22.
- Gosse, J.C., Klein, J., Evenson, E.B., Lawn, B., Middleton, R., 1995, Beryllium-10 dating of the duration and retreat of the last Pinedale glacial sequence, *Science* 268, 1329-1333.
- Hughes, P.D., Gibbard, P.L., Ehlers, J., 2013, Timing of glaciation during the last glacial cycle: evaluating the concept of a global 'Last Glacial Maximum' (LGM), *Earth-Science Reviews*, 125, 171-198.
- Janecke, S.U., 1992, Geologic map of part of the Big Windy Peak and Moffet Springs 7.5' quadrangles, Lemhi and Custer Counties, Idaho, *Idaho Geological Survey Technical Report*, 92-96.
- Johnson, B.G., Thackray, G.D., Van Kirk, R., 2007, The effect of topography, latitude, and lithology on rock glacier distribution in the Lemhi Range, central Idaho, USA, *Geomorphology*, 91.1, 38-50.
- Kaufman, D. S., Porter, S. C., and Gillespie, A. R., 2003, Quaternary alpine glaciation in Alaska, the Pacific Northwest, Sierra Nevada, and Hawaii, in Gillespie, A. R., Porter, S. C., and Atwater, B. F., eds., *The Quaternary Period in the United States: Developments in Quaternary Science: Amsterdam*, Elsevier, 1, 77-103.
- Kenworthy, M.K., Rittenour, T.M., Pierce, J.L., Sutfin, N.A., Sharp, W.D., 2014, Luminescence dating without sand lenses: An application of OSL to coarse-grained alluvial fan deposits of the Lost River Range, Idaho, USA, *Quaternary Geochronology*, 23, 9-25.
- Knoll, K.M., 1977, Chronology of alpine glacier stillstands, east-central Lemhi Range, Idaho, *Idaho State University Museum of Natural History*.
- Laabs, B.J.C., Refsnider, K.A., Munroe, J.S., Mickelson, D.M., Applegate, P.J., Singer, B.S., Caffee, M.W., 2009, Latest Pleistocene glacial chronology of the Uinta

- Mountains: support for moisture-driven asynchrony of the last deglaciation, *Quaternary Science Reviews*, 28, 1171-1187.
- Licciardi, J.M., Clark, P.U., Brook, E.J., Elmore, D., Sharma, P., 2004, Variable responses of western U.S. glaciers during the last deglaciation, *Geology*, 32.1, 81-84.
- Licciardi, J.M., Pierce, K. L., 2008, Cosmogenic exposure-age chronologies of Pinedale and Bull Lake glaciations in greater Yellowstone and Teton Range, USA, *Quaternary Science Reviews*, 27, 814-831.
- Link, P.K., Janecke, S.U., 1999, Geology of east-central Idaho: geologic roadlogs for the Big and Little Lost River, Lemhi, and Salmon River valleys, *Guidebook to the Geology of Eastern Idaho: Idaho Museum of Natural History, Pocatello*, 295-334.
- Lisiecki, L.E., Raymo, M.E., 2005, A Pliocene-Pleistocene stack of 57 globally distributed benthic $\delta^{18}\text{O}$ records, *Paleoceanography*, 20, PA1003, doi:10.1029/2004PA001071.
- Lund, K.I., Evans, K.V., Tysdal, R.G., Winkler, G.R., 2003, Geologic Map of the Eastern Part of the Salmon National Forest, *United States Geological Survey*, 1:100,000.
- Lundeen, K.A., 2001, Refined late Pleistocene glacial chronology for the eastern Sawtooth Mountains, Central Idaho, *M.S. Thesis Idaho State University*, 117.
- Marshall, K.J., 2013, Expanded Late Pleistocene glacial chronology for Western Washington, U.S.A and the Wanaka-Hawea Basin, New Zealand, using luminescence dating of glaciofluvial outwash, *M.S. Thesis Idaho State University*, 357.
- Martinson, D.G., Pisias, N.G., Hays, J.D., Imbrie, J., Moore, T.C., Shackleton, N.S., 1987, Age dating and the orbital theory of the ice ages: Development of a high-resolution 0 to 300,000-year chronostratigraphy, *Quaternary Research*, 27, 1-29.
- Meier, M.F., Post, A.S., 1962, Recent variations in mass net budgets of glaciers in western North America, *IASH Publ*, 58, 63-77.
- Meierding, T.C., 1982, Late Pleistocene glacial equilibrium-line altitudes in the Colorado Front Range: a comparison of methods, *Quaternary Research*, 18.3, 289-310.
- Meyer, G.A., Fawcett, P.J., Locke, W.W., 2004, Late-Pleistocene equilibrium-line altitudes, atmospheric circulation, and timing of mountain glacier advances in the interior northwestern United States, in Haller, K., Wood, S.H., eds., *Geological Field Trips in Southern Idaho, Eastern Oregon, and Northern Nevada: Geological Society of America Field Guide*, 61-66.

- Mix, A.C., Bard, E., Schneider, R., 2001, Environmental processes of the ice age: land, ocean, glaciers (EPILOG), *Quaternary Science Reviews*, 20, 627-657.
- Pellitero, R., Rea, B. R., Spagnolo, M., Bakke, J., Hughes, P., Ivy-Ochs, S., Ribolini, A., 2015, A GIS tool for automatic calculation of glacier equilibrium-line altitudes, *Computers & Geosciences*, 82, 55-62.
- Pierce, K.L., Scott, W.E., 1982, Pleistocene episodes of alluvial gravel deposition, southeastern Idaho. In: Bonnicksen, B., Breckenridge, R.M. (Eds.), *Cenozoic Geology of Idaho, Idaho Bureau of Mines and Geology Bulletin*, 26, 685-702.
- Pisias, N. G., Martinson, D. G., Moore, T. C., Shackleton, N. J., Prell, W., Hays, J., & Boden, G., 1984, High resolution stratigraphic correlation of benthic oxygen isotopic records spanning the last 300,000 years, *Marine Geology*, 56, 119-136.
- Porter, S.C., 1964, Composite Pleistocene snow line of the Olympic Mountains and Cascade Range, Washington, *Geological Society of America Bulletin*, 75, 477-482.
- Porter, S.C., 1975, Equilibrium-line altitudes of late Quaternary glaciers in the Southern Alps, New Zealand, *Quaternary Research*, 5.1, 27-47.
- Porter, S.C., Swanson, T.W., 2008, ³⁶Cl dating of the classic Pleistocene glacial record in the northeastern Cascade Range, Washington, *American Journal of Science*, 308, 130-166, DOI 10.2475/02.2008.02.
- Prism Climate Group, 2015, Average annual precipitation for Idaho 1981-2010, <http://www.prism.oregonstate.edu/gallery/view.php?state=ID>.
- Putnam, A.E., Schaefer, J.M., Denton, G.H., Barrell, D.J., Birkel, S.D., Andersen, B.G., Kaplan, M.R., Finkel, R.C., Schwartz, R., Doughty, A.M., 2013, The Last Glacial Maximum at 44°S documents by a ¹⁰Be moraine chronology at Lake Ohau, Southern Alps of New Zealand, *Quaternary Science Reviews*, 62, 114-141.
- Refsnider, K.A., Laabs, B.C., Plummer, M.A., Mickelson, D.M., Singer, B.S., Caffee, M.W., 2008, Last glacial maximum climate inferences from cosmogenic dating and glacier modeling of the western Uinta ice field, Uinta Mountains, Utah, *Quaternary Research*, 69, 130-144.
- Rother, H., Lehmkuhl, F., Fink, D., Nottebaum, V., 2014, Surface exposure dating reveals MIS-3 maximum in the Khangai Mountains of Mongolia, *Quaternary Research*, 82, 297-308.
- Ruppel, E.T., Lopez, D.A., 1981, Geologic map of the Gilmore quadrangle, Lemhi and Custer counties, Idaho, *United States Geological Survey*, 1:62,500.

- Ruppel, E.T., Lopez, D.A., 1988, Regional geology and mineral deposits in and near the central part of the Lemhi Range, Lemhi County, Idaho, *United States Geological Survey Professional Paper*, No. 1480, 1-122.
- Shulmeister, J., Fink, D., Hyatt, O.M., Thackray, G.D., Rother, H., 2010, Cosmogenic ¹⁰Be and ²⁶Al exposure ages of moraines in the Rakaia Valley, New Zealand and the nature of the last termination in New Zealand glacial systems, *Earth and Planetary Science Letters*, 297.3, 558-566.
- Staley, A.E., 2015, Glacial geomorphology and chronology of the Quinault Valley, Washington, and broader evidence of marine isotope stages 4 and 3 glaciation across northwestern United States, *M.S. Thesis Idaho State University*, 188.
- Thackray, G.D., 1996, Glaciation and neotectonic deformation on the Western Olympic Peninsula, Washington, *Ph.D. Dissertation University of Washington*, 152.
- Thackray, G.D., 2001. Extensive early and middle Wisconsin glaciation on the western Olympic Peninsula, Washington, and the variability of Pacific Moisture delivery to the Pacific Northwest. *Quaternary Research*, 55, 257-270.
- Thackray, G.D., 2004, Late Pleistocene alpine glacier advances in the Sawtooth Mountains, Idaho, USA: Reflections of midlatitude moisture transport at the close of the last glaciation, *Geology*, 32, 225-228.
- Thackray, G.D., 2008, Varied climatic and topographic influences on Late Pleistocene mountain glaciations in the western United States, *Journal of Quaternary Science* 23, 671-681.
- Thackray, G.D., Staley, A.E., *in review*, Fault scarp offsets document extensive MIS 4-3 glaciation in western interior North America, Teton Range, Wyoming, USA, *Quaternary Research*.
- Western Regional Climate Center, 2015, Western United States precipitation map 1961-1990, http://www.wrcc.dri.edu/pcpn/westus_precip.gif.
- Wyshnytzky, C.E., Rittenour, T.M., Nelson, M.S., Thackray, G.D., 2015, Luminescence dating of Late Pleistocene proximal glacial sediments in the Olympic Mountains, Washington, *Quaternary International*, 362, 116-123.

Chapter 2. Surficial Geologic Map of the Gilmore 7.5-Minute Quadrangle and the Northeastern Quarter of the Big Windy Peak 7.5-Minute Quadrangle, Lemhi Range, East-Central Idaho

Abstract

The Gilmore 7.5-minute quadrangle and the northeastern quarter of the Big Windy Peak 7.5-minute quadrangle, located in the central Lemhi Range, east-central Idaho, encompass a series of glacially sculpted valleys along the eastern flank that host well preserved moraine systems. Late Pleistocene to Holocene glacial, alluvial, periglacial, and mass movement features were mapped in this study using detailed field mapping techniques, 1:24,000 USGS topographic maps, aerial photographs, Google Earth and NAIP imagery, and 10 m resolution DEMs in ArcMap 10.3.1. Surficial mapping of glacial features delineates four distinct glacial advances on the bases of spatial positioning and relative dating. These glacial advances are evidenced by mapped Qm1-Qm4 end moraines and coeval Qf1-Qf4 outwash fans. The geomorphic characteristics of the mapped end moraines, including moraine crest angularity, moraine relief, and distal moraine slope steepness, were analyzed semi-quantitatively from transverse profiles to determine the relative age of each mapped moraine system. Assessment of moraine morphology suggests that slope angle, crest angularity, and relief decrease as moraine age increases. The glacial advances are correlated to the Marine Isotope Stages (MIS), reflecting inferred ages of each advance. The glacial advances of the Lemhi Range include: Lemhi Advance 1 (MIS 6), Lemhi Advance 2 (MIS 4-3), Lemhi Advance 3 (MIS 2), and Lemhi Advance 4 (late MIS 2). Glacial recession from terminal positions was punctuated by a series of temporary halts in the final retreat of the glaciers, evidenced by a series of end moraine systems up-valley from the more extensive glacial moraine systems. Glacial recession in the Lemhi Range is inferred to be

completed by 14 ± 0.5 cal ka BP, as determined by radiocarbon dating of organic sediment from a sediment core from Meadow Lake. Since deglaciation, mass wasting and periglacial processes have modified the upland landscape and developed a suite of associated landforms.

2.1 Introduction

The Gilmore and Big Windy Peak 7.5-minute quadrangles are located in the south-central portion of the Lemhi Range, east-central Idaho, about 32 km south of Leadore. The Lemhi Range lies east of the Lost River Range and north of the Eastern Snake River Plain (ESRP) (Figure 2.1). These two quadrangles encompass well preserved evidence of multiple episodes of Pleistocene glaciation (Figure 2.2) and postglacial mass wasting and periglacial processes, Proterozoic to upper Paleozoic sedimentary rocks, and Tertiary igneous intrusions (Figure 2.3). Most notably for this project, these two quadrangles include exquisitely preserved glacial moraine and outwash systems in a high relief mountainous landscape and a low relief range front (Figure 2.2). This surficial geologic map includes the entire Gilmore 7.5-minute quadrangle, and focuses on the northeastern quadrant of the Big Windy Peak 7.5-minute quadrangle, due to previous studies (Dort, 2003) that examined the glacial and outwash sequences exposed at Spring Mountain Canyon. The map also extends slightly into adjoining quadrangles where necessary for complete mapping of the moraine systems.

For many years, it has been generally assumed that mountain glacier systems fluctuated synchronously with the Cordilleran and Laurentide Ice Sheets (e.g., Chadwick et al., 1997; Thackray, 2008), primarily during the Last Glacial Maximum (LGM). While ice sheet fluctuations are well represented in the Marine Isotope Stage (MIS) record of

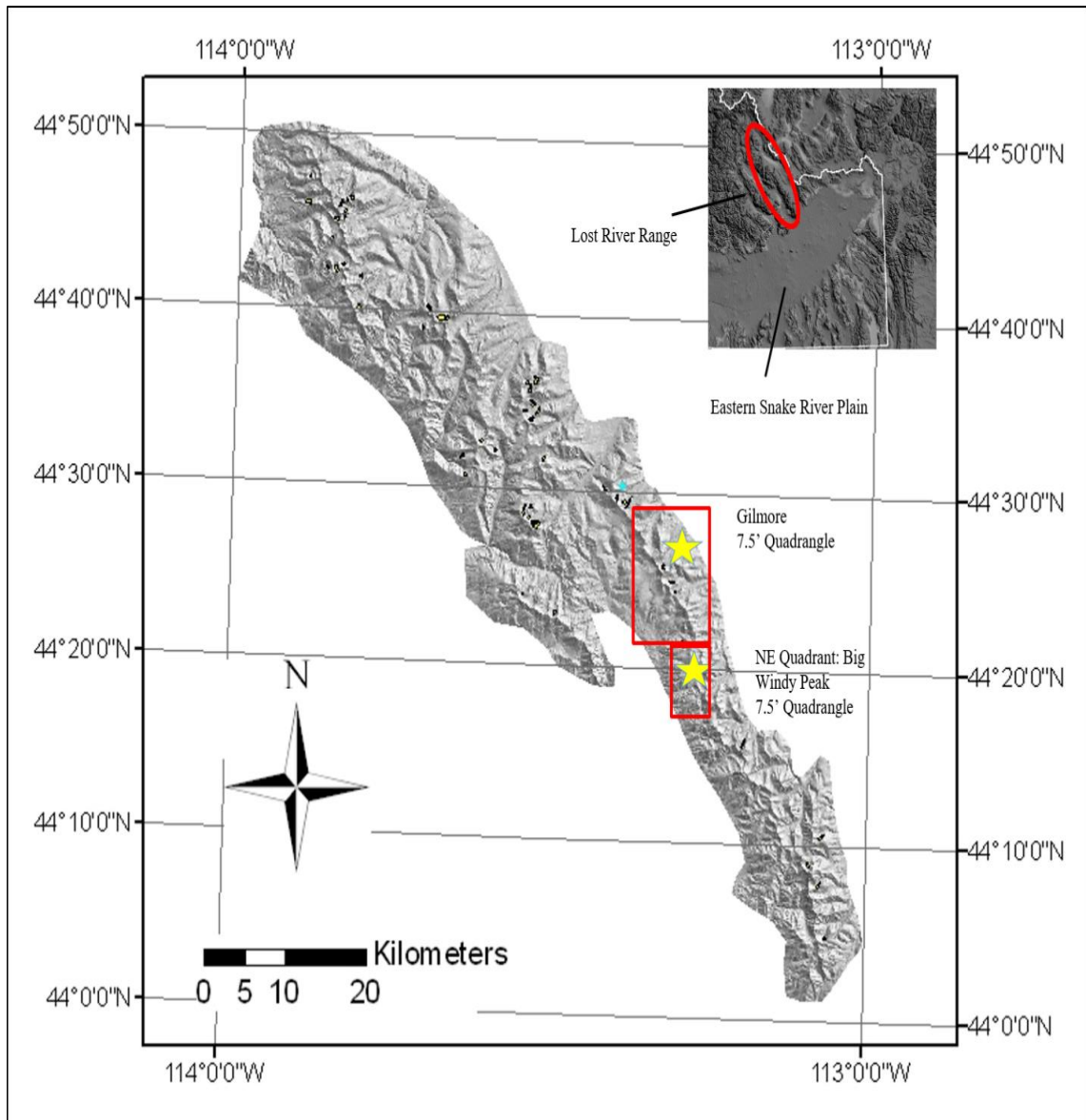


Figure 2.1 Location map of the Gilmore and the northeast quadrant of the Big Windy Peak Quadrangles, Lemhi Range, east-central Idaho, denoted by red bounding boxes. Inset map shows the location of the Lemhi Range in relation to the Eastern Snake River Plain and the Lost River Range. Stars indicate the location of Gilmore and Big Windy Peak, Idaho. Figure modified from Johnson et al. (2007).



Figure 2.2 10 m DEM Slope map of Long Canyon along the eastern flank of the Lemhi Range showing a steeply sloping, high relief, younger, inner moraine and a degraded, shallow sloping, low relief, older, outer moraine, indicative of multiple episodes of Pleistocene glaciation.

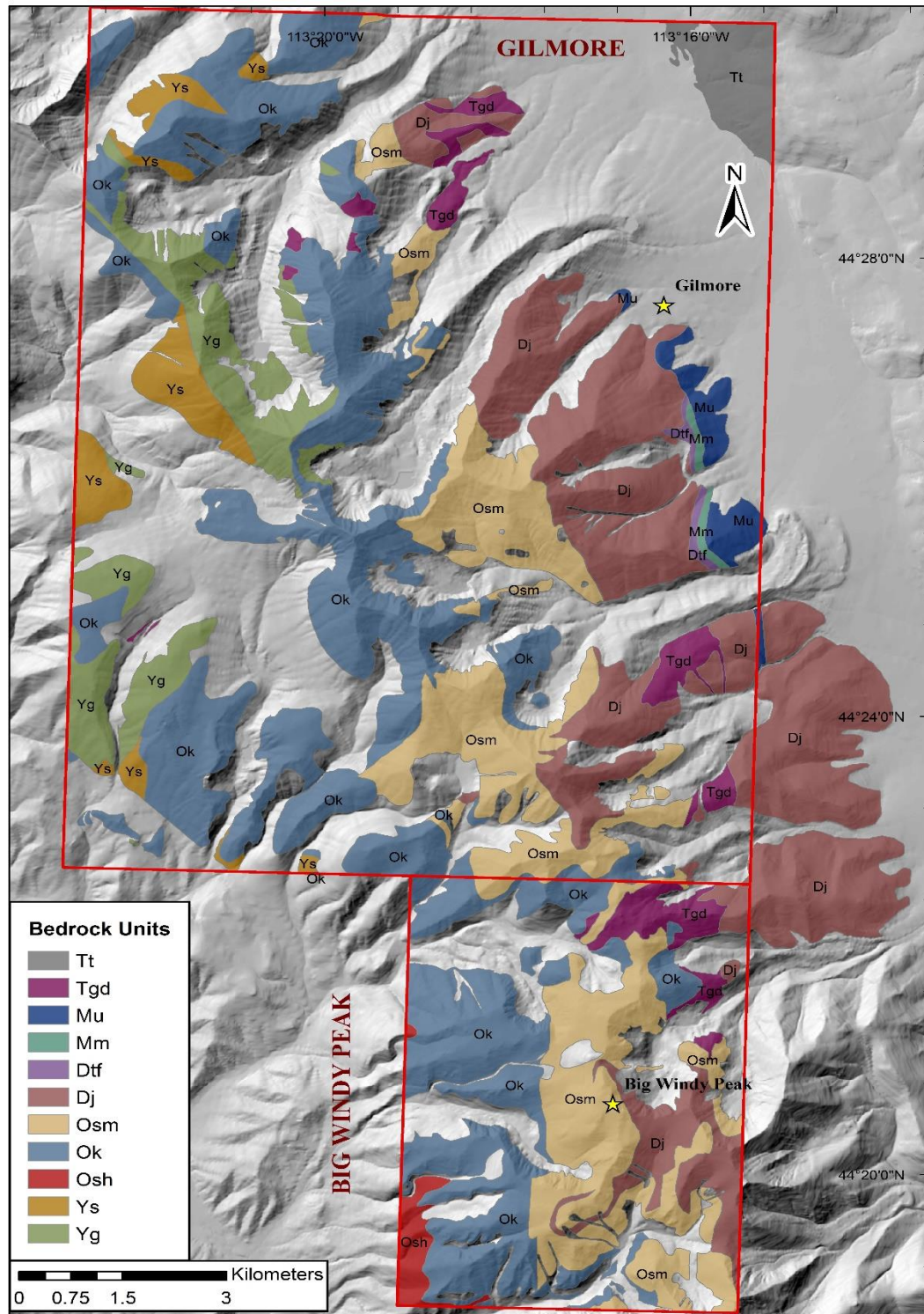


Figure 2.3 Proterozoic to Tertiary-age bedrock units exposed in the Gilmore and northeastern quadrant of the Big Windy Peak 7.5-minute quadrangles. Red bounding boxes and labels delineate the outer limits of the quadrangles and the quadrangle names, respectively. Yellow stars indicate locations of Gilmore and Big Windy Peak, Idaho. Bedrock units mapped by Ruppel and Lopez (1981).

global ice volume (Mix et al., 2001), evidence of pre-LGM ice sheet advances is uncommon in the terrestrial record due to more recent and extensive MIS 2 glaciation. Mountain glacier systems are better suited to preserve pre-LGM glacial and outwash deposits, as they respond to small-magnitude, regional climatic fluctuations.

The Lemhi range was chosen for this project because of the likelihood of preserving pre-LGM moraine systems. The semi-arid, inland environment of the Lemhi Range suggests that the extent and erosional capacity of glaciers was limited during episodes of Pleistocene glaciation (Figure 2.2). Therefore, the range should record and preserve detailed records of regional climatic fluctuations through the Late Pleistocene because landforms of earlier episodes of glaciation have not been removed by later advances (Dort, 1962). Pre-LGM advances may potentially exceed the extent of LGM advances, permitting preservation of those deposits.

The Lemhi Range is geologically and tectonically active, bounded by a NW-trending, SW-dipping normal fault on the western flank. The range has also experienced extensive glaciation during Middle to Late Pleistocene time, with glacial extent, as well as glacial and periglacial erosional capacity, increasing northward along the range (Foster et al., 2008). The central portion of the range was chosen for mapping because of the accessibility to multiple glaciated valleys through dirt roads and mining tracks, and access to proximal vantage points along ridgelines. Mapping within these quads was undertaken to better understand the spatial relationships between glacial landforms, timing of maximum and lesser ice extent within the range, and the climatic conditions driving glaciation. This information can then be combined with other inland mountain

glacier studies to elucidate the climatic conditions of glaciation across the northwestern United States during the Late Pleistocene.

This surficial geologic map of the central Lemhi Range builds upon previous bedrock and surficial mapping across the range (Ruppel and Lopez, 1988; Janecke, 1992), and utilizes aerial photography and National Agriculture Imagery Program (NAIP) scenes, USGS topographic maps (1:24,000), 10 m digital elevation models (DEM), Google Earth imagery, and detailed field observations. This mapping documents the extent of glaciers in the central Lemhi Range through end moraine complexes and recessional glacial features, coupled with coeval outwash fan and terrace sequences. Surficial mapping depicts relative age relationships between surficial landforms, and defines three individual glacial advance sequences, described here as Lemhi Advance 1-4. These advances are hypothesized to correlate to MIS 6 through MIS 2 (Bull Lake to late Pinedale) based on moraine morphometry (i.e., crest angularity, crest width), relief of moraine deposits (i.e., degree of degradation), and the spatial positioning of moraine deposits.

2.2 Geologic Overview

The Lemhi Range is a northwest trending, normal-faulted mountain range located north of the eastern Snake River Plain in east-central Idaho, located within the Cordilleran fold and thrust belt, and in the Basin and Range province. The range is bounded by the Pahsimeroi and Lost River valleys to the west, and the Lemhi and Birch Creek valleys to the east (Link and Janecke, 1999; Johnson et al., 2007).

The strata exposed in the Lemhi Range were deposited in the Mesoproterozoic Belt intracratonic rift basin, and episodically during the late Neoproterozoic through

Paleozoic Cordilleran miogeoclinal phase (Link and Janecke, 1999). The oldest rocks in the Lemhi Range are included in the Middle Proterozoic Yellowjacket Formation, composed of predominantly feldspathic quartzite and siltite, while the youngest rocks are Tertiary conglomerates, composed of angular to subrounded boulders of Kinnikinic Quartzite, Saturday Mountain Formation, and Jefferson Dolomite. Strata within the Lemhi Range were deformed in the Late Cretaceous when the Medicine Lodge thrust moved eastward. (Ruppel and Lopez, 1981, 1988). Extension along numerous normal faults began prior to Middle Eocene Challis volcanism, which generated Tertiary half graben systems (Link and Janecke, 1999). Strata were then intruded during Eocene time by small stocks of monzogranite, granodiorite, quartz monzodiorite, and quartz monzonite (Ruppel and Lopez, 1988). The coarse topography of the Lemhi Range seen today is mainly a result of uplift and erosional processes correlating to normal faulting. These processes allow for the exposure of Proterozoic to upper-Paleozoic sedimentary and meta-sedimentary rocks that were folded and thrust-faulted during the Sevier Orogeny (Lund et al., 2003). The ice-sculpted central part of the Lemhi Range allows for exposure of an underlying geologic framework (Ruppel and Lopez, 1981, 1988).

The Gilmore and Big Windy Peak 7.5-minute quadrangles are located in the east-central portion of the Lemhi Range. Extensive geologic bedrock mapping has been previously conducted in these quadrangles, and is relatively well understood. The mapping patterns reveal the structural, tectonic, and mineral deposition history of the range (Ruppel and Lopez, 1981, 1988). Ruppel and Lopez (1981) constructed a 1:62,500 scale bedrock geologic map of the Gilmore quadrangle, published by the Department of the Interior, United States Geological Survey. It is important to note that this map over

emphasizes the mapping of thrust faults to explain unit contacts and therefore may not exhibit reliable bedrock contacts and fault structures. However, the lithologies and location of contacts provided in this geologic map are assumed to be mostly correct and are used as a basis for this study. Their mapping details Proterozoic to upper-Paleozoic sedimentary and meta-sedimentary rocks and Eocene intrusive rocks, as well as detailed fault mapping and numerous cross-sections. However, minimal detail is provided on Pleistocene glacial and outwash deposits, as well as modern Holocene deposits such as talus and landslides. Surficial mapping has been limited to areas along and adjacent to the Lemhi Fault. Janecke (1992) mapped the portion of the Big Windy Peak quadrangle in the vicinity of the active fault, leading to the conclusion that the Lemhi Fault cuts Latest Pleistocene outwash fan deposits. Glaciation and surficial mapping in the central Lemhi Range has therefore received scant attention.

2.2.1 Description of Bedrock Units

The stratigraphic units pertinent to this thesis are those that are exposed and mapped in the Gilmore and the northeastern quadrant of the Big Windy Peak 7.5-minute quadrangles (Figure 2.3). The bedrock units within the mapping area are of particular importance to the study because cirque headwalls are composed of specific lithologies, which provide the source material for glacial and outwash features, as well as boulders for cosmogenic radionuclide (CRN) dating (Appendix A). The following bedrock unit descriptions are derived from, and are described in further detail by, Ruppel and Lopez (1981, 1988):

Tertiary Volcanic Rocks

- Tt Tuff, Tuffaceous Conglomerate, and Limestone (Pliocene)** – Primarily light gray, friable, vitric, well-sorted tuff in beds as much as 1 m thick. Interbedded with light gray to brown, medium-grained tuff and tuffaceous conglomerate. Exposed only in the northeast corner of the Gilmore quadrangle.
- Tgd Porphyritic Intrusive Rocks (Eocene)** – Primarily medium-light gray, medium-grained, porphyritic granodiorite containing approximately 30 percent quartz, 25 percent potassium feldspar, 35 percent plagioclase feldspar, and 10 percent combined biotite and hornblende. The largest stock is located at Gilmore, intruding rocks mainly of Ordovician and Devonian age. The stock is almost certainly continuous at shallow depth, reaching from Long Canyon to Spring Mountain Canyon.

Paleozoic Sedimentary Rocks

- Mu Limestone Undivided (Upper Mississippian)** – Medium- to dark-gray, thin bedded, cherty limestone that weathers to light-gray to yellow brown. Brecciated by thrust faulting, and metamorphosed to light-gray, crystalline marble adjacent to granodiorite intrusions in Gilmore. Unmetamorphosed rocks are exposed in small outcrops in the east-central portion of the Gilmore quadrangle.
- Mm McGowan Creek Formation (Lower Mississippian)** – Medium- to dark-gray, chippy, siltstone, mudstone, and shale, that is locally carbonaceous. Thin interbeds of dark-gray, crystalline limestone persist throughout. Exposed in relatively thin stratigraphic sections exclusively south of Gilmore.

- Dtf **Three Forks Formation (Upper Devonian)** – Medium-gray, finely crystalline, thin-bedded, platy limestone with locally silty limestone and siltstone interbeds that weather yellowish orange. Exposed in relatively thin stratigraphic sections exclusively south of Gilmore.
- Dj **Jefferson Dolomite (Upper and Middle Devonian)** – Medium- to dark-gray crystalline to sugary, fetid dolomite, including limestones, limestone sedimentary breccia, and sandstones within. Formation is separated into six discrete members (further described by Ruppel and Lopez, 1981, 1988). Exposed as bedrock ridges in relatively thick stratigraphic sections across the eastern segment of the Gilmore and Big Windy Peak quadrangles.
- Osm **Saturday Mountain Formation (Middle Ordovician)** – Medium- to light-gray, finely crystalline, thick-bedded to massive, partly fossiliferous dolomite. Certain beds contain nodules of black chert. Primarily exposed in cirque headwalls as relatively thick stratigraphic sections in the east-central segments of the Gilmore and Big Windy Peak quadrangles.
- Ok **Kinnikinic Quartzite (Middle Ordovician)** – White- to light-gray, fine- to medium grained, vitreous quartzite; composed of greater than 90 percent quartz; dappled with reddish-brown to reddish-orange sandstone cemented by ferrodolomite. Exposed in higher-altitude ridgelines and cirque headwalls in relatively thick stratigraphic sections in the central segment of the Gilmore quadrangle and in the northeast-central segment of the Big Windy Peak quadrangle.

Osh **Summerhouse Formation (Lower Ordovician)** – Sandstone with locally pebbly limestone and quartzite beds. From top to base includes an upper 60 m of pale-red to nearly white *Skolithos*-bearing sandstone underlain by about 50 m of yellowish-brown *Skolithos*-bearing calcareous glauconitic sandstone; 150 m of interbedded pink to white sandstone and quartzite; 25 m of sandy fossiliferous limestone; at the base resides about 20 m of light gray, fine- to very-fine-grained, vitreous quartzite. Located in the southwestern quarter of the northwestern quarter Big Windy Peak quadrangle.

Proterozoic Sedimentary Rocks

Ys **Swauger Formation** – Grayish-pink to pale purple, pale-red-purple, or light-brown to grayish-green, medium coarse-grained, hematitic quartzite. Quartz grains are glassy, well-sorted, and well-rounded. Exposed as moderately thick stratigraphic sequences, forming the west side of major ridgelines in the northwest-central segment of the Gilmore quadrangle, and as isolated patches of bedrock in the western segment,. Also forms the west side of major ridgelines in the northeast quarter of the Big Windy Peak quadrangle.

Yg **Lemhi Group: Gunsight Formation** – Light-brownish-gray and medium-light to purplish-gray and grayish-red purple, fine- to medium-grained, feldspathic quartzite. Feldspar content is typically 20 percent. Deformation present from local soft sediment slumping; cross-laminated; siltstone and argillite bedding partings. Exposed as moderately-thick to thick stratigraphic sections forming cirque headwalls in the north-central segment of the Gilmore quadrangle, and as isolated patches of bedrock in the south-west segment.

2.3 Quaternary Geology Nomenclature and Regional Glacial Overview

2.3.1 Terminology

Stratigraphic nomenclature of mountain glacier sequences across the northwestern United States has been a point of contention, stemming from the use of the same terms in a morpho-, time-, and climate-stratigraphic sense (Evenson et al., 1982). Rocky Mountain terminology has been widely employed to describe deposits of first-order glacial origin, referred to as Pinedale (younger) and Bull Lake (older). Older deposits of glacial origin were recognized as Pre-Bull Lake, indicating greater antiquity (Evenson et al., 1982; Wigley and others, 1978; Evenson and others, 1979; Colman and Pierce, 1986). A more focused nomenclature system (Table 2-1) has been developed by Evenson et al. (1982) in the Pioneer Mountains, Idaho, termed the “Idaho Glacial Model”. Although this model has not been widely used, it is acknowledged here for its correlation to Lemhi Range glaciation. This model recognizes and allocates titles to three distinct periods of glaciation. The three glacial periods are, from youngest to oldest: Potholes glaciation, Copper Basin glaciation, and Pioneer glaciation. This system yields independent, informal stratigraphic units which can then be correlated with local and regional stratigraphic units (Evenson et al., 1982).

The pattern and chronology of Late Pleistocene glacial sequences in the Lemhi Range has received minimal attention. Previous studies in central Idaho (e.g. Schmidt and Mackin, 1970; Colman and Pierce, 1981) briefly described moraine morphometry correlating to Midwestern chronology, such as Wisconsinan or Nebraskan, or have used nomenclature of the Rocky Mountain Glacial Model (Evenson et al., 1982). In the central Lemhi Range, Dort (1962) first mapped and delineated Neoglacial moraine and

mass wasting deposits which he separated into Temple Lake (3000-5000 ka) and Little Ice age (1300-1850) sequences. Temple Lake deposits were mapped in Meadow Lake Creek, Long Canyon, Deer Creek, and Bruce Canyon. Little Ice Age deposits were mapped in these same valleys, as well as Spring Mountain Canyon.

Knoll (1977) documented Holocene and Pleistocene glacial landforms in Meadow Lake Creek (termed Meadow Lake Canyon by Knoll) and Long Canyon in the central Lemhi Range. He describes eighteen moraines in the lower half of Meadow Lake Canyon composed of till and stratified drift and ranging from 100 m to greater than 2.4 km in length. Knoll additionally describes five outwash fans derived from Meadow Lake Canyon that vary in size and slope, and formed at different times, representing at least three separate glaciations. In Long Canyon, Knoll (1977) describes nine moraines in the upper reaches, representing recessional glacier stillstands, and twenty-two moraines in the lower reaches ranging in length from 100 m to 2.3 km. He additionally describes outwash distributed in three major fans associated with different groups of end moraines around the mouth of Long Canyon, Knoll associates the identified glacial features in these canyons with individual glaciations, and their inferred ages, in a series of sketch maps as: Glaciation I (Pre-Bull Lake), Glaciation II (Bull Lake), Glaciation III (Pinedale), and Glaciation IV (Neoglaciation), with Glaciations II and III having multiple defined stadial events.

Fresh end moraines at canyon mouths, at about 7200-7400 feet along the eastern flank of the range, are briefly described and interpreted by Dort (2003) as Pinedale-age features. Dort (2003) also inferred that subdued landforms that lie close in front of fresh end moraines are Bull Lake-age ice-derived features. Where subdued glacial features do

not exist, Dort (2003) suggests that Pinedale ice extended beyond the older Bull Lake ice limits, eradicating the older deposits. Decades later, Dort sampled boulders of Jurassic quartzite from Middle Ridge, which lies approximately 4 km east of the Lemhi Range front in the center of the adjacent basin. The boulders returned ^{10}Be exposure dates of ca. 500-350 ka (uncorrected for erosion), suggesting (but not clearly demonstrating) a pre-Bull Lake ice advance (John Gosse, personal communication, 2015). The depositional record of the episodic retreat phases of Pinedale ice conveys the greatest detail. Lateral and terminal moraines of Pinedale age were formed and preserved because of minimal postglacial runoff erosion (Dort, 2004).

Knoll (1977) and Butler (1984, 1986) have described Neoglacial moraines, rock glaciers, protalus, and talus deposits within Long Canyon and Meadow Lake Creek, as well as Hilltop Valley, based on dendrochronology and relative-age and dating techniques. Knoll (1977) also identified two to three stadials of Bull Lake glaciation and nine stadials of Pinedale glaciation. Evenson et al., (1982) provide a correlation between the Pinedale and Bull Lake glaciations identified by Dort and Knoll to the Potholes and Copper Basin glaciations respectively, using the Idaho Glacial Model (Table 2-1).

Table 2-1 Time stratigraphic glacial chronologies throughout Idaho correlated to the Idaho Glacial Model with Lemhi Range correlation highlighted (red box) signifying key importance to this thesis. Figure from Evenson et al., (1982).

IDAHO GLACIAL MODEL	STANLEY BASIN WILLIAMS, 1961	BEAR VALLEY SCHMIDT AND MACKIN, 1970	LEMHI MOUNTAINS KNOLL, 1977	LONG VALLEY SCHMIDT & MACKIN, 1970; COLMAN & PIERCE, 1981
	NEOGLACIAL		GANNETT PEAK NEOGLACIAL TEMPLE LAKE	NEOGLACIAL
POTHOLES GLACIATION	PINEDALE	PINEDALE	PINEDALE LATE MIDDLE LAKE	PINEDALE 20,000 YRS INTERMEDIATE 60,000 YRS
COPPER BASIN GLACIATION	BULL LAKE LATE EARLY	BULL LAKE	BULL LAKE LATE EARLY	BULL LAKE 140,000 YRS
PIONEER GLACIATION	PRE-BULL LAKE		SACAGAWEA RIDGE	PRE-BULL LAKE

2.3.2 Western Wyoming and Central Idaho Glaciation

Mountain glacier systems have demonstrated sensitive behavior to both long-term and short-term climatic fluctuations, assimilating variations in regional temperature and precipitation. Chronological data have been extracted from mountain glacier systems to elucidate paleoclimatic conditions. The glacial sequences exposed in the Sawtooth Mountains, central Idaho, the Lost River Range, central Idaho, and the Teton Range, western Wyoming, have been well examined from a geomorphic and chronological standpoint (Thackray, 2004; Kenworthy et al., 2014; Licciardi and Pierce, 2008; Thackray and Staley, in review), allowing the timing of maximum ice extent to be well understood. The close proximity of the Lemhi Range to these ranges suggests similar glacial and climatic patterns.

The Sawtooth Mountains, located in central Idaho, experienced extensive glaciation following the LGM (17,000 – 16,000 cal yr BP) and during early-late-glacial time (ca. 14,000 – 13,000 cal yr BP) (Thackray et al., 2004). Thackray and others (2004) applied surficial geologic mapping, relative weathering assessment of glacial landforms, analysis of sediment cores, and radiocarbon dating to moraine sequences in the Sawtooth Mountains. These techniques revealed that the extensive mountain glacier advances responded strongly to enhanced winter precipitation and westerly flow from moist Pacific air masses following the LGM.

The Lost River Range (LRR) is located within the northeastern Basin and Range Province in east-central Idaho. Kenworthy and others (2014) applied optically stimulated luminescence (OSL) dating to alluvial fans along the western flank of the LRR, which are typically composed of pebble- to cobble-sized sheetflood gravels with sandy matrices, lacking identifiable sand lenses. OSL age assessments for these deposits identify six periods of fan aggradation, ranging from 4 to 120 ka.

The Teton Range is located in the northeastern Basin and Range province in western Wyoming, and has evolved through extensive Pleistocene glaciation. Licciardi and Pierce (2008) focused on the greater Yellowstone glacial system, which formed the largest coalesced Pleistocene mountain glacier complex in the western United States. Sixty-nine ^{10}Be surface exposure ages were obtained from boulders on moraines deposited by glaciers of the greater Yellowstone glacial system and the Teton Range (Licciardi and Pierce, 2008). The Yellowstone glacial system consisted of an ice-cap fed by glaciers from higher mountain areas. Prior to ice-cap formation, Pinedale glaciers grew in the adjacent mountains (e.g., Teton Range, Beartooth Mountains, and Absaroka

Mountains). The results obtained from the Teton Range mountain glacier system are best suited for comparison to the Lemhi Range. Licciardi and Pierce (2008) obtained twenty-four boulder and two bedrock exposure ages from Pinedale moraines and surfaces associated with the prominent valley glacier that flowed down Cascade Canyon and terminated at Jenny Lake. Ten boulders from the outermost set of end moraines at Jenny Lake yield a mean age of 15.9 ± 0.9 ^{10}Be ka and eight boulders from the inner set of Jenny Lake end moraines yield an average age of 14.7 ± 1.1 ^{10}Be ka (Licciardi and Pierce, 2008, with ages recalculated using the Heyman et al. (2014) production rates by J. Licciardi). Ages derived from the Jenny Lake moraine complex also constrain the ages of Pinedale deposits of the southern Jackson Hole outlet lobe of the greater Yellowstone glacial system. The Teton Range has also developed through the influence of Quaternary faulting. Thackray and Staley (in review) measured the vertical offset for 15 scarp locations along the Teton Fault cutting glacial landforms, using bare-Earth LiDAR from the Teton Conservation District (2008) and EarthScope Intermountain Seismic Belt LiDAR Project (2008), to determine fault offset rates and age estimates for older glacial landforms. Late Pleistocene glacial and outwash landforms are offset by scarps 11.2-37.6 m high. Scarps that cut the deglacial surface are ca. 11.2 to 13.5 m high. Assuming a range-front deglaciation occurred uniformly along the range front (ca. 15 ka) (Licciardi and Pierce, 2008), Thackray and Staley (in review) calculate an offset rate of 0.80 m/ka and use this offset rate to estimate ages for the older range-front landforms to be 17-48 ka. These data suggest that MIS 2 and MIS 3 glaciation influenced the Teton Range and likely other inland mountain ranges across the northwestern United States.

2.4 Methods

2.4.1 Mapping Glacial and Outwash Landforms

Surficial mapping relied on satellite and digital terrain data interpretation, along with field investigation that took place between July 2nd and October 9th, 2015. Field mapping followed techniques described by Hyatt and Shulmeister (2013) and was executed using USGS topographic maps of 1:24,000 scale. Field mapping was based on detailed field observations of landform relationships, which reveal relative age relationships. Relative age relationships (or relative dating) are based on the premise that weathering and erosion parameters are time dependent and therefore can be used to distinguish episodes of deposition (Burke and Birkeland, 1979). The parameters utilized for relative dating and identification between individual glacial units in the Lemhi Range include moraine morphology (number and freshness of ice disintegration hollows, preservation of original moraine form, and degree of degradation and secondary dissection), extent of glaciation down-valley and on valley sides (older moraine deposits are located beyond the extent of younger moraine deposits), and outwash fan and outwash terrace relationships with moraines (Evenson et al., 1982). In addition to these qualitative parameters, transverse profiles (perpendicular to moraine crests) were generated in ArcGIS 10.3.1 and surveyed to compare crest angularity, relief, and the degree of degradation, providing a semi-quantitative perspective on the relative ages of the glacial units. Additional surficial landforms such as mass wasting deposits and alluvial features, are mapped based on their morphology and depositional processes.

Surficial mapping in the Lemhi Range requires extensive exploration and investigation of the range. Dense vegetation obstructs glacial landforms, making

delineation of glacial sequences difficult, which limits the effective use of satellite imagery and aerial photography. In addition, treacherous slopes and wildlife hindered navigation to particular areas within the field site. With the absence of bare-Earth LiDAR DEMs in this portion of the Lemhi Range (which would improve mapping detail by removing vegetation and delineating small landforms), aerial photographs and Google Earth imagery were used in conjunction with NAIP imagery and 10 m resolution DEMs in ArcMap 10.3.1 to refine and aid field mapping techniques and observations. Four major glacial advances are identified for the Lemhi Range, based on surficial mapping and the above mentioned relative dating techniques, and are correlated to MIS and Pinedale/Bull Lake-age nomenclature.

2.5 Results

2.5.1 Surficial Geologic Map of the Gilmore 7.5-Minute Quadrangle and the Northeastern Quarter of the Big Windy Peak 7.5-Minute Quadrangle, Lemhi Range, East-Central Idaho

Ice flowed down many valleys in the central Lemhi Range, with ice extending beyond the eastern range-front at Deer Creek, Meadow Lake Creek, Long Canyon, and Spring Mountain Canyon. These low-gradient valley mouths provide well preserved evidence of multiple episodes of glaciation. Identification of glacial moraine and outwash sequences are based on clear geomorphic relationships. Sharp, broad (0.1-0.4 km wide), arcuate, high and low relief landforms with identifiable crests mantled with boulders are identified as end moraine complexes and indicate distinct ice marginal positions (Figure 2.4). Hummocky landforms, referred to in this study as dead ice landforms, are nested within Qm3 end moraines and were constructed as the ice margin fluctuated and ice blocks detached from the main toe of the glacier (Figure 2.5).

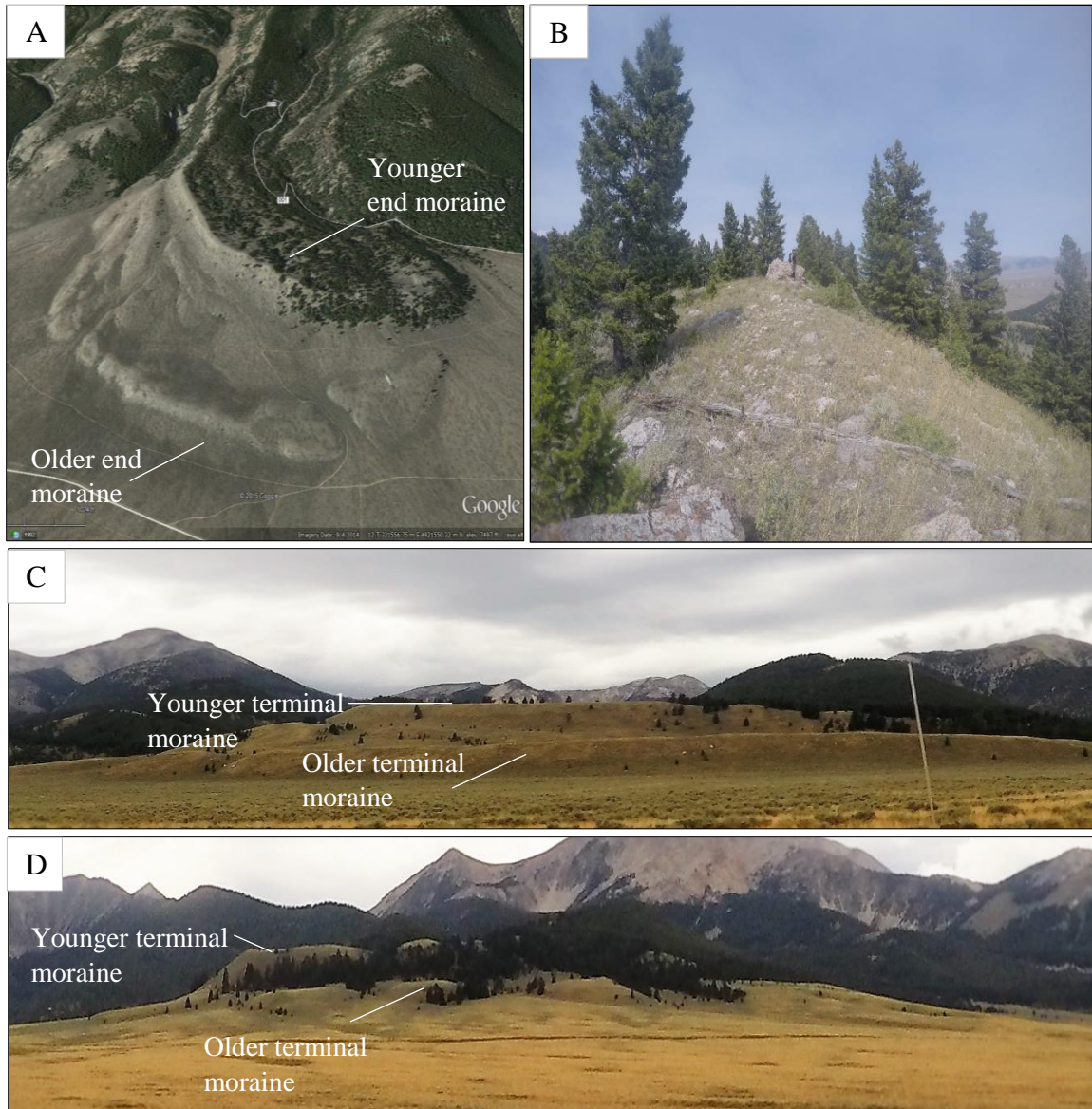


Figure 2.4 Prominent crests of moraine sequences at (A) Long Canyon, (B) Lemhi Union Gulch, and (C) Meadow Lake Creek, Lemhi Range, Idaho. (A) Google Earth (2015) satellite imagery depicting the broad arcuate nature of both older and younger end moraine complexes at Long Canyon. (B) Field photo of a sharp terminal moraine crest riddled with Osm and Dj boulders at Lemhi Union Gulch. (C) Range front photo of Long Canyon and (D) Meadow Lake Creek depicting older, low elevation, and low relief terminal moraines and younger, high elevation, high relief terminal moraines. Each moraine sequence marks a separate ice terminal position.



Figure 2.5 Field photograph of Spring Mountain Canyon depicting the hummocky dead ice landform within Qm3 moraines.

End moraines of individual advances are spatially separated by ca. 0.3-0.6 km of flat, gently sloping, coeval outwash fan surfaces. These outwash fan surfaces are composed of moderately sorted, silt- to boulder-sized sediment and grade up-valley to end moraines, indicating deposition from glacial meltwater streams. Older moraine sequences at Deer Creek, Meadow Lake Creek, Long Canyon, and Spring Mountain Canyon are neighbored by older outwash fan remnants that lie at higher elevations than the surrounding, younger outwash fan surface. In valleys such as Deer Creek, moraines of individual advances merge (with no outwash fan surfaces between them), and are only differentiated by the degree of degradation of their arcuate crests.

Pleistocene glacial and outwash landforms, which include end moraines and outwash fans, are assigned to a Lemhi Advance term to identify glacial advance sequences (Plate 1). For example, Lemhi Advance 1 is the earliest Quaternary advance for which evidence remains, and is evidenced by Qm1 (end moraine 1) and Qf1 (outwash fan 1) map units. This nomenclature repeats for Lemhi Advance 2-4. Retreat phase landforms are discussed on an individual basis.

2.5.2 Description of Map Units

Holocene Non-Glacial Landforms

Postglacial Alluvial Deposits and Landforms

- Qfp **Active flood plain** – Flat, level, vegetated plain composed of fine-grained sand and silt that borders the active Texas Creek stream channel located in the northeast corner of the Gilmore quadrangle. The active flood plain in the Gilmore quadrangle is approximately 3 km in length and is susceptible to inundation at high flow by slow moving overbank waters.
- Qal **Alluvium** – Unconsolidated, clastic material subaerially deposited by running water, dominated by gravel, sand, silt, and clay, with variable amounts of cobbles and boulders. Commonly includes channelized deposits of streams incised into bedrock. Locally includes alluvial plains, assemblages of active and abandoned channels forming low gradient broad, flat, regional ramps along the western flanks of the range.
- Qt8 **Alluvial terrace 8** – Youngest alluvial terrace, including modern terraces within alluvial deposits in the western portion of Gilmore quadrangle. They are flat-topped remnants of constructional valley floors thickly mantled with alluvium in

stream valleys that flank and parallel active or abandoned stream channels. They are dominantly composed of silt with moderate amounts of sand and pebbles.

Boulders and cobbles are sparse, and lithologies are consistent with bedrock units on the western portion of the Gilmore quadrangle.

Mass Movement Deposits and Landforms

- Qc **Colluvium** – Unconsolidated, unsorted earth material deposited, or in the act of being transported, on side slopes, and at the base of slopes in valleys by gravitational force and by local, concentrated runoff. Composed of silt- to boulder sized-sediment, dominated by pebble- to boulder-sized sediment.
- Qls **Landslide deposits** – Rotational slumps and translational slides of blocky bedrock, boulders, pebbles, sand, and silt of varying lithologies. Clasts are angular to subangular, unsorted, and unstratified. Commonly occurring as slumps composed of single lithologic units. Landslides are locally marked by steep unvegetated slopes, tilted or toppled trees, head scarps, planar or concave-upward failure surfaces, subsided material at the head of the slide, and accumulated rock and/or soil at the toe of the slide, generating a lobate deposit.
- Qtc **Talus cones** – Steeply sloping, cone-shaped accumulation of angular to subangular debris at the base of a hillslope or escarpment that heads in a narrow ravine. Deposits are typically loose and unsorted to poorly sorted. Talus cones are typically derived from, and are therefore composed of, single lithologic units that have accumulated by convergent topography channelizing episodic rockfalls, and topples. Cones of accumulated material occasionally spread across or along valley floors.

- Qts Talus slopes** – Steeply sloping accumulation of angular to subangular boulders, cobbles, pebbles, and gravel lying at the base of very steep rock slopes. Broader and more continuous than talus cones. Deposits are typically loose and unsorted to poorly sorted. Talus slopes are typically derived from, and are therefore composed of, single lithologic units that have accumulated chiefly by incremental block-by-block failure, falling, toppling or sliding. Deposits typically terminate at the base of hillslopes and do not extend across valley bottoms.
- Qdf Debris Flows** – Deposits of rapid, downslope movements or collapses of detached, unconsolidated rock and sediment. Deposits range from silt- to boulder-sized sediment. They commonly originate in cirque headwalls, convex ridgelines/hilltops, and side slopes. They commonly occur due to saturation of hillslopes and are characterized by narrow channels, spreading of material at the toe of the mass movement, and toppled trees.

Periglacial Landforms

- Qtl Protalus lobes** – Arcuate, lobate accumulations of angular to subangular boulders, cobbles, and pebbles, located beyond the outer limit of talus cones. Deposits are typically loose and poorly to moderately sorted. Protalus lobes are inferred to develop in response to slow incremental permafrost creep of single lithologic talus combined with minimal slope wash. Commonly form where rock glaciers are absent, though most rock glaciers are associated with protalus lobes (Johnson et al. et al., 2007). They are more prominent on north-west facing slopes, although exist locally on north-east facing slopes.

Qrg **Rock Glacier** – Masses of poorly sorted, angular to subangular boulders, cobbles, pebbles, gravel, and occasional fine material, marked by transverse, arcuate ridges that indicate slow movement, with the fastest movement along the longitudinal axis. They are typically around 0.5 km in length. Exist locally in high elevation cirque headwalls at Meadow Lake Creek and Ridgeway Mine valleys.

Mid-Late Pleistocene Glacial Landforms

End Moraines

Qm1 **End moraine 1** – Oldest and smallest end moraine in the Lemhi glacial sequence and categorized as representative of Lemhi Advance 1. Broad-crested, arcuate, shallow gradient, low relief moraine, exclusively exposed at Deer Creek as the outermost ice limit. Unconsolidated deposits predominantly composed of silt with common sand and pebbles. Boulders and cobbles moderately abundant to scarce. Clasts are subangular and poorly sorted. Clast lithologies are dominated by Osm, Dj, and Yg, with moderately abundant amounts of Ok. No boulders meet specifications for sampling on this moraine. No evidence of blockfields exist within this moraine.

Qm2 **End moraine 2** – Second oldest end moraine in the Lemhi glacial sequence and categorized as representative of Lemhi Advance 2. Moderately sharp- to broad-crested, gently sloping, low relief moraine exposed as ridge remnants in the landscape, following the arcuate trend of Qm3, at Meadow Lake Creek and Long Canyon. Exposed as a continuous, arcuate, degraded ridge at Deer Creek and as lateral moraine remnants at Lemhi Union Gulch and Spring Mountain canyon. Unconsolidated deposits predominantly composed of silt with common sand and

pebbles. Boulders and cobbles are abundant to moderately abundant. Clasts are subangular and poorly sorted. The maximum boulder size is about 2 m long, 1.5 m wide, and 2.5 m tall. Boulders exhibit moderately common spalling, lichen cover and jointing, with glacial polish being rare. The lithologies of clasts include Tgd, Dj, Osm, Ok, and Yg. Ok clasts are dominant, with moderate amounts of Osm and Dj, at Meadow Lake Creek and Long Canyon. Yg, Ok, and Dj clasts are in nearly equal proportions at Deer Creek. No evidence of blockfields exist within this moraine sequence. Lemhi Advance 2 sequences at Deer Creek, Meadow Lake Creek, and Long Canyon extend beyond the range-front.

Qm3 End moraine 3 – Third oldest end moraine in the Lemhi glacial sequence, representing Lemhi Advance 3. Exposed at Deer Creek, Meadow Lake Creek, Long Canyon, west side of Long Canyon ridgeline divide, Spring Mountain Canyon, Ridgeway Mine, Silver Moon Gulch, Lemhi Union Gulch, and Bruce Canyon. Sharp-crested, arcuate, steeply sloping, high relief end moraine complex. Unconsolidated deposits predominantly composed of silt with common sand and pebbles. Boulders and cobbles are abundant to moderately abundant. Clasts are subangular and poorly sorted. The maximum boulder size is about 2.5 m long, 1.5 m wide, and 2 m tall. Boulders exhibit moderately frequent spalling, lichen cover and jointing, with glacial polish being rare. The lithologies of clasts include Tgd, Dj, Osm, Ok, and Yg. Lemhi Advance 3 sequences at Deer Creek, Meadow Lake Creek, Long Canyon, and Spring Mountain Canyon extend beyond the range-front and into the Lemhi Valley. Ok clasts are dominant in Meadow Lake Creek and Long Canyon. Yg, Ok, and Dj clasts are in nearly equal proportions at Deer

Creek. Osm, Dj, and Tgd clasts are dominant in Spring Mountain Canyon. Lemhi Advance 3 sequences at Ridgeway Mine, Silver Moon Gulch, Lemhi Union Gulch, and Bruce Canyon are less extensive and reside at higher elevations in the landscape. Ok clasts are dominant on the Ridgeway Mine moraines and the northern moraine of Bruce Canyon. Dj clasts are dominant on the Silver Moon Gulch moraine. Osm and Dj clasts are dominant on the Lemhi Union Gulch moraines. Tgd boulders are dominant on the southern moraine of Bruce Canyon. Lemhi Advance 3 sequences at Ridgeway Mine, Meadow Lake Creek, and Bruce Canyon exhibit blockfields/felsenmeer that mark the termini and lateral portions of moraines. Blockfields are predominantly composed of Ok with uncommon volcanics and are of possible periglacial origin.

Qm3 Moraine Talus 3 – Steeply sloping accumulation of angular to subangular boulders, cobbles, pebbles, and gravel, locally occurring along the terminal and lateral portions of Qm3 moraines and on Qf3 outwash fan surfaces at Deer Creek, Ridgeway Mine, Meadow Lake Creek, and Bruce Canyon. Deposits are typically composed predominantly of Kinnikinic Quartzite and are loose and unsorted to poorly sorted. These deposits are of possible periglacial origin, and are termed “blockfields” or “felsenmeer”, or are of supra-glacial rockfall origin.

Qm4 End moraine 4 – Fourth oldest end moraine in the Lemhi glacial sequence, representing Lemhi Advance 4. Sharp-crested, arcuate, steeply sloping, high relief end moraine complex, exclusively exposed at Spring Mountain Canyon and Bruce Canyon. Additionally, Qm4 end moraine complexes are exposed as linear ridges up-valley of Qm3 end moraine complexes at Deer Creek, Ridgeway Mine,

Meadow Lake Creek, Silver Moon Gulch, Long Canyon, and Lemhi Union Gulch as a result of subsequent retreat from the prior terminal position. Lemhi Advance 4 moraine sequences lie in the upper to lower reaches of the valleys, but do not extend beyond the range-front. Sharp crested, arcuate, steeply sloping moraine terminus. Unconsolidated deposits predominantly composed of silt with common sand and pebbles. Boulders and cobbles are abundant to moderately abundant. Clasts are subangular and poorly sorted. The maximum boulder size is 3 m long, 1 m wide, and 1 m tall. Boulders exhibit moderately frequent spalling, lichen cover and jointing. Excessive jointing occurs in Tgd boulders at Spring Mountain Canyon, glacial polish is rare and clasts are predominantly Tgd with moderately abundant amounts of Osm and Dj, and minimal amounts of Ok. The Qm4 end moraines complexes exposed as linear features up-valley contain lithologies that contrast between valleys and are consistent with lithologies present on terminal moraine sequences (see terminal moraine descriptions). No evidence of blockfields.

Qm5 End moraine 5 – Fifth oldest end moraine in the glacial sequence. Moderately sharp- to broad-crested, shallow gradient, low relief, linear ridgelines located up-valley of Qm4 end moraines at Deer Creek, Meadow Lake Creek, Long Canyon, and Spring Mountain Canyon. Unconsolidated deposits predominantly composed of silt with common sand and pebbles. Boulders and cobbles are moderately abundant, with boulders that are greater than 1 m tall being rare. Clasts are subangular and poorly sorted. Lithologies contrast between valleys and are consistent with lithologies present on terminal moraine sequences (see terminal

moraine descriptions). Interpreted to have been constructed during a temporary halt in the final retreat of the glaciers, indicating a period of equilibration.

Qm6 End moraine 6 – Sixth oldest end moraine in the glacial sequence. Moderately sharp- to broad-crested, gently sloping, low relief, linear ridgelines located up-valley of Qm5 end moraines at Deer Creek, Meadow Lake Creek, Long Canyon, and Spring Mountain Canyon. Constructed by multiple lobes of ice at Deer Creek and Spring Mountain Canyon. Unconsolidated deposits predominantly composed of silt with common sand and pebbles. Boulders and cobbles are moderately abundant, with boulders greater than 1 m tall being scarce. Clasts are subangular and poorly sorted. Qm6 at Meadow Lake Creek is composed of talus containing abundant boulders and cobbles. Lithologies contrast between valleys and are consistent with lithologies present on terminal moraine sequences (see terminal moraine descriptions). Interpreted to have been constructed during a temporary halt in the final retreat of the glaciers, indicating a period of equilibration.

Qm7 End moraine 7 – The youngest of the end moraine complexes. Moderately sharp- to broad-crested, shallow gradient, low relief, linear ridgelines located up-valley of Qm6 end moraines at Deer Creek and Long Canyon; constructed by multiple lobes of ice at Deer Creek and Spring Mountain Canyon. Exposed as an end moraine complex with an identifiable terminus in the center cirque headwall of Long Canyon. Unconsolidated deposits predominantly composed of silt with common sand and pebbles. Talus containing abundant boulders and cobbles is moderately abundant. Clasts are subangular and poorly sorted. Lithologies contrast between valleys and are consistent with lithologies present on terminal

moraine sequences (see terminal moraine descriptions). Interpreted to have been constructed during a temporary halt in the final retreat of the glacier, or as a re-advance of the ice front during a period of overall recession, indicating a period of equilibration.

Dead Ice Features

- Qdl Dead ice landforms** – Hummocky landforms (depressions and mounds/ridges) nested within the ice limits of Qm1 at Deer Creek, Qm2 at Deer Creek, Qm3 at Deer Creek, Meadow Lake Creek, Long Canyon, Lemhi Union Gulch, and Spring Mountain Canyon, and Qm4 at Spring Mountain Canyon end moraine complexes. These features formed from melting of large, detached ice blocks of stagnant ice. The landform characteristics are similar to those of the terminal moraine ice limit in which the dead ice landform lies within (see terminal moraine unit descriptions).
- Qgu Undifferentiated glacial landforms** – Extensive, low relief landforms having uneven or undulating surfaces composing the beds of glaciated valleys, and are exposed in each glaciated valley. Unconsolidated deposits predominantly composed of silt with common sand and pebbles. Boulders and cobbles are abundant. Clasts are subangular and poorly sorted. Deposited by processes including basal lodgment and release from downwasting stagnant ice by ablation. (May also be classified as ground moraine or ablation moraine).

Mid-Late Pleistocene Outwash Landforms

Outwash Fans

- Qf1 **Outwash fan 1** – Oldest outwash fan deposit, coeval with Qm1, and exclusively exposed at Deer Creek. Broad, flat, down-valley sloping, gently sloping, ridge remnant exposed in the landscape. The sediment is unconsolidated, moderately to well sorted, dominantly composed of silt, sand, and gravel, with moderately abundant cobbles and boulders. The maximum boulder size is about 0.5 m long, 0.5 m wide, and 0.5 m tall. Clasts are subangular to subrounded. Lithologies present and the distribution of lithologies vary between valleys and are similar to those of Qm1 (see Qm1 unit description).
- Qf2 **Outwash fan 2** – Second oldest outwash fan deposit, coeval with Qm2, and exposed at Deer Creek, Meadow Lake Creek, Long Canyon, and Spring Mountain Canyon. Broad, flat, gently sloping, fan-shaped surface exposed as fan-shaped remnants in the landscape sloping down-valley, either connected to or detached from a coeval moraine or a younger end moraine. The sediment is unconsolidated, moderately to well sorted, dominantly composed of silt, sand, and gravel, with moderately abundant cobbles and boulders. The maximum boulder size is about 2.5 m long, 2 m wide, and 2 m tall. Lithologies present and the distribution of lithologies vary between valleys and are similar to those of Qm2 (see Qm2 unit description).
- Qf3 **Outwash fan 3** – Third oldest and most extensive outwash fan deposit, coeval with Qm3, and exposed in every mapped valley and along the entire eastern range-front. Broad, flat, fan-shaped surface that gently slopes down-valley. This

fan is exposed as a low relief surface meandering through higher elevation remnants of Qf1 and Qf2 due to incision of older outwash fan surfaces, and grades into Qm3 terminal moraine sequences. The sediment is unconsolidated, moderately to well sorted, dominantly composed of silt, sand, and gravel, with moderately abundant cobbles and boulders. The maximum boulder size is about 2 m long, 1 m wide, and 1.5 m tall. Lithologies present and the distribution of lithologies vary between valleys and are similar to those of Qm3 (see Qm3 unit description). Blockfields, or talus deposits, of Ok with few intermixed volcanics are exposed in Qf3 at Bruce Canyon near the terminus of the northern Qm3 end moraine.

- Qf4 **Outwash fan 4** – Youngest outwash fan deposit, coeval with Qm4, and exposed at Bruce Canyon and Spring Mountain Canyon. Broad, flat, fan-shaped surface that gently slopes down-valley at Bruce Canyon. This fan exhibits a ridge-like shape, as it is compressed by the northern canyon bedrock wall and the northern outside portion of Qm3 at Spring Mountain Canyon. The sediment is unconsolidated, dominantly composed of silt, sand, and gravel, with moderately abundant cobbles and boulders. The maximum boulder size is 1 m long, 1 m wide, and 1 m tall. Lithologies present and the distribution of lithologies vary between valleys and are similar to those of Qm4 (see Qm4 unit description).

Alluvial Terraces

- Qt4 **Alluvial terrace 4** – Oldest alluvial terraces. Terraces are graded to coeval Qm4 end moraines and occupy fluvial cuts in older Qm3 moraines. They are flat-topped remnants of constructional valley floors mantled with alluvium in stream

valleys that flank and parallel active or abandoned stream channels. They originally formed at a previous stream level and are exposed at Meadow Lake Creek, Silver Moon Gulch, Long Canyon, Bruce Canyon, and Spring Mountain Canyon. The sediment is unconsolidated, well sorted, and dominantly composed of silt with moderately common sand and pebbles. Boulders and cobbles are sparse. The lithologies present are consistent with end moraines and outwash fans in corresponding valleys.

Qt5 Alluvial terrace 5 – Alluvial terraces that grade to a coeval Qm5 moraine and occupy fluvial cuts in older Qm4 moraines. They are flat-topped remnants of constructional valley floors mantled with alluvium in stream valleys that flank and parallel active or abandoned stream channels. They are exposed at Meadow Lake Creek, Long Canyon, and Spring Mountain Canyon. The sediment is unconsolidated, well sorted, and dominantly composed of silt with moderately common sand and pebbles. Boulders and cobbles are sparse. The lithologies present are consistent with end moraines and outwash fans in corresponding valleys.

Qt6 Alluvial terrace 6 – Alluvial terraces that grade to a coeval Qm6 moraine and occupy fluvial cuts in older Qm5 moraines. They are flat-topped remnants of constructional valley floors mantled with alluvium in stream valleys that flank active or abandoned stream channels. They are exposed at Meadow Lake Creek, Long Canyon, and Spring Mountain Canyon. The sediment is unconsolidated, well sorted, and dominantly composed of silt with moderately common sand and

pebbles. Boulders and cobbles are sparse. The lithologies present are consistent with end moraines and outwash fans in corresponding valleys.

Qt7 Alluvial terrace 7 – Youngest Pleistocene alluvial terrace formed within the Qgu deposit at Spring Mountain Canyon cirque headwall. This terrace is a flat-topped remnant of constructional valley fill mantled with alluvium in a stream valley that flanks and parallels an abandoned stream channel. The sediment is unconsolidated, well sorted, and dominantly composed of silt with moderately common sand and pebbles. Boulders and cobbles are sparse. The lithologies present are consistent with the undifferentiated glacial material and talus deposits at Spring Mountain Canyon.

2.6 Interpretation of Map Units

Figure 2.6A and Figure 2.6B (Plate 1) depict the mapped surficial geologic units of the Gilmore and northeastern quarter of the Big windy Peak 7.5-minute quadrangles, as well as the names of the major glaciated valleys and their associated moraine sequences. Relative age relationships between landforms, deduced from surficial mapping, are used to correlate the timing and extent of glaciation between valleys, revealing the glacial history of the central Lemhi Range. Valleys in the Lemhi Range preserve evidence of multiple advances, although this evidence is less well preserved in the steeper, small valleys. Glacial advances are correlated with the Pinedale and Bull Lake nomenclature described by Dort (2003) and provisionally the Marine Isotope Stages (Martinson et al., 1987). Cosmogenic radionuclide ages will provide a reconnaissance chronology that will be used to support the established relative age relationships.

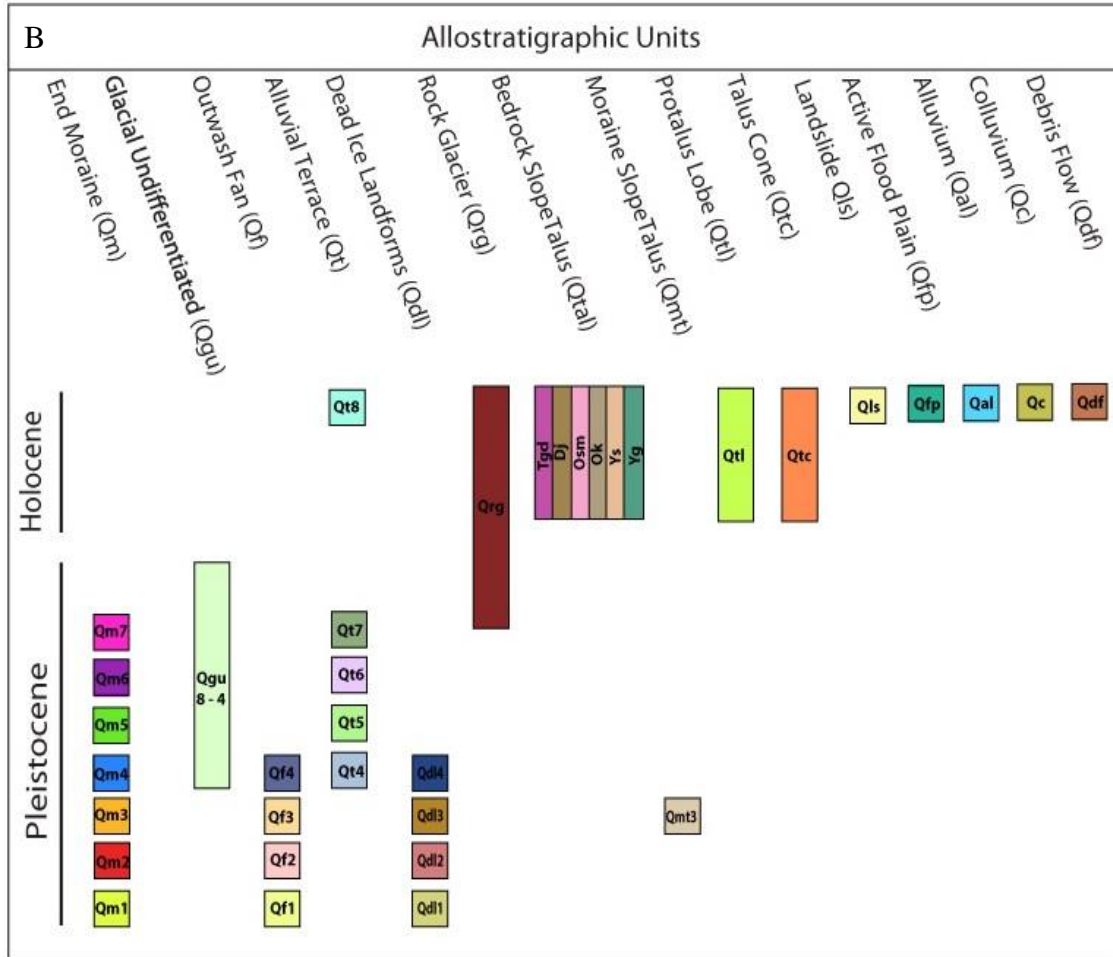


Figure 2.6B Correlation of surficial map units, depicted in Figure 2.6A, show the relationship between the mapped surficial features type and relative ages.

Details regarding the background of cosmogenic radionuclide dating, sampling strategies, sample preparation, and the status of collected samples are discussed in Appendix A.

2.6.1 Timing of Glacial Events

The timing of glacial advance in the Lemhi Range is inferred from surficial mapping of late Pleistocene glacial features and semi-quantitative analysis of moraine morphology. These techniques assess the spatial positioning of glacial features, as well as moraine crest angularity, relief, distal slope angles, and overall degree of degradation.

Four major glacial advances are identified in the Lemhi Range and are given inferred ages relative to the Marine Isotope Stages based on the applied relative dating techniques. Figure 2.13, which depicts the correlation of glacial advances with their inferred ages, is located at the end of this section.

Lemhi Advance 1

Lemhi Advance 1 advance is evidenced by mapped Qm1 and Qf1 landforms in the central Lemhi Range and is the most extensive ice advance at Deer Creek, located in the northern portion of the Gilmore quadrangle, with landforms exclusively preserved there (Figure 2.7). There, Lemhi Advance 1 is represented by a small area and low relief Qm1 end moraine with a spatially related Qf1 outwash fan lying 5-10 m above the adjacent, younger Qf3 fan. No chronological evidence was extracted from landforms of Lemhi Advance 1, so a numerical age was not determined. Surficial mapping shows that Qm1 is older than the up-valley Qm2 end moraine of Deer Creek (Figure 2.6A) (Plate 1). The Qm1 longitudinal profile (Figure 2.8A) shows a moderately broad terminal crest that peaks at ca. 2190 meters above sea level (masl), with the toe of the moraine at ca. 2175 masl (relief of 15 m), and a distal slope of ca. 0.2 (ca. 11°). The broad crest, and low slope and relief provide evidence for a high degree of degradation of the Qm1 end moraine. Therefore, the landforms representing Lemhi Advance 1 indicate an older glacial sequence.

Bull Lake age moraines have been previously identified across the intercontinental United States in both a qualitative and quantitative manner. Chadwick (1997) described fifteen Bull Lake moraines in the Wind River Range (WRR), Wyoming, using relative age criteria and described the moraines as having low relief and shallow

slopes. Additionally, Phillips (1997) measured ^{36}Cl ages for boulders in Bull Lake complexes in the WRR. Both Chadwick (1997) and Phillips (1997) determined ages of Bull Lake moraines to be ca. 130-95 ^{36}Cl ka, correlative with MIS 6-5b. Based on the degree of degradation, shallow slopes, and low relief observed in the Lemhi Range and WRR, I infer that Lemhi Advance 1 correlates to MIS 6 and Glaciation II (Bull Lake-age) described by Knoll (1977).

Lemhi Advance 2

Lemhi Advance 2 is evidenced by the mapped Qm2 and Qf2 landforms and represents the second most extensive ice advance at Deer Creek. However, this advance either extended over landforms representing Lemhi Advance 1 in some valleys or advanced into area in which Qm1 and Qf1 had been eroded, making Lemhi Advance 2 the most extensive advance with preserved evidence at Meadow Lake Creek and Long Canyon (Figure 2.7) (Figure 2.9-2.11). In addition, lateral remnants of Qm2 and Qf2 fan remnants are exposed at Lemhi Union Gulch and Spring Mountain Canyon (Figure 2.6A). Landforms of Lemhi Advance 2 include Qf2 fan remnants, isolated by ca. 20 m of incision from the younger Qf3 outwash fan sequence, and reside at similar elevations between valleys of ca. 2200 – 2300 masl. Surficial mapping shows that landforms representing Lemhi Advance 2 are located up-valley from the landforms representing Lemhi Advance 1. Morphological characteristics of Qm2 termini, extracted from Qm2 longitudinal profiles (Figure 2.8A, B, C), provide semi-quantitative evidence for a younger glacial advance.

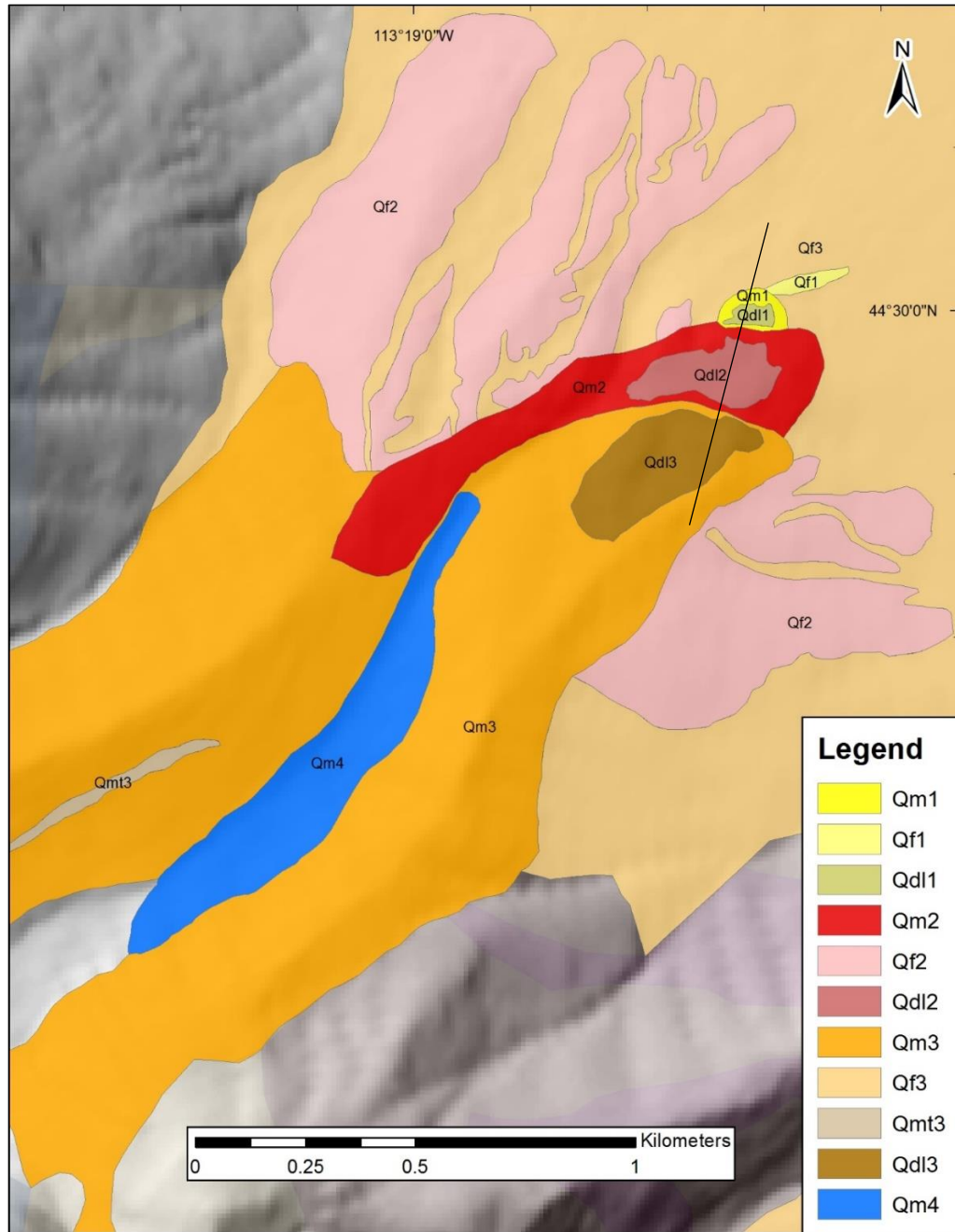


Figure 2.7 10 m hillshade DEM depicting the mapped glacial moraine and outwash features associated with Lemhi Advance 1-4 at Deer Creek. Black line denotes the location of the transverse moraine profile in Figure 2.8A.

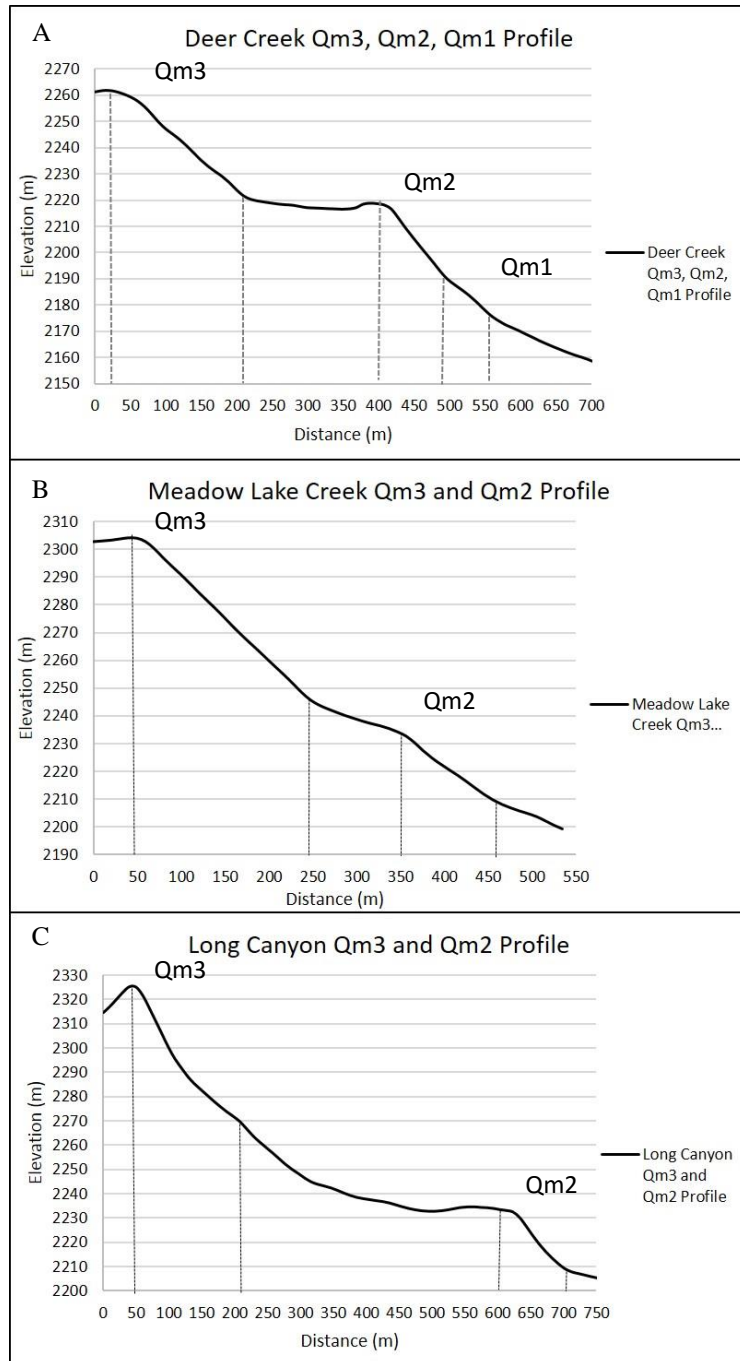


Figure 2.8 A) Deer Creek longitudinal profile depicting the relief and crest sharpness of the Qm3, Qm2, and Qm1 end moraines. B) Meadow Lake Creek end moraine profiles depicting relief and crest sharpness of Qm3 and Qm2 end moraines. C) Long Canyon end moraine profiles depicting relief and crest sharpness of Qm3 and Qm2 end moraines. Gray dashed lines indicate the approximate horizontal extent of the end moraines (from crest to toe). Slope is inferred from the change in elevation divided by the change in distance (from crest to toe). Deer Creek and Meadow Lake Creek profiles were extracted from the exposed terminal moraines, while the Long Canyon profile was extracted from the exposed lateral moraines.

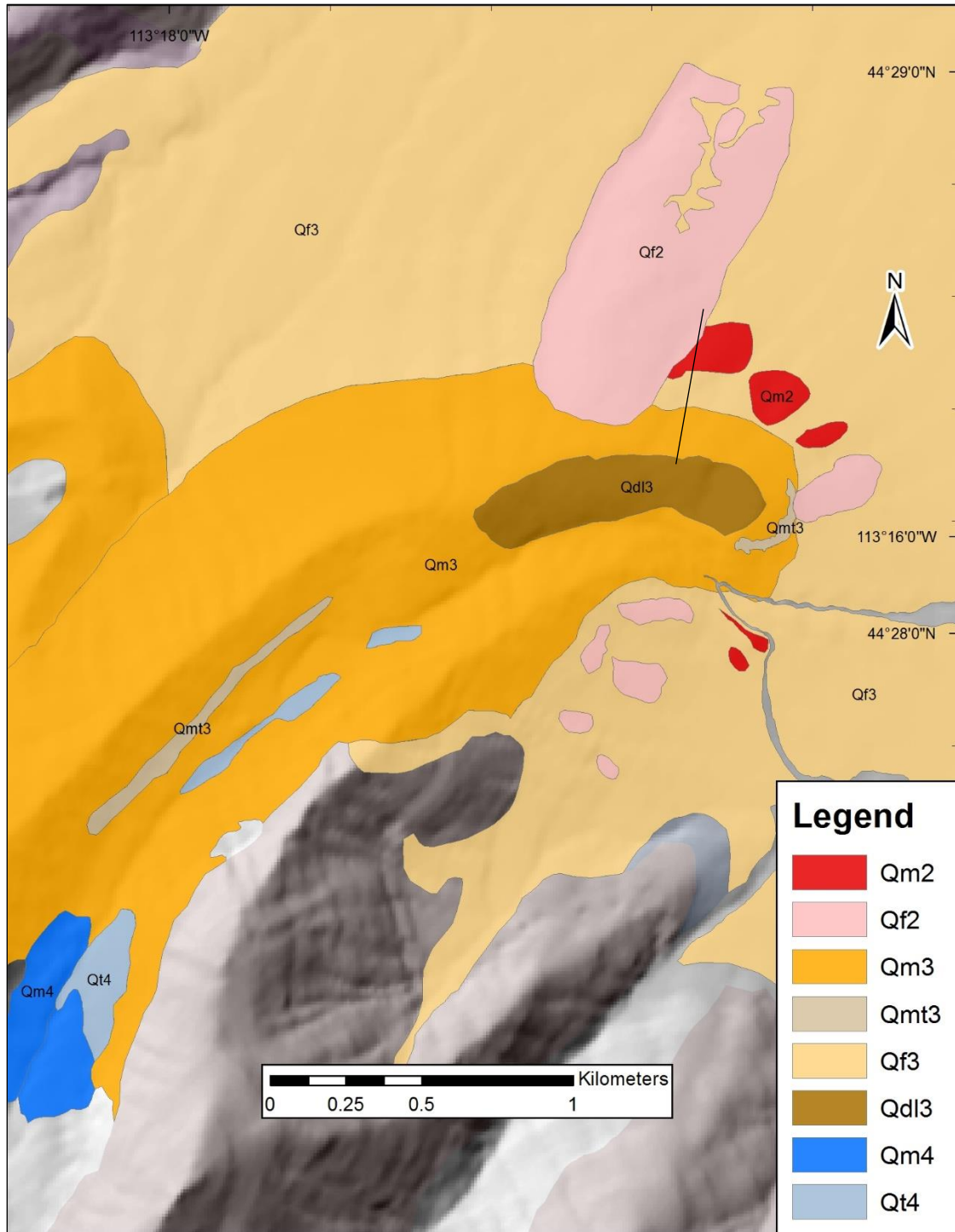


Figure 2.9 10 m hillshade DEM depicting the mapped glacial moraine, glacial outwash, and alluvial features associated with Lemhi Advance 1-4 at Meadow Lake Creek. Black line denotes the location of the transverse moraine profile in Figure 2.8B

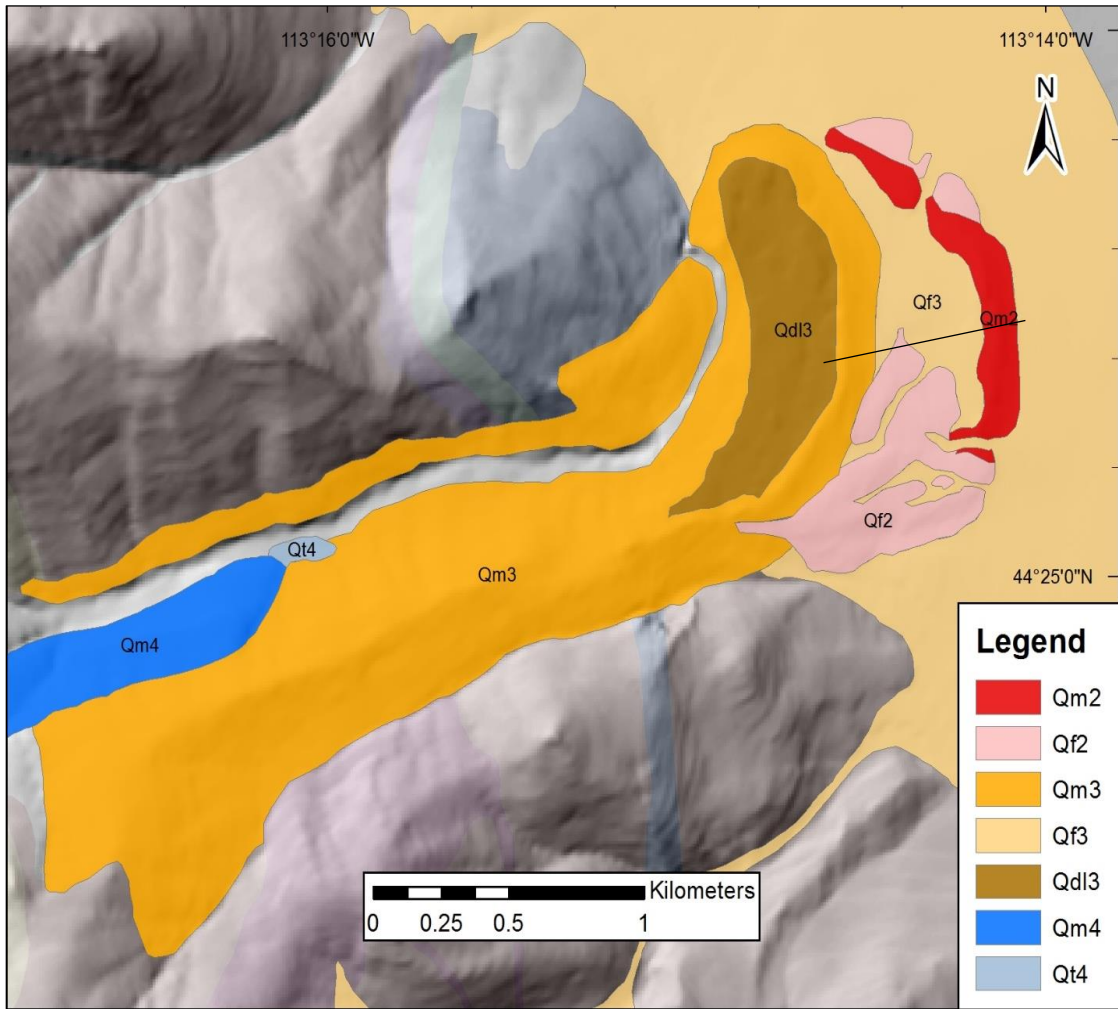


Figure 2.10 10 m hillshade DEM depicting the mapped glacial moraine, glacial outwash, and alluvial features associated with Lemhi Advance 1-4 at Long Canyon. Black line denotes the location of the transverse moraine profile in Figure 2.8C

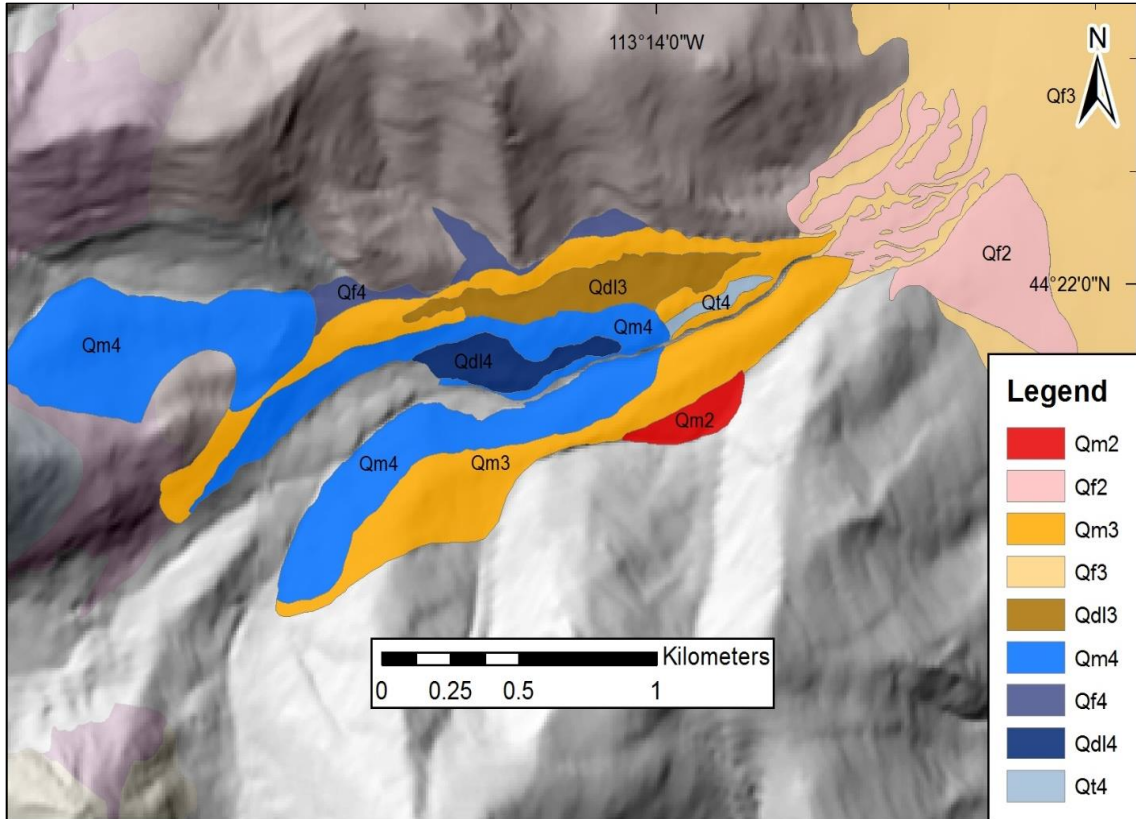


Figure 2.11 10 m hillshade DEM depicting the mapped glacial moraine, glacial outwash, and alluvial features associated with Lemhi Advance 1-4 at Spring Mountain Canyon.

Lemhi Advance 2 – Spatial Comparison of Landforms Between Valleys

Lemhi Advance 2 at Deer Creek exposes a cohesive, intact Qm2 end moraine that exhibits an arcuate shape. Qm2 contains dead ice landforms within the terminus of the moraine. Qf2 fan remnants form linear, fan-shaped features with prominent ridgelines that extend towards the valley and grade to Qm2 moraines (Figure 2.7). Lemhi Advance 2 at Meadow Lake Creek is evidenced by Qm2 end moraine and Qf2 fan remnants. Qm2 remnants parallel the arcuate trend of Qm3 (Figure 2.9), and Qf2 remnants are similar to those of Deer Creek. The landform representing Lemhi Advance 2 at Silver Moon Gulch is exposed as a small, intact Qm2 end moraine, with no evidence of Qf2 fan remnants. The Qm2 deposit and associated trimlines can be faintly traced up-valley to the cirque

headwall (Figure 2.6A). Lemhi Advance 2 at Long Canyon is represented by a well preserved, nearly continuous Qm2 end moraine remnant and Qf2 fan remnants in the landscape (Figure 2.10). The Qm2 moraine remnant parallels the arcuate trend of Qm3. Qf2 remnants are similar to those of Deer Creek. Lemhi Advance 2 at Spring Mountain Canyon and Lemhi Union Gulch is represented by a single lateral Qm2 moraine remnant in each valley, outside of the younger Qm3 lateral moraine. Qf2 fan remnants persist in the landscape near the range-front (exclusively at Spring Mountain Canyon). Qf2 remnants are similar to those of Deer Creek (Figure 2.11).

These relationships imply that ice lobes formed in the high elevation cirques of these valleys. Multiple ice lobes coalesced in Deer Creek, Long Canyon, and Spring Mountain Canyon, while a single ice lobe formed in Meadow Lake Creek, Silver Moon Gulch, and Lemhi Union Gulch. As ice flowed east-northeast down the eastern valleys of the central Lemhi Range, Qm2 and Qf2 were created simultaneously when the glaciers reached an equilibrium state at or near their maximum extent. Recessional glacier features, representing Lemhi Advance 2, are nonexistent due to later glacial advances covering or eroding older features up-valley. Later glacial advances (i.e., Lemhi Advance 3) initiated erosion and meltwater incision of older landforms representing the Lemhi Advance 2 advance, leaving remnants of these landforms perched in the surrounding landscape.

Lemhi Advance 2 – Morphological Comparisons of Moraines Between Valleys

The morphology of the Qm2 end moraine at Deer Creek (Figure 2.8A) shows a moderately sharp crest that peaks at ca. 2,220 masl, with the toe of the moraine at ca. 2,190 masl (relief of ca. 30 m), and a distal slope of ca. 0.33 (ca. 18°). This Qm2 end

moraine exhibits a higher relief, sharper crest, and a similar slope to that of the Qm1 moraine, indicating a younger glacial advance. The morphology of the Qm2 end moraine at Meadow Lake Creek (Figure 2.8B) shows a moderately broad crest that peaks at ca. 2,235 masl, with the toe of the moraine at ca. 2,210 masl (relief of 25 m), and a distal slope of ca. 0.25 (ca. 14°). This Qm2 moraine exhibits a similar relief, crest angularity, and a slightly steeper slope relative to the Qm1 moraine. These similar characteristics may contradict the spatial patterns and be indicative of a similar age/glacial advance. The morphology of the Qm2 end moraine at Long Canyon (Figure 2.8C) shows a sharp crested moraine that peaks at ca. 2,235 masl, with the toe of the moraine at ca. 2,210 masl (relief of 25 m), and a distal slope of 0.25 (ca. 14°). This Qm2 moraine, though measured in the lateral moraine rather than the terminal moraine, exhibits a sharper crest, higher relief, and a steeper slope angle relative to the Qm1 moraine. These morphologic characteristics of Qm2 end moraines provide evidence for a glacial advance that is younger than Lemhi Advance 1 based on the lower degree of degradation, more abundant exposure, and up-valley location relative to Lemhi Advance 1 representative landforms. However, the similar characteristics between Qm1 at Deer Creek and Qm2 at Meadow Lake Creek may be indicative of a similar age. Throughout these valleys, the spatial separation of these landforms from the landforms representing Lemhi Advance 3 are not well understood, with Lemhi Advance 2 landforms potentially being buried, or slope angles being altered, by deposition of Lemhi Advance 3 associated landforms.

Lemhi Advance 2 – Regional Comparison

The relative age criteria and morphology of the Qm2 moraines can be compared to previous regional studies to further elucidate the relative timing of Lemhi Advance 2.

The general morphology of Qm2 moraines in the study area is degraded, with broad to moderately sharp crests and shallow to moderately shallow distal slopes. Lundeen (2001) used moraine morphometry, in which crest width, proximal slope, distal slope, and crest angularity were measured to determine the relative age of moraines in the Pettit Lake, Yellow Belly Lake, and Hell Roaring Lake valleys in the Sawtooth Mountains. Lundeen (2001) determined that crest width showed an age trend in Pettit Lake valley, with crest width decreasing with decreasing age. In addition, it was determined that crest angularity decreases with increasing moraine age in all three valleys. Moraines were grouped into an older, low-angularity group and a younger, high-angularity group. The morphology of these moraines are described by Lundeen (2001) as fresh with angular crests, steep slopes, and thin soils, consistent with regional descriptions of MIS 3-2 age moraines in the Pioneers (Evenson et al., 1982) and McCall (Colman and Pierce, 1986). Conversely, Bull Lake deposits in these areas have been described as more subdued and dissected, lacking kettles, and having well developed soils. The Qm2 end moraines described here do not exhibit the steep slopes and angular crests, as described in previous studies, thus indicating greater antiquity. Based on the spatial mapping, general morphology, and regional comparisons of moraine morphology, I infer that Lemhi Advance 2 is of MIS 4-3 age relating to Glaciation III (Middle Pinedale age), with the Qm2 moraine at Meadow Lake Creek being of possible MIS 6 age relating to Glaciation II (Bull Lake) described by Knoll (1977).

Lemhi Advance 3

Lemhi Advance 3 is evidenced by Qm3 and Qf3 mapped landforms and represents the third most extensive ice advance in the central Lemhi Range. Landforms

representing Lemhi Advance 3 are exposed at Deer Creek, Ridgeway Mine, Meadow Lake Creek, Silver Moon Gulch, Long Canyon, Lemhi Union Gulch, Bruce Canyon, and Spring Mountain Canyon (Figure 2.6A) (Figure 2.9-2.11). This includes nearly all of the eastern range-front valleys, indicating extensive glaciation during this time. Qm3 end moraines extend to, or beyond, the range-front at Deer Creek, Meadow Lake Creek, Long Canyon, and Spring Mountain Canyon, residing at similar elevations (ca. 2200 – 2300 masl). Qm3 end moraines are also located at higher elevations in the smaller valleys of Ridgeway Mine, Silver Moon Gulch, Lemhi Union Gulch, and Bruce Canyon, residing at similar elevations (ca. 2400 – 2500 masl). Qm3 end moraine complexes are composed of extensive, intact, sharp crested terminal and lateral moraines. Qf3 is exposed as a single, continuous outwash fan unit across the eastern range-front that grades to all Qm3 moraines and dissects older glacial and outwash features.

Lemhi Advance 3 – Spatial Comparison of Landforms Between Valleys

The up-valley location of Qm3 relative to Qm2 and Qf2 and the lower elevation of Qf3 relative to Qf2 indicate that landforms of Lemhi Advance 2 are older than those of Lemhi Advance 3. Lemhi Advance 3 landforms contrast between large and small valleys. Advances in the larger valleys (i.e., Deer Creek, Meadow Lake Creek, Long Canyon, and Spring Mountain Canyon) develop from larger, and in some cases multiple, ice tributaries on the east-northeast-facing slopes of the high peaks that receive minimal insolation (Figure 2.12). This engenders greater accumulation, in the form of precipitation and

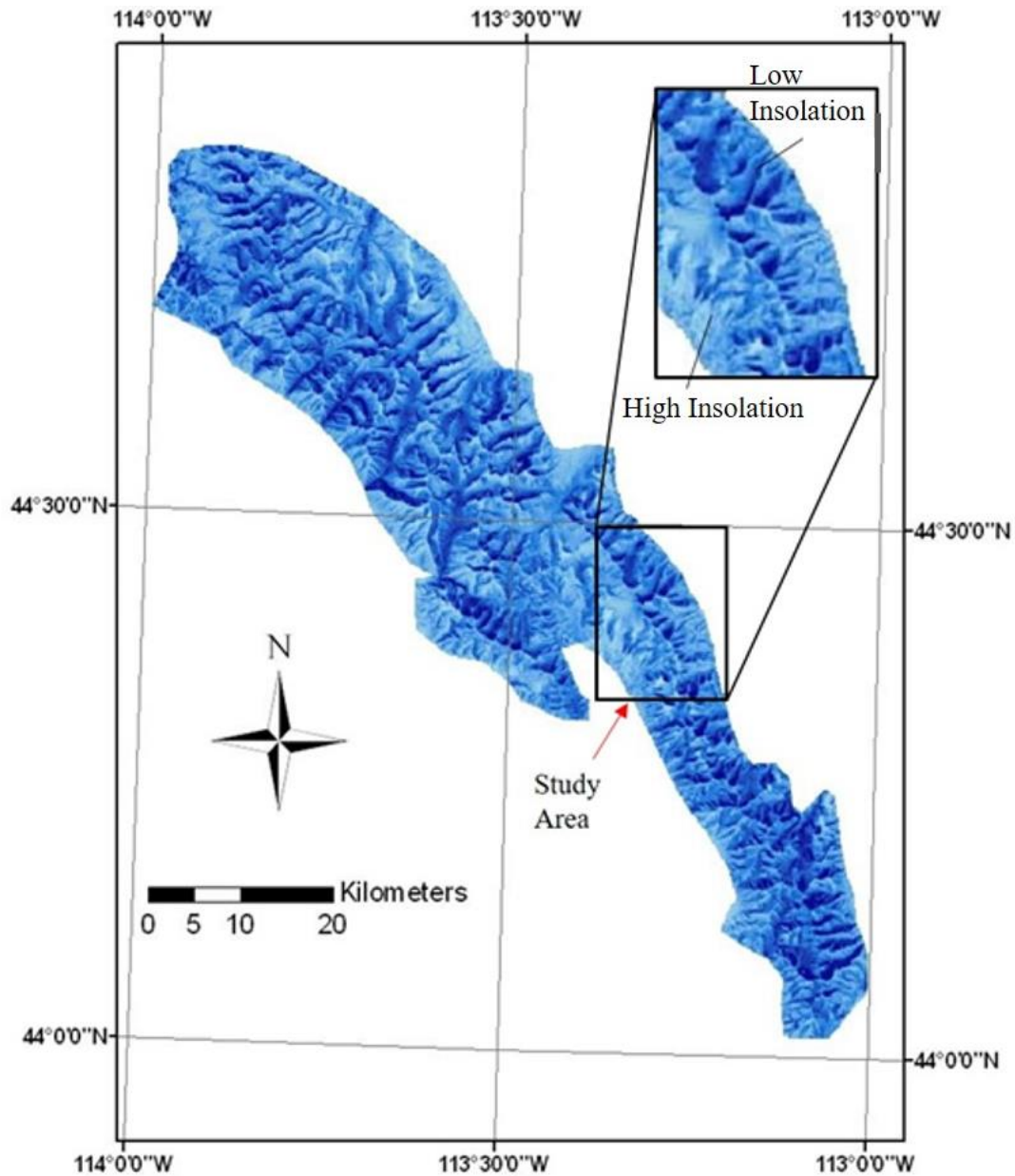


Figure 2.12 Hillshade image of the Lemhi Range depicting the influence of aspect, relief, and slope on solar insolation. Dark blues represent areas of low duration of insolation. Light blues represent areas of high duration insolation. Figure is based on modern insolation values. Inset map focuses on the slopes of the Gilmore and Big Windy Peak quadrangles. It is important to note that Figure 2.13 is based on modern insolation values. These values could have potentially been different during the Middle-Late Pleistocene due to orbital variations influencing insolation maxima and minima. However, the relative values are likely to be similar due to strong topographic influence, which is assumed to be similar. Figure modified from Johnson et al. (2007).

wind-blown snow, and evasion of sun exposure, maintaining colder temperatures, with these factors together yielding more extensive advances. Glaciers at Ridgeway Mine, Silver Moon Gulch, Lemhi Union Gulch, and Bruce Canyon also originate on the flanks of cold, east-northeast-facing slopes, but have carved smaller cirque headwalls at lower elevations east of the divide. The differences of cirque headwall elevation and glacier morphology contribute to variability in the equilibrium-line altitudes (ELAs) across the central Lemhi Range (Chapter 3).

Lemhi Advance 3 – Morphological Comparisons of Moraines Between Valleys

Geomorphic relationships of Qm3 end moraines provide evidence for the relative age of Lemhi Advance 3. The morphology of the Qm3 end moraine at Deer Creek (Figure 2.8A) shows a sharp crest that peaks at ca. 2,260 masl, with the toe of the moraine at ca. 2,220 masl (relief of ca. 40 m), and a distal slope of ca. 0.5 (ca. 27°). The morphology of the Qm3 end moraine at Meadow Lake Creek (Figure 2.8B) shows a sharp crest that peaks at ca. 2,305 masl, with the toe of the moraine at ca. 2,245 masl (relief of ca. 60 m), and a distal slope of ca. 0.4 (ca. 22°). The morphology of the Qm3 end moraine at Long Canyon (Figure 2.8C) shows a sharp crest, with the lateral portion peaking at ca. 2,325 masl, the toe of the moraine at ca. 2,270 masl (relief of ca. 55 m), and a distal slope of ca. 0.4 (ca. 22°). The Qm3 end moraines are sharp crested, have higher relief, and similar or steeper slope angles compared to Qm2 end moraines, indicating a lower degree of degradation, and allowing age-contrast inferences with other landform units. The up-valley terminal position, sharp crests, steep slopes, and high relief of Qm3 end moraines, relative to Qm2 and Qm1, provide evidence that Lemhi Advance 3 is a more recent advance. The three distinct groupings of glacial features based on spatial

positioning and relative weathering criteria must represent events that are distinctly spaced in age by at least ca. 10 ka (the estimated minimum amount of time to produce discernable ages by relative weathering). Therefore, I infer that Lemhi Advance 3 is of MIS 2 age, relating to Glaciation III (Late Pinedale) described by Knoll (1977).

Additionally, Qm3 end moraines at Deer Creek, Ridgeway Mine, Meadow Lake Creek, and Bruce Canyon are mantled with talus composed of Ok quartzite boulders, exposed along their termini and lateral portions. This exposure provides two possible interpretations of the timing of deposition of these matrix-free moraine slopes. First, if the deposits are blockfields that were generated by glacial and periglacial conditions, the Qm3 end moraines persisted through a period of extreme cold, most likely the LGM. The extreme cold would have initiated frost jacking, driving large, blocky material to the surface of these features. If this occurred, then the moraines likely pre-date the LGM. The second interpretation is that the deposits originated from rockfalls that occurred while ice was at or near its stabilized position, with the debris transported supraglacially and concentrated in the moraines (see, for example, Shulmeister et al., 2009). These deposits are missing from both Qm1 and Qm2 end moraine complexes, indicating that the rockfalls would have occurred only during the construction of Qm3 end moraines.

Lemhi Advance 3 – Regional Comparison

The general morphology of Qm3 end moraines in the study area is fresh, with sharp crested ridges and steeply slopes, nested kettle topography, and high relief relative to Qm1 and Qm2 end moraines indicating minimal degradation and no incision associated with later glacial advances. These moraine descriptions are consistent with the younger, high angularity moraine groups at Pettit Lake, Yellow Belly Lake, and Hell Roaring Lake valleys in the Sawtooth Mountains described by Lundeen (2001). The

morphology of these moraines also compares well with the younger moraines at McCall, Idaho, in which Colman and Pierce (1986) described the Pilgrim Cove and McCall deposits as being narrower and having steeper slopes, with weathering rind thickness suggesting MIS 2/Pinedale age deposits. Evenson et al. (1982) also recognized fresh surface, sharp crested, and kettle preserved moraines with high surface boulder frequencies in the Pioneer Mountains, which were correlated to Pinedale age (Potholes glaciation). These moraines are also numerous and located up-valley from older Copper Basin moraines. Regionally, MIS 2 moraines are described as having fresh morphology, sharp crests, and common kettles. The similar morphology, spatial positioning, and kettle abundance between regional Pinedale/MIS 2 age moraines and the Qm3 end moraines in the Lemhi Range provide additional evidence for the inference that Qm3 moraines are MIS 2 age.

Lemhi Advance 4

Lemhi Advance 4 is evidenced by mapped Qm4 and Qf4 landforms and represents the youngest ice advance in the central Lemhi Range. Qm4 end moraines associated with this advance represent equilibration of ice at terminal positions during the latest advance phase and earliest retreat phases of glaciation. Qm4 moraines and the coeval Qf4 outwash fan are exposed at Bruce Canyon and Spring Mountain Canyon (Figure 2.6A) (Figure 2.11). The landforms representing Lemhi Advance 4 reside at elevations of ca. 2400 – 2600 masl. Qm4 end moraines are intact, sharp crested, transverse ridges located up-valley of Qm3 end moraines. However, Qm4 exposed in the main valley of Spring Mountain Canyon shows evidence of incision either from, post-glacial stream incision or a glacial outburst flood. Qf4 is exposed as small, continuous

outwash fan surfaces, grading to Qm4 moraines and filling incised channels through older glacial and outwash features. The relatively pristine character and up-valley terminal and retreat positions indicate the youngest glacial sequence. I infer this advance to be of late MIS 2 age (latest Pinedale age or late-glacial).

Western Flank Glacial Extent

Converse to the pattern of glaciation along the eastern flank of the central Lemhi Range, the western flank exhibits little evidence of glaciation. Detailed aerial photograph and satellite imagery analysis revealed very few glacial landforms, contradicting Ruppel and Lopez (1981), who mapped extensive morainal areas there. A likely explanation of the contrast of glaciation on the eastern and western flanks of the range can be found in relief and aspect contrasts. West-southwest facing slopes and lower relief dominate this portion of the range and the area thus experiences longer durations of sun exposure than the east side (Figure 2.12). Longer duration insolation hinders the long-term accumulation and preservation of snow, ultimately yielding little to no ice cover. This pattern is converse to that of the eastern slopes.

Glacial Recession

Recession of Lemhi Advance 1-4

During the retreat phase of Lemhi Advance 1-3, large blocks of ice detached and stagnated slightly up-valley from the outer ice limit, causing depressions in the landscape and ultimately creating hummocky, undulating, dead ice landforms. Dead ice landforms are not present in all end moraine complexes. The later glacial advances (i.e., Lemhi Advance 2-4) initiated erosion and meltwater incision of Lemhi Advance 1-3 end moraines and outwash fans, yielding scarce remnants of the landforms representing

Lemhi Advance 1, moderately extensive remnants of Lemhi Advance 2 landforms perched in the surrounding landscape, and intact remnants of Lemhi Advance 3 landforms, along with dead ice landforms within the terminal positions of Qm1 and Qm2 moraines at Deer Creek, Qm3 moraines in nearly all valleys, and Qm4 moraines at Spring Mountain Canyon. As the ice front of Lemhi Advance 3 receded up-valley, meltwater channels initiated incision of older glacial deposits. Continued recession was punctuated by a series of temporary halts in the final retreat of the glacier, evidenced by Qm4-Qm7 end moraine sequences at Deer Creek, Meadow Lake Creek, Long Canyon, Lemhi Union Gulch, and Spring Mountain Canyon (Figure 2.6A) (Plate 1). These lateral moraine sequences potentially correlate to late-glacial Temple Lake deposits identified by Dort (1962). Coevally constructed alluvial terraces fill the inner valleys. Deposition of undifferentiated glacial debris/ablation moraine material (Qm8) occurred in all glaciated valleys during this period of recession from downwasting of stagnant ice.

Recession of the ice front eventually reached the cirque headwalls, leaving a cirque lake at Meadow Lake, and in several valleys outside of the study area. Radiocarbon dating of a sediment core from Meadow Lake reveals that final glacial retreat past that cirque lake was completed by 14 ± 0.5 cal ka BP (B. Finney, personal communication, 2015).

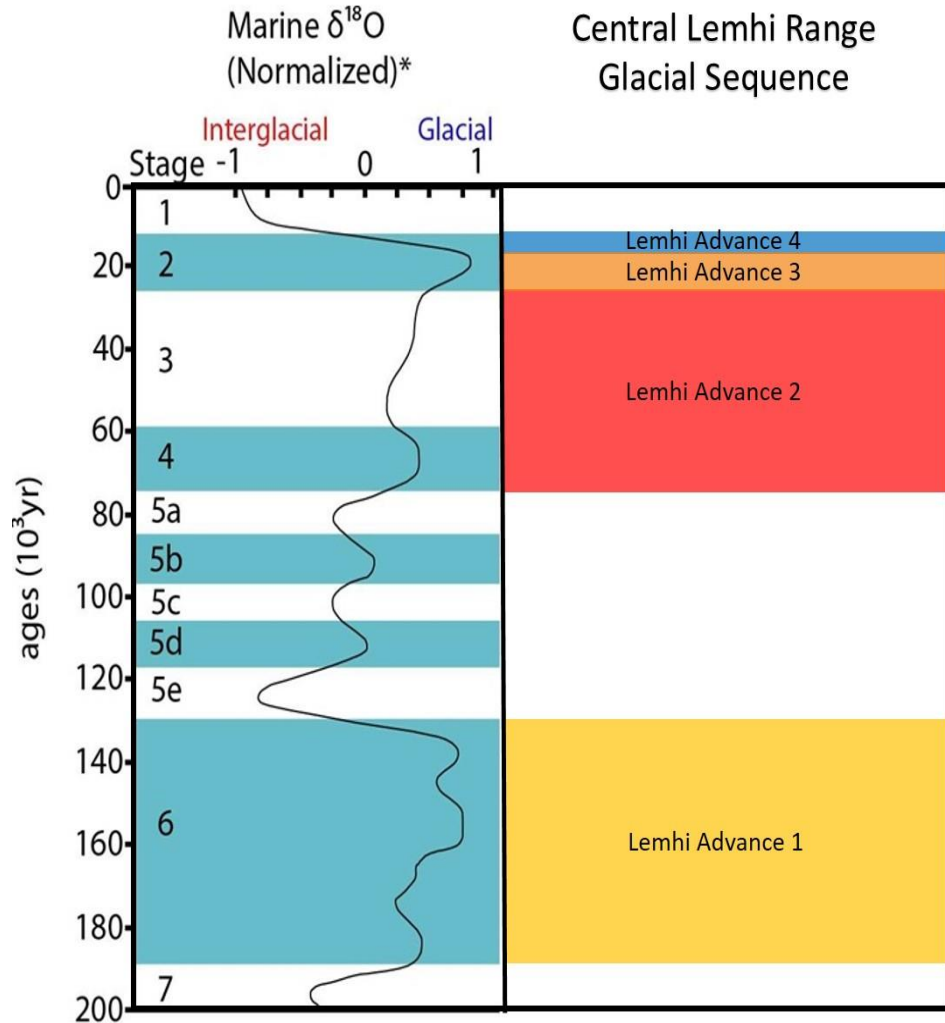


Figure 2.13 The central Lemhi Range glacial sequence (right) correlated with the Marine Isotope Stages (MIS) (left) based on relative dating techniques. From oldest to youngest the advances are: Lemhi Advance 1 (yellow) (MIS 6), Lemhi Advance 2 (red) (MIS 4-3), Lemhi Advance 3 (orange) (middle MIS 2), and Lemhi Advance 4 (blue) (latest MIS 2 or late-glacial). Colors of advances are intended to match the mapped end moraines, and represent the range of inferred ages. Actual events were likely limited to narrow time windows within MIS 6 and MIS 4-3, rather than extending through those periods. Figure modified from Kaufman et al. (2003), based on original data from Martinson et al. (1987).

2.6.2 Timing of Post-Glacial Events

Following glaciation, extended periods of erosion have taken place. Erosional processes have created talus slopes and cones, debris flow deposits, and colluvium.

Periglacial, freeze-thaw, and debris flow mass wasting drive the formation of arcuate

proglacial lobe features at the base of talus slopes. Holocene precipitation drives the formation of active flood plains that are seen in the Lemhi Range today.

2.7 Conclusion

The east-central Lemhi Range preserves a detailed record of mountain glaciation for the last glacial cycle. This study has generated a new geomorphological sequence for Lemhi Range glacial events that, with forthcoming CRN chronology, can be correlated to published chronologies of glacial events from central Idaho and western Wyoming. Surficial mapping of the Gilmore and northeast quadrant of the Big Windy Peak 7.5-minute quadrangles, east-central Lemhi Range, and analysis of the geomorphic characteristics of mapped moraine systems delineates multiple glacial advances in this range. The overall east-central Lemhi Range glacial sequence timing is inferred as: Lemhi Advance 1 (MIS 6), Lemhi Advance 2 (MIS 4-3), Lemhi Advance 3 (MIS 2), and Lemhi Advance 4-8 (late MIS 2), with glacial recession completed by 14 ± 0.5 cal ka BP.

References

- Burke, R.M., Birkeland, P.W., 1979, Reevaluation of multiparameter relative dating techniques and their application to the glacial sequence along the eastern escarpment of the Sierra Nevada, California, *Quaternary Research*, 11, 21-51.
- Butler, D.R., 1984, A late Quaternary chronology of mass wasting for a small valley in the Lemhi Mountains of Idaho, *Northwest Science*, 58.1, 1-13.
- Butler, D.R., 1986, Pinedale deglaciation and subsequent Holocene environmental changes and geomorphic responses in the central Lemhi Mountains, Idaho, USA, *Géographie physique et Quaternaire*, 40.1, 39-46.
- Chadwick, O. A., Hall, R.D., Phillips, F.M., 1997, Chronology of Pleistocene glacial advances in the central Rocky Mountains, *Geological Society of America Bulletin*, 109, 1443-1452.
- Colman, S.M., Pierce, K.L., 1981, Weathering rinds on andesitic and basaltic stones as a Quaternary age indicator, western United States, *Geological Survey Professional Paper*, No. 1210, 1-56.
- Colman, S.M., Pierce, K.L., 1986, Glacial sequence near McCall, Idaho: Weathering rinds, soil development, morphology, and other relative-age criteria, *Quaternary Research*, 25, 25-42.
- Dort, W., 1962, Multiple glaciation of southern Lemhi Mountains, Idaho: preliminary reconnaissance report, *Tebiwa*, 5.2, 2-17.
- Dort, W., 2003, Multiple Pre-Bull Lake glaciations, eastern side of Lemhi Range, east-central Idaho, *Geological Society of America Abstracts with Programs*, 35.5.
- Dort, W., 2004, Records of multiple Pinedale glacier retreat/readvance pulses, Lemhi Mountains, east-central Idaho, *Geological Society of America Abstracts with Programs*, 36.4.
- EarthScope Intermountain Seismic Belt LiDAR Project, 2008, EarthScope Intermountain 223 Seismic Belt LiDAR Project: <http://opentopo.sdsc.edu>, doi: 10.5069/G9VD6WCS 224.
- ESRI, 2015, ArcGIS 10.3.1 software: ESRI Corporation, Redlands, California.
- Evenson, E.B., Pasquini, T.A., Stewart, R.A., Stephens, G., 1979, Systematic provenance investigations in areas of alpine glaciation: applications to glacial geology and mineral exploration, in *Moraines and Varves*, 25-42.
- Evenson, E.B., Cotter, J.F.P., and Clinch, M.J., 1982, Glaciation of the Pioneer Mountains: A proposed model for Idaho, ed. Bonnicksen and Breckenridge,

- Cenozoic Geology of Idaho, *Idaho Bureau of -Mines and Geology Bulletin*, 26, 653-665.
- Foster, D., Brocklehurst, S.H., Gawthorpe, R.L., 2008, Small valley glaciers and the effectiveness of the glacial buzzsaw in the northern Basin and Range, *Geomorphology*, 624-639.
- Heyman, J., 2014, Paleoglaciation of the Tibetan Plateau and surrounding mountains based on exposure ages and ELA depression estimates, *Quaternary Science Reviews*, 91, 30-41.
- Hyatt, O.M., Shulmeister, J., 2013, Methods in geomorphology: mapping glacial features, *Treatise on Geomorphology*, 14, 92-104, DOI 10.1016/B978-0-12-374739-6.00375-4
- Janecke, S.U., 1992, Geologic map of part of the Big Windy Peak and Moffet Springs 7.5' quadrangles, Lemhi and Custer Counties, Idaho, *Idaho Geological Survey Technical Report*, 92-96.
- Johnson, B.G., Thackray, G.D., Van Kirk, R., 2007, The effect of topography, latitude, and lithology on rock glacier distribution in the Lemhi Range, central Idaho, USA, *Geomorphology*, 91.1, 38-50.
- Kaufman, D. S., Porter, S. C., and Gillespie, A. R., 2003, Quaternary alpine glaciation in Alaska, the Pacific Northwest, Sierra Nevada, and Hawaii, in Gillespie, A. R., Porter, S. C., and Atwater, B. F., eds., *The Quaternary Period in the United States: Developments in Quaternary Science: Amsterdam*, Elsevier, 1, 77-103
- Kenworthy, M.K., Rittenour, T.M., Pierce, J.L., Sutfin, N.A., Sharp, W.D., 2014, Luminescence dating without sand lenses: An application of OSL to coarse-grained alluvial fan deposits of the Lost River Range, Idaho, USA, *Quaternary Geochronology*, 23, 9-25.
- Knoll, K.M., 1977, Chronology of Alpine glacier stillstands, east-central Lemhi Range, Idaho, *Idaho State University Museum of Natural History*.
- Licciardi, J.M., Pierce, K. L., 2008, Cosmogenic exposure-age chronologies of Pinedale and Bull Lake glaciations in greater Yellowstone and Teton Range, USA, *Quaternary Science Reviews*, 27, 814-831.
- Link, P.K., Janecke, S.U., 1999, Geology of east-central Idaho: geologic roadlogs for the Big and Little Lost River, Lemhi, and Salmon River valleys, *Guidebook to the Geology of Eastern Idaho: Idaho Museum of Natural History, Pocatello*, 295-334.
- Lund, K.I., Evans, K.V., Tysdal, R.G., Winkler, G.R., 2003, Geologic Map of the Eastern Part of the Salmon National Forest, *United States Geological Survey*, 1:100,000.

- Lundeen, K.A., 2001, Refined late Pleistocene glacial chronology for the eastern Sawtooth Mountains, Central Idaho, *M.S. Thesis Idaho State University*, 117.
- Martinson, D.G., Pisias, N.G., Hays, J.D., Imbrie, J., Moore, T.C., Shackleton, N.S., 1987, Age dating and the orbital theory of the ice ages: Development of a high-resolution 0 to 300,000-year chronostratigraphy, *Quaternary Research*, 27, 1-29.
- Mix, A.C., Bard, E., Schneider, R., 2001, Environmental processes of the ice age: land, ocean, glaciers (EPILOG), *Quaternary Science Reviews*, 20, 627-657.
- Phillips, F.M., Zreda, M.G., Gosse, J.C., Klein, J., Evenson, E.B., Hall, R.D., Chadwick, O.A., Sharma, P., 1997, Cosmogenic ³⁶Cl and ¹⁰Be ages of Quaternary glacial and fluvial deposits of the Wind River Range, Wyoming, *Geological Society of America Bulletin*, 109, 11, 1453-1463.
- Ruppel, E.T., Lopez, D.A., 1981, Geologic map of the Gilmore quadrangle, Lemhi and Custer counties, Idaho, *United States Geological Survey*, 1:62,500.
- Ruppel, E.T., Lopez, D.A., 1988, Regional geology and mineral deposits in and near the central part of the Lemhi Range, Lemhi County, Idaho, *United States Geological Survey Professional Paper*, No. 1480, 1-122.
- Schmidt, D.L., Mackin, J.H., 1970, Quaternary geology of Long and Bear Valleys, west-central Idaho, *United States Government*, No. 1311-A.
- Shulmeister, J., Davies, T.R., Evans, D.J.A., Hyatt, O.M., Tovar, D.S., 2009, Catastrophic landslides, glacier behavior and moraines formation – a view from an active plate margin, *Quaternary Science Reviews*, 28, 1085-1096.
- Teton Conservation District, 2008, Teton Conservation District, Wyoming LiDAR: 294 <http://opentopo.sdsc.edu>, doi: 10.5069/G9F769GN.
- Thackray, G.D., 2004, Late Pleistocene alpine glacier advances in the Sawtooth Mountains, Idaho, USA: Reflections of midlatitude moisture transport at the close of the last glaciation, *Geology*, 32, 225-228.
- Thackray, G.D., 2008, Varied climatic and topographic influences on Late Pleistocene mountain glaciations in the western United States, *Journal of Quaternary Science* 23, 671-681.
- Thackray, G.D., Staley, A.E., *in review*, Fault scarp offsets document extensive MIS 4-3 glaciation in western interior North America, Teton Range, Wyoming, USA, *Quaternary Research*.

Wigley, W.C., Pasquini, T.P., Evenson, E.B., 1978, Glacial history of the Copper Basin, Idaho - A pedologic, provenance, and morphologic approach, *Quaternary soils: Norwich, England, Geological Abstracts*, 265-307.

Chapter 3. Late Pleistocene Glacial Geomorphology and Paleoclimatology in the East-Central Lemhi Range, Idaho, U.S.A.

Abstract

Mountain glaciation in continental interiors, from a global to continental perspective, has been well documented in many areas, with results suggesting that the timing of major mountain glacier events is highly variable through the last glacial cycle (e.g., Evenson, 1982; Colman and Pierce, 1992; Lundeen, 2001; Thackray, 2004; Licciardi and Pierce, 2008; Kenworthy, 2014; Staley, 2015; Hughes et al., 2013; Chapter 2 of this thesis). The Lemhi Range, east-central Idaho, offers significant information regarding the glacial history of western North America, as it exposes well preserved glacial deposits and landforms. Surficial mapping of glacial features in the central Lemhi Range delineates four distinct glacial advances evidenced by mapped Qm1-Qm4 end moraines and coeval Qf1-Qf4 outwash fans. The geomorphic characteristics of the mapped end moraines, including moraine crest angularity, moraine relief, and distal moraine slope steepness, were analyzed semi-quantitatively from transverse profiles, yielding patterns indicating that slope angle, crest angularity, and relief decrease as moraine age increases. The glacial advances of the Lemhi Range are correlated to the Marine Isotope Stages as: Lemhi Advance 1 (MIS 6), Lemhi Advance 2 (MIS 4-3), Lemhi Advance 3 (MIS 2), and Lemhi Advance 4 (late MIS 2). Glacial recession in the Lemhi Range is inferred to have been completed by 14 ± 0.5 cal ka BP, as determined from radiocarbon dating from a Meadow Lake sediment core. Paleo-glacier surfaces were reconstructed for seven glaciated valleys across the eastern flank of the range from inferred MIS 2-age Qm3 end moraines. Equilibrium-line altitudes (ELAs) were calculated for the ice surfaces using the accumulation-area-ratio (AAR) method and the

toe-to-headwall-altitude-ratio (THAR) method. The average AAR- and THAR-derived ELAs across reconstructed glaciers is 2650 m and 2690 m respectively. Both ELAs show similarities to Last Glacial Maximum (LGM)/Pinedale age glacier ELAs in the Sawtooth Mountains, Idaho (2640 m), and Beaverhead Mountains, Montana (2650 m). The eastward increase of ELAs across these ranges likely reflect orographic and ice sheet influence of westerly flow and moisture delivery. Similarities between the Lemhi Range and Sawtooth Mountains can be interpreted as 1) the inland mountainous region of Idaho experienced uniform cooling during the last glacial cycle, superimposed on consistent precipitation contrasts, or 2) limited delivery of precipitation to the Sawtooth Mountains from decreased westerly winds and an increased temperature depression in the Lemhi Range due to cold winds from the Cordilleran and Laurentide ice sheets. It is likely that cold and dry climatic conditions were generated by the anticyclonic, ice-sheet influenced circulation during the LGM, allowing cold, easterly winds to progress westward over the low portions of the Beaverhead Mountains, reaching the Lemhi Range. These cold easterly winds may have caused cold summer temperatures, allowing low winter accumulation to support glaciation. This suggests that moist air masses may have been diverted around these mountain ranges, allowing the Sawtooths to experience reduced precipitation, while the Lemhi Range experienced a greater temperature depression.

3.1 Introduction

Previous studies of glacial geomorphology, paleoclimatology, and geochronology in the western United States have focused intently on Northern Hemisphere ice sheet fluctuations and the resulting influence on sea level during the Last Glacial Maximum (LGM) (ca.26-18 ka) (Clark and Alley, 1999; Clark and Mix, 2002; Lambeck, 2010). The

LGM has been widely defined as the most recent interval when global ice sheets reached their maximum integrated volume during the last glaciation (Mix et al., 2001), and has been correlated to maximum mountain glacier extent by either geochronology or inferences from relative age data. However, mountain glaciers are more highly sensitive to short-term climatic fluctuations (changes in temperature and precipitation) than are ice sheets, and are more likely to respond to short-term climatic variations independent of the ice-sheet maximum. Therefore, records of paleo-mountain glacier responses to climate change provide sources for high-resolution proxy data for elucidating the spatial and temporal patterns, as well as the climatic drivers, of Pleistocene glaciation. These data can improve understanding of paleoclimatic processes spanning the length of the last glacial cycle and encompassing marine isotope stages (MIS) 5-2.

Decades of mountain glacier studies have revealed patterns of glaciation in space and time across the northwestern United States. Many of those studies have revealed maximum Late Pleistocene glaciation during or shortly following the LGM, such as in the Wind River Range, Wallowa Mountains, Uinta Mountains, and the greater Yellowstone and Teton Range (Gosse et al., 1995; Licciardi et al., 2004; Refsnider, 2008; Licciardi and Pierce, 2008, respectively). However, studies have also revealed evidence for MIS 4-3 glaciation being more extensive than LGM glaciation in the Olympic Mountains, Cascade Range, Sawtooth Mountains, Lost River Range, and the Teton Range (Thackray, 2001; Marshall, 2013; Thackray et al., 2004; Kenworthy, 2014, Thackray and Staley, in review; Staley, 2015) (Figure. 3.1). Dating techniques such as radiocarbon, optically stimulated luminescence (OSL), and cosmogenic radionuclide (CRN) have been applied in these areas to provide evidence for climatic variability and

Existing Late Pleistocene Geochronology of Mountain Glacier Systems

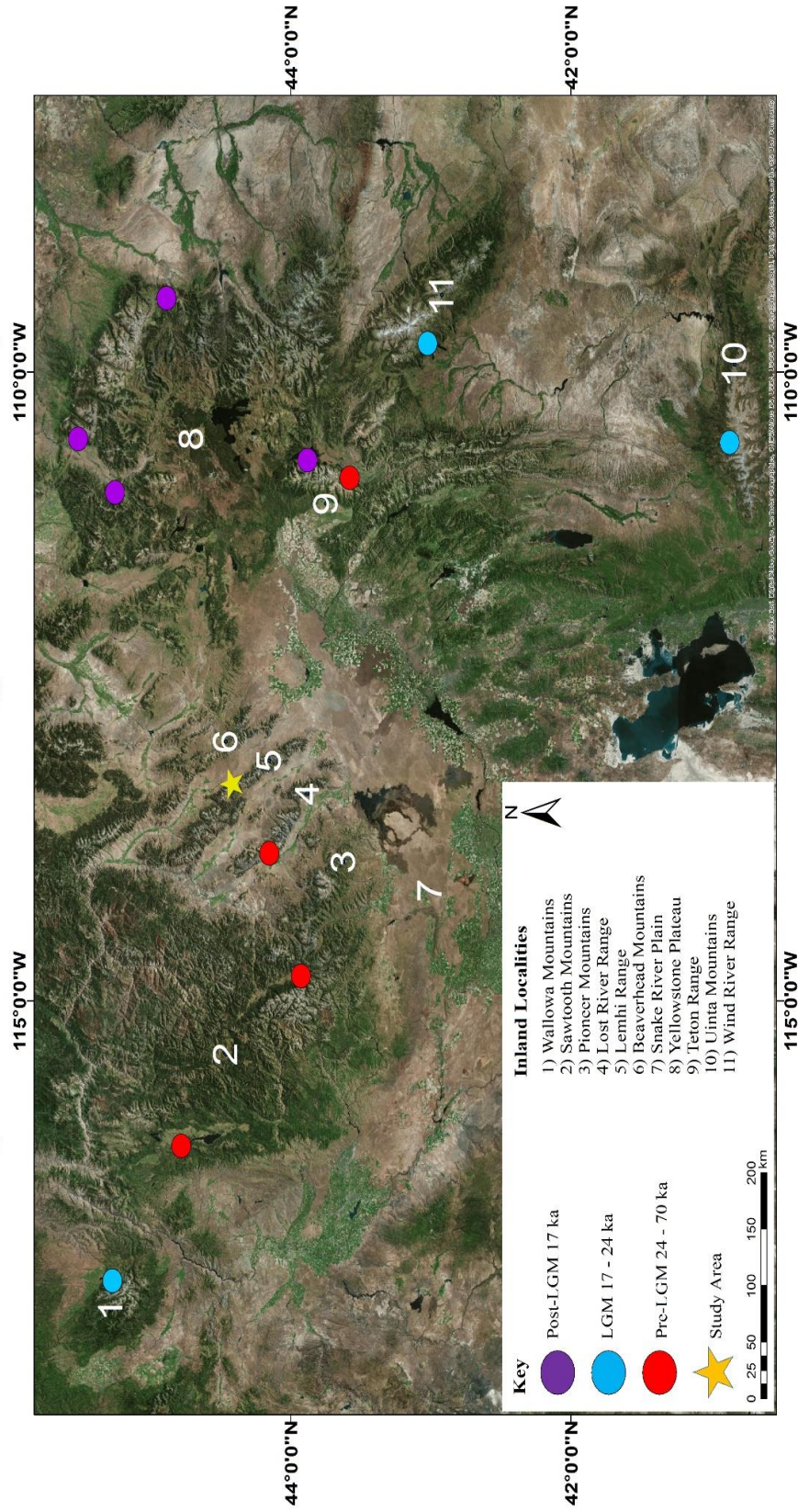


Figure 3.1 Regional topographic image of east-central Idaho, Wyoming, and southwestern Montana showing locations of inland mountain glacier systems and Late Pleistocene geochronologies of maximum ice extent. Ages were determined through cosmogenic radionuclide, optically stimulated luminescence, fault offset, and erosional weathering dating criteria. Some areas with LGM or post-LGM geochronology also have moraines that may pre-date LGM. See Chapter 1 for discussion of geochronology and references.

the relationship between glacier fluctuation and climate change during the last glacial cycle. However, detailed chronologies remain limited in geographic coverage, and additional detailed studies are needed to elucidate the spatial and temporal glacial patterns.

This study focuses on the Lemhi Range, east-central Idaho, to test the following hypotheses: 1) Pre-LGM (MIS 4-3; 25-75 ka) climatic events produced extensive mountain glaciers in east-central Idaho, and 2) MIS 4-3 temperature and precipitation variations influenced extensive glaciation in the Lemhi Range, similar to glaciation in nearby inland mountain glacier systems (i.e., Lost River Range and Sawtooth Mountains). To test these hypotheses, and better understand the climatic drivers behind Lemhi Range glaciation, extensive surficial mapping of glacial and alluvial deposits and semi-quantitative analysis of moraine morphometry were conducted to develop relative age relationships (see Chapter 2). The target moraine sequences have been previously interpreted as Pinedale and Bull Lake deposits by Dort (2003). Equilibrium-line altitudes (ELAs) were calculated for seven reconstructed glacier surfaces correlated to inferred MIS 2 moraines along the eastern range-front of the Lemhi Range to explore and correlate regional climate patterns. The paleo-ELAs were compared with modern ELAs of glaciers across three mountain ranges in the region.

If the hypotheses posed above are correct, we would expect that: 1) moraine characteristics and, ultimately, ^{10}Be ages will document MIS 4-3 and MIS 2 moraine ages and 2) MIS 4-3 glaciers in the Lemhi Range would exhibit similar ELAs to those of the nearby mountain ranges containing evidence of MIS 4-3 glaciers. The new CRN ages and equilibrium line altitudes, synthesized with previously published chronological data and

ELAs, will establish a record of inland mountain glacier system fluctuations and climatic regimes during the Late Pleistocene.

3.2 Setting

The Lemhi Range, east-central Idaho, is a northwest trending, 150 km-long, normal-faulted mountain range located north of the eastern Snake River Plain and northeast of the Lost River Range (Foster et al., 2008) (Figure. 3.2). The range crest has a mean altitude of 3,050 m (Butler, 1986). The Lemhi Range receives approximately 500-1000 mm/yr precipitation, with the high peaks receiving approximately 750 mm/yr in the form of snow. The Lemhi Range was extensively glaciated during the last glacial cycle, and presumably previous glacial cycles, leaving an incised system of glacially-scoured valleys that dominate the eastern flank and are oriented nearly perpendicular to the range (Figure. 3.3). Glaciers occupied most major east-facing valley heads in late Pinedale time (30-14 ka) (Dort, 2003; Colman and Pierce, 1986). Glacial advance, recession, and deposition have produced intricate patterns of moraine and kettle topography in many valleys (Knoll, 1977; Butler, 1984). Pleistocene ELAs decline southeast to northwest along the range (Foster et al., 2008).

The bedrock strata exposed in the Lemhi Range were deposited in the Mesoproterozoic Belt intracratonic rift basin, and episodically in the late Neoproterozoic and Paleozoic Cordilleran miogeocline (Link and Janecke, 1999). Strata were deformed in Late Cretaceous time when the Medicine Lodge thrust moved eastward during the Sevier Orogeny (Ruppel and Lopez, 1981, 1988) and were intruded during Eocene time by small stocks of monzogranite, granodiorite, quartz monzodiorite, and quartz monzonite (Ruppel and Lopez, 1988). The coarse topography of the Lemhi Range seen

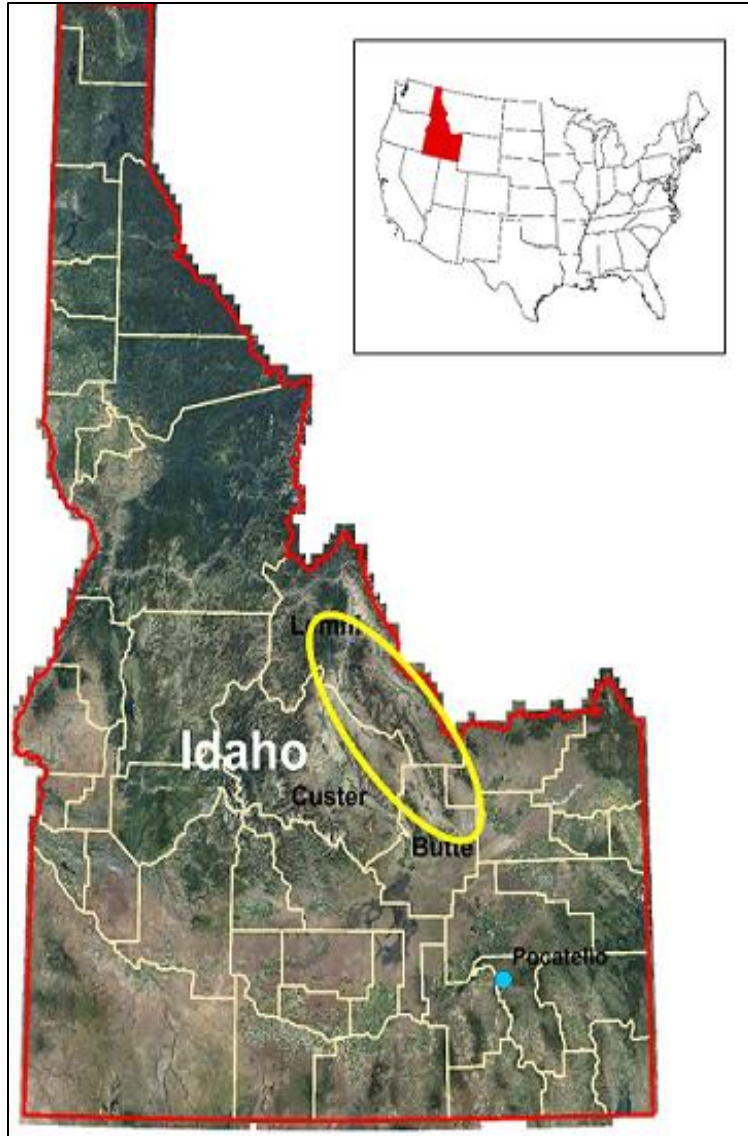


Figure 3.2 Location map of the Lemhi Range, east-central Idaho, identified by yellow bounding oval. The state of Idaho is segmented by counties, with counties of close proximity to the Lemhi Range labeled.

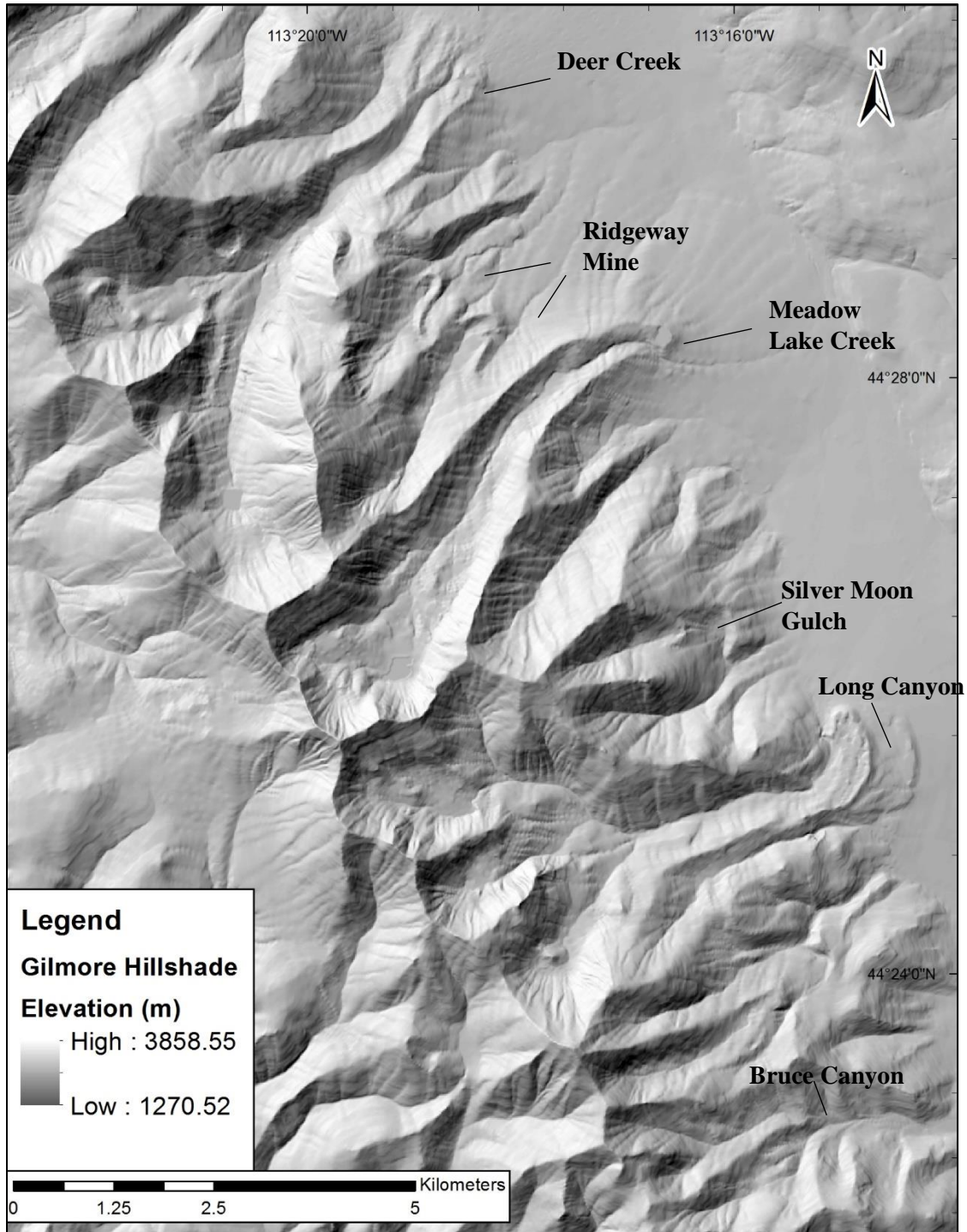


Figure 3.3 Hillshade image of the Gilmore 7.5-minute Quadrangle depicting the elevation of the glacially scoured valleys present today. The valleys are, from northwest to southeast: Deer Creek, Ridgeway Mine, Meadow Lake Creek, Silver Moon Gulch, Long Canyon, and Bruce Canyon. Qm3 moraines mapped in these valleys are utilized for paleo-glacier reconstruction in these valleys. See Chapter 2 for details regarding surficial mapping.

today is mainly a result of uplift correlating to normal faulting and fluvial, hillslope, and glacial erosional processes. These processes exposed Proterozoic-upper Paleozoic sedimentary and meta-sedimentary rocks. Of the bedrock units exposed in the range, this study emphasizes the Middle Ordovician Kinnikinic Quartzite, Middle Ordovician Saturday Mountain Formation, Upper and Middle Devonian Jefferson Dolomite, and Tertiary intrusive rocks. These lithologies comprise the cirque headwalls and lateral valley walls of the glaciated valleys, which host the glacial depositional features and associated boulders suitable for CRN dating.

3.3 Previous Work

Previous studies have produced age estimates of extensive glacial sequences across northwestern inland mountain glacier systems using a variety of chronological techniques. These chronologies, integrated with forthcoming ages, display the degree of temporal understanding for pre-LGM and LGM glaciation and the climatic conditions driving glaciation during the last glacial cycle.

3.3.1 Previous Work Suggesting Variability in Glaciation across Northwestern Inland Mountain Glacier Systems

From a global to continental perspective, the timing of major mountain glacier events is highly variable through the last glacial cycle. It is relatively well known that mountain glaciers reached their respective maximum extent at different times during the last glacial cycle, often prior to the LGM (Hughes et al., 2013). It has also been regionally documented that northwestern United States maritime mountain glacier systems (i.e., Olympic Mountains, Washington) show a dominance of pre-LGM maximum extent. The Olympic Mountains represent a prime range for pre-LGM

maximum ice extent, displaying extensive MIS 4-3 advances in the Quinault, Hoh, and Queets valleys under the influence of moderate cooling and sustained Pacific Ocean-sourced precipitation (Thackray, 2001; Marshall, 2013; Staley, 2015).

While many regional glacial systems have yielded cosmogenic exposure ages indicating extensive LGM and post-LGM glaciation (Licciardi et al., 2004; Laabs et al., 2009; Licciardi and Pierce, 2008), the record is incomplete. Glacial landforms and sediments in several regional mountain ranges suggest that pre-LGM glaciation was widespread. Glacial deposits near McCall, Idaho, were deposited by piedmont lobes of Pleistocene glaciers. Weathering rind thicknesses were measured on basaltic clasts and used as relative age indicators, distinguishing four different ages of deposits within the McCall glacial sequence. The yielded age estimates fall within MIS 2, MIS 4-3, and MIS 6 (Colman and Pierce, 1986, 1992). New ^{10}Be dating on erratic boulders near McCall yield ages of 158 ± 2.8 ka (Bull Lake), corrected for 1.7 mm/ky erosion rate, and 19.3 ± 0.2 ka, 17.4 ± 0.5 ka, and 15.9 ± 0.5 ka (Pinedale), uncorrected for erosion (Staley, 2015). However, the age of one intermediate moraine system (Williams Creek), estimated from weathering and morphologic evidence, was inferred to be ca. 60 ka, yet remains undated.

Major valleys along the eastern flank of the Sawtooth Mountains, Idaho, located ca. 130 km west of the central Lemhi Range, hosted large valley glaciers that constructed a broad moraine belt in the adjacent extensional basin. Moraine morphometry (crest angularity) and soil characteristics (depth to the B horizon) provide relative age indices for and delineation of two moraine groups: Perkins Lake moraine group and the Busterback Ranch moraine group (Lundeen, 2001; Thackray et al., 2004). Radiocarbon ages from sediment cores produced minimum limiting ages of 16,860 and 13,980 cal yr

BP within the Perkins Lake moraine group (Lundeen, 2001; Thackray et al., 2004). Cirque lake radiocarbon ages determined by Mijal (2008), support a deglaciation timing of ca. 14,000 cal yr BP. The Busterback Ranch moraine group was inferred to have been constructed during MIS 4-3, based on the ages of the Perkins Lake moraine group, and differences in soil profiles and moraine weathering characteristics, though limited CRN dating by Sherard (2006) suggests that the Busterback moraines date to MIS 2.

In the Pioneer Mountains, Idaho, (Figure 3.1), located ca. 100 km southwest of the central Lemhi Range, glacial and glacial-fluvial mapping, moraine morphometry, and relative dating techniques resulted in the differentiation of three regional glacial events: the Potholes, Copper Basin, and Pioneer, which are correlated to Pinedale (MIS 2), Bull Lake (MIS 6), and pre-Bull Lake (pre-MIS 6) (Evenson, 1982). However, Kenworthy et al. (2014) derived an OSL age of 38.0 ± 5.3 ka for an alluvial fan/terrace deposit along the East Fork of the Big Lost River. Staley (2015) extracted a single OSL sample yielding a preliminary OSL age of 23.5 ± 4.9 ka. This date indicates an MIS 2 ice marginal position, suggesting ages during MIS 3 or 4 for undated, post-Bull Lake ice marginal positions down-valley.

The Lost River Range (LRR) (Figure. 3.1), Idaho, is located ca. 45 km southwest of the central Lemhi Range. The faulted, western front of the LRR is characterized by numerous moraine sequences and low-gradient alluvial fans. Moraine morphometry and relative age sequences, applied in conjunction with surficial mapping of Doublespring Pass, delineated seven distinct glacial advance cycles correlating to Late Pinedale, Middle Pinedale, and Bull Lake (Cluer, 1989). OSL dating of Ramshorn, Birch Springs, and King Canyon alluvial fans and fill-cut terraces in the LRR by Kenworthy et al.

(2014) revealed ages of approximately 10-20 ka, 25-35 ka (MIS 2-3), and > 40 ka (MIS 3-4). Staley (2015) measured offset rates of three outwash terraces and one outwash fan in the nearby Rock Creek drainage and applied a published fault dip and slip rate to estimate terrace ages corresponding to MIS 5-3 and MIS 2, in broad agreement with the fan alluvium OSL ages of Kenworthy et al. (2014).

The Teton Range and Yellowstone Plateau ice systems lie ca. 220 km east-southeast of the central Lemhi Range (Figure. 3.1). Both systems are strongly affected by moisture-laden storms from the Pacific Ocean that are funneled eastward by the Snake River Plain. CRN ^{10}Be ages from boulders on moraines marking the southern limit of the Yellowstone Plateau glacial system in Jackson Hole provide evidence for Bull Lake (MIS 6) and Pinedale (MIS 2) glaciations (Licciardi and Pierce, 2008). CRN ^{10}Be ages from boulders on the outer and inner end moraines enclosing Jenny Lake provide evidence of late Pinedale (MIS 2) glaciation (Licciardi and Pierce, 2008), confirmed by extensive additional dating (Licciardi et al., 2015). Thermoluminescence ages determined from accumulated loess in the Jackson Hole area, combined with meteoric and cosmogenic ^{10}Be ages and soil development characteristics, suggest an MIS 4-3 glacial interval (Pierce, 2011). Thackray and Staley (in review) measured the vertical offset at 15 scarp locations along the Teton Fault where it cuts glacial landforms to determine postglacial fault offset rates and age estimates for older glacial landforms. Assuming that range-front deglaciation occurred uniformly along the range front (ca. 15 ka, Licciardi and Pierce, 2008), Thackray and Staley (in review) calculated a vertical offset rate of 0.80 m/ka and used this offset rate to estimate ages for the older range-front landforms to be 17-48 ka.

This suggests either that the fault experienced dramatic variations in offset rate during MIS 2, or that MIS 3 and MIS 4 glacial sequences influenced the Teton Range.

Modern ELAs

Rock glaciers remain as the only active glacial features in the Lemhi Range (Johnson et al., 2007). Although these features persist, ELAs cannot be deduced, as the rock glaciers are covered by and comprised of rockfall debris, with no evidence of snowlines. The Otto glacier was discovered and recorded as the only active alpine glacier in Idaho, located on the north face of Borah Peak in the LRR at an elevation of ca. 10,400 feet, in the Rock Creek drainage (Otto, 1977) (Figure 3.4). The dimensions of the glacier were found to be approximately 550 m in length (including a terminal moraine), 250 m in width (widest portion), an area of 137,500 m², and a thickness, determined from seismic depth soundings, of 64 meters. The moraines present are typical of most alpine glacial moraines in that they extend around the entire lobate portion of the ice (Otto, 1977). Keeley (2015) conducted a reconnaissance survey of the Otto glacier and used remote sensing techniques and historical Google Earth imagery over a three-year period (2011-2014) to track the movement of large rocks. Keeley (2015) determined that the Otto glacier moves downslope between 50 and 200 cm per year. Although this is the only apparently active glacier in the range, it serves as the most appropriate modern ELA analogue to the Lemhi Range, as it lies ca. 50 km southwest of the study area. The Otto glacier provides a remnant ice elevation of 3260 masl, extracted from Google Earth aerial imagery (Staley, 2015). Seven modern glacier ELAs were determined in the Teton Range by Reynolds (2011), revealing an average ELA of ca. 3175 masl.

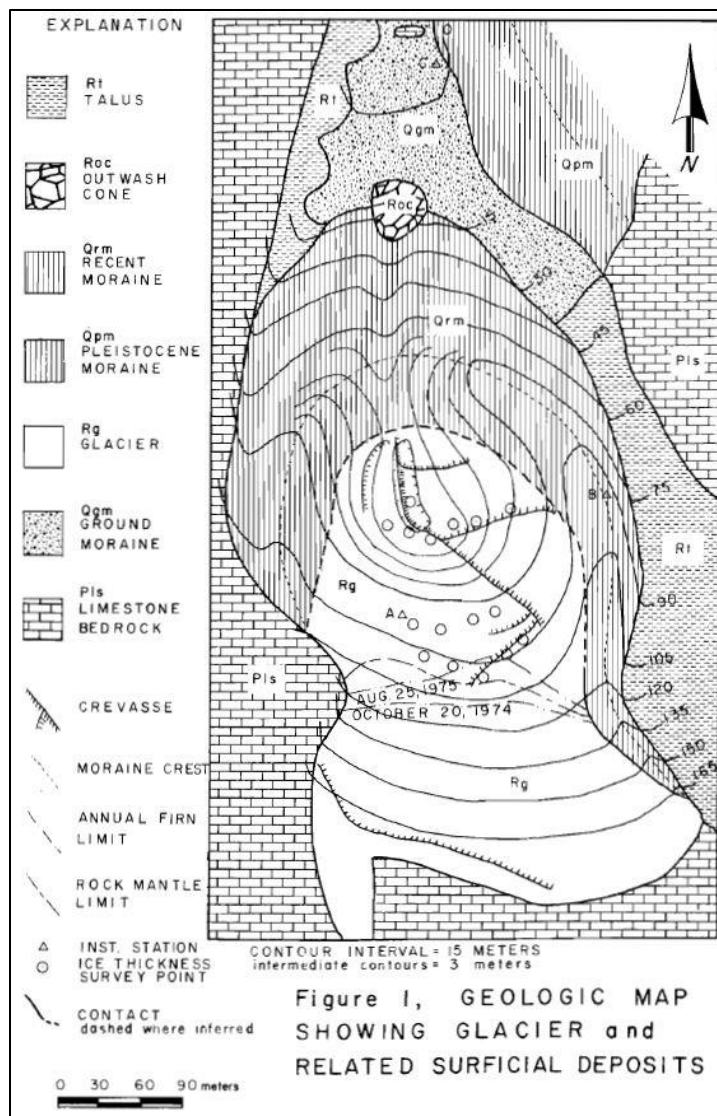


Figure 3.4 Geologic map of Rock Creek Cirque showing the Otto Glacier, associated surficial deposits, seismic stations, 1974 firn limits, crevasses, bedrock, and elevation contours. Figure from Otto (1977).

This average ELA estimate compares relatively well with the Otto glacier ELA estimate, justifying the use of the Otto glacier ELA as a basis for Lemhi Range ELA comparisons.

Other modern ELAs include the Mammoth Glacier located in the Wind River Range, Wyoming, showing an ELA of 3610 m (Davies, 2011). Temperature depression determination from comparison of paleo- and modern ELAs is discussed in Appendix C.

3.4 Methods

Techniques for reconstructing alpine paleo-glaciers and their associated ELAs have been used across the northwestern U.S. to evaluate the probable paleoclimatic conditions (i.e., temperature and precipitation) that engendered and sustained glaciers during the last glacial cycle (Brugger, 1996; Lundeen, 2001; Foster et al., 2008; Refsnider et al., 2008; Staley, 2015). In order to place glacial reconstructions into a spatial and temporal context, extensive surficial mapping must be conducted, establishing relative age relationships based on semi-quantitative moraine morphometry and geomorphology. In addition, a reliable chronology of past glacial advances must be determined. This study utilizes surficial geologic mapping, paleo-ELA reconstruction, and ^{10}Be CRN exposure dating to reveal the patterns, timing, and drivers of Late Pleistocene glaciation.

3.4.1 Surficial Mapping of the Gilmore 7.5-Minute Quadrangle and the Northeastern Quarter of the Big Windy Peak 7.5-Minute Quadrangle, Lemhi Range, East-Central Idaho

Surficial mapping of the Gilmore 7.5-minute quadrangle and the northeast quadrant of the Big Windy Peak 7.5-minute quadrangle (Figure 3.5) relied on satellite and digital terrain data interpretation and field investigation. Field mapping was executed using USGS topographic maps of 1:24,000 scale and was based on detailed field observations of landform relationships, which reveal relative age relationships (Plate 1). Relative age relationships (or relative dating) are based on the premise that weathering parameters are time dependent and therefore can be used to distinguish episodes of deposition (Burke and Birkeland, 1979). The parameters utilized for relative dating between individual glacial units in the Lemhi Range include moraine morphology

(number and freshness of ice disintegration hollows, preservation of original moraine form, degree of degradation and secondary dissection), extent of glaciation down-valley (older moraine deposits are located beyond the extent of younger moraine deposits), and spatial relationships of moraines, alluvial/outwash fans, and terraces (alluvial/outwash fans graded to the termini of corresponding, coeval moraines; outwash terraces graded to a coeval moraine and filling narrow cuts in older moraines and terraces) (Evenson et al., 1982). In addition to these qualitative parameters, longitudinal profiles perpendicular to moraine crests were generated in ArcGIS 10.3.1 and surveyed to compare crest angularity, relief, and the degree of degradation, providing a semi-quantitative perspective on the relative ages of the glacial units. Additional landforms, such as talus cones, talus lobes, and debris flows, are delineated on the basis of morphology, grain-size, angularity, sorting, and depositional processes. Greater detail regarding surficial mapping, unit descriptions, and glacial advance sequences are provided in Chapter 2 of this thesis.

Surficial mapping in the Lemhi Range requires extensive exploration and investigation of the range. Dense vegetation obstructs glacial landforms, making it difficult to delineate glacial sequences and limits the effective use of satellite imagery and aerial photography. In addition, treacherous slopes and wildlife hindered navigation to particular areas within the field site. Therefore, aerial photography of the central Lemhi Range and Google Earth imagery were used in conjunction with NAIP imagery and 10 m resolution DEMs in ArcMap 10.3.1 to refine and aid field mapping techniques and observations.

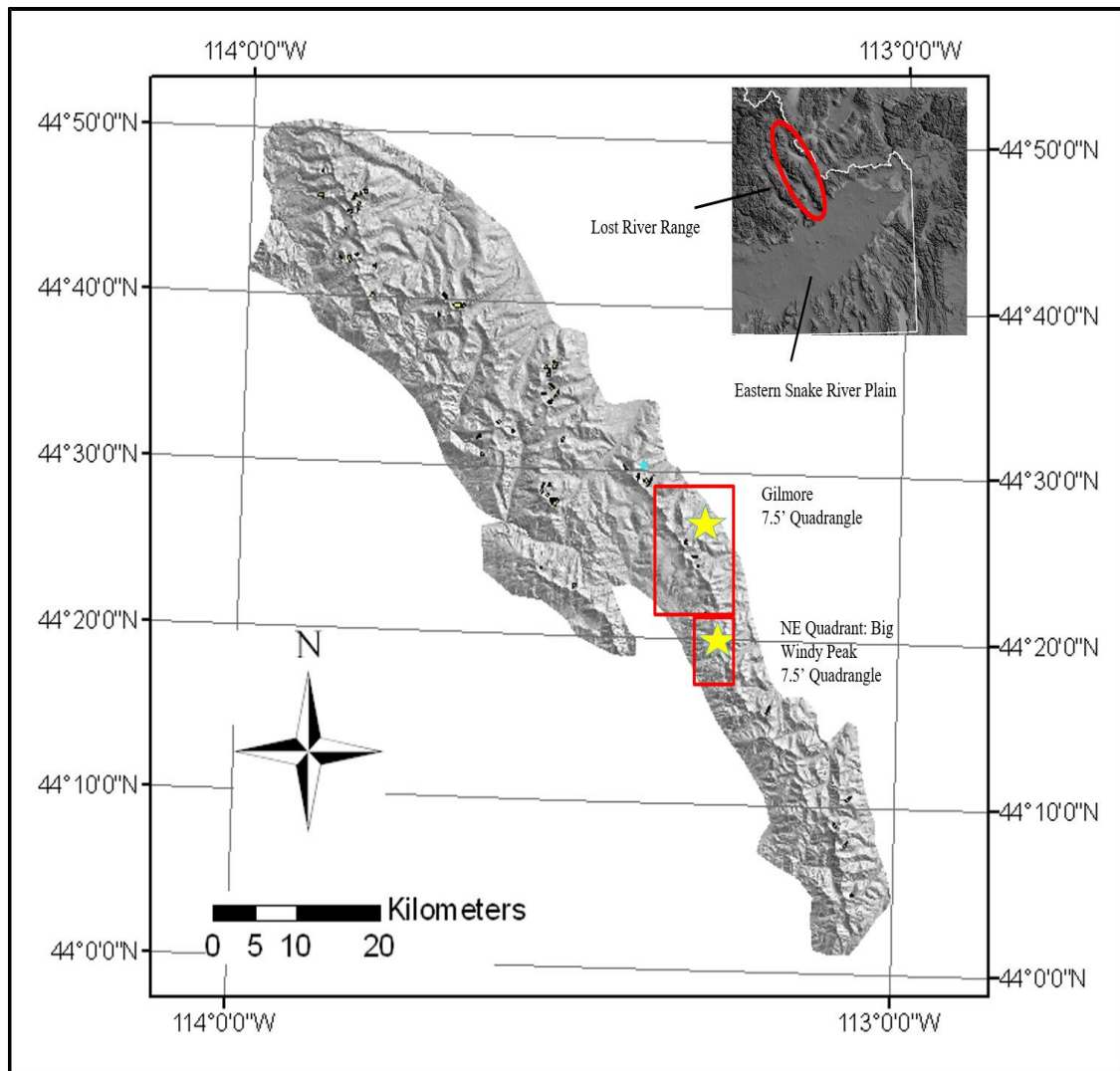


Figure 3.5 Location map of the Gilmore and the northeast quadrant of the Big Windy Peak Quadrangles, Lemhi Range, east-central Idaho, modified from Johnson et al. (2007). Inset map shows the location of the Lemhi Range in relation to the Eastern Snake River Plain and the Lost River Range.

3.4.2 Cosmogenic Radionuclide Dating

To constrain the timing of glacial advances developed by surficial mapping, I collected eight rock samples for cosmogenic ^{10}Be measurement from the tops of boulders resting on Qm2 and Qm3 terminal moraine crests exposed at Deer Creek, Meadow Lake Creek, and Long Canyon, as well as the southern Qm3 sequence at Bruce Canyon (Appendix A, Figure A.3). All samples were collected using a hammer and chisel from

boulders 1 m in height or greater. Six of the eight samples were collected from Ordovician Kinnikinic Quartzite boulders at Deer Creek (LRDC-S3, LRDC-S5), Meadow Lake Creek (LRML-S4, LRML-S2), and Long Canyon (LRLC-S6, LRLC-S7) in which samples were collected from the Qm2 moraine and the other from Qm3 moraine respective to the listing of sample names (Ruppel and Lopez, 1981, 1988). Three of the six samples were extracted from a milky-white, polished surface on the quartzite boulders. The remaining two samples were collected from Tertiary granodiorite boulders along the terminal crest (LRBC-S9) and the left lateral portion (LRBC-S8) of the southern Bruce Canyon Qm3 moraine. These samples came from boulders ≥ 1 meter in height, exhibiting no glacial polish. Further information regarding the sample locations, sampling strategies, preparation of samples, and status of samples are located in Appendix A.

3.4.3 Glacier and Paleoclimate Modeling

The spatial extent of glacial deposits has been constrained across the eastern drainages in the central Lemhi Range (Chapter 2), revealing exceptionally well preserved lateral and terminal moraines marking former ice extent. The mapped moraines define ice limits and provide a means of converting glacial geomorphology into paleoclimatology, allowing for inferences about the Pleistocene climate of the central Lemhi Range. The equilibrium line is a climatically influenced line or zone that joins points on a glacier where average annual accumulation balances average annual ablation. It is thus the elevation where the annual net budget, or mass balance, is zero (Porter, 1975). Glacier ELAs have been widely used to infer past climate and paleoclimatic conditions through the use of relationships derived from modern measurements. Paleo-glacier

reconstructions infer the ELA under the assumption that the glacier was in equilibrium with climate (Pellitero et al., 2015). In order to calculate the paleo-ELA, an inferred topographic map of the glacier surface must be reconstructed. This was accomplished for Qm3 end moraines through a series of well-defined steps using widely available digital methods described below, with a goal of objectivity and repeatability.

3.4.3.1 Glacier Longitudinal Profiles

The former ice surface of a glacier possesses the necessary information to determine the paleoclimatic conditions that drove former glaciations. Former glacier surfaces, in the form of equilibrium longitudinal profiles, have been reconstructed using the *Profiler V.2 Excel*TM spreadsheet program developed by Benn and Hulton (2010). This model implements simple, steady-state conditions which assume a ‘perfectly plastic’ ice rheology. This model is built on the assumption that ice deforms in response to the driving stress (τ_D) only when a specified yield stress (τ_y) is reached. If the driving stress is less than the yield stress, no ice movement is enabled, allowing the glacier to thicken and/or steepen in response to accumulation and melting, ultimately increasing τ_D (Benn and Hulton, 2010). Since the ice surface profile is assumed to adjust continuously, the condition of $\tau_D = \tau_y$ is withheld and expressed as

$$\tau_D = \tau_y = \rho g H \frac{\delta h}{\delta x} \quad (\text{Eq. 1})$$

Where ρ is the density of glacier ice ($\sim 900 \text{ kg}\cdot\text{m}^{-3}$), g is the gravitational acceleration ($9.81 \text{ m}\cdot\text{s}^{-2}$), H is the glacier thickness, h is the ice surface elevation and x is the horizontal co-ordinate, with the x -axis parallel to glacier flow.

The ExcelTM spreadsheet program *Profiler V.2* requires inputs of the longitudinal profile of the glacier bed, determined as elevation (z) at horizontal distances (x) on a line from the former ice terminus, marked by a down-valley moraine, and along an inferred glacial flowline. These points begin at the terminus and end on the cirque headwall. A shape factor is calculated to determine side drag, which is a function of the shape of the confining valley walls. The shape factor, f , is defined as

$$f = \frac{A}{Hp} \quad (\text{Eq. 2})$$

Where A is the area of the glacier cross section, H is the ice thickness, and p is the glacierized perimeter (where glacier ice is in contact with valley walls and channel bed). A yield stress for each step in the x -direction is the final input necessary to generate a glacier surface and is assumed to be a maximum of 100 kPa, with yield stress decreasing up-valley.

In this study, glacier surface longitudinal profiles were reconstructed for Qm3 end moraines in seven glaciated valleys (Deer Creek, Ridgeway Mine (North and South), Meadow Lake Creek, Silver Moon Gulch, Long Canyon, and Bruce Canyon). Qm3 moraines are the best and most extensively preserved moraines in these valleys, and former ice surfaces were not reconstructed for end moraines of other units due to their degraded nature. Using ESRI ArcMap 10.3.1 software, NAIP imagery, and 1:24,000 scale topographic maps, a flowline was drawn down the center of each valley extending from terminus to headwall, representing the center of flow of ice at maximum extent. Points were then constructed from each line at intervals ranging from 50-200 meters, depending on the length of the glaciated valley. Valley floor elevation data, as well as x - and y -coordinates, were extracted to these points from a 10 m Digital Elevation Model

(DEM), downloaded from the National Map Viewer (USGS website). X- and y-coordinates were extracted using the Calculate Geometry function within the attribute tables of ArcMap 10.3.1. These extracted data serve as the horizontal (x) and vertical (z) inputs into the spreadsheet of *Profiler V.2* (utilization of coordinates is described in the subsequent section). Shape factor values were extracted in the same manner but from cross-sections of Qm3 end moraines. Points were constructed from lines, when determining shape factor, at intervals ranging from 20-50 meters. Basal shear stress values of 100 kPa were chosen as inputs for the down-valley segments of the glacier, as this is a typical upper bound for mountain glaciers. As stated by Equation 1, shear stress decreases with increasing ice slope, causing the shear stress to decrease up-valley (Benn and Hulton, 2010). Shear stress values decreasing from the standardized 100 kPa are arbitrary and were adjusted to coincide with slope and glacier dynamics. That is, where slopes are steep, glacier ice thins, and where slopes are shallow, glacier ice thickens. Theoretically, little to no glacier ice will exist on the steep slopes of cirque headwalls. Therefore, shear stress values of zero, or nearly zero, were used in the model to achieve an ice thickness of zero at these points. From these inputs, paleo-glacier longitudinal profiles were generated. For valleys with multiple cirque headwalls/ice tributaries, glacier longitudinal profiles were reconstructed from the terminus to each individual cirque headwall.

3.4.3.2 Glacier Surface and Equilibrium-Line Altitude Reconstructions

Glacier Surface Reconstruction

Paleo-glacier surfaces were reconstructed for Qm3 end moraines, inferred to date to MIS 2, in seven valleys across the eastern flank of the central Lemhi Range (Figure.

3.3), based on former glacier geometries derived from surficial mapping of Qm3 moraines (Plate 1; Chapter 2). In reconstructing glacier surfaces, maximum ice extent within steady-state conditions was assumed. Centerline ice elevations were constructed in the *Profiler V.2 Excel*TM spreadsheet program (Benn and Hulton, 2010; above). The ice elevations for each valley were then imported into ArcMap 10.3.1 based on the x- and y-coordinates calculated for each point. This new set of points overlies the valley floor elevation points, denoting the elevation of the ice surface centerline. Identification of lateral and terminal moraines, based on surficial mapping, and trimlines provide ice elevation constraints along the glacier's former margin, whereas up-valley from geomorphic features, little control exists and ice elevations have to be assumed from the glacier profile (Porter, 2001). Trimlines for these valleys are not well preserved because of high canyon wall erosion rates, and were often inferred based on changes in slope, talus bedrock interfaces, vegetation bedrock interfaces, and lateral moraine elevations. Paleo-ice marginal elevations were extracted from a 10 m DEM using ArcMap 10.3.1. Points were then constructed from this line at the same horizontal interval as the points constructed for the center ice elevation. X- and y-coordinates were then calculated for these points. Center and marginal paleo-ice elevations were then exported and compiled into a single ExcelTM spreadsheet with headings of "x" "y" and "z" which denote the coordinates and ice surface elevations. These data were then imported into ArcMap 10.3.1 and exported as a new shapefile, providing inferred elevation points on a paleo-glacier surface.

From this point dataset, a paleo-glacier surface was interpolated in ArcGIS. Under the Geostatistical Analyst tool, the Geostatistical Wizard was used to begin the

interpolation. A first order universal kriging method, along with a Gaussian model type with “true” anisotropy and “4 sectors with 45° offset” were selected as the parameters for glacier reconstruction (S. Godsey, personal communication, 2016). This process produced an interpolated map of the glacier surface, which was then exported as a raster file. This raster file represents a DEM of the glacier surface and additional surrounding topography. The DEM was then further classified, to eliminate roughness in the surface elevation. A polygon was created, expanding the area of the outlined glacier surface. The interpolated DEM was then clipped to this polygon using the “extract by mask” tool. The clipped DEM was then categorized using the “stretched” symbology, with light blue colors marking the high elevations and the dark blue colors marking the low elevations.

Equilibrium-Line Altitude Reconstruction

Accumulation-Area Ratio

Equilibrium-line altitudes (ELAs) were calculated for each of the reconstructed paleo-glacier surfaces to deduce possible climatic conditions of glaciation associated with Qm3 moraines. ELAs were calculated using the accumulation-area ratio (AAR) method within a new ArcGIS based toolbox developed by Pellitero et al. (2015). The AAR method is the most widely applied technique for ELA estimation and has been used to reconstruct and infer paleo-glacier-paleoclimate conditions in mountain ranges across the world (Porter, 1975, 2001; Meierding, 1982; Lundeen, 2001; Benn et al., 2005). The AAR refers to the ratio of area above the equilibrium line (accumulation area) to the total glacier area (Porter, 1975, 2001). This method is based on the assumption that under steady-state conditions, the accumulation area of the glacier occupies a fixed proportion of the total glacier area (Benn et al., 2005).

Empirical studies of modern glaciers have revealed an average AAR of 0.6 ± 0.05 (Meier and Post, 1962) meaning the accumulation area occupies approximately 60 percent of the total glacier area (Porter, 2001). To calculate the ELAs, the “AAR (and MGE)” tool was selected from the toolbox and the reconstructed glacier surface DEMs were supplied as the main input. A scratch folder was then created to host the exported ELA shapefiles. Two additional parameters were required for the operation. The first is the contour interval for the glacier area calculation. This was set to 10 m to reflect the vertical resolution of the DEM. The smaller this value, the more accurate the calculation. Setting the interval to 10 m results in ELA calculation errors of ± 5 m (Pellitero et al., 2015). The second parameter is the ratio for the AAR method. Former steady-state AARs may differ considerably from modern ones in the same region due to changes climate, debris cover, and glacier hypsometry, so care is required to choose an appropriate ratio (Benn et al., 2005). AAR ratios of 0.55, 0.6, and 0.65 were used to calculate former ELAs across the seven reconstructed glacier surfaces. An AAR of 0.6 resulted in the lowest variance of calculated ELAs between valleys and was chosen for overall analysis. An inferred average ELA was then calculated. The results of the ELAs calculated using 0.55 and 0.65 AAR values are presented in Appendix C.

Toe-to-Headwall-Altitude Ratio

Equilibrium-line altitudes were additionally calculated using the toe-to-headwall-altitude Ratio (THAR) to compare more accurately the ELAs of the Lemhi Range to those determined using the THAR method in other inland mountain glacier systems across the northwestern U.S. The THAR method calculates the ELA by multiplying a predetermined THAR value for a specified region by the difference between glacier

headwall and terminus altitudes. This value is then added to the terminus elevation to determine the ELA (Meierding 1982; Porter 2001). For this calculation, elevations were extracted from the terminus and highest inferred point of ice at the cirque headwall in the reconstructed glacier surfaces. Meierding (1982) reported that the most accurate results were created by THAR values of 0.35-0.40 in the Colorado Front Range. However, a THAR value of 0.6 is used in this study to calculate ELAs, chosen in order to compare ELAs calculated by Staley (2015) across a broad transect of regional mountain ranges.

3.5 Results

3.5.1 Surficial Mapping

The central Lemhi Range houses a well preserved geomorphic record of Pleistocene glaciation. Pleistocene ice originated in the high altitude reaches of the central Lemhi Range, carving steep cirque headwalls. Ice flowed down many valleys in the central Lemhi Range with ice extending beyond the eastern range-front at Deer Creek, Meadow Lake Creek, Long Canyon, and Spring Mountain Canyon. These low-gradient valley mouths provide well preserved evidence of multiple episodes of glaciation. Identification of glacial moraine and outwash sequences are based on clear geomorphic relationships. Sharp, broad (0.1-0.4 km wide), arcuate, high and low relief landforms with identifiable crests mantled with boulders are identified as end moraine complexes and indicate distinct ice marginal positions (Figure 3.6). Hummocky landforms, referred to in this study as dead ice landforms, are nested within Qm3 end moraines and were constructed as the ice margin fluctuated and ice blocks detached from the main toe of the glacier (Figure 3.7).

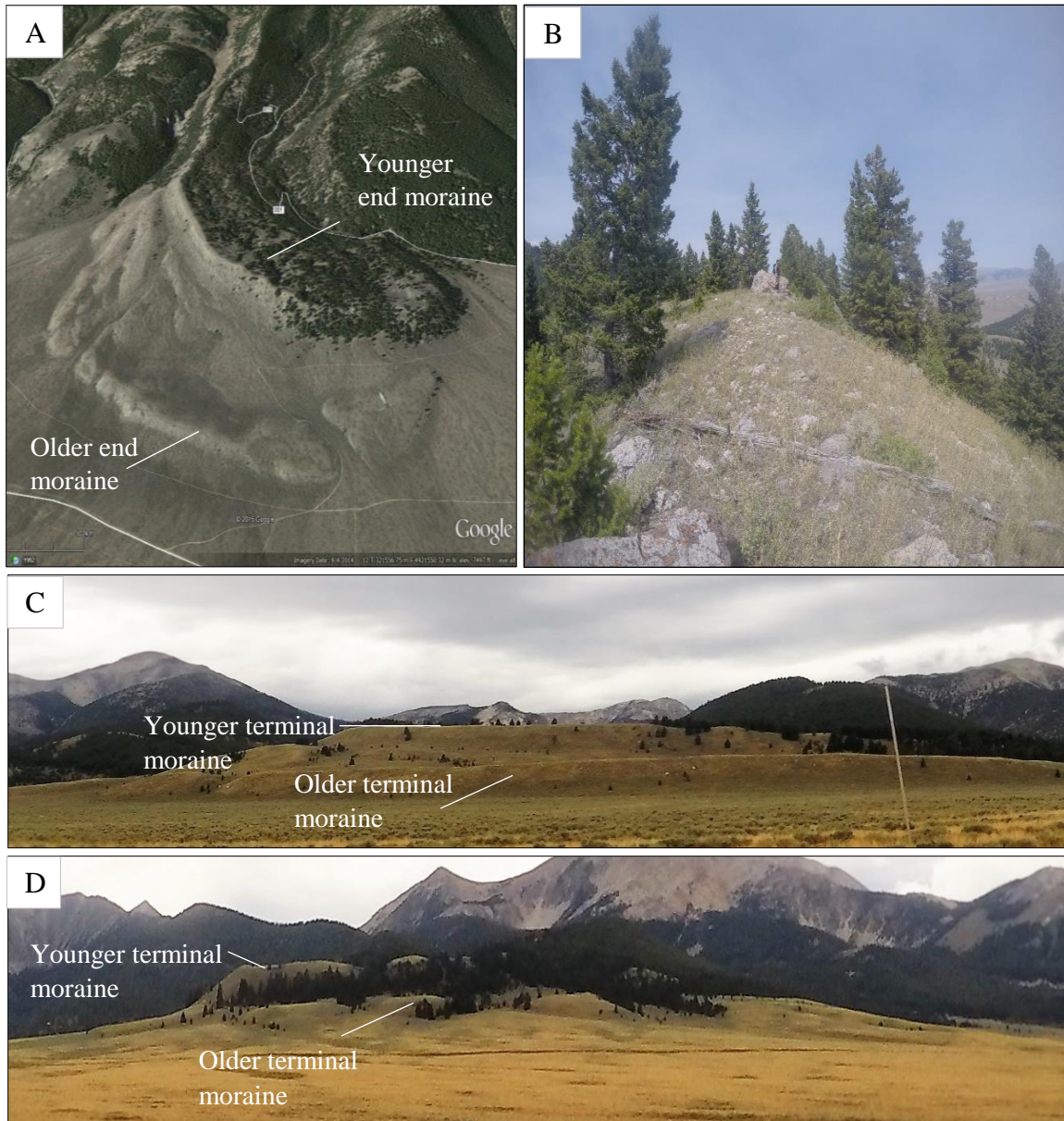


Figure 3.6 Prominent crests of moraine sequences at (A) Long Canyon, (B) Lemhi Union Gulch, and (C) Meadow Lake Creek, Lemhi Range, Idaho. (A) Google Earth satellite imagery depicting the broad arcuate nature of both older and younger end moraine complexes at Long Canyon. (B) Field photo of a sharp terminal moraine crest riddled with Osm and Dj boulders at Lemhi Union Gulch. (C) Range front photo of Long Canyon and (D) Meadow Lake Creek depicting older, low elevation, and low relief terminal moraines and younger, high elevation, high relief terminal moraines. Each moraine sequence marks a separate ice terminal position. Image from Google Earth (2015).

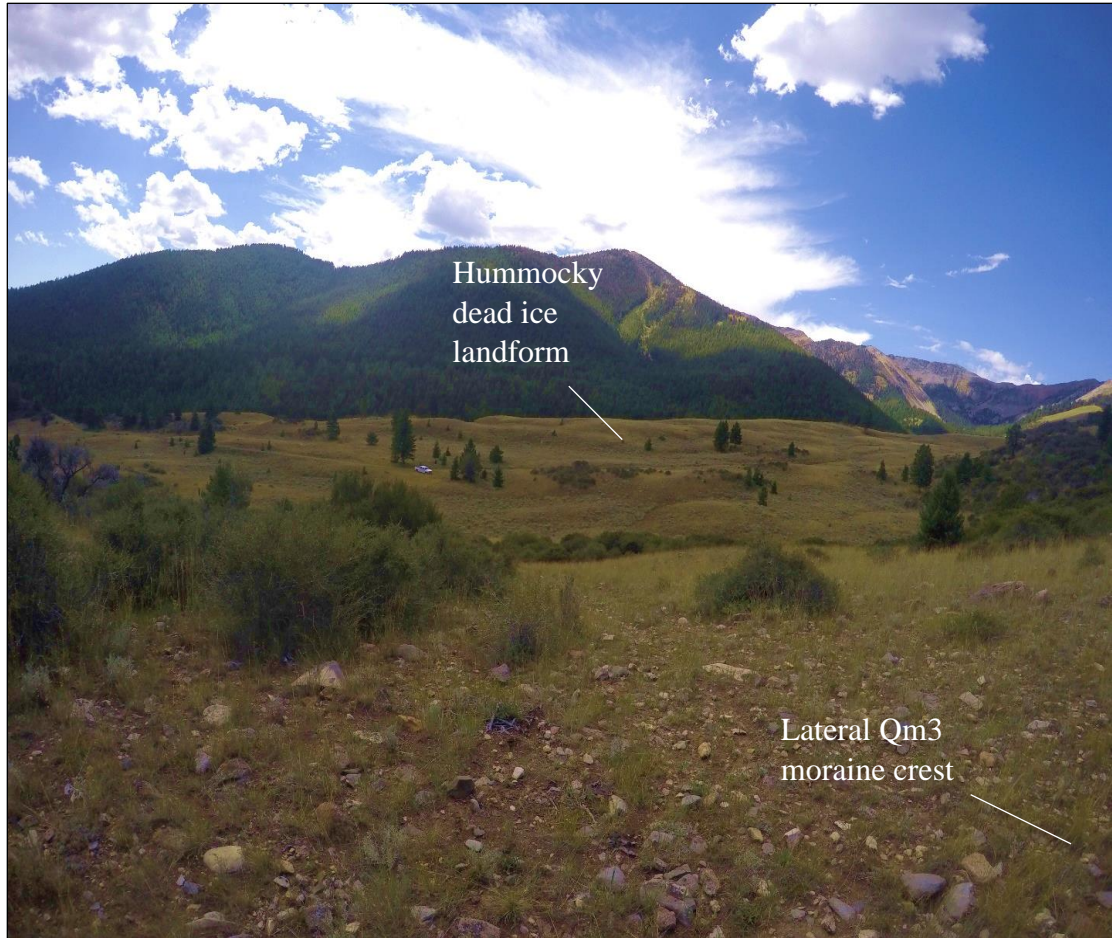


Figure 3.7 Field photograph of Spring Mountain Canyon depicting the hummocky dead ice landform within Qm3 moraines.

End moraines of individual advances are spatially separated by ca. 0.3-0.6 km of flat, gently sloping, coeval outwash fan surfaces. These outwash fan surfaces are composed of moderately sorted, silt- to boulder-sized sediment and grade up-valley to end moraines, indicating deposition from glacial meltwater streams. Older moraine sequences at Deer Creek, Meadow Lake Creek, Long Canyon, and Spring Mountain Canyon are neighbored by older outwash fan remnants that lie at higher elevations than the surrounding, younger outwash fan surface. In valleys such as Deer Creek, moraines of

individual advances merge (with no outwash fan surfaces between them), and are only differentiated by the degree of degradation of their arcuate crests.

Pleistocene glacial and outwash landforms, which include end moraines and outwash fans, are assigned a Lemhi Advance term to identify glacial advance sequences (Plate 1). For example, Lemhi Advance 1 is the earliest Quaternary advance for which evidence remains, and is evidenced by Qm1 (end moraine 1) and Qf1 (outwash fan 1) map units. This nomenclature repeats for Lemhi Advance 2-4. Retreat-phase landforms are discussed on an individual basis.

3.5.2 Glacier Modeling and Equilibrium-Line Altitudes

As noted, paleo-glacier longitudinal profiles and paleo-glacier surfaces were reconstructed for Qm3 (inferred MIS 2) end moraines in seven mapped valleys (Figure 3.8, 3.9). The entirety of glacier longitudinal profiles and individual reconstructed paleo-glacier surfaces are located in Appendix B. ELAs were then calculated for each of these valleys using the AAR and THAR methods (Figure 3.10). ELAs calculated using the THAR method are, on average, ca. 45 meters higher than ELAs calculated using the AAR method (Table 3-1, 3-2). The AAR method reveals a segregation of ELAs into two assemblages. The valleys that exhibit multiple, high elevation cirque headwalls and ice tributaries, along with a more extensive advance (i.e., Deer Creek, Meadow Lake Creek, Long Canyon, and Bruce Canyon) have ELAs averaging ca. 2700 m. The valleys that exhibit a single low elevation cirque headwall (i.e., Ridgeway Mine (North and South) and Silver Moon Gulch) have ELAs averaging ca. 2600 m. Thus, the AAR method produces a ca. 100 m difference in ELAs between the large and small reconstructed glaciers. The difference in ELAs may be attributed to the hypsometry of the landscape

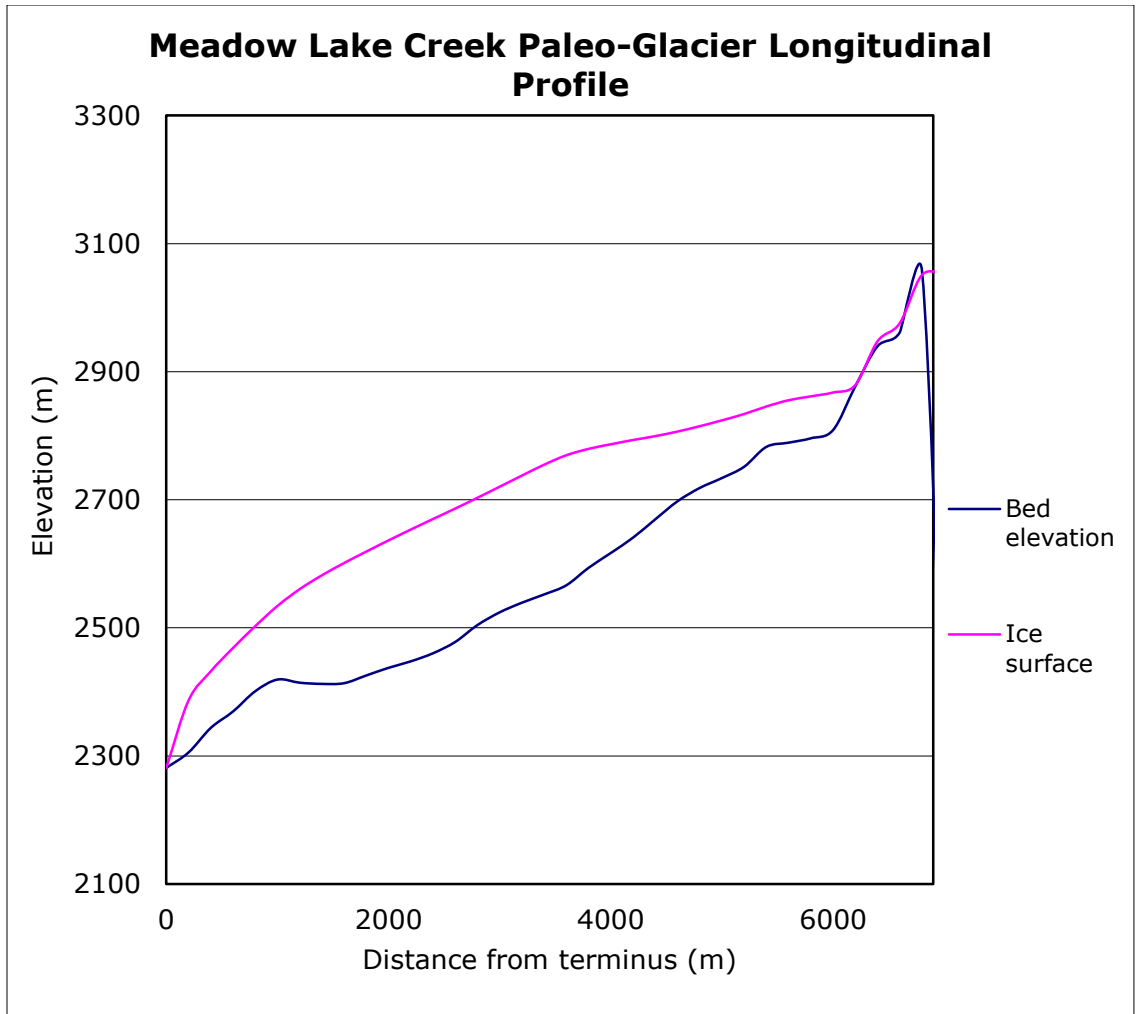


Figure 3.8 Meadow Lake glacier longitudinal profile determine from the *Profiler V.2 Excel™ Spreadsheet Program* (Benn and Hulton, 2010). The profile extends from the terminus of the glacier to the steep cirque headwall reaches. The pink line indicates the ice surface elevation along a center flowline. The blue line indicates the bed elevation. Glacier thickness decreases in the steep cirque headwall region, exhibiting negative ice thickness at certain elevations. Longitudinal profiles for the remaining reconstructed glaciers can be found Appendix B.

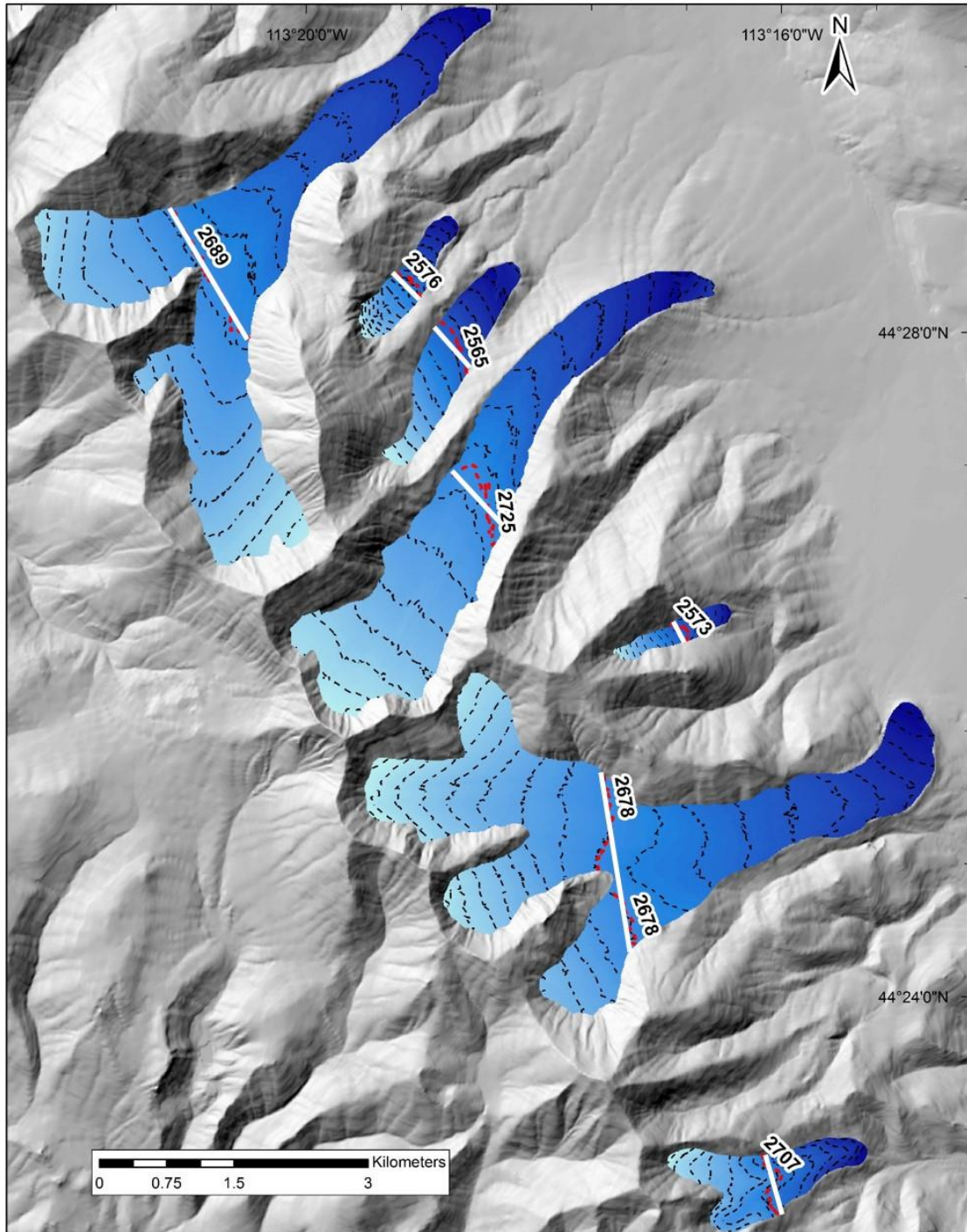


Figure 3.9 Glacier surface reconstructions and their corresponding equilibrium-line altitudes (ELAs) for the seven glaciated valleys corresponding to Figure 3.3. Black dashed lines are contour lines depicting glacier surface elevations. Red dashed lines and the corresponding numeric value are the ELAs calculated by the ELA toolbox (Pellitero et al., 2015). The white solid line refers to a generalized ELA for the glacier surface to eliminate the assertion of precision.

Table 3-1 Equilibrium-line altitudes (ELAs) for reconstructed glacier surfaces in the central Lemhi Range using an AAR value of 0.6. The average ELA is rounded to 2650 m to avoid inferences of precision.

Lemhi Range Paleo-Glacier ELAs			
Location	Valley Name	ELA (m)	Method
1	Deer Creek	2689	AAR
2	Ridgeway Mine North	2576	AAR
3	Ridgeway Mine South	2565	AAR
4	Meadow Lake Creek	2725	AAR
5	Silver Moon Gulch	2573	AAR
6	Long Canyon	2678	AAR
7	Bruce Canyon North	2707	AAR
Average		2645	

Table 3-2 Equilibrium-line altitudes (ELAs) for reconstructed glacier surfaces in the central Lemhi Range using a THAR value of 0.6. The average ELA is rounded to 2700 m to avoid inferences of precision.

Lemhi Range Paleo-Glacier ELAs			
Location	Valley Name	ELA (m)	Method
1	Deer Creek	2686	THAR
2	Ridgeway Mine North	2648	THAR
3	Ridgeway Mine South	2634	THAR
4	Meadow Lake Creek	2760	THAR
5	Silver Moon Gulch	2651	THAR
6	Long Canyon	2694	THAR
7	Bruce Canyon North	2746	THAR
Average		2690	

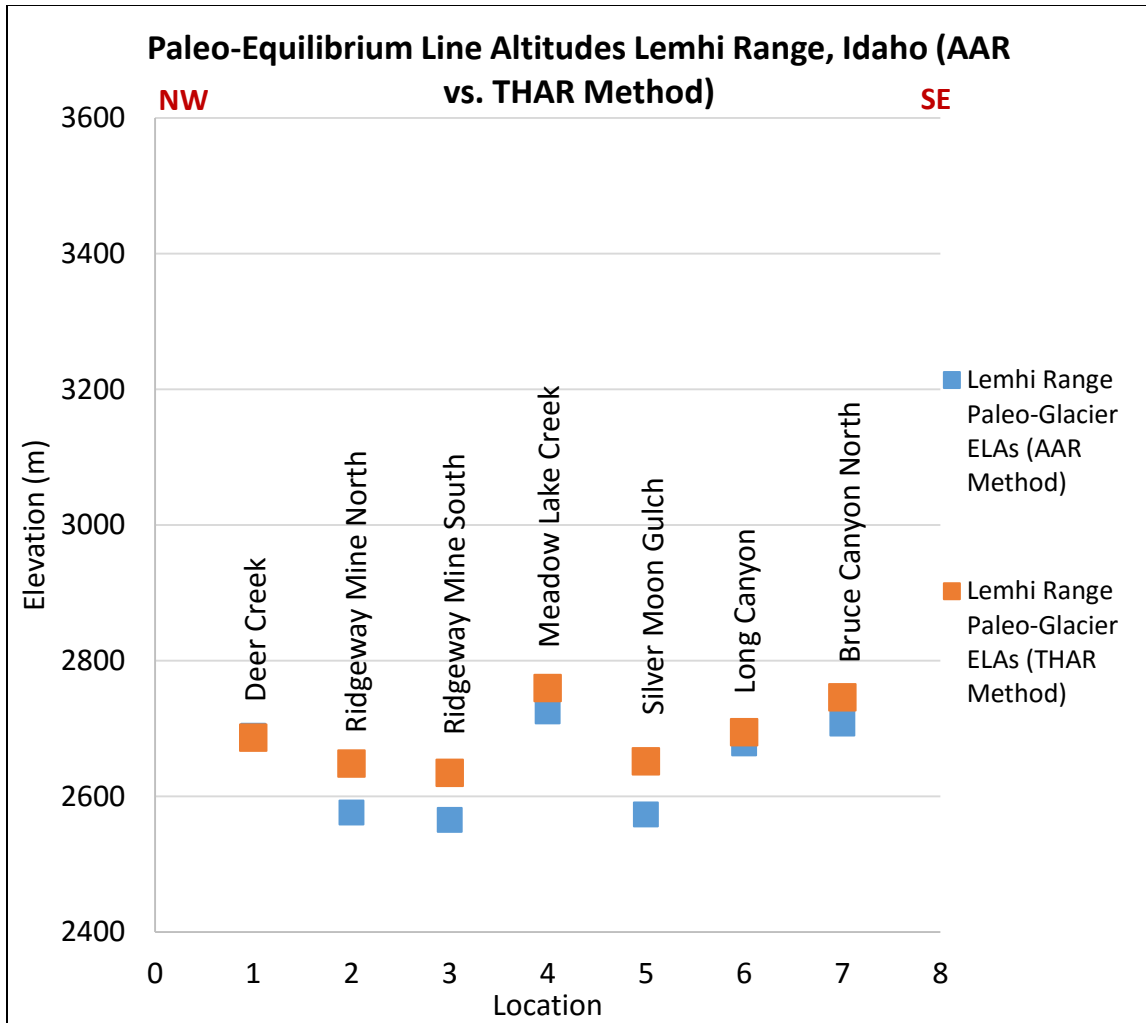


Figure 3.10 Equilibrium-line altitudes (ELAs) across the glaciated valleys (denoted for each location number) of the central Lemhi Range, Idaho, corresponding to Figure 3.9. ELAs were calculated using the accumulation-area ratio (AAR) method (blue squares), using an AAR of 0.6, and the toe-to-headwall-altitude ratio (THAR) method (orange squares), using a THAR of 0.6. ELAs, all are within the generally accepted methodological uncertainties of ± 50 m (Porter, 1975).

and the surface area available for snow and ice accumulation. It is possible that as the ELA falls below the hypsometric maximum, the rate of change in ice volume decreases, as modeled for the Bitterroot Range, USA, and Sierra Nevada, Spain, in a study by Pedersen and Egholm (2013). Additionally, the separation of the large and small valley glacier ELAs may also represent two separate glacial advances, due to the substantial

difference in the ELAs. However, this possibility does not fit the mapped moraine correlations.

The THAR method produces relatively similar results to those of the AAR method, with the larger valleys having higher ELAs than the smaller valleys. However, the THAR-derived ELAs exhibit a scatter of values with no obvious pattern between valleys. The 120 m spread of these ELAs is similar to that of the AAR method, however, Meierding (1982) suggested that the AAR method has a more satisfactory physical basis than the THAR method, thus producing more accurate results, because it integrates surfaces areas, absolute elevations, and gradients of ice accumulation and ablation, while the THAR method only utilizes the latter two criteria. He also suggests that the THAR method should be applied for initial reconnaissance of ELAs in mountain ranges where the ages of Pleistocene terminal moraines are known. Calculated Lemhi THAR and AAR estimates are within assumed uncertainty of ± 50 m (Porter 1975, 2001; Meierding, 1982). Average AAR and THAR ELAs are determined across the range in order to make regional comparisons between modern and paleo-ELAs. This study therefore focuses on ELAs derived from the AAR method, using an AAR value of 0.6, for regional comparisons. ELAs that were calculated using AAR values of 0.55 and 0.65 are located in Appendix C.

Modern ELAs have been calculated by Otto (1977), Reynolds (2011), and Davies (2011) for the Lost River Range, Teton Range, and the Wind River Range, respectively. Modern ELAs for these ranges rise to a maximum of ca. 3600 m (Wind River Range), with the average of the two most proximal modern ELA estimates (Lost River and Teton ranges) being ca. 3220. In comparison, average paleo-glacier ELAs, for both methods of

calculation used in this study, are ca. 2670 m. Modern ELAs are ca. 500-1000 m higher than the paleo-glacier ELAs calculated using the AAR and THAR methods (Figure 3.11). Primary emphasis is placed on the modern ELA of 3260 m (Staley, 2015) of the Lost River Range, because it is the most proximal active glacier to the Lemhi Range and is broadly similar to the average modern ELA of 3175 m, determined by Reynolds (2011), in the Teton Range (discussed in section 3.3.1). The average Lemhi paleo-ELAs are ca. 600 m lower than the estimated modern Otto Glacier ELA.

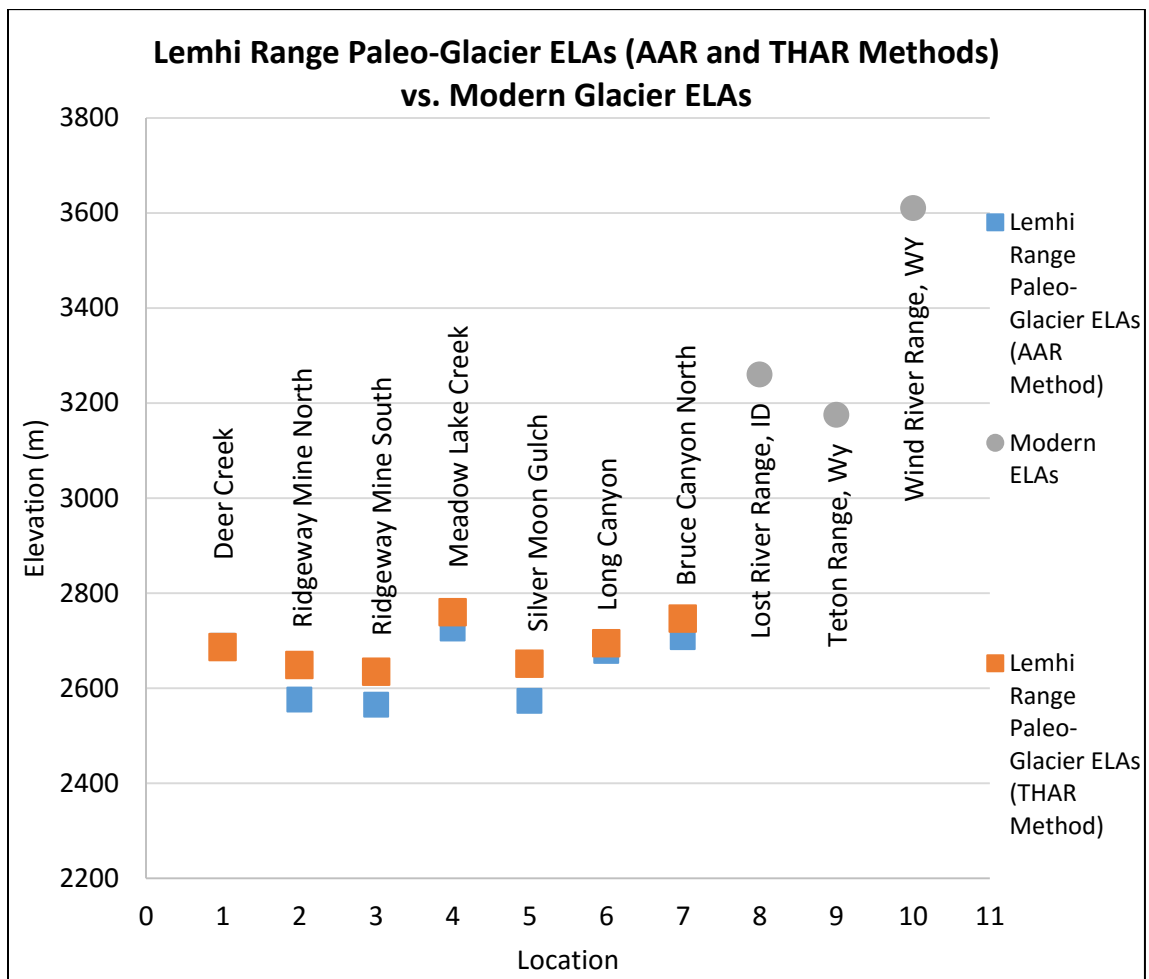


Figure 3.11 Comparison of the Paleo-glacier ELAs of the Lemhi Range calculated using the AAR method (blue squares) and the THAR method (orange squares) to modern ELAs (gray circles) of proximal mountain ranges.

3.6 Discussion

3.6.1 Glacial Advance Sequences

The timing of glacial advance in the Lemhi Range is inferred from moraine and outwash fan geomorphic positions determined through surficial mapping and from semi-quantitative analysis of moraine morphology. These techniques assess the spatial positioning of glacial features, as well as moraine crest angularity, relief, distal slope angles, and overall degree of degradation. This study identifies four major glacial advances, based on morphologic sequences, and suggests possible correlations relative to Marine Isotope Stages based on the relative dating analysis. Figure 3.17, which depicts the correlation of glacial advances with their inferred ages, is located at the end of this section.

Lemhi Advance 1

Lemhi Advance 1 advance is evidenced by mapped Qm1 and Qf1 landforms in the central Lemhi Range and is the most extensive ice advance at Deer Creek, located in the northern portion of the Gilmore quadrangle, with landforms exclusively preserved there (Figure 3.13A). There, Lemhi Advance 1 is represented by a small area and low relief Qm1 end moraine with a spatially related Qf1 outwash fan lying 5-10 m above the adjacent, younger Qf3 fan. No chronological evidence was extracted from landforms of Lemhi Advance 1, so a numerical age was not determined. Surficial mapping shows that Qm1 is older than the up-valley Qm2 end moraine of Deer Creek (Plate 1). The Qm1 longitudinal profile (Figure 3.12A) shows a moderately broad terminal crest that peaks at ca. 2190 meters above sea level (masl), with the toe of the moraine at ca. 2175 masl (relief of 15 m), and a distal slope of ca. 0.2 (ca. 11°). The broad crest, and low slope and

relief provide evidence for a high degree of degradation of the Qm1 end moraine. Therefore, the landforms representing Lemhi Advance 1 indicate an older glacial sequence.

Bull Lake age moraines have been previously identified across the intercontinental United States in both a qualitative and quantitative manner. Chadwick (1997) described fifteen Bull Lake moraines in the Wind River Range (WRR), Wyoming, using relative age criteria and described the moraines as having low relief and shallow slopes. Additionally, Phillips (1997) measured ^{36}Cl ages for boulders in Bull Lake complexes in the WRR. Both Chadwick (1997) and Phillips (1997) determined ages of Bull Lake moraines to be ca. 130-95 ^{36}Cl ka, correlative with MIS 6-5b. Based on the degree of degradation, shallow slopes, and low relief observed in the Lemhi Range and WRR, I infer that Lemhi Advance 1 correlates to MIS 6 relating to Glaciation II (Bull Lake-age) described by Knoll (1977)

Lemhi Advance 2

Lemhi Advance 2 is evidenced by the mapped Qm2 and Qf2 landforms and represents the second most extensive ice advance at Deer Creek. However, this advance either extended over landforms representing Lemhi Advance 1 in some valleys or advanced into area in which Qm1 and Qf1 had been eroded, making Lemhi Advance 2 the most extensive advance with preserved evidence at Meadow Lake Creek and Long Canyon (Plate 1) (Figure 3.13A-D). In addition, lateral remnants of Qm2 and Qf2 fan remnants are exposed at Lemhi Union Gulch and Spring Mountain Canyon (Figure 2.6A). Landforms of Lemhi Advance 2 include Qf2 fan remnants, isolated by ca. 20 m of incision from the younger Qf3 outwash fan sequence, and reside at similar elevations

between valleys of ca. 2200 – 2300 masl. Surficial mapping shows that landforms representing Lemhi Advance 2 are located up-valley from the landforms representing Lemhi Advance 1. Morphological characteristics of Qm2 termini, extracted from Qm2 longitudinal profiles (Figure 3.12A, B, C), provide semi-quantitative evidence for a younger glacial advance.

Lemhi Advance 2 – Spatial Comparison of Landforms Between Valleys

Lemhi Advance 2 at Deer Creek exposes a cohesive, intact Qm2 end moraine that exhibits an arcuate shape. Qm2 contains dead ice landforms within the terminus of the moraine. Qf2 fan remnants form linear, fan-shaped features with prominent ridgelines that extend towards the valley and grade to Qm2 moraines (Figure 3.13A). Lemhi Advance 2 at Meadow Lake Creek is evidenced by Qm2 end moraine and Qf2 fan remnants. Qm2 remnants parallel the arcuate trend of Qm3 (Figure 3.13B), and Qf2 remnants are similar to those of Deer Creek. The landform representing Lemhi Advance 2 at Silver Moon Gulch is exposed as a small, intact Qm2 end moraine, with no evidence of Qf2 fan remnants. The Qm2 deposit and associated trimlines can be faintly traced up-valley to the cirque headwall (Plate 1). Lemhi Advance 2 at Long Canyon is represented by a well preserved, nearly continuous Qm2 end moraine remnant and Qf2 fan remnants in the landscape (Figure 3.13C). The Qm2 moraine remnant parallels the arcuate trend of Qm3. Qf2 remnants are similar to those of Deer Creek. Lemhi Advance 2 at Spring Mountain Canyon and Lemhi Union Gulch is represented by a single lateral Qm2 moraine remnant in each valley, outside of the younger Qm3 lateral moraine. Qf2 fan remnants persist in the landscape near the range-front (exclusively at Spring Mountain Canyon). Qf2 remnants are similar to those of Deer Creek (Figure 3.13D).

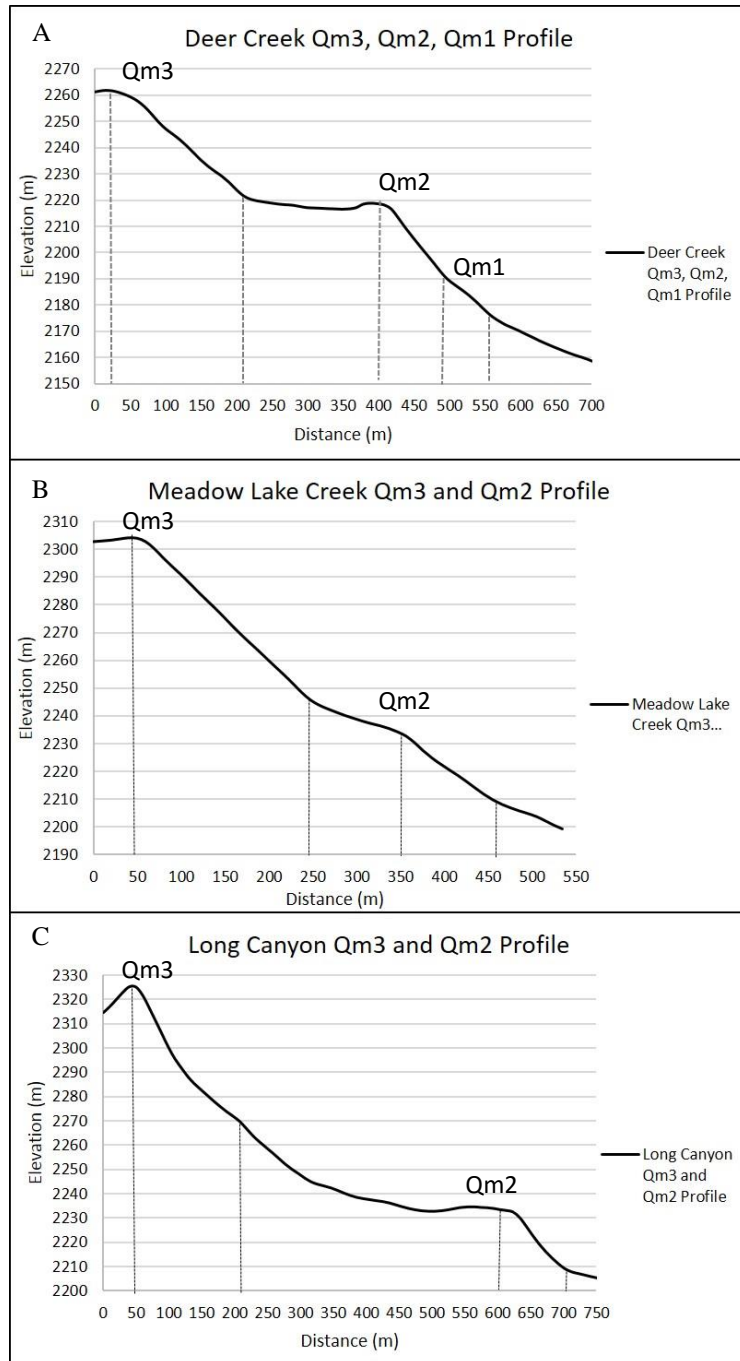


Figure 3.12 A) Deer Creek longitudinal profile depicting the relief and crest sharpness of the Qm3, Qm2, and Qm1 end moraines. B) Meadow Lake Creek end moraine profiles depicting relief and crest sharpness of Qm3 and Qm2 end moraines. C) Long Canyon end moraine profiles depicting relief and crest sharpness of Qm3 and Qm2 end moraines. Gray dashed lines indicate the approximate horizontal extent of the end moraines (from crest to toe). Slope is inferred from the change in elevation divided by the change in distance (from crest to toe). Deer Creek and Meadow Lake Creek profiles were extracted from the exposed terminal moraines, while the Long Canyon profile was extracted from the exposed lateral moraines.

These relationships imply that ice lobes formed in the high elevation cirques of these valleys. Multiple ice lobes coalesced in Deer Creek, Long Canyon, and Spring Mountain Canyon, while a single ice lobe formed in Meadow Lake Creek, Silver Moon Gulch, and Lemhi Union Gulch. As ice flowed east-northeast down the eastern valleys of the central Lemhi Range, Qm2 and Qf2 were created simultaneously when the glaciers reached an equilibrium state at or near their maximum extent. Recessional glacier features, representing Lemhi Advance 2, are nonexistent due to later glacial advances covering or eroding older features up-valley. Later glacial advances (i.e., Lemhi Advance 3) initiated erosion and meltwater incision of older landforms representing the Lemhi Advance 2 advance, leaving remnants of these landforms perched in the surrounding landscape.

Lemhi Advance 2 – Morphological Comparisons of Moraines Between Valleys

The morphology of the Qm2 end moraine at Deer Creek (Figure 3.12A) shows a moderately sharp crest that peaks at ca. 2,220 masl, with the toe of the moraine at ca. 2,190 masl (relief of ca. 30 m), and a distal slope of ca. 0.33 (ca. 18°). This Qm2 end moraine exhibits a higher relief, sharper crest, and a similar slope to that of the Qm1 moraine, indicating a younger glacial advance. The morphology of the Qm2 end moraine at Meadow Lake Creek (Figure 3.12B) shows a moderately broad crest that peaks at ca. 2,235 masl, with the toe of the moraine at ca. 2,210 masl (relief of 25 m), and a distal slope of ca. 0.25 (ca. 14°). This Qm2 moraine exhibits a similar relief, crest angularity, and a slightly steeper slope relative to the Qm1 moraine. These similar characteristics may contradict the spatial patterns and be indicative of a similar age/glacial advance. The morphology of the Qm2 end moraine at Long Canyon (Figure 3.12C) shows a sharp

crested moraine that peaks at ca. 2,235 masl, with the toe of the moraine at ca. 2,210 masl (relief of 25 m), and a distal slope of 0.25 (ca. 14°). This Qm2 moraine, though measured in the lateral moraine rather than the terminal moraine, exhibits a sharper crest, higher relief, and a steeper slope angle relative to the Qm1 moraine. These morphologic characteristics of Qm2 end moraines provide evidence for a glacial advance that is younger than Lemhi Advance 1 based on the lower degree of degradation, more abundant exposure, and up-valley location relative to Lemhi Advance 1 representative landforms. However, the similar characteristics between Qm1 at Deer Creek and Qm2 at Meadow Lake Creek may be indicative of a similar age. Throughout these valleys, the spatial separation of these landforms from the landforms representing Lemhi Advance 3 are not well understood, with Lemhi Advance 2 landforms potentially being buried, or slope angles being altered, by deposition of Lemhi Advance 3 associated landforms.

Lemhi Advance 2 – Regional Comparison

The relative age criteria and morphology of the Qm2 moraines can be compared to previous regional studies to further elucidate the relative timing of Lemhi Advance 2. The general morphology of Qm2 moraines in the study area is degraded, with broad to moderately sharp crests and shallow to moderately shallow distal slopes. Lundeen (2001) used moraine morphometry, in which crest width, proximal slope, distal slope, and crest angularity were measured to determine the relative age of moraines in the Pettit Lake, Yellow Belly Lake, and Hell Roaring Lake valleys in the Sawtooth Mountains. Lundeen (2001) determined that crest width showed an age trend in Pettit Lake valley, with crest width decreasing with decreasing age. In addition, it was determined that crest angularity decreases with increasing moraine age in all three valleys. Moraines were grouped into an

older, low-angularity group and a younger, high-angularity group. The morphology of these moraines are described by Lundeen (2001) as fresh with angular crests, steep slopes, and thin soils, consistent with regional descriptions of MIS 3-2 age moraines in the Pioneers (Evenson et al., 1982) and McCall (Colman and Pierce, 1986). Conversely, Bull Lake deposits in these areas have been described as more subdued and dissected, lacking kettles, and having well developed soils. The Qm2 end moraines described here do not exhibit the steep slopes and angular crests, as described in previous studies, thus indicating greater antiquity. Based on the spatial mapping, general morphology, and regional comparisons of moraine morphology, I infer that Lemhi Advance 2 is of MIS 4-3 age, relating to Glaciation III (Middle Pinedale age), with the Qm2 moraine at Meadow Lake Creek being of possible MIS 6 age, relating to Glaciation II (Bull Lake).

Lemhi Advance 3

Lemhi Advance 3 is evidenced by Qm3 and Qf3 mapped landforms and represents the third most extensive ice advance in the central Lemhi Range. Landforms representing Lemhi Advance 3 are exposed at Deer Creek, Ridgeway Mine, Meadow Lake Creek, Silver Moon Gulch, Long Canyon, Lemhi Union Gulch, Bruce Canyon, and Spring Mountain Canyon (Plate 1) (Figure 3.13A-D). This includes nearly all of the eastern range-front valleys, indicating extensive glaciation during this time. Qm3 end moraines extend to, or beyond, the range-front at Deer Creek, Meadow Lake Creek, Long Canyon, and Spring Mountain Canyon, residing at similar elevations (ca. 2200 – 2300 masl). Qm3 end moraines are also located at higher elevations in the smaller valleys of Ridgeway Mine, Silver Moon Gulch, Lemhi Union Gulch, and Bruce Canyon, residing at similar elevations (ca. 2400 – 2500 masl). Qm3 end moraine complexes are composed of

extensive, intact, sharp crested terminal and lateral moraines. Qf3 is exposed as a single, continuous outwash fan unit across the eastern range-front that grades to all Qm3 moraines and dissects older glacial and outwash features.

Lemhi Advance 3 – Spatial Comparison of Landforms Between Valleys

The up-valley location of Qm3 relative to Qm2 and Qf2 and the lower elevation of Qf3 relative to Qf2 indicate that landforms of Lemhi Advance 2 are older than those of Lemhi Advance 3. Lemhi Advance 3 landforms contrast between large and small valleys. Advances in the larger valleys (i.e., Deer Creek, Meadow Lake Creek, Long Canyon, and Spring Mountain Canyon) develop from larger, and in some cases multiple, ice tributaries on the east-northeast-facing slopes of the high peaks that receive minimal insolation (Figure 3.14). This engenders greater accumulation, in the form of precipitation and wind-blown snow, and evasion of sun exposure, maintaining colder temperatures, with these factors together yielding more extensive advances. Glaciers at Ridgeway Mine, Silver Moon Gulch, Lemhi Union Gulch, and Bruce Canyon also originate on the flanks of cold, east-northeast-facing slopes, but have carved smaller cirque headwalls at lower elevations east of the divide. The differences of cirque headwall elevation and glacier morphology contribute to variability in the equilibrium-line altitudes (ELAs) across the central Lemhi Range (Chapter 3).

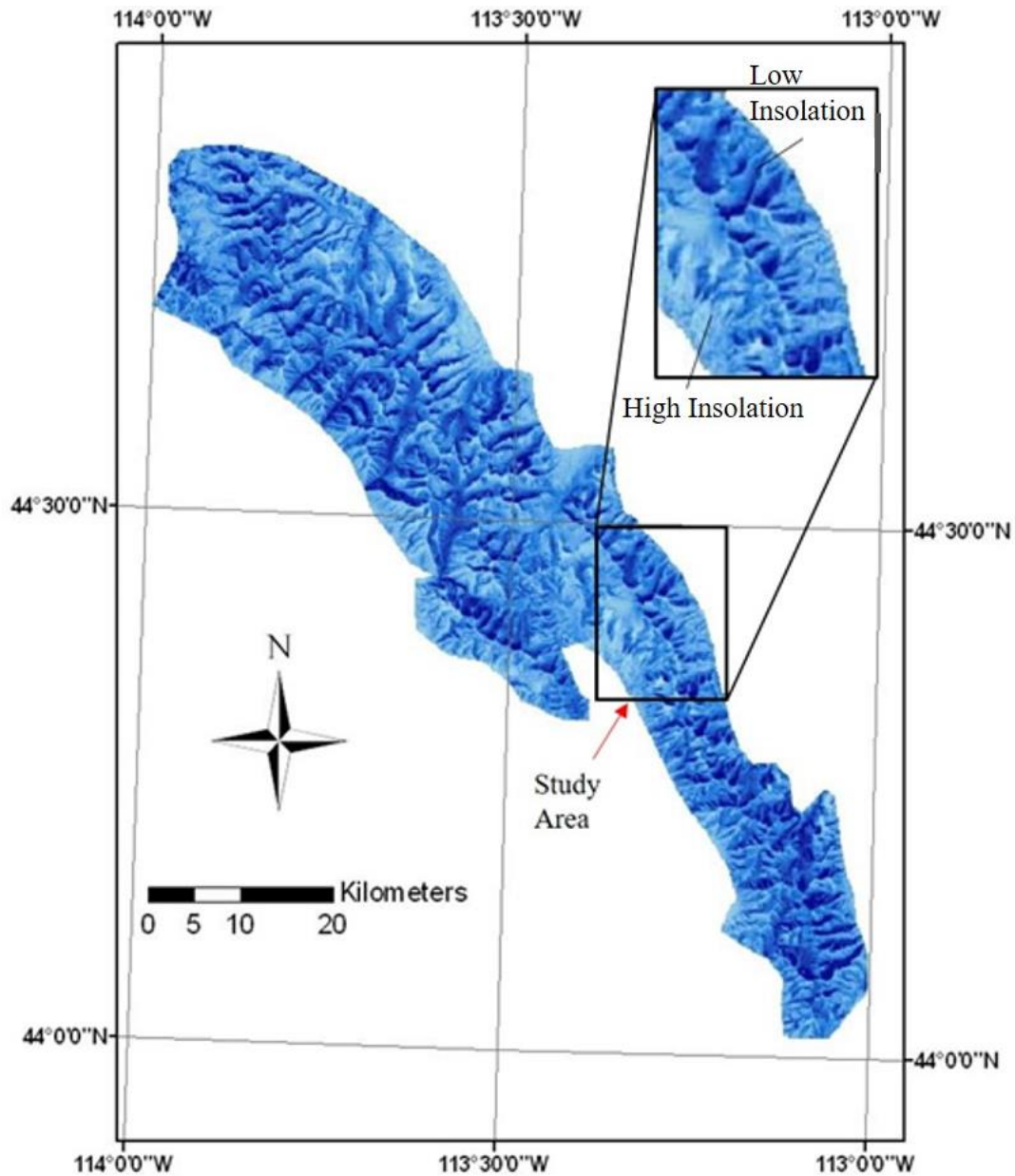


Figure 3.14 Hillshade image of the Lemhi Range depicting the influence of aspect, relief, and slope on solar insolation. Dark blues represent areas of low duration of insolation. Light blues represent areas of high duration insolation. Figure is based on modern insolation values. Inset map focuses on the slopes of the Gilmore and Big Windy Peak quadrangles. It is important to note that Figure 2.13 is based on modern insolation values. These values could have potentially been different during the Middle-Late Pleistocene due to orbital variations influencing insolation maxima and minima. However, the relative values are likely to be similar due to strong topographic influence, which is assumed to be similar. Figure modified from Johnson et al. (2007).

Lemhi Advance 3 – Morphological Comparisons of Moraines Between Valleys

Geomorphic relationships of Qm3 end moraines provide evidence for the relative age of Lemhi Advance 3. The morphology of the Qm3 end moraine at Deer Creek (Figure 3.12A) shows a sharp crest that peaks at ca. 2,260 masl, with the toe of the moraine at ca. 2,220 masl (relief of ca. 40 m), and a distal slope of ca. 0.5 (ca. 27°). The morphology of the Qm3 end moraine at Meadow Lake Creek (Figure 3.12B) shows a sharp crest that peaks at ca. 2,305 masl, with the toe of the moraine at ca. 2,245 masl (relief of ca. 60 m), and a distal slope of ca. 0.4 (ca. 22°). The morphology of the Qm3 end moraine at Long Canyon (Figure 3.12C) shows a sharp crest, with the lateral portion peaking at ca. 2,325 masl, the toe of the moraine at ca. 2,270 masl (relief of ca. 55 m), and a distal slope of ca. 0.4 (ca. 22°). The Qm3 end moraines are sharp crested, have higher relief, and similar or steeper slope angles compared to Qm2 end moraines, indicating a lower degree of degradation, and allowing age-contrast inferences with other landform units. The up-valley terminal position, sharp crests, steep slopes, and high relief of Qm3 end moraines, relative to Qm2 and Qm1, provide evidence that Lemhi Advance 3 is a more recent advance. The three distinct groupings of glacial features based on spatial positioning and relative weathering criteria must represent events that are distinctly spaced in age by at least ca. 10 ka (the estimated minimum amount of time to produce discernable ages by relative weathering). Therefore, I infer that Lemhi Advance 3 is of MIS 2 age, relating to Glaciation III (Late Pinedale) described by Knoll (1977).

Additionally, Qm3 end moraines at Deer Creek, Ridgeway Mine, Meadow Lake Creek, and Bruce Canyon are mantled with talus composed of Ok quartzite boulders, exposed along their termini and lateral portions. This exposure provides two possible

interpretations of the timing of deposition of these matrix-free moraine slopes. First, if the deposits are blockfields that were generated by glacial and periglacial conditions, the Qm3 end moraines persisted through a period of extreme cold, most likely the LGM. The extreme cold would have initiated frost jacking, driving large, blocky material to the surface of these features. If this occurred, then the moraines likely pre-date the LGM. The second interpretation is that the deposits originated from rockfalls that occurred while ice was at or near its stabilized position, with the debris transported supraglacially and concentrated in the moraines (see, for example, Shulmeister et al., 2009). These deposits are missing from both Qm1 and Qm2 end moraine complexes, indicating that the rockfalls would have occurred only during the construction of Qm3 end moraines.

Lemhi Advance 3 – Regional Comparison

The general morphology of Qm3 end moraines in the study area is fresh, with sharp crested ridges and steeply slopes, nested kettle topography, and high relief relative to Qm1 and Qm2 end moraines indicating minimal degradation and no incision associated with later glacial advances. These moraine descriptions are consistent with the younger, high angularity moraine groups at Pettit Lake, Yellow Belly Lake, and Hell Roaring Lake valleys in the Sawtooth Mountains described by Lundeen (2001). The morphology of these moraines also compares well with the younger moraines at McCall, Idaho, in which Colman and Pierce (1986) described the Pilgrim Cove and McCall deposits as being narrower and having steeper slopes, with weathering rind thickness suggesting MIS 2/Pinedale age deposits. Evenson et al. (1982) also recognized fresh surface, sharp crested, and kettle preserved moraines with high surface boulder frequencies in the Pioneer Mountains, which were correlated to Pinedale age (Potholes glaciation). These moraines are also numerous and located up-valley from older Copper

Basin moraines. Regionally, MIS 2 moraines are described as having fresh morphology, sharp crests, and common kettles. The similar morphology, spatial positioning, and kettle abundance between regional Pinedale/MIS 2 age moraines and the Qm3 end moraines in the Lemhi Range provide additional evidence for the inference that Qm3 moraines are MIS 2 age.

Lemhi Advance 4

Lemhi Advance 4 is evidenced by mapped Qm4 and Qf4 landforms and represents the youngest ice advance in the central Lemhi Range. Qm4 end moraines associated with this advance represent equilibration of ice at terminal positions during the latest advance phase and earliest retreat phases of glaciation. Qm4 moraines and the coeval Qf4 outwash fan are exposed at Bruce Canyon and Spring Mountain Canyon (Plate 1) (Figure 3.13D). The landforms representing Lemhi Advance 4 reside at elevations of ca. 2400 – 2600 masl. Qm4 end moraines are intact, sharp crested, transverse ridges located up-valley of Qm3 end moraines. However, Qm4 exposed in the main valley of Spring Mountain Canyon shows evidence of incision either from, post-glacial stream incision or a glacial outburst flood. Qf4 is exposed as small, continuous outwash fan surfaces, grading to Qm4 moraines and filling incised channels through older glacial and outwash features. The relatively pristine character and up-valley terminal and retreat positions indicate the youngest glacial sequence. I infer this advance to be of late MIS 2 age (latest Pinedale age or late-glacial).

Western Flank Glacial Extent

Converse to the pattern of glaciation along the eastern flank of the central Lemhi Range, the western flank exhibits little evidence of glaciation. Detailed aerial photograph

and satellite imagery analysis revealed very few glacial landforms, contradicting Ruppel and Lopez (1981), who mapped extensive morainal areas there. A likely explanation of the contrast of glaciation on the eastern and western flanks of the range can be found in relief and aspect contrasts. West-southwest facing slopes and lower relief dominate this portion of the range and the area thus experiences longer durations of sun exposure than the east side (Figure 3.14). Longer duration insolation hinders the long-term accumulation and preservation of snow, ultimately yielding little to no ice cover. This pattern is converse to that of the eastern slopes.

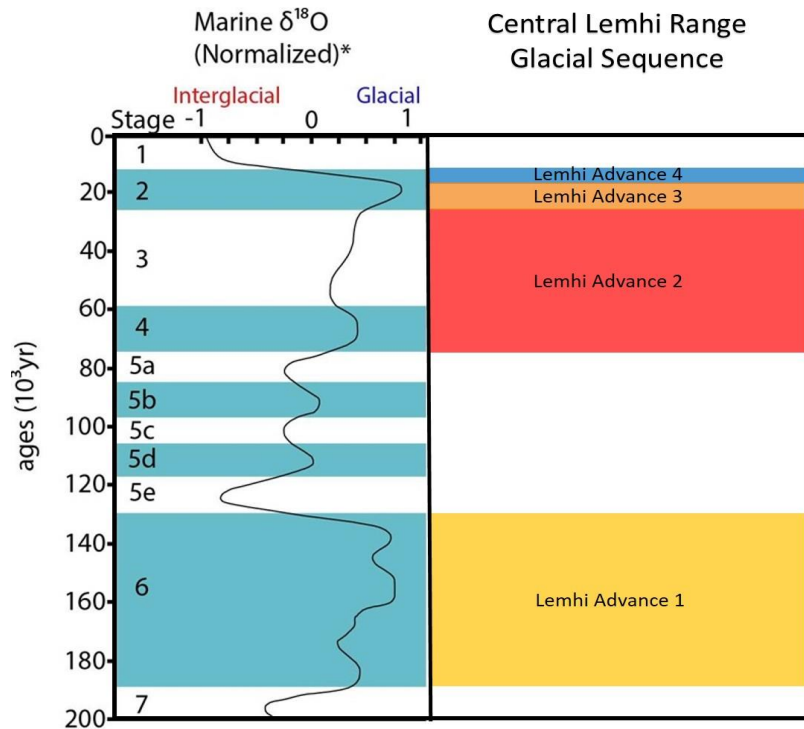


Figure 3.15 The central Lemhi Range glacial sequence (right) correlated with the Marine Isotope Stages (MIS) (left) based on relative dating techniques. From oldest to youngest the advances are: Lemhi Advance 1 (yellow) (MIS 6), Lemhi Advance 2 (red) (MIS 4-3), Lemhi Advance 3 (orange) (middle MIS 2), and Lemhi Advance 4 (blue) (latest MIS 2 or late-glacial). Colors of advances are intended to match the mapped end moraines, and represent the range of inferred ages. Actual events were likely limited to narrow time windows within MIS 6 and MIS 4-3, rather than extending through those periods. Figure modified from Kaufman et al. (2003), based on original data from Martinson et al. (1987).

3.6.2 Inferences from Insolation

The moraine sequences exposed in the Gilmore and Big Windy Peak quadrangles are hypothesized from morphological evidence to date to MIS 6-2. Interpretation of the spatial and temporal patterns of glaciation in the Lemhi Range and the region must consider the relationship between ice sheets, mountain glaciers, and their associated climatic conditions. Continental climatic regimes influence ice sheets, while mountain glacier systems respond to regional climatic fluctuations and are more responsive to short-lived climatic excursions. Milankovitch cycles indicate that summer insolation at high northern latitudes paces the growth and reduction of Northern Hemisphere ice sheets, showing an approximate 100,000-year periodicity of gradual growth and fast termination, since 800 ka (Abe-Ouchi et al., 2013). Insolation variations can influence mountain glacier systems, although regional temperature and precipitation contrasts provide a greater influence on glacier growth and retreat. Based on the Milankovitch cycles, periods of insolation minima at 65°N latitude for summer months (correlative to June 21st) are apparent for the early and late stages of MIS 6, as well as MIS 4 and MIS 2 (Figure 3.16).

If the ages of all of the Lemhi moraines are revealed to be MIS 6 and MIS 2, then dry, cold climatic conditions (cool, dry summers) likely influenced glaciation most strongly. As first proposed by Kutzbach et al. (1993), and Thompson et al. (1993) weakened westerly flow caused by anticyclonic ice-sheet circulation may have caused substantial aridity accompanying cold temperatures in the northern US during MIS 2. During MIS 3, insolation peaked around 34 ka and 60 ka, and declined around 50 ka at 65°N latitude for summer months (Figure 3.16). If the ages of the moraines are revealed

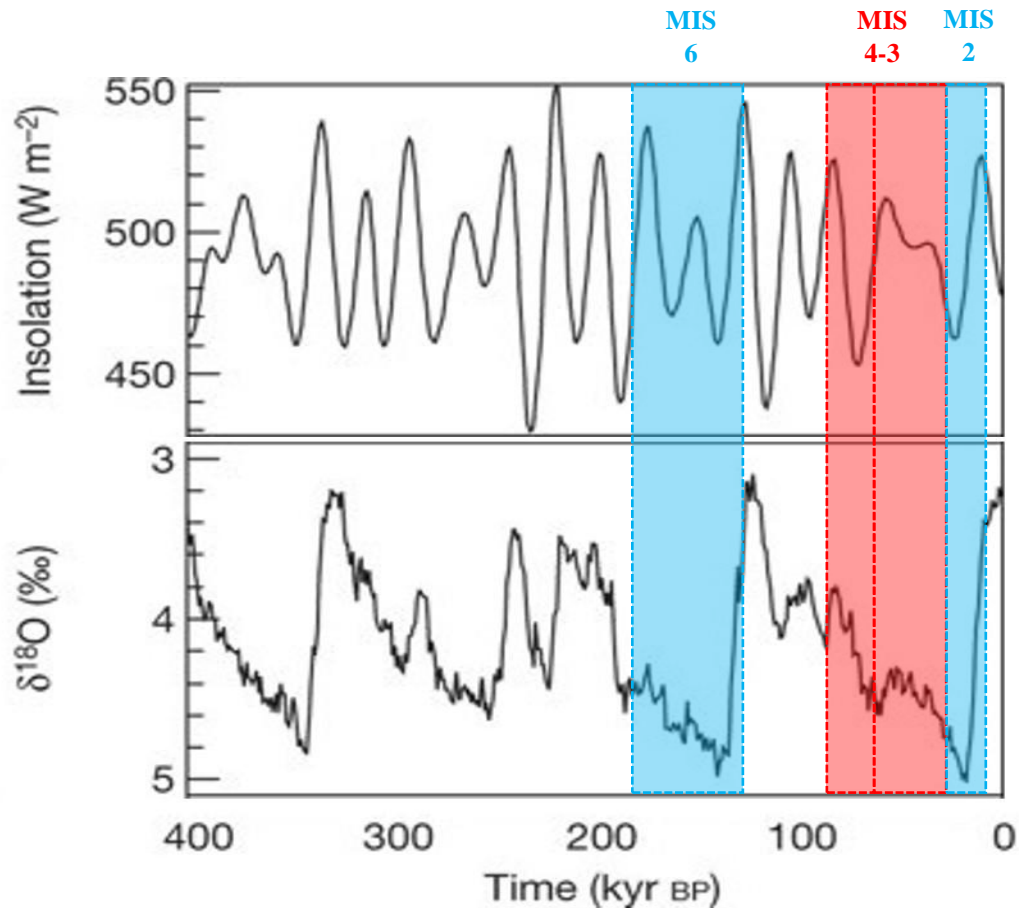


Figure 3.16 Time series of forcing and responses of Northern Hemisphere ice sheets. Emphasis is placed on the mean atmospheric insolation at latitude $65^{\circ}N$ on 21 June of each year (top graph) and ice volume (bottom graph). The blue shaded regions depict periods of insolation minima during MIS 2 and MIS 6. The red shaded region depicts a period of increasing insolation during MIS 4-3. Figure modified from Abe-Ouchi et al. (2013).

to correlate with MIS 3 insolation peaks (as in the Olympic Mountains; Thackray, 2008, and Staley, 2015), solar radiation must have been nearing relative peak conditions for that time interval, and warm, and potentially wet, climatic conditions (especially wet winters) overcame the relatively probable less cold summer temperatures to enhance glaciation. Although these hypothesized scenarios are plausible, CRN ages will ultimately quantify the timing of glaciation across the central Lemhi Range. The criteria presented above, as well as subsequent assessment of deglaciation, ELAs, and climatic inferences, provide substantial evidence for the timing of glaciation, independent of numerical ages.

3.6.3 Regional Glacial Recession

The final phases of deglaciation began as glaciers receded from Qm4 terminal positions. A basal sediment date of ca. 14 ± 0.5 cal ka BP, indicating a minimum timing of final deglaciation of the cirque, was determined from lake cores taken from Meadow Lake, located at the head of the Meadow Lake Creek valley within the Gilmore quadrangle (B. Finney, personal communication, 2015).

A terminal age for deglaciation of 14 ± 0.5 cal ka BP for the Lemhi Range can be compared to regional ages of maximum advance, onset of retreat, and completion of retreat to better understand the variability in timing of glacial retreat. Butler (1986), suggested that deglaciation was completed before $\sim 11,500 \pm 500$ ^{14}C years before present (yr BP), determined from radiocarbon dating of organic-rich sediments in meadows across the eastern front of the Lemhi Range. Approximate calibration of this age to calendar years produces a minimum deglaciation age of 13.6 ± 0.6 cal ka BP. The ages reported by Finney (2015) and Butler (1986) are indistinguishable at the reported uncertainties, as the uncertainty in ages overlap. Thackray et al. (2004) determined two distinct limiting dates of ca. 16.9 cal ka BP and 13.95 cal ka BP for glacial stillstands in the Sawtooth Mountains, Idaho, based on radiocarbon dating from sediment cores. Later, Mijal (2008) determined a minimum timing of deglaciation in the Sawtooths of ca. 14 cal ka BP from a depth-age model developed for a series of ^{14}C AMS radiocarbon samples from low-organic basal sediments in cirque lakes and tephra deposits. Sedimentation rates were determined from the models and ages were extrapolated for intervals between radiocarbon samples assuming a constant sedimentation rate. Collectively, these

radiocarbon ages reflect the onset of glaciation occurring 17-14 cal ka BP and a minimum limiting of recession completion of ca. 14 cal ka BP.

Gosse et al. (1995) determined that the entire glacial system in the Wind River Range, Wyoming, retreated to the cirque basin by $12,100 \pm 500$ ^{10}Be years, determined from ^{10}Be CRN dating of moraine crests and bedrock knobs, and applying a production rate of 6.01 ± 0.4 atoms $\text{g}^{-1} \text{yr}^{-1}$ for Pinedale. This published date uses much higher than currently accepted ^{10}Be production rate (3.99 ± 0.22 atoms $\text{g}^{-1} \text{yr}^{-1}$; Heyman, 2014) but the date may be close to the age that would result from re-calculation with the higher production rate, due to a ca. 15% correction that was applied to raw AMS data in the opposite direction of the re-standardization (owing to the changes in the accepted ^{10}Be decay constant since that time) (J. Gosse, personal communication, 2015).

Licciardi et al. (2004) describe three late Pleistocene ice advances in the Willowa Mountains, Oregon, documented with ^{10}Be CRN ages of 24.9 ± 0.9 ka, 19.7 ± 0.8 ka, and 12.9 ± 2.0 ka (Licciardi et al., 2004; recalculated by Licciardi, 2015 personal communication, using the new production rate of 3.99 ± 0.22 atoms $\text{g}^{-1} \text{yr}^{-1}$ in CRONUS 2.2 online calculator, Heyman, 2014; Staley, 2015). Licciardi et al. (2004) also described initiation of widespread deglaciation across the western U.S. of ca. 17 ka based on ^{10}Be CRN dating. Since the glacial advance ages are ca. 4 ka older when recalculated, recalculating the deglacial ages are assumed to be ca. 4 ka older as well, inferring that the onset of deglaciation began ca. 21 ka.

Licciardi and Pierce (2008) determined ages of the outer and inner sets of Pinedale end moraines at Jenny Lake in the Teton Range to be 14.6 ± 0.7 and 13.5 ± 1.1 ^{10}Be ka respectively, using a production rate of 4.96 ± 0.43 atoms $\text{g}^{-1} \text{yr}^{-1}$. Recalibration

of these ages using the updated production rate of 3.99 ± 0.22 atoms $\text{g}^{-1} \text{yr}^{-1}$ (Heyman, 2014) reveals ages of 15.9 ± 0.8 and 14.7 ± 1.1 ka for the outer and inner Jenny Lake moraines respectively, with an approximate deglaciation age of 15 ka (J. Licciardi, personal communication, 2015). Young et al. (2011) determined that deglaciation initiated in the Arkansas River basin, Colorado, between 16 and 15 ka from ^{10}Be CRN dating of inner most range-front moraines using a ^{10}Be production rate of 4.49 ± 0.39 atoms $\text{g}^{-1} \text{yr}^{-1}$. Additionally, Young et al. (2011) hypothesized that the demise of glaciers across the western U.S. occurred between 15 and 13 ka. The relative proportion of this production rate to the updated production rate suggests that the ages reported by Young et al. (2011) are approximately 10% younger than the ages would be using the updated production rate. Therefore, an estimated recalibration of these ages suggests that deglaciation initiated between 18 and 17 ka.

Kenworthy (2011) determined nearly complete deposition of Willow Creek alluvial fan surfaces of the Lost River Range, Idaho, to be 13-15 ka from optically stimulated luminescence (OSL) dating and fan morphology. This study is not directly comparable, as this reported age suggests proglacial fan aggradation and is therefore not correlative to the onset of deglaciation, nor completed cirque deglaciation.

Recalibration of radiocarbon and CRN ages is necessary to accurately compare the maximum extent of ice advances, onset of glacial retreat, and completion of glacial retreat. Broad recalibration of radiometric ages suggests that the onset of deglaciation began ca. 14-21 ka with glacial retreat completed by ca. 13-15 ka across the region. CRN ages will allow comparison of Lemhi deglacial onset with these areas.

3.6.4 Equilibrium-Line Altitudes

3.6.4.1 Equilibrium-Line Altitude Comparisons for Paleoclimatic Inferences

Equilibrium-line altitudes were calculated using both the AAR and THAR methods, and are associated with mapped Qm3 moraine deposits inferred to date to MIS 2. The average paleo-ELA for the Lemhi Range, calculated using an AAR of 0.6, is 2650 m, while the average paleo-ELA, calculated using a THAR of 0.6, is 2690 m. THAR and AAR estimates are within estimated uncertainty of ± 50 m (Porter 1975, 2001; Meierding, 1982), though the AAR calculation using the ELA toolbox reports a stated uncertainty of ± 5 m (Pellitero et al., 2015). The ELAs calculated using the AAR method can be compared to previously determined paleo-ELAs for the Lemhi Range, as well as to nearby mountain glacier systems, to deduce the climatic conditions corresponding to construction of Qm3 moraine units. THAR-derived ELAs, regional THAR comparisons, additional AAR-derived ELAs, and temperature depression are discussed in Appendix C.

This study and one other have focused on Lemhi Range glaciation and determination of ELAs to infer paleoclimatic conditions, although Meyer et al. (2004) also considered the Lemhi Range in the determination of ELAs and paleoclimatic conditions across the western U.S. Foster et al. (2008) focused on the influence of glacial erosion on limiting topography across the Teton Range, Beaverhead-Bitterroot Mountains, Lemhi Range, and Lost River Range. Glacier surfaces and ELAs were reconstructed for 20 valleys in the Lemhi Range. ELAs in that study were assumed to be correlated to the LGM and were calculated using the accumulation-area-balance ratio (AABR) and THAR methods (Figure 3.17). ELAs calculated by Foster et al. (2008) range from ca. 2500-2800 meters along the Lemhi Range. In the areas of the Gilmore and Big

Windy Peak quadrangles, the calculated ELAs range from ca. 2650-2750 meters. Thus, the ELAs calculated by Foster et al. (2008) are similar to the ELAs calculated in this study using the THAR method. However, it is difficult to compare the ELAs between the AAR and AABR methods, as the AABR method utilizes glacier hypsometry and mass balance gradients (Benn and Lehmkuhl, 2000).

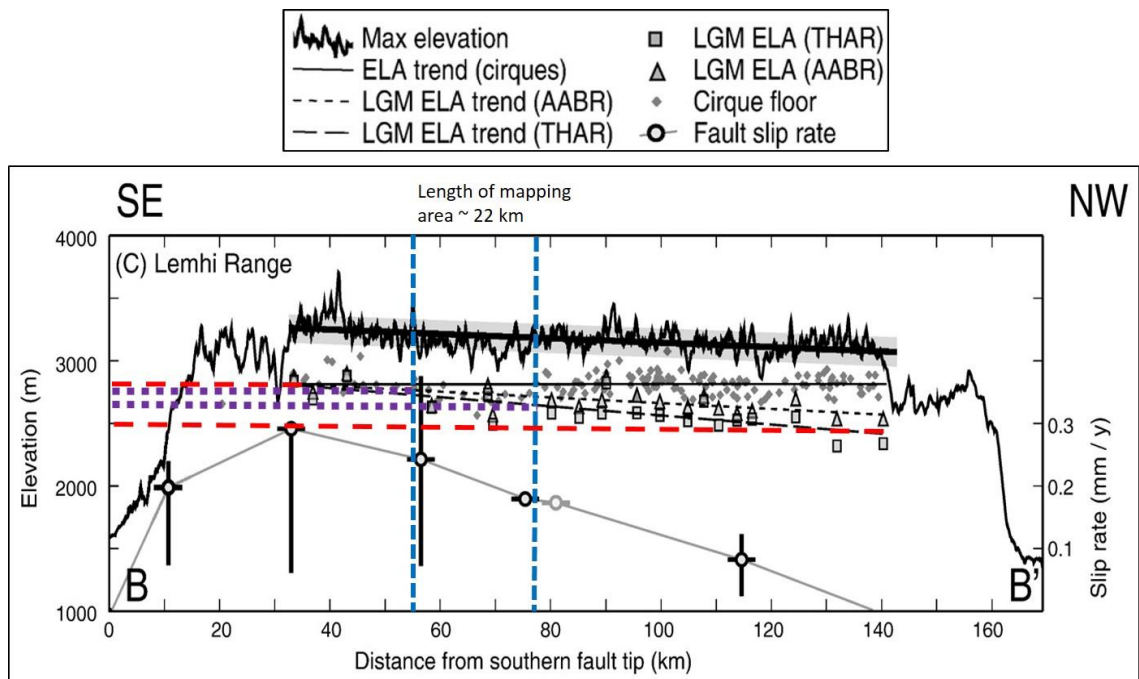


Figure 3.17 Assumed LGM equilibrium-line altitudes calculated across the Lemhi Range using the THAR (thick black dashed line and squares) and AABR (thick black dashed line and triangles). The horizontal red dashed line marks the upper and lower boundaries of the calculated ELAs for both methods used by Foster (2008). The vertical blue dashed lines bound the Gilmore and northeast quadrant of the Big Windy Peak quadrangles. The horizontal purple dashed line marks the upper and lower boundaries of inferred LGM ELAs calculated by Foster (2008) for the quadrangles. Figure modified from Foster et al. (2008).

Additionally, Meyer et al. (2004) reconstructed 510 paleo-ELAs for small late Pleistocene (inferred LGM/Pinedale) alpine glaciers in the Lemhi Range and other ranges across interior northwestern United States. That study applied an AAR of 0.65, which produced paleo-ELAs of ca. 2600-2900 m for the Lost River and Lemhi Ranges (Figure

3.18). An average ELA of 2700 m is determined from Figure 3.18, which coincides well with the average AAR ELA in this study.

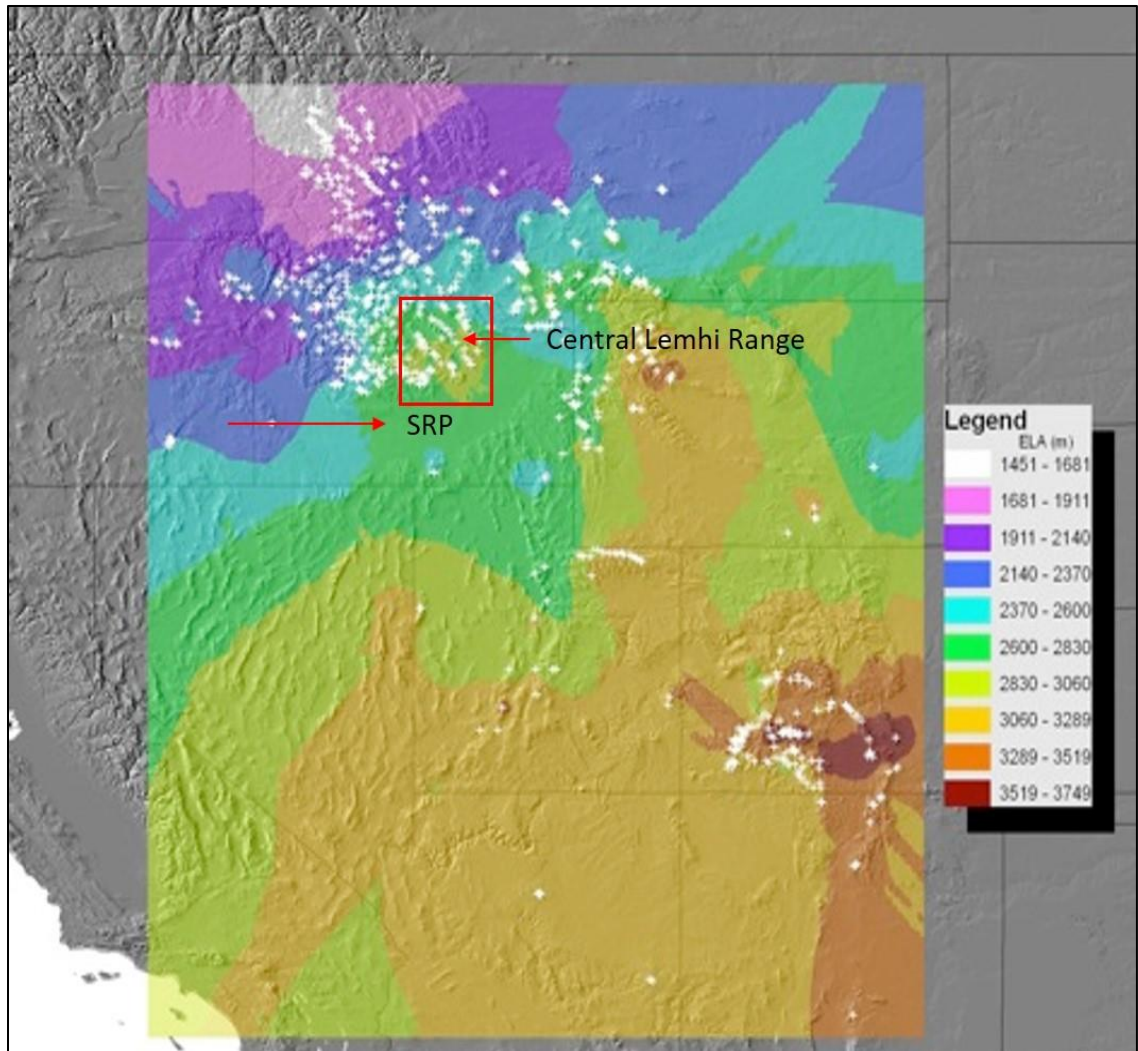


Figure 3.18 ELA contour map of the western United States produce assuming Pleistocene ELA maximums and utilizing the AAR method with an AAR of 0.65. Red bounding box denotes the location of the central Idaho Mountains. Arrows mark the locations of the central Lemhi Range and the Snake River Plain (SRP), Idaho. Figure modified from Meyer (unpublished data).

Previous regional studies have produced ELAs using the AAR method (Brugger, 1996; Lundeen 2001; Meyer et al., 2004) and the THAR method (Staley, 2015) to determine paleoclimatic conditions during glacial periods. Inland mountain glacier ELAs

reflect mainly continental climatic conditions and are potentially subject to both cooling and changes in precipitation patterns. The newly calculated AAR-derived ELAs for the central Lemhi Range can be compared to inferred LGM ELAs of other inland mountain ranges to infer the climatic conditions that produced glaciation relative to Lemhi Advance 3 sequences. These ELAs and corresponding locations are summarized for the AAR method in Table 3-3.

Table 3-3 Equilibrium-line altitudes calculated for inland mountain glacier systems using the Accumulation-Area Ratio (AAR) method. Uncertainty is approximately ± 50 m (Porter, 1975, 2001; Meierding, 1982).

Regional Paleo-ELAs (AAR Method)					
Location	Range Name	ELA (m)	Age	Source	Method
12	Sawtooth Mountains, ID	2670	MIS 2	Lundeen (2001)	AAR
12	Sawtooth Mountains, ID	2470	MIS 3	Lundeen (2001)	AAR
12	Sawtooth Mountains, ID	2600	LGM/Pinedale	Meyer et al. (2004)	AAR
13	Pioneer Mountains, ID	2730	MIS 3-2	Brugger (1996)	AAR
14	Lost River Range, ID	2950	LGM/Pinedale	Meyer et al. (2004)	AAR
15	Lemhi Range, ID	2650	Inferred MIS 2	Colandrea (2016)	AAR
15	Lemhi Range, ID	2720	LGM/Pinedale	Meyer et al. (2004)	AAR
16	Beaverhead Mountains, MT	2650	LGM/Pinedale	Locke (1990)	AAR

Similarities in ELA patterns are revealed when comparing the inferred MIS 2 ELAs of the Lemhi Range (average 2690 m) and the Sawtooth Mountains (average 2640 m) (average of values from Table 3-3). These similarities can be interpreted as 1) the inland mountainous region of Idaho experienced uniform cooling during the last glacial cycle, superimposed on consistent precipitation contrasts, or 2) limited delivery of precipitation to the Sawtooth Mountains from decreased westerly winds, coupled with

increased temperature depression in the Lemhi Range due to cold winds from the Cordilleran and Laurentide ice sheets, coincidentally produced similar ELA depressions of ca. 500m and ca. 600 m across these ranges, respectively. The following regional ELA comparisons are made to further elucidate the climatic conditions that produced inferred MIS 2 ELAs in the Lemhi Range and are depicted in Figure 3.19 at the end of this section. Lundeen (2001) used the AAR method for ELA calculation in the Sawtooth Mountains, Idaho, revealing average ELAs of ca. 2670 m for the dated MIS 2 moraine group, and ca. 2470 m for the inferred MIS 3 correlative moraine group. That MIS 2 ELA is ca. 20 m higher than the average Lemhi Range ELA, determined in this study, of 2650 m, while the MIS 3 ELA is ca. 180 m lower than the average Lemhi Range ELA. Meyer et al. (2004) determined an average LGM/Pinedale ELAs in the Sawtooths of ca. 2600 m (determined from Figure 3.18), ca. 50 m lower than the average Lemhi Range ELA of this study. The Sawtooths have previously been identified as a range that receives high amounts of precipitation, serving as an orographic barrier that intercepts moist Pacific air masses (Lundeen, 2001; Thackray et al., 2004; Staley, 2015), exemplifying a wetter climatic regime. A consistent precipitation pattern across regional mountain ranges, or an extreme temperature decrease in the Lemhi Range, could produce similar ELA patterns between the Sawtooth Mountains and the Lemhi Range.

Brugger (1996) used the AAR method for ELA calculation in the Pioneer Mountains, Idaho, revealing an average ELA of 2730 m for the Wildhorse Advance 1, inferred to correlate to MIS 3 or 2 (Staley, 2015). Meyer et al. (2004) determined LGM/Pinedale ELAs of ca. 2950, and 2720 for the Lost River Range and Lemhi Range respectively. These are average values determined from Figure 3.18 and are 300 and 70

m higher, respectively, than the inferred MIS 2 ELAs in the Lemhi Range determined in this study. Although the Lemhi Range ELA determined by Meyer et al. (2004) is beyond the ± 50 m uncertainty, it remains as a relatively close value, determined from a wide range of ELA values, and is used for comparison. The Pioneer Mountain and the Lost River Range ELAs are 80 and 300 m higher, respectively, than the average Lemhi Range ELA determined in this study. These values lie beyond the estimated ± 50 m uncertainty, making these ELA contrasts insignificant. Locke (1990) determined a range of ELAs for the Beaverhead Mountains using the AAR, THAR, and a variety of other methods, yielding an average LGM/Pinedale ELA of 2650 m.

To interpret Pleistocene paleoclimates, Locke (1990) estimated paleo-ELAs using the AAR (0.65), THAR (0.4), and a variety of other methods from 500 different former cirque and valley glaciers throughout western and central Montana that he assumed represented the climate at the peak of the last glaciation. Locke (1990) determined that the gradient of Montana paleo-ELA surfaces is the same for present glaciers in the region, decreasing from southeast to northwest, but that the paleo-ELAs lie ca. 450 m lower than modern ones.

Assuming that temperatures were 10° C lower than present and that paleo-precipitation is similar to modern precipitation, Locke (1990) determined that summer temperatures in the Beaverheads were ca. 2.5° C during the Pleistocene and that the latitudinal paleotemperature gradient was affected by the presence of the ice sheets, causing a change in wind-flow patterns. Those temperature estimates are influenced by a relatively low assumed winter accumulation (400-600 mm) required to support glaciation in the Beaverhead Mountains. Meyer et al. (2004) determined a similar pattern for the

northwestern continental interior, finding that the Lemhi Range, Lost River Range, and Idaho Pioneer Mountains exhibit high ELAs, suggesting a combination of precipitation shadows and moist air-mass diversion up the Snake River Plain, resulting in relatively dry climate. Pleistocene paleo-ELAs of the Beaverhead Mountains (ca. 25 km east-northeast of the Lemhi Range) range from ca. 2600-2700 m (Locke, 1990). Similar ELA values and depressions between these two adjacent ranges suggest that both ranges experienced similar climatic conditions during the late Pleistocene.

These relationships suggest that cold and dry climatic conditions were generated in the continental interior by cold easterly and katabatic winds during the LGM. It is plausible that the inferred easterly winds, generated by the anticyclone ice sheet circulation, were able to progress westward over and through the low portions of the Beaverhead Mountains, such as Railroad Canyon, eventually reaching the Lemhi Range. These cold easterly winds may have caused cold summer temperatures, suggesting that relatively low winter accumulation was required to support glaciation in these ranges. This suggests that moisture may have been transported in the lower atmosphere (less than 2 km above ground level), diverting moist air masses around these mountain ranges (Locke, 1990). Therefore, it is likely that at the LGM the Sawtooths experienced reduced precipitation from the glacial anticyclone weakening westerly winds, while the Lemhi Range experienced a greater temperature depression from cold katabatic winds from the ice sheets. These opposing temperature and precipitation conditions between ranges coincidentally produced similar ELA depressions of ca. 500 m, determined by Meyer (2004) and ca. 600 m, determined in this study across the Sawtooth Mountains and Lemhi Range respectively. This cold and dry climatic pattern would allow for ELAs of the

eastern flank of the Lemhi Range to be lower than the LRR and equivalent to the wetter Sawtooth Mountains to the west. The migration of cold easterly winds, summer temperatures, and diversion of precipitation are the likely cause of similarities in glaciation and ELAs between the Lemhi Range and Beaverhead Mountains.

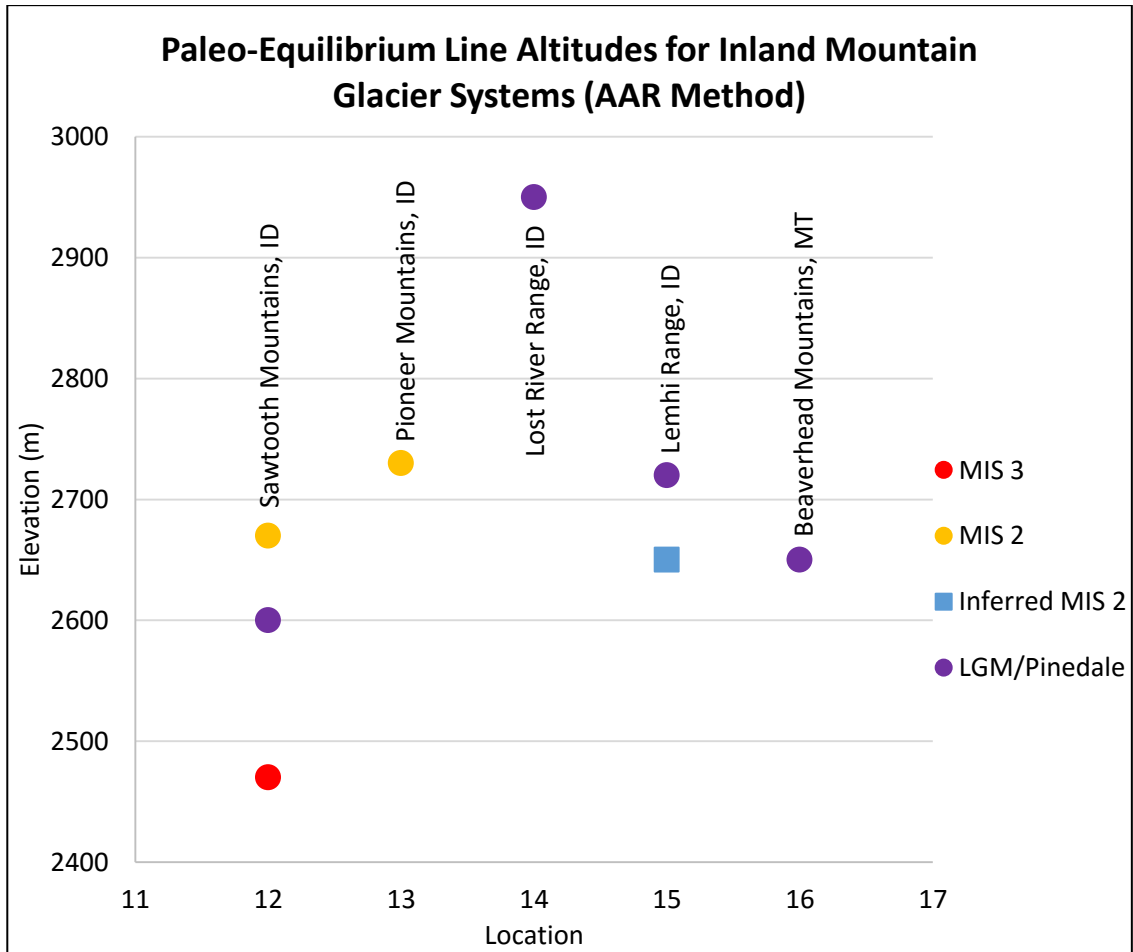


Figure 3.19 Comparison of equilibrium-line altitudes (shown in Table 3-3) calculated using the accumulation-area ratio method across the inland mountain glacier systems of the Sawtooth Mountains, Pioneer Mountains, Lost River Range, Lemhi Range, and Beaverhead Mountains. MIS 3 is inferred for the Sawtooths. Data modified from Locke (1990), Brugger (1996), Lundeen (2001), Meyer et al. (2004), and Staley (2015).

3.6.4.2 MIS 4-3 Paleoclimatic Inferences

Patterns of MIS 4-3 glaciation have been documented in regional mountain ranges (e.g., Sawtooth Mountains) that receive greater amounts of precipitation from westerly moisture sources (Lundeen, 2001; Staley, 2015). Climatic conditions, broadly similar to these nearby mountain ranges, may have influenced the Lemhi Range, producing extensive glaciation during MIS 4-3. The spatial relationships of mapped end moraine complexes and semi-quantitative moraine morphometry conclude that the relative age of Qm2 end moraines is MIS 4-3. Although the Qm2 end moraines exhibit a greater degree of degradation, they are located between 0.25-0.55 km down-valley of the Qm3 end moraines. Therefore, Lemhi Advance 2 was only slightly more extensive than Lemhi Advance 3, indicating that the ELA depression was only slightly greater than the ELA depression determined for inferred MIS 2 age Qm3 end moraines. This inferred ELA pattern suggests that MIS 4-3 climatic conditions in the Lemhi Range must have been relatively similar to MIS 2 climatic conditions. The absence of continental ice sheets during this time suggests that intercontinental temperatures may have been slightly warmer and westerly winds were prevailing, allowing moist Pacific air masses to penetrate further inland. The Lemhi Range may have experienced slightly cooler summers, slightly warmer winters, and a slight increase in precipitation, potentially sourced from the Snake River Plain, to account for a more extensive MIS 4-3 age Lemhi Advance 2.

3.7 Conclusions

This study employs surficial mapping, semi-quantitative analysis of moraine morphometry, paleo-glacier surface reconstruction, and ELA calculation to determine the

spatial and temporal patterns of glaciation in the central Lemhi Range. Surficial mapping documents the spatial relationships between glacial landforms, denoting younger and older sequences based on landform characteristics. The geomorphic characteristics of the mapped end moraines, including moraine crest angularity, moraine relief, and distal moraine slope steepness, indicate that slope angle, crest angularity, and relief decrease as moraine age increases. This study has revealed evidence of four glacial advances in the Lemhi Range, which are correlated to the Marine Isotope Stages as: Lemhi Advance 1 (MIS 6), Lemhi Advance 2 (MIS 4-3), Lemhi Advance 3 (MIS 2), and Lemhi Advance 4 (late MIS 2). A minimum limiting date for glacier retreat in the central Lemhi Range, determined from radiocarbon dating of lake cores taken from Meadow Lake, suggests that glacial recession was completed by 14 ± 0.5 cal ka BP. Similar AAR-derived ELAs are determined for the Lemhi Range, Sawtooth Mountains, and Beaverhead Mountains. AAR-derived ELAs for the Lemhi Range, determined in this study and by Meyer et al. (2004), correlate well with southwestern Montana ELAs (Locke, 1990). This consistent ELA pattern likely results from decreases in precipitation from rain shadowing by the Sawtooths and other western ranges, moisture diversion around these high ELA ranges to the north and south into the Snake River Plain, weakening of westerly flow from glacial anticyclonic easterly winds, and likely penetration of cold easterly winds over and through low portions (i.e., Railroad Canyon) of the Beaverhead Mountains, directly to the Lemhi Range. This allows the Lemhi Range to directly experience cold and dry climatic conditions similar to those of the Beaverheads during the last glaciation. The similarities in ELA patterns between the Lemhi Range and Sawtooth Mountains are interpreted as 1) the inland mountainous region of Idaho experienced uniform cooling during the last

glacial cycle, superimposed on consistent precipitation contrasts, or, 2) limited delivery of precipitation to the Sawtooth Mountains from decreased westerly winds and an increased temperature depression in the Lemhi Range due to cold katabatic winds from the continental ice sheets, coincidentally produced similar ELA depressions of ca. 500 m and ca. 600 m across these ranges respectively.

MIS 4-3 glaciation has been determined in previous studies for inland mountain glacier systems near the Lemhi Range on the basis of evidence from radiometric dating techniques, fault offset, and erosional characteristics. Glacial landforms in the Lemhi Range have strongly documented MIS 2 glaciation and may also document MIS 4-3 glaciation. New CRN ages, currently in process, will help evaluate that possibility.

References

- Abe-Ouchi, A., Saito, F., Kawamura, K., Raymo, M.E., Okuno, J.I., Takahashi, K., Blatter, H., 2013, Insolation-driven 100,000-year glacial cycles and hysteresis of ice-sheet volume. *Nature*, 500, 190-193, doi:10.1038/nature12374.
- Benn, D.I., Lehmkuhl, F., 2000, Mass balance and equilibrium-line altitudes of glaciers in high-mountain environments, *Quaternary International*, 65, 15-29.
- Benn, D.I., Owen, L.A., Osmaston, H.A., Seltzer, G.O., Porter, S.C., Mark, B., 2005, Reconstruction of equilibrium-line altitudes for tropical and sub-tropical glaciers, *Quaternary International*, 138, 8-21.
- Benn, D.I., N. Hulton, 2010, An Excel™ spreadsheet program for reconstructing the surface profile of former mountain glaciers and ice caps, *Computers & Geosciences*, 605-610.
- Brugger, K.A., 1996, Implications of till-provenance studies for glaciological reconstructions of the paleoglaciers of Wildhorse Canyon, Idaho, U.S.A., *Annals of Glaciology*, 22, 93-101.
- Burke, R.M., Birkeland, P.W., 1979, Reevaluation of multiparameter relative dating techniques and their application to the glacial sequence along the eastern escarpment of the Sierra Nevada, California, *Quaternary Research*, 11, 21-51.
- Butler, D.R., 1984, A late Quaternary chronology of mass wasting for a small valley in the Lemhi Mountains of Idaho, *Northwest Science*, 58.1, 1-13.
- Butler, D.R., 1986, Pinedale deglaciation and subsequent Holocene environmental changes and geomorphic responses in the central Lemhi Mountains, Idaho, USA, *Géographie physique et Quaternaire*, 40.1, 39-46.
- Chadwick, O.A., Hall, R.D., Phillips, F.M., 1997, Chronology of Pleistocene glacial advances in the central Rocky Mountains, *Geological Society of America Bulletin*, 109, 1443-1452.
- Clark, P.U., Alley, R.B., Pollard, D., 1999, Northern Hemisphere ice-sheet influences on global climate change, *Science*, 286, 1104-1111.
- Clark, P.U., Mix, A.C., 2002, Ice sheets and sea level of the Last Glacial Maximum. *Quaternary Science Reviews*, 21, 1-7.
- Cluer, K.J., 1989, Surficial geology and geomorphology of the Doublespring Pass area, Lost River Range, east-central Idaho, *Rocky Mountain Geology*, 27, 44-62.

- Colman, S.M., Pierce, K.L., 1986, Glacial sequence near McCall, Idaho: Weathering rinds, soil development, morphology, and other relative-age criteria, *Quaternary Research*, 25, 25-42.
- Colman, S.M., Pierce, K.L., 1992, Varied records of early Wisconsinan alpine glaciations in the western United States derived from weathering-rind thicknesses, in Clark, P.U., and Lea, P.D., eds., *The Last Interglacial-Glacial Transition in North America: Boulder, Colorado, Geological Society of America Special Paper 270*, 269-278.
- Davies, N., 2011, Holocene glaciation of the Green River drainage, Wind River Range, Wyoming, *M.S. Thesis Western Washington University*.
- Dort, W., 2003, Multiple Pre-Bull Lake glaciations, eastern side of Lemhi Range, east-central Idaho, *Geological Society of America Abstracts with Programs*, 35.5.
- ESRI, 2015, ArcGIS 10.3.1 software: ESRI Corporation, Redlands, California.
- Evenson, E.B., Cotter, J.F.P., and Clinch, M.J., 1982, Glaciation of the Pioneer Mountains: A proposed model for Idaho, ed. Bonnicksen and Breckenridge, *Cenozoic Geology of Idaho, Idaho Bureau of -Mines and Geology Bulletin*, 26, 653-665.
- Foster, D., Brocklehurst, S.H., Gawthorpe, R.L., 2008, Small valley glaciers and the effectiveness of the glacial buzzsaw in the northern Basin and Range, *Geomorphology*, 624-639.
- Gosse, J.C., Klein, J., Evenson, E.B., Lawn, B., Middleton, R., 1995, Beryllium-10 dating of the duration and retreat of the last Pinedale glacial sequence, *Science* 268, 1329-1333.
- Heyman, J., 2014, Paleoglaciation of the Tibetan Plateau and surrounding mountains based on exposure ages and ELA depression estimates, *Quaternary Science Reviews*, 91, 30-41.
- Hughes, P.D., Gibbard, P.L., Ehlers, J., 2013, Timing of glaciation during the last glacial cycle: evaluating the concept of a global 'Last Glacial Maximum' (LGM), *Earth-Science Reviews*, 125, 171-198.
- Johnson, B.G., Thackray, G.D., Van Kirk, R., 2007, The effect of topography, latitude, and lithology on rock glacier distribution in the Lemhi Range, central Idaho, USA, *Geomorphology*, 91.1, 38-50.
- Kaufman, D. S., Porter, S. C., and Gillespie, A. R., 2003, Quaternary alpine glaciation in Alaska, the Pacific Northwest, Sierra Nevada, and Hawaii, in Gillespie, A. R.,

- Porter, S. C., and Atwater, B. F., eds., *The Quaternary Period in the United States: Developments in Quaternary Science: Amsterdam*, Elsevier, 1, 77-103.
- Keeley, J., Warbritton, M., 2015, The Otto Glacier, Lost River Range, Custer County Idaho: Reconnaissance survey finds further evidence for active glacier, *Watershed Monitoring Program, Salmon-Challis National Forest*, 1-32
- Kenworthy, M.K., 2011, Optically stimulated luminescence dating of gravelly alluvial fan deposits: links between climate and geomorphic response in the Lost River Range, Idaho, *M.S. Thesis Boise State University*, 197.
- Kenworthy, M.K., Rittenour, T.M., Pierce, J.L., Sutfin, N.A., Sharp, W.D., 2014, Luminescence dating without sand lenses: An application of OSL to coarse-grained alluvial fan deposits of the Lost River Range, Idaho, USA, *Quaternary Geochronology*, 23, 9-25.
- Knoll, K.M., 1977, Chronology of alpine glacier stillstands, east-central Lemhi Range, Idaho, *Idaho State University Museum of Natural History*.
- Kutzbach, J.E., Guetter, P.J., Behling, P.J., Selin, R., 1993, Simulated climatic changes: Results of the COHMAP Climate-Model Experiments, *in*, Wright, H.E. Jr., Kutzbach, J.E., Webb, T. III, Ruddiman, W.F., Street-Perrott, P.A., Bartlein, P.J., University of Minnesota Press, Minneapolis, MN, *Global climates since the Last Glacial Maximum*, 24-93.
- Laabs, B.J.C., Refsnider, K.A., Munroe, J.S., Mickelson, D.M., Applegate, P.J., Singer, B.S., Caffee, M.W., 2009, Latest Pleistocene glacial chronology of the Uinta Mountains: support for moisture-driven asynchrony of the last deglaciation, *Quaternary Science Reviews*, 28, 1171-1187.
- Lambeck, K., Purcell, A., Zhao, J., Svensson, N.O., 2010, The Scandinavian ice sheet: from MIS 4 to the end of the Last Glacial Maximum, *Boreas*, 39, 410-435, DOI 10.1111/j.1502-3885.2010.00140.x.
- Licciardi, J.M., Clark, P.U., Brook, E.J., Elmore, D., Sharma, P., 2004, Variable responses of western U.S. glaciers during the last deglaciation, *Geology*, 32.1, 81-84.
- Licciardi, J.M., Pierce, K. L., 2008, Cosmogenic exposure-age chronologies of Pinedale and Bull Lake glaciations in greater Yellowstone and Teton Range, USA, *Quaternary Science Reviews*, 27, 814-831.
- Licciardi, J., 2015, Cosmogenic ¹⁰Be chronologies of moraines and glacially scoured bedrock in the Teton Range, with implications for paleoclimatic events and tectonic activity, *in 2015 AGU Fall Meeting*. Agu.

- Link, P.K., Janecke, S.U., 1999, Geology of east-central Idaho: geologic roadlogs for the Big and Little Lost River, Lemhi, and Salmon River valleys, *Guidebook to the Geology of Eastern Idaho: Idaho Museum of Natural History, Pocatello*, 295-334.
- Locke, W.W., 1990, Late Pleistocene glaciers and the climate of western Montana, USA, *Arctic and Alpine Research*, 22, 1-13.
- Lundeen, K.A., 2001, Refined late Pleistocene glacial chronology for the eastern Sawtooth Mountains, Central Idaho, *M.S. Thesis Idaho State University*, 117.
- Marshall, K.J., 2013, Expanded Late Pleistocene glacial chronology for Western Washington, U.S.A and the Wanaka-Hawea Basin, New Zealand, using luminescence dating of glaciofluvial outwash, *M.S. Thesis Idaho State University*, 357.
- Martinson, D.G., Pisias, N.G., Hays, J.D., Imbrie, J., Moore, T.C., Shackleton, N.S., 1987, Age dating and the orbital theory of the ice ages: Development of a high-resolution 0 to 300,000-year chronostratigraphy, *Quaternary Research*, 27, 1-29.
- Meier, M.F., Post, A.S., 1962, Recent variations in mass net budgets of glaciers in western North America, *IASH Publ*, 58, 63-77.
- Meierding, T.C., 1982, Late Pleistocene glacial equilibrium-line altitudes in the Colorado Front Range: a comparison of methods, *Quaternary Research*, 18.3, 289-310.
- Meyer, G.A., Fawcett, P.J., Locke, W.W., 2004, Late-Pleistocene equilibrium-line altitudes, atmospheric circulation, and timing of mountain glacier advances in the interior northwestern United States, in Haller, K., Wood, S.H., eds., *Geological Field Trips in Southern Idaho, Eastern Oregon, and Northern Nevada: Geological Society of America Field Guide*, 61-66.
- Meyer, G.A., unpublished equilibrium-line altitudes calculated across western U.S.A. using the AAR method.
- Mijal, B., 2008, Holocene and latest Pleistocene glaciations in the Sawtooth Mountains, central Idaho, *Western Washington University M.S. Thesis*, 90.
- Mix, A.C., Bard, E., Schneider, R., 2001, Environmental processes of the ice age: land, ocean, glaciers (EPILOG), *Quaternary Science Reviews*, 20, 627-657.
- Otto, B.R., 1977, An active alpine glacier, Lost River Range, Idaho, *Northwest Geology*, 6, 85-87.
- Pedersen, V.K., Egholm, D.L., 2013, Glaciations in response to climate variations preconditioned by evolving topography. *Nature*, 493, 206-210, doi:10.1038/nature11786.

- Pellitero, R., Rea, B. R., Spagnolo, M., Bakke, J., Hughes, P., Ivy-Ochs, S., Ribolini, A., 2015, A GIS tool for automatic calculation of glacier equilibrium-line altitudes, *Computers & Geosciences*, 82, 55-62.
- Phillips, F.M., Zreda, M.G., Gosse, J.C., Klein, J., Evenson, E.B., Hall, R.D., Chadwick, O.A., Sharma, P., 1997, Cosmogenic ^{36}Cl and ^{10}Be ages of Quaternary glacial and fluvial deposits of the Wind River Range, Wyoming, *Geological Society of America Bulletin*, 109, 11, 1453-1463.
- Pierce, K.L., Muhs, D.R., Fosberg, M.A., Mahan, S.A., Rosenbaum, J.G., Licciardi, J.M., Pavich, M.J., 2011, A loess-paleosol record of climate and glacial history of the past two glacial-interglacial cycles (~150 ka), southern Jackson Hole, Wyoming, *Quaternary Research*, 76, 119-141.
- Porter, S.C., 1975, Equilibrium-line altitudes of late Quaternary glaciers in the Southern Alps, New Zealand, *Quaternary Research*, 5.1, 27-47.
- Porter, S.C., 2001, Snowline depression in the tropics during the Last Glaciation, *Quaternary Science Reviews*, 20, 1067-1091.
- Refsnider, K.A., Laabs, B.C., Plummer, M.A., Mickelson, D.M., Singer, B.S., Caffee, M.W., 2008, Last glacial maximum climate inferences from cosmogenic dating and glacier modeling of the western Uinta ice field, Uinta Mountains, Utah, *Quaternary Research*, 69, 130-144.
- Reynolds, H. A., 2011, Recent glacier fluctuations in Grand Teton National Park, Wyoming, *M.S. Thesis Idaho State University*.
- Ruppel, E.T., Lopez, D.A., 1981, Geologic map of the Gilmore quadrangle, Lemhi and Custer counties, Idaho, *United States Geological Survey*, 1:62,500.
- Ruppel, E.T., Lopez, D.A., 1988, Regional geology and mineral deposits in and near the central part of the Lemhi Range, Lemhi County, Idaho, *United States Geological Survey Professional Paper*, No. 1480, 1-122.
- Sherard, C., 2006, Regional correlations of late Pleistocene climatic changes based on cosmogenic nuclide exposure dating of moraines in Idaho, *M.S. Thesis Western Washington University*, 87.
- Shulmeister, J., Davies, T.R., Evans, D.J.A., Hyatt, O.M., Tovar, D.S., 2009, Catastrophic landslides, glacier behavior and moraines formation – a view from an active plate margin, *Quaternary Science Reviews*, 28, 1085-1096.
- Staley, A.E., 2015, Glacial geomorphology and chronology of the Quinault Valley, Washington, and broader evidence of marine isotope stages 4 and 3 glaciation across northwestern United States, *M.S. Thesis Idaho State University*, 188.

- Thackray, G.D., 2001. Extensive early and middle Wisconsin glaciation on the western Olympic Peninsula, Washington, and the variability of Pacific Moisture delivery to the Pacific Northwest. *Quaternary Research*, 55, 257-270.
- Thackray, G.D., 2004, Late Pleistocene alpine glacier advances in the Sawtooth Mountains, Idaho, USA: Reflections of midlatitude moisture transport at the close of the last glaciation, *Geology*, 32, 225-228.
- Thackray, G.D., Staley, A.E., *in review*, Fault scarp offsets document extensive MIS 4-3 glaciation in western interior North America, Teton Range, Wyoming, USA, *Quaternary Research*.
- Thompson, R. S., Whitlock, C., Bartlein, P. J., Harrison, S. P., Spaulding, W. G., 1993, Climatic changes in the western United States since 18,000 yr BP, *in Global climates since the last glacial maximum*, H.E. Wright, Jr., J.E. Kutzbach, T. Webb III, W.F. Ruddiman, F.A. Street-Perrott, and P.J. Bartlein, eds, University of Minnesota Press, 468-513.
- Young, N.E., Briner, J.P., Leonard, E.M., Licciardi, J.M., and Keenan, L., 2011, Assessing climatic and nonclimatic forcing of Pinedale glaciation in the western United States, *Geology*, 39, 2, 171-174.

Chapter 4. Conclusion

4.1 Lemhi Range Glaciation and Climatic Conditions

4.1.1 Surficial Mapping of the Gilmore 7.5-Minute Quadrangle and the Northeastern Quarter of the Big Windy Peak 7.5-Minute Quadrangle: Evidence for Multiple Glacial Advances

The surficial map of the Gilmore 7.5-minute quadrangle and the northeastern quarter of the Big Windy Peak 7.5-minute quadrangle is built upon previous bedrock and surficial mapping across the range (Ruppel and Lopez, 1988; Janecke, 1992), detailed field observations, and geomorphic relationships between landforms, generating a newly detailed glacial sequence for the Lemhi Range. Relative age relationships are determined from the mapping to distinguish episodes of deposition, based on the premise that weathering and landform erosion parameters are time dependent (Burke and Birkeland, 1979).

The central Lemhi Range hosts a well preserved geomorphic record of Pleistocene glaciation. Pleistocene ice originated in the high altitude reaches of the central Lemhi Range, carving steep cirque headwalls. Ice flowed down many valleys with ice extending beyond the eastern range-front at Deer Creek, Meadow Lake Creek, Long Canyon, and Spring Mountain Canyon. Several sequences of end moraines (Qm1-Qm4), indicating distinct ice marginal positions, and coeval outwash fans (Qf1-Qf4) have been identified across the central portion of the Lemhi Range, providing evidence for multiple glacial advances. Additionally, end moraines are identified up-valley, reflecting ice equilibration positions during glacial retreat (Qm5-Qm7, Qgu). Dort (2003, 2004) described pre-Bull Lake, Bull Lake, and Pinedale age moraines across the central Lemhi Range, yet the four glacial advances across the central Lemhi Range identified in this

study and their hypothesized ages stem from more detailed consideration of relative dating and geomorphic relationships, determined from semi-quantitative analysis of moraine morphometry, as well as comparisons of moraines with nearby mountain ranges. Semi-quantitative analysis of the geomorphic characteristics of the mapped end moraines, including moraine crest angularity, moraine relief, and distal moraine slope steepness, suggests that the slope angle, crest angularity, and relief decrease with increasing moraine age. The glacial advances and their hypothesized ages are: Lemhi Advance 1 (MIS 6), Lemhi Advance 2 (MIS 4-3), Lemhi Advance 3 (MIS 2), and Lemhi Advance 4 (late MIS 2). Small-scale climatic fluctuations are recorded in the semi-arid environment of the Lemhi Range, as evidenced by the relationships between end moraines and recessional glacial features, as well as minimal subsequent incision during retreat up-valley. The semi-arid climate limits the extent and erosional capacity of glaciers and the power of interglacial streams, allowing older glacial features to be preserved.

4.1.2 Cosmogenic Radionuclide Dating: Quantitative Evidence of Glaciation

To further constrain and support the hypothesized ages of Lemhi Advance 1-4 developed by surficial mapping, the timing of glacial advance must be quantified. Eight samples were collected for cosmogenic radionuclide (CRN) ^{10}Be measurement from Qm2 and Qm3 terminal moraine crests. Forthcoming CRN ages are anticipated to be correlative with the hypothesized ages of Lemhi Advance 2-3, thus providing relative age constraints on Lemhi Advance 1 and 4. However, the dates may reveal a variety of possible ages ranging from MIS 6 to MIS 2, potentially disproving the hypothesis of this thesis. Details regarding CRN dating and the collected CRN samples are located in Appendix A.

The geomorphic relationships, coupled with a detailed chronological record of multiple glaciations, will help elucidate the drivers behind climatic shifts. The hypothesized ages of the glacial sequence allow for inferences regarding the climatic regimes that influenced glaciation across the Lemhi Range to be made. A Northern Hemisphere insolation peak during MIS 3 would allow for persistent westerly winds and increased precipitation delivery and accumulation, leading to cool, and potentially wet, climatic conditions (especially wet winters) taking precedent over the relatively warm summer temperatures to enhance glaciation. In addition, a Northern Hemisphere insolation minimum during MIS 6 and MIS 2 could generate a decrease in precipitation delivery and accumulation, as well as cold climatic conditions (cool, dry summers) driving glaciation. These climatic conditions may result from weakened westerly flow caused by anticyclonic ice-sheet circulation from the Cordilleran and Laurentide ice sheets. Cold, easterly winds generated from these ice sheets may have caused substantial aridity in the intercontinental interior during MIS 6 and MIS 2. The final phases of deglaciation across the range began as glaciers receded from Qm4 terminal positions. A basal retreat date of ca. 14 ± 0.5 cal ka BP, indicating a minimum age of final deglaciation of the cirque, was determined from lake cores taken from Meadow Lake, located at the head of the Meadow Lake Creek valley within the Gilmore quadrangle (B. Finney, personal communication, 2015).

4.1.3 Equilibrium-Line Altitudes: Inferences of Climatic Conditions

The paleoclimatic conditions that drove glaciation the Lemhi Range are inferred based on paleo-glacier reconstruction, calculation of equilibrium-line altitudes (ELAs), comparison of ELAs between proximal inland mountain ranges, and temperature

depression calculations. ELAs were calculated for seven reconstructed Pleistocene glaciers across the central Lemhi Range associated with Qm3 end moraines using the AAR and THAR methods. ELAs calculated across the range show a separation into two distinct groups. ELAs reside at higher elevations (ca. 2700 m) in the larger valleys. These valleys contain high elevation cirque headwalls near the divide, housing single and multiple ice tributaries, and evidence of multiple episodes of extensive ice advance (i.e., Deer Creek, Meadow Lake Creek, Long Canyon, and Bruce Canyon). ELAs reside at lower elevations (ca. 2600 m) in the smaller valleys that exhibit a single, low elevation cirque headwall (i.e., Ridgeway Mine (North and South) and Silver Moon Gulch). Both the AAR and THAR methods expose ca. 100 m separation between the two clusters of ELAs across the eastern flank of the central Lemhi Range. ELAs across a relatively small transect should not vary by that much, as the ELA for a single advance is relatively consistent across the associated glaciers due to balances between precipitation and temperature. The difference in ELAs may be attributed to the hypsometry of the valleys and the surface area available for snow and ice accumulation. It is possible that as the ELA falls below the hypsometric maximum, the rate of change in ice volume decreases, as modeled for the Bitterroot Range, USA and Sierra Nevada, Spain, in a study by Pedersen and Egholm (2013). Additionally, the separation of the large and small valley glacier ELAs may also represent two separate glacial advances, due to the large difference in the ELAs.

Similar AAR and THAR derived ELAs are determined for the Lemhi Range, Sawtooth Mountains, and Beaverhead Mountains (regional comparison of THAR ELAs is discussed in Appendix C). AAR-derived ELAs for the Lemhi Range, determined in

this study and by Meyer et al. (2004), are similar to those calculated for southwestern Montana ELAs (Locke, 1990). This consistent ELA pattern likely results from decreases in precipitation from rain shadowing by the Sawtooths, moisture diversion around these high ELA ranges to the north and south into the Snake River Plain, weakening of westerly flow from glacial anticyclone easterly winds, and likely penetration of cold easterly winds over and through low portions (i.e., Railroad Canyon) of the Beaverhead Mountains, directly to the Lemhi Range. This allows the Lemhi Range to directly experience cold and dry climatic conditions similar to those of the Beaverheads during the last glaciation. Broadly similar ELA depressions of ca. 450 m, 500 m, and 600 m of the Sawtooth Mountains, Lemhi Range, and Beaverhead Mountains respectively, have been determined. These similarities are interpreted as 1) the inland mountainous region of Idaho experienced uniform cooling during the last glacial cycle, superimposed on consistent precipitation contrasts, or, 2) limited delivery of precipitation to the Sawtooth Mountains from decreased westerly winds and an increased temperature depression in the Lemhi Range due to cold katabatic winds from the continental ice sheets, coincidentally produced similar ELA depressions across these ranges.

4.2 Suggestions for Future Work

High-resolution chronologies spanning the last glacial cycle are scarce across inland mountain glacier systems and must be generated to provide continued evidence for the timing of glaciation. Evidence for MIS 4-2 glaciation extends from the Olympic Mountains, Washington, to as far inland as the Teton Range, Wyoming. However, radiometric dating techniques, especially CRN dating, have been underutilized for pre-MIS 2 landforms. Relative dating methods such as fault offset of glacial landforms,

moraine morphometry, and weathering-based techniques provide a broad sense for MIS 4-3 glaciation. Continued surficial mapping within inland mountain glacier systems, coupled with reevaluation of existing chronologies, development of new chronologies, and the inferences for MIS 6-2 glaciation described in Chapters 2 and 3, would increase the overall understanding of the northwestern United States glacial and climatic history over the past ca. 130 ka.

Future work within the Lemhi Range should include continued exploration and surficial mapping of glaciated valleys north and south of the Gilmore quadrangle and Big Windy Peak quadrangle. Application of mapping and relative dating techniques will allow for correlations of glacial sequences to be made across the range. In addition, pursuing samples for CRN dating across similar landforms within the range will build a greater, and higher resolution, chronological sequence, as eight collected samples in this study provides only limited chronologic information.

Additionally, other methods for dating glacier sequences in the Lemhi Range should be applied. Luminescence dating has been applied in the Lost River Range, providing valuable data of correlations of alluvial fan construction proximal to glacier margins (Kenworthy et al., 2014). Sediment for luminescence dating may be revealed through excavation of the eastern range-front outwash fans, providing an opportunity for extracting new chronological data. Continued lake coring of additional lakes, such as Nez Perce Lake to the north and Mill Creek Lake to the west of Gilmore, Idaho, will yield a more detailed, range-wide, glacial retreat age. Surficial mapping and CRN dating should additionally be applied to proximal inland mountain ranges where evidence of glaciation exists.

Future work should also include collection of Light Detection and Ranging (LiDAR) topographic data for the central Lemhi Range, and eventually the entire range. Development of LiDAR will allow for a more detailed delineation and identification of glacial landforms and features to be made by eliminating the dense forest cover that persists throughout the majority of the range. This would substantially improve surficial mapping, producing a more detailed relative age sequence between glacial landforms. Development of LiDAR may potentially improve the reconstruction of paleo-glaciers in this study by revealing trimlines that are otherwise indistinguishable. This will generate a more accurate reconstruction of the glacier surface by more accurately constraining the lateral extent of glaciers and the elevation of glacier surfaces throughout the range, and thus more accurate ELAs.

Reconstruction of paleo-ELAs can be improved upon in this range, and other proximal ranges, by utilizing the newly developed ArcGIS based ELA toolbox (Pellitero et al., 2015) and implementing the more robust accumulation-area ratio and accumulation-area-balance ratio (AABR) methods. The AAR method is the most widely applied method for ELA reconstruction. Therefore, a better understanding of climatic conditions between ranges can be made if the same ELA calculation method is implemented. The AABR method is more robust and accurate than other methods of ELA calculation; however, glacier hypsometry and glacier mass-balance gradients are necessary for the application of this method, and therefore must be implemented.

This study provides evidence for MIS 6-2 glaciation in the Lemhi Range, east-central Idaho. Forthcoming CRN ages will potentially support or refute the premise that MIS 4-3 glaciation in the Lemhi Range was more extensive than LGM glaciation. The

evidence supplied by this study can then be incorporated with former glacial chronological evidence to further improve our understanding of the climatic conditions that drove glaciation across the northwestern United States. Subsequent studies will continue to provide additional chronological and geomorphic evidence of glaciation and climatic conditions of inland mountain glacier systems.

References

- Burke, R.M., Birkeland, P.W., 1979, Reevaluation of multiparameter relative dating techniques and their application to the glacial sequence along the eastern escarpment of the Sierra Nevada, California, *Quaternary Research*, 11, 21-51.
- Dort, W., 2003, Multiple Pre-Bull Lake glaciations, eastern side of Lemhi Range, east-central Idaho, *Geological Society of America Abstracts with Programs*, 35.5.
- Dort, W., 2004, Records of multiple Pinedale glacier retreat/readvance pulses, Lemhi Mountains, east-central Idaho, *Geological Society of America Abstracts with Programs*, 36.4.
- Janecke, S.U., 1992, Geologic map of part of the Big Windy Peak and Moffet Springs 7.5' quadrangles, Lemhi and Custer Counties, Idaho, *Idaho Geological Survey Technical Report*, 92-96.
- Kenworthy, M.K., Rittenour, T.M., Pierce, J.L., Sutfin, N.A., Sharp, W.D., 2014, Luminescence dating without sand lenses: An application of OSL to coarse-grained alluvial fan deposits of the Lost River Range, Idaho, USA, *Quaternary Geochronology*, 23, 9-25. 22.
- Locke, W.W., 1990, Late Pleistocene glaciers and the climate of western Montana, USA, *Arctic and Alpine Research*, 22, 1-13.
- Meyer, G.A., Fawcett, P.J., Locke, W.W., 2004, Late-Pleistocene equilibrium-line altitudes, atmospheric circulation, and timing of mountain glacier advances in the interior northwestern United States, in Haller, K., Wood, S.H., eds., *Geological Field Trips in Southern Idaho, Eastern Oregon, and Northern Nevada: Geological Society of America Field Guide*, 61-66.
- Pedersen, V.K., Egholm, D.L., 2013, Glaciations in response to climate variations preconditioned by evolving topography. *Nature*, 493, 206-210, doi:10.1038/nature11786.
- Pellitero, R., Rea, B. R., Spagnolo, M., Bakke, J., Hughes, P., Ivy-Ochs, S., Ribolini, A., 2015, A GIS tool for automatic calculation of glacier equilibrium-line altitudes, *Computers & Geosciences*, 82, 55-62.
- Ruppel, E.T., Lopez, D.A., 1988, Regional geology and mineral deposits in and near the central part of the Lemhi Range, Lemhi County, Idaho, *United States Geological Survey Professional Paper*, No. 1480, 1-122.

APPENDICES

Appendix A: Terrestrial Cosmogenic Radionuclide Dating – Background, Sampling Methods, Preparation, and Status of Collected Samples Not Included in Text

Background

This study applies cosmogenic radionuclide (CRN) dating techniques to develop a new chronology of MIS 6-2 glaciation and understand the drivers of spatial and temporal patterns of glaciation. New chronologies extracted from the Lemhi Range will fill an important gap between maritime and inland glacier records by identifying responses to climate change before and during the LGM. I expand upon the spatial and temporal coverage of glaciation in the central Lemhi Range by developing eight new Beryllium-10 (^{10}Be) CRN ages, in a region with little glacial-chronologic data, from boulders on undated moraines in several valleys across the eastern range front.

Terrestrial Cosmogenic Radionuclide dating (also referred to as surface exposure dating and Cosmogenic-exposure dating) is a principal tool to date glacial landforms such as moraines, erratic boulders, and glacially eroded bedrock (Briner, 2011). Cosmogenic Radionuclide (CRN) exposure dating begins with cosmic radiation constantly being propelled toward the Earth from supernova explosions in the galaxy. The trajectories of particles are altered due to forces exerted by the Sun and their paths are dependent upon the angle at which they enter the Earth's magnetic field lines. High-energy cosmic rays collide with atoms in the upper atmosphere, producing a cascade of nuclear reactions which generate cosmogenic nuclides that progress toward the Earth's surface. Certain high-energy neutrons, and low-mass muons, survive these collisions and can then penetrate a few meters of rock, producing in situ cosmogenic nuclides, such as ^{10}Be , in minerals at a greater rate than decay (Brown et al., 1991; von Blanckenburg, 2014). Over

time ^{10}Be will accumulate in rocks as a measure of the time that the surface has been exposed to cosmic-ray bombardment (Granger, 2001). The production rates of in situ nuclides are incredibly low, reaching only a few atoms per gram of mineral per year (von Blanckenburg, 2014). CRN dating measures the concentration of a specified nuclide in a rock surface to be dated, and then a nuclide production rate is applied to transform the concentration measurement to an age (Balco, 2009). The rates of in situ production of cosmogenic nuclides vary with time, location, latitude, longitude, elevation, sample thickness and density, topographic shielding, and erosion, allowing uncertainties to arise (Heyman, 2014). To reduce uncertainty, production rate calibration sites that are similar in location and age to the site being dated are located (Balco, 2009), or a global average production rate from multiple, high quality calibration sites are used to determine an average production rate (Heyman, 2014). Gosse and Phillips (2001) provide further detail on background and fundamental principles.

This study focuses on the accumulation of ^{10}Be in quartz crystals that comprise approximately 95% of the Ordovician age Kinnikinic Quartzite and about 30% of the Tertiary age granodiorite boulders. CRN dating requires careful sample selection due to topographic shielding, isotopic inheritance, and boulder exhumation on glacial moraines. Topographic shielding refers to topographic irregularities or surface coverage that inhibit the accumulation of incident cosmic radiation of samples on sloping surfaces. Common types of surface coverage shielding include cover by winter snow, sand, soil, or peat (Gosse and Phillips, 2001). Isotopic inheritance refers to cases where moraine boulders are deposited on a moraine surface, containing an inventory of cosmogenic isotopes accumulated from prior exposure. Inheritance may result from inefficient glacial erosion,

rockfalls onto glacial surfaces, or reworking of older materials (Briner, 2011). Because moraines are depositional features, gravity and erosion will degrade slope angles allowing subsurface boulders to be exhumed. This yields cosmogenic ages that are younger than the true age of moraine deposition (Bursik, 1991; Briner, 2011). Glacial boulders may exhibit surface textures such as glacial polish, scour marks, or fluvially smoothed textures, that provide strong evidence for insignificant erosion since the event that is intended to be dated (Gosse and Phillips, 2001). The effective range of CRN dating depends on the nuclides being used. For ^{10}Be in quartz, ages range from 0.1 ka to 1 Ma (Granger, 2001; Gosse and Phillips, 2001).

The objective of sampling is to collect and describe the attributes of a sample that accurately represent the exposure history of a given landform (Gosse and Phillips, 2001). Moraines selected for sampling are characterized by sharp-crested and well-preserved ridge morphology and a relative abundance of surface boulders. Boulders are moderately abundant in the Lemhi Range. However, boulders that meet the required sampling specifications are uncommon. Boulders selected for sampling primarily reside on terminal moraine crests, exhibit glacial polish and smoothing (indicating minimal erosion) and are 1 meter or greater in height to reduce concerns of snow cover and past soil cover. (Figure A.1) (Licciardi et al., 2004; Licciardi and Pierce, 2008). Boulders selected for sampling that are 1 meter or greater in height have proven to produce more accurate chronologies (Heyman, 2016). Boulders sampled also have minimal surface erosion characteristics such as granular disintegration, spalling, soil build-up, and formation of dissolution pits. GPS coordinates were recorded to document the location of each boulder. Topographic shielding angles were measured using a Brunton compass at

points of inflection in the topography surrounding the boulder sample. These measurements will correct for the influence of topographic shielding.

After a particular boulder is chosen, a specific point of sampling must be considered. Eight samples were collected using a rock/sledge hammer and chisel from horizontal and dipping surfaces that mark the uppermost portion of the boulder. For samples taken from dipping surfaces, the strike and dip of the surface was recorded. In order to obtain the maximum concentration of CRN production, samples weighing 1-4 kg were collected, and the upper 1-2 cm of the surface was isolated for processing (Figure A.2).



Figure A.1 Field photograph depicting an Ordovician age Kinnikinic Quartzite boulder resting on a prominent moraine crest that was selected for sampling. Minimal spalling and soil build-up is observed. Some glacial polish is extant on the surface and the boulder is greater than 1 meter tall.



Sample of Ordovician age Kinnikinic Quartzite that was collected in the field. The approximate upper 1-2 cm was extracted from a nearly horizontal surface on the boulder.

Sampling Strategies

A series of strict guidelines were followed when extracting samples for cosmogenic radionuclide dating. CRN sampling strategies followed those described by Licciardi et al. (2001, 2004), Licciardi and Pierce (2008), and from personal communication by Joe Licciardi (2015), and are described here. Moraines selected for sampling are characterized by a distinctly preserved ridge morphology, lined with abundant boulders. The boulder of interest must be in its original depositional position on the crest of a terminal moraine and ideally exhibit glacial polish and minimal evidence of spalling (Figure A.4). This ensures that that the boulder of interest is derived from a

specific glacial advance and that the original boulder surface is sampled. Universal Transverse Mercator (UTM) coordinates and elevations of each boulder location were documented using a handheld Garmin Oregon 600t GPS unit. The boulder dimensions were measured using a tape measure, with the height equaling or exceeding 1 m in height (Heyman, 2016). This assertion reduces the concern of exhumation influences, as well as soil and snow cover. The lithology of the boulder was also described. Descriptions of the degree of spalling, the degree of erosion and fragility, the degree of soil erosion and buildup, evidence of exhumation and soil cover, and the degree of lichen cover are considered when selecting a boulder for sampling. Ideally, samples were collected from near-horizontal boulder surfaces marking the boulder tops, with little evidence of water pooling. However, some samples in this study were extracted from dipping, lower elevation surfaces. Strike and dip of the sampled surface was recorded to allow for shielding correction. The upper 1-2 cm of the boulder surface was extracted with desired sample size ca. 1 kg (depending on the quartz content of the rock). Samples were then annotated with arrows, indicating the top surface of the sample. Topographic shielding influences were accounted for by sighting/measuring the angle of inflection points of the surrounding landscape in relation to the boulder location using the clinometer on a Brunton compass.

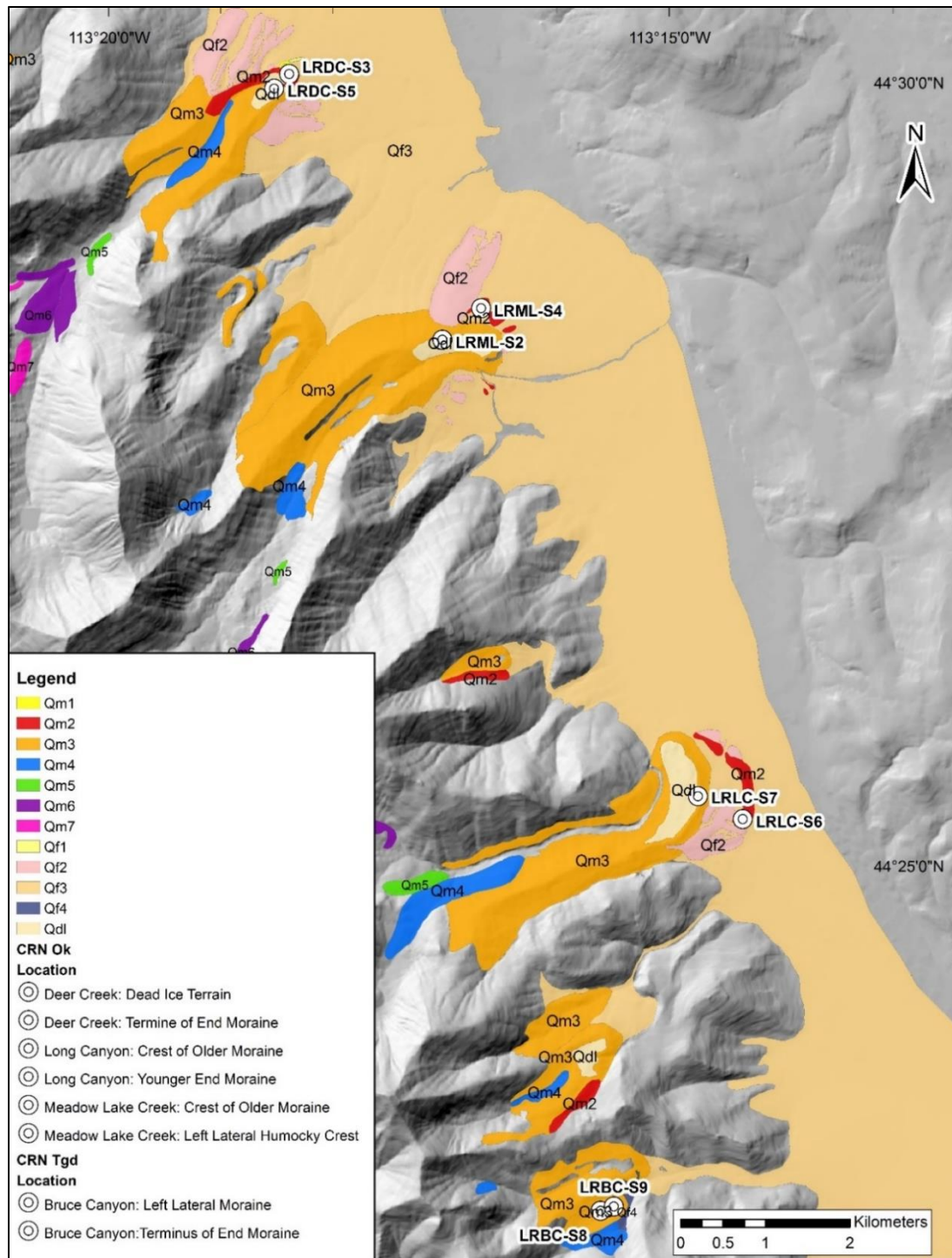


Figure A.3 Hillshade image (10 m DEM) showing the location of CRN samples on the corresponding mapped glacial moraines.

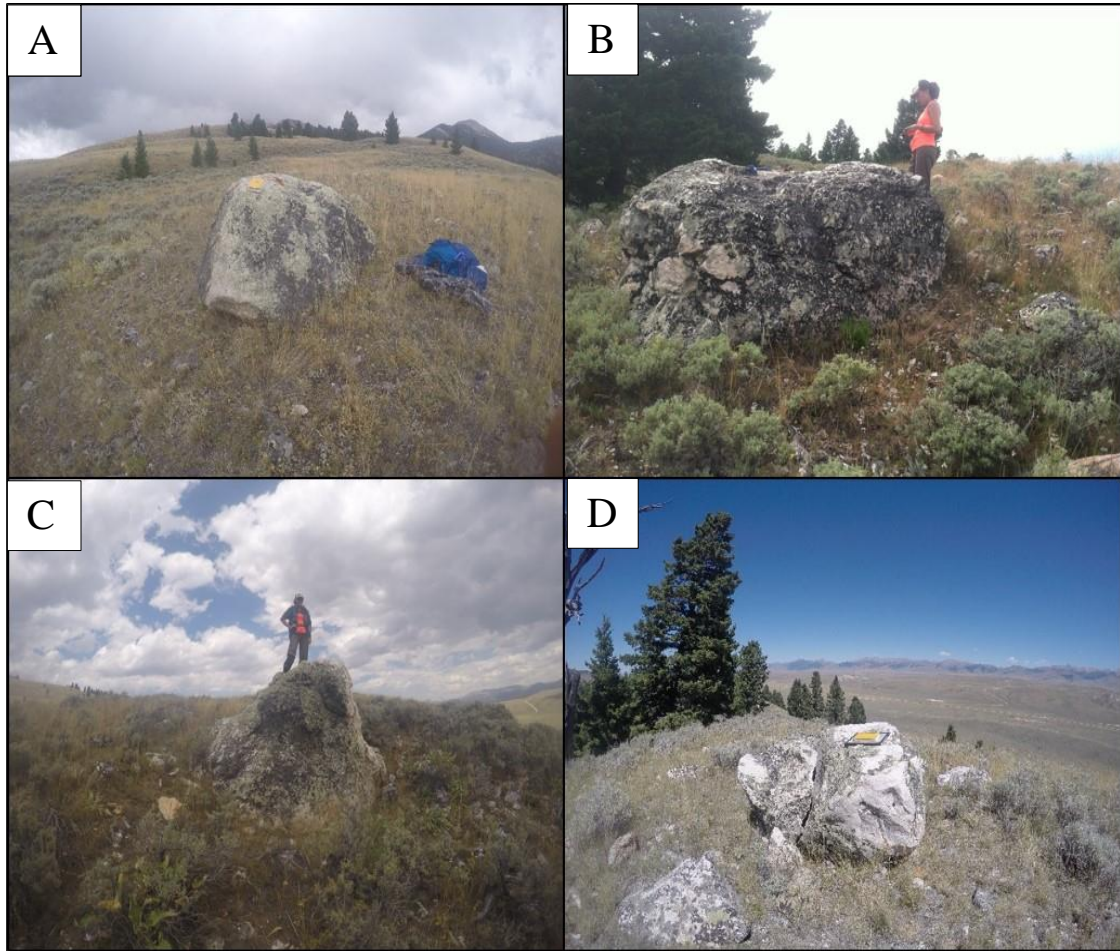


Figure A.4 Photographs of quartzite boulders selected for sampling and the corresponding moraine in which they reside. A) Dead ice landform at Deer Creek, B) Left lateral segment of Qm3 moraine at Meadow Lake Creek, C) Qm2 moraine at Long Canyon, D) Qm3 moraine at Long Canyon.

¹⁰Be Preparation and Measurements

Beryllium concentrates were extracted from quartzite and granodiorite samples to produce purified BeO target material for accelerator mass spectrometry (AMS) analysis. The outer boulder surface from each sample was isolated for processing. Samples were trimmed using a rock saw, to isolate the upper 1-2 cm, and were ground between 250 and 725 micrometers in the grinding lab at Idaho State University. Six ground quartzite samples of approximately 200 g and two ground granodiorite samples of approximately

400 g were further prepared for beryllium-isotope analysis following methods described by Gosse and Phillips (2001), Bierman et al. (2002), and Laabs (2009) at the University of Vermont Cosmogenic Nuclide Laboratory. AMS measurements of Beryllium-10 concentrations were conducted at the Lawrence Livermore National Laboratory Center for Accelerator Mass Spectrometry.

Age Calculations

All exposure ages based on ^{10}Be concentration will be calculated using the CRONUS-Earth (Cosmic-Ray prOduced NUclide Systematics on Earth) online CRN age calculator code (Version 2.2) (Balco et al., 2008; <http://hess.ess.washington.edu/>) and an updated production rate of 3.99 ± 0.22 atoms/g/yr (Heyman, 2014).

Sample Status

CRN samples are currently being processed by the University of Vermont Cosmogenic Nuclide Laboratory under the supervision of Paul Bierman and will subsequently be sent to the Lawrence Livermore National Laboratory Center for Accelerator Mass Spectrometry. Beryllium-10 concentrations (10^5 atoms $\cdot\text{g}^{-1}$) will likely be received by or before August 2016. These concentrations will then be used to calculate CRN ages. These ages will then reveal a reconnaissance chronology of the extent of glaciation in the central Lemhi Range.

References

- Balco, G., Stone, J.O., Lifton, N.A., Dunai, T.J., 2008, A complete and easily accessible means of calculating surface exposure ages or erosion rates from ^{10}Be and ^{26}Al measurements, *Quaternary Geochronology*, 3, 174-195.
- Balco, G., Briner, J., Finkel, R.C., Rayburn, J.A., Ridge, J.C., Schaefer, J.M., 2009, Regional beryllium-10 production rate calibration for late-glacial northeastern North America, *Quaternary Geochronology*, 4, 93-107.
- Bierman, P.R., Caffee, M.W., Davis, P.T., Marsella, K., Pavich, M., Colgan, P., Mickelson, D., Larsen, J., 2002, Rates and timing of earth surface processes from in situ-produced cosmogenic Be-10, *Reviews in mineralogy and geochemistry*, 50.1, 147-205.
- Borgert, J.A., Lundeen, K.A., Thackray, G.D., 1999, Glacial geology of the southeastern Sawtooth Mountains, in Hughes, S.S., and Thackray, G.D., eds., *Guidebook to the Geology of Idaho: Pocatello, Idaho Museum of Natural History*, 205-217.
- Briner, J.P., 2011, Dating Glacial Landforms, *Encyclopedia of Snow, Ice and Glaciers*, 175-176.
- Brown, E.T., Edmond, J.M., Raisbeck, G.M., Yiou, F., Kurz, M.D., Brook, E.J., 1991, Examination of surface exposure ages of Antarctic moraines using in situ produced ^{10}Be and ^{26}Al , *Geochimica et Cosmochimica Acta*, 55.8, 2269-2283.
- Bursik, M., 1991, Relative dating of moraines based on landform degradation, Lee Vining Canyon, California, *Quaternary Research*, 35.3, 451-455.
- Gosse, J.C., Phillips, F.M., 2001, Terrestrial in situ cosmogenic nuclides: theory and application, *Quaternary Science Reviews*, 20.14, 1475-1560.
- Granger, D.E., Muzikar, P.F., 2001, Dating sediment burial with in situ-produced cosmogenic nuclides: theory, techniques, and limitations, *Earth and Planetary Science Letters*, 188.1, 269-281.
- Heyman, J., 2014, Paleoglaciation of the Tibetan Plateau and surrounding mountains based on exposure ages and ELA depression estimates, *Quaternary Science Reviews*, 91, 30-41.
- Heyman, J., Applegate, P.J., Blomdin, R., Gribenski, N., Harbor, J.M., Stroeven, A.P., 2016, Boulder height – exposure age relationships from global ^{10}Be compilation, *Quaternary Geochronology*, 34, 1-11.
- Laabs, B.J.C., Refsnider, K.A., Munroe, J.S., Mickelson, D.M., Applegate, P.J., Singer, B.S., Caffee, M.W., 2009, Latest Pleistocene glacial chronology of the Uinta

Mountains: support for moisture-driven asynchrony of the last deglaciation, *Quaternary Science Reviews*, 28, 1171-1187.

Licciardi, J.M., 2000, Alpine glacier and pluvial lake records of late Pleistocene climate variability in the western United States, *Ph.D.Thesis Oregon State University*, 155.

Licciardi, J.M., Clark, P.U., Brook, E.J., Pierce, K.L., Kurz, M.D., Elmore, D., Sharma, P., 2001, Cosmogenic ^3He and ^{10}Be chronologies of the late Pinedale northern Yellowstone ice cap, Montana, USA, *Geology*, 29, 1095-1098.

Licciardi, J.M., Clark, P.U., Brook, E.J., Elmore, D., Sharma, P., 2004, Variable responses of western U.S. glaciers during the last deglaciation, *Geology*, 32.1, 81-84.

Licciardi, J.M., Pierce, K. L., 2008, Cosmogenic exposure-age chronologies of Pinedale and Bull Lake glaciations in greater Yellowstone and Teton Range, USA, *Quaternary Science Reviews*, 27, 814-831.

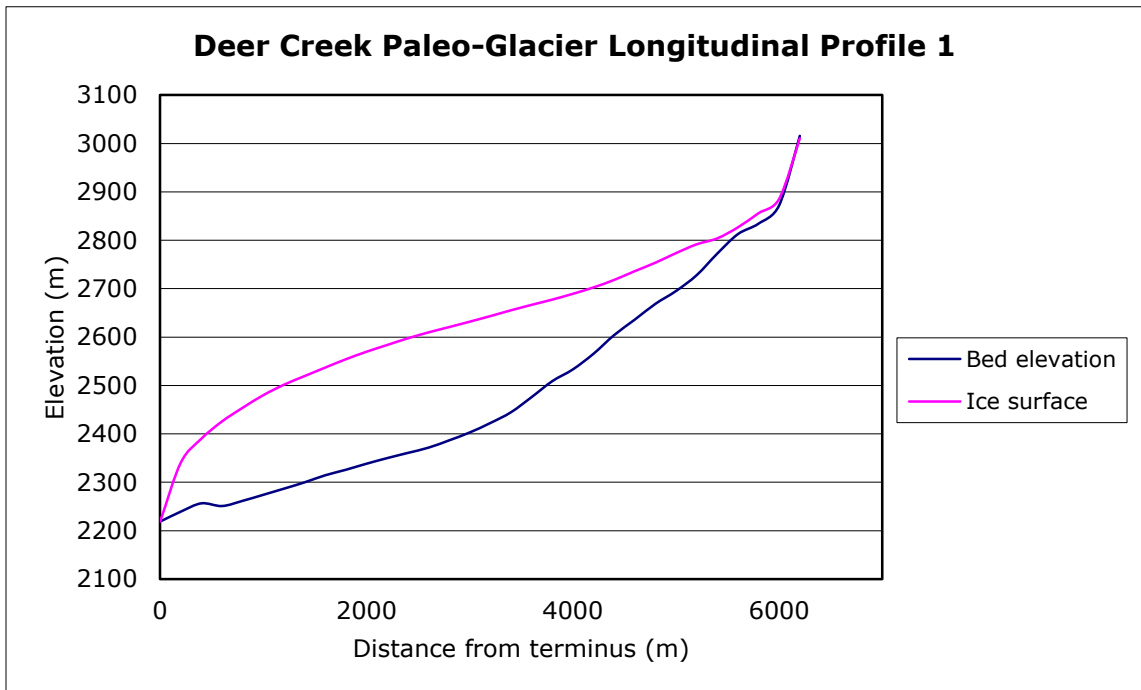
von Blanckenburg, F., Willenbring, J.K., 2014, Cosmogenic nuclides: Dates and rates of Earth-surface change, *Elements*, 10.5, 341-346.

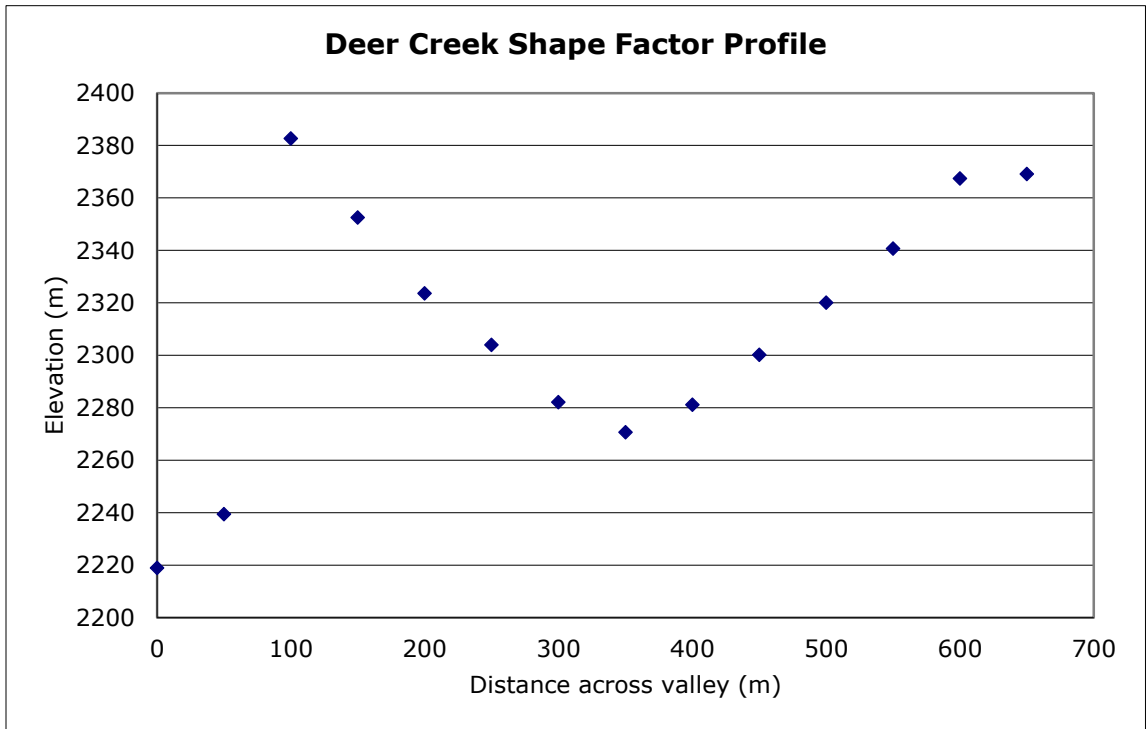
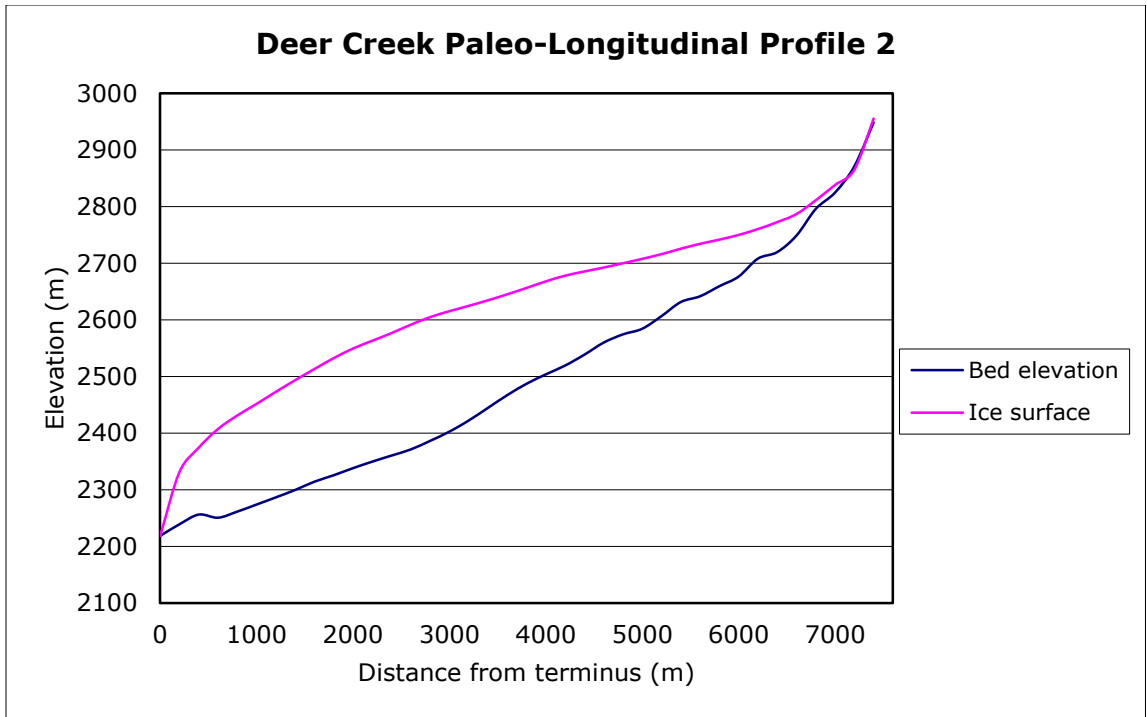
Appendix B: Paleo-Glacier Reconstructions – Paleo-Glacier Longitudinal Profiles and Individual Paleo-Glacier Surfaces

Paleo-Glacier Longitudinal Profiles and Shape Factor Cross-Sectional Profiles

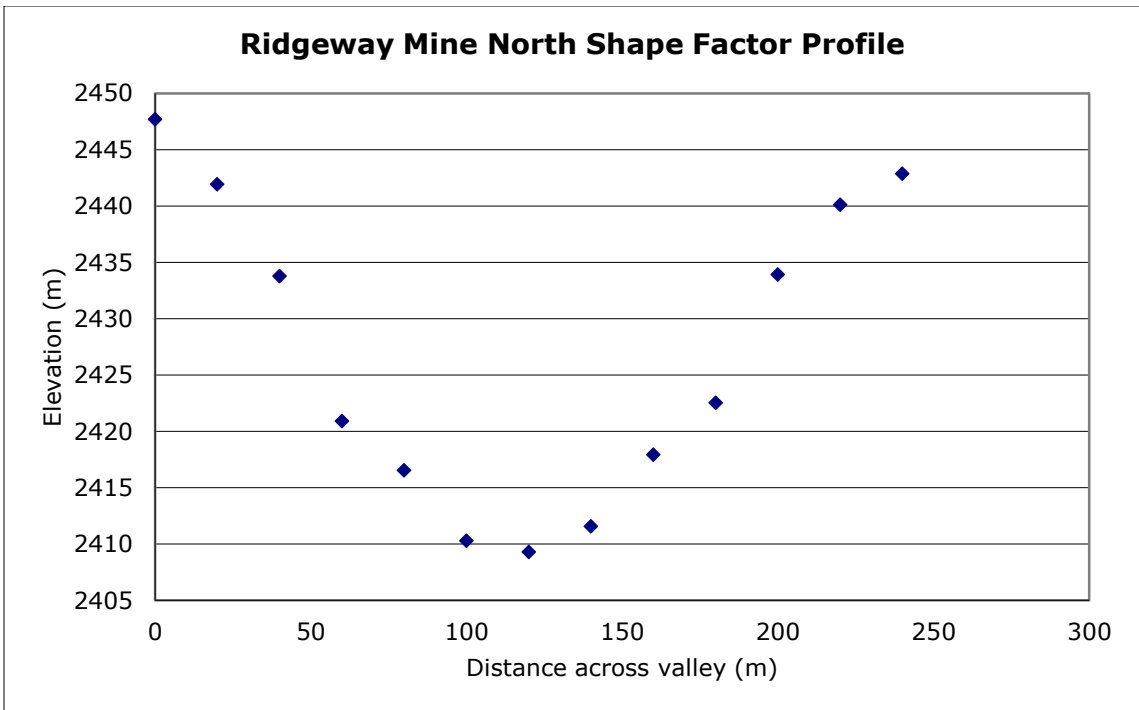
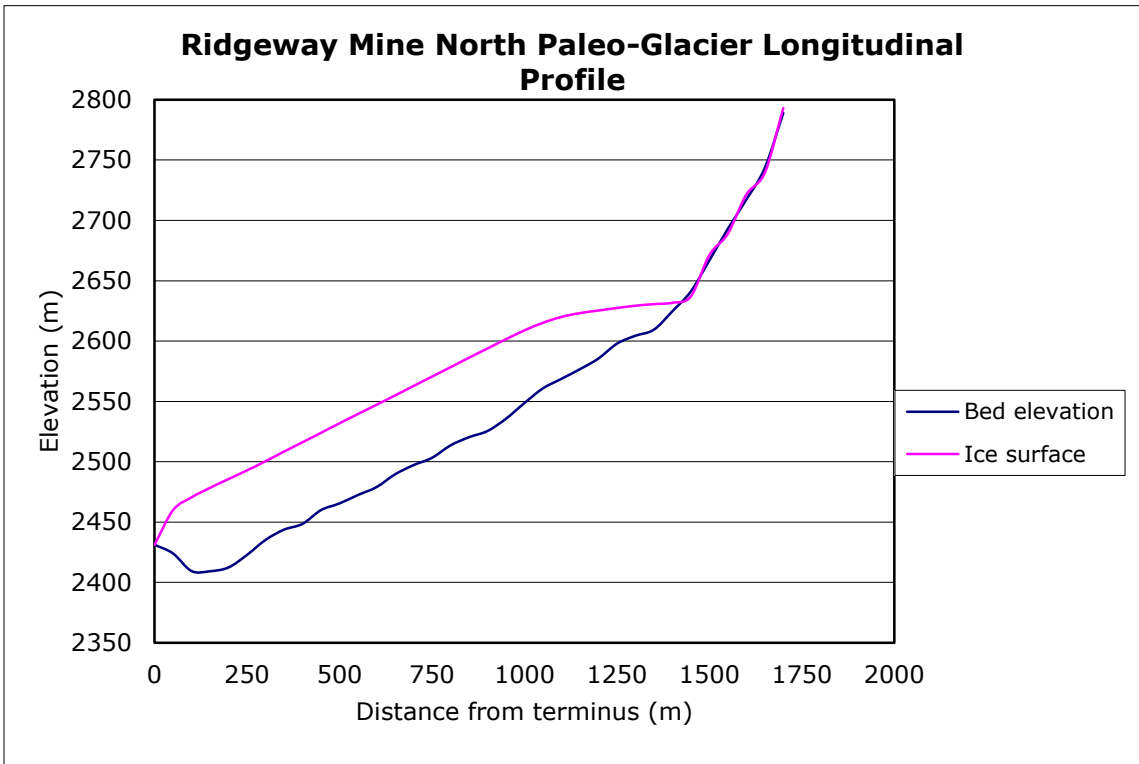
Multiple glacier profiles were constructed in valleys with multiple ice tributaries in order to generate the entirety of the glacier surface for that valley, and were generated from north to south (ex: Profile 1 reflects the tributary furthest north). The following figures depict the longitudinal profiles and shape factor profiles for each reconstructed glacier surface. Shape Factor (F) values are denoted in valley name headings:

Deer Creek: F = 0.35

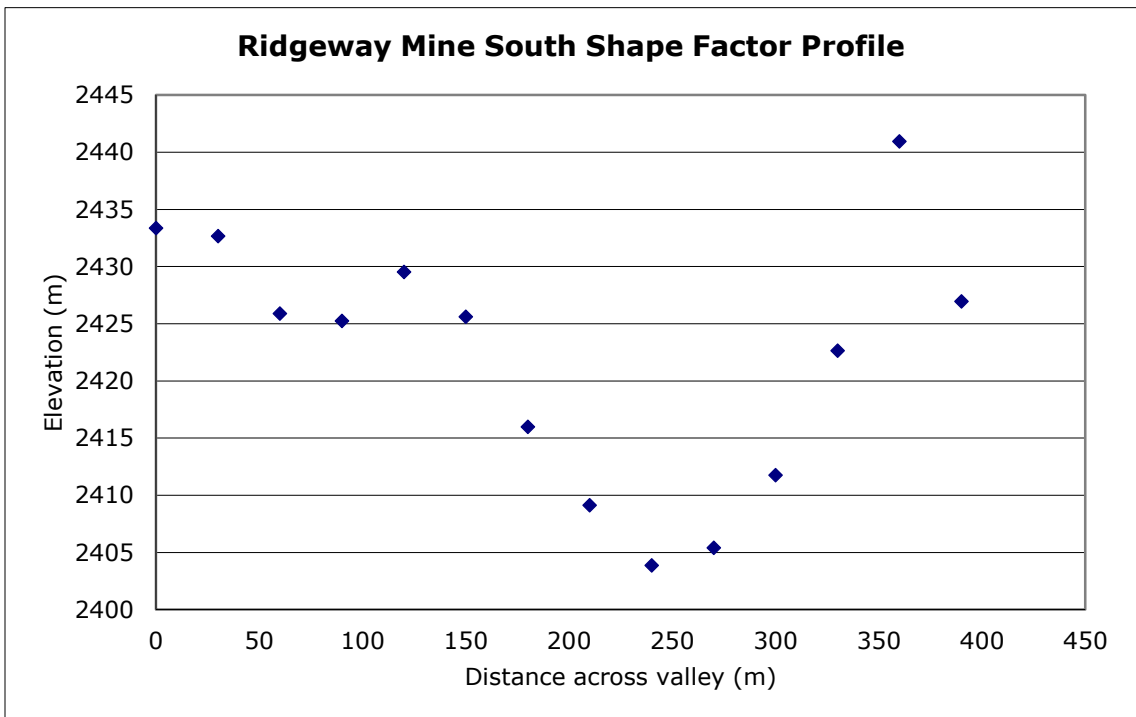
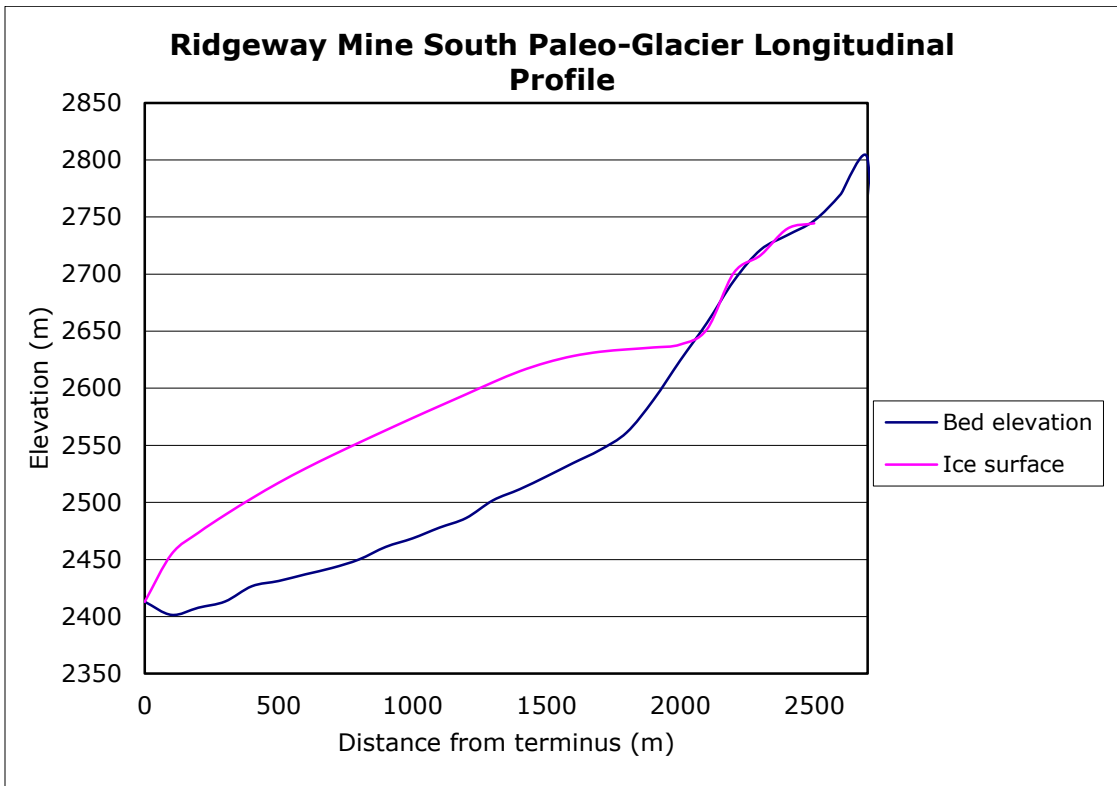




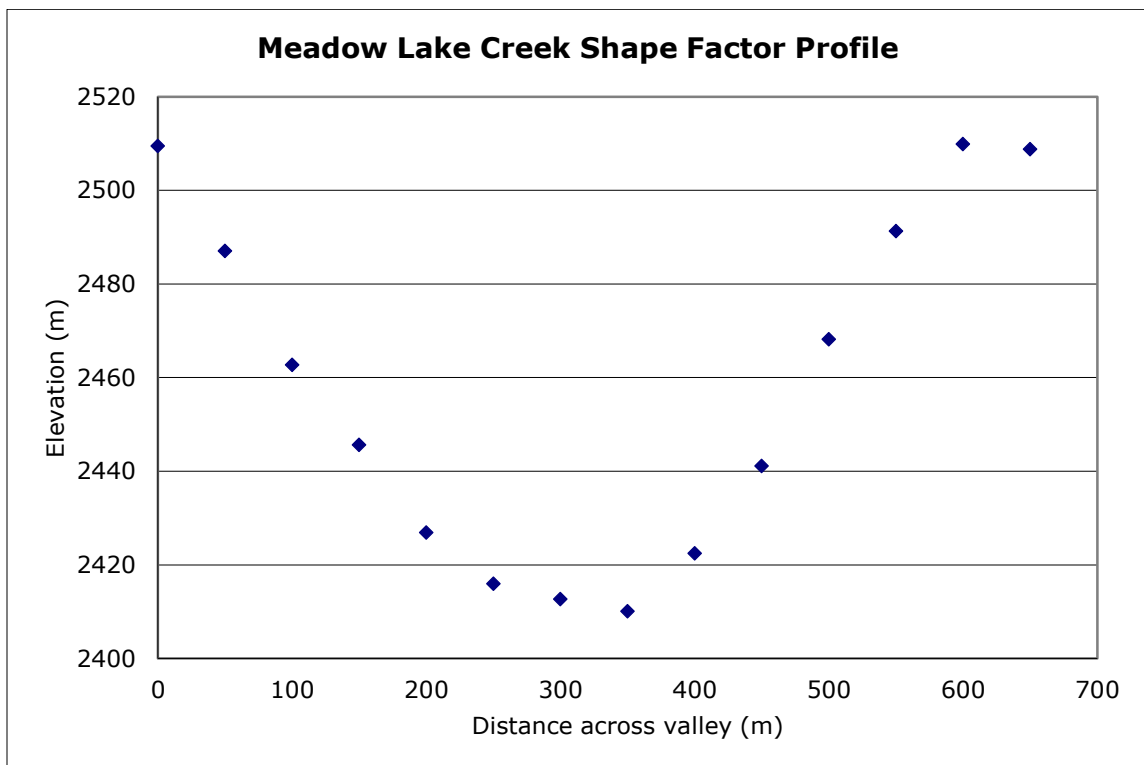
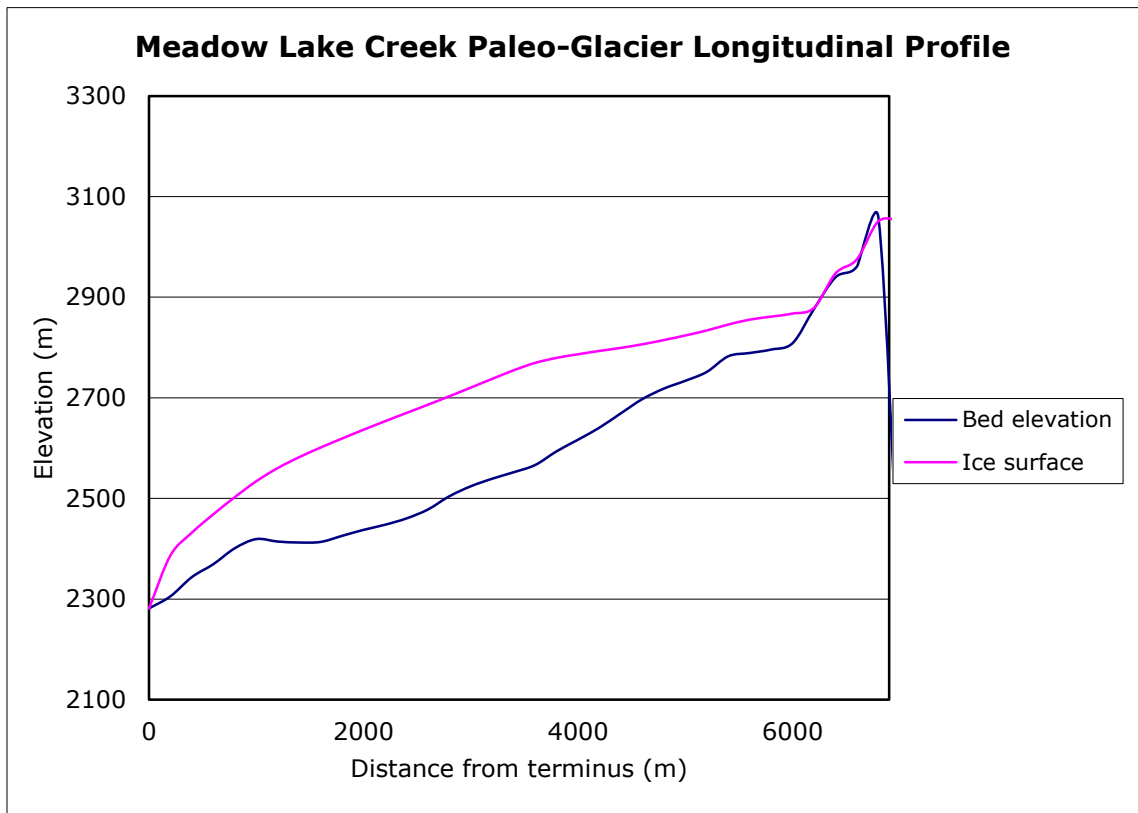
Ridgeway Mine North: $F = 0.55$



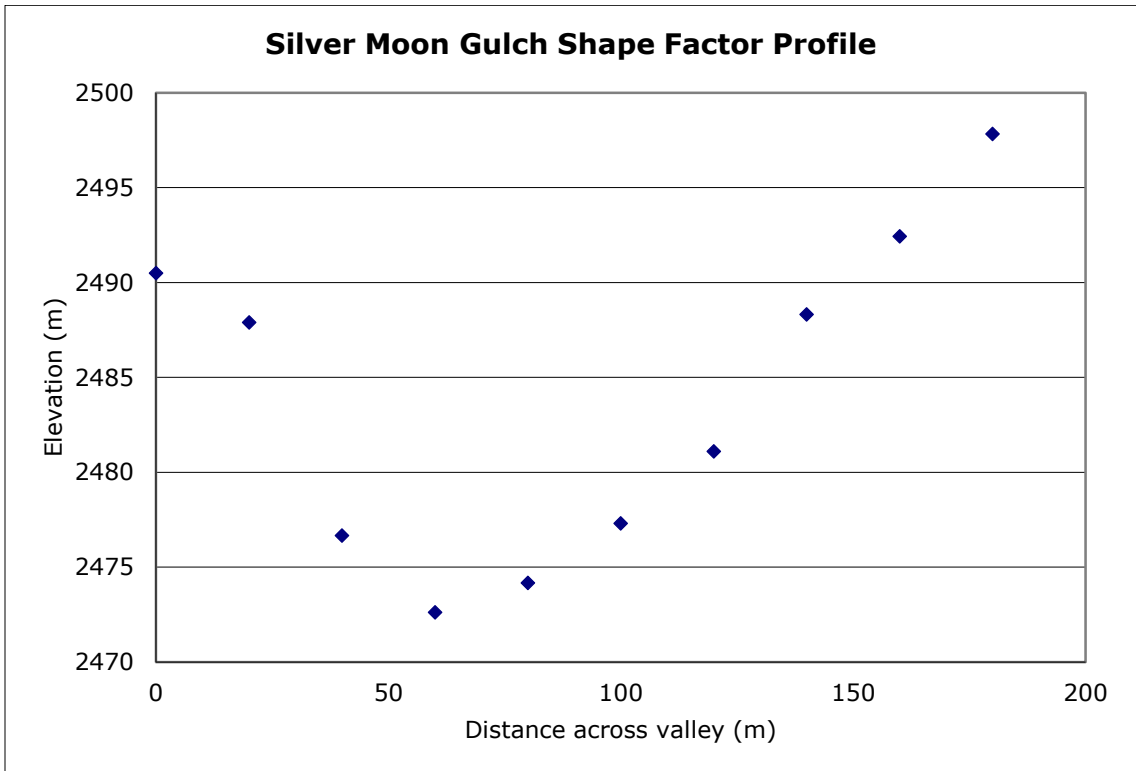
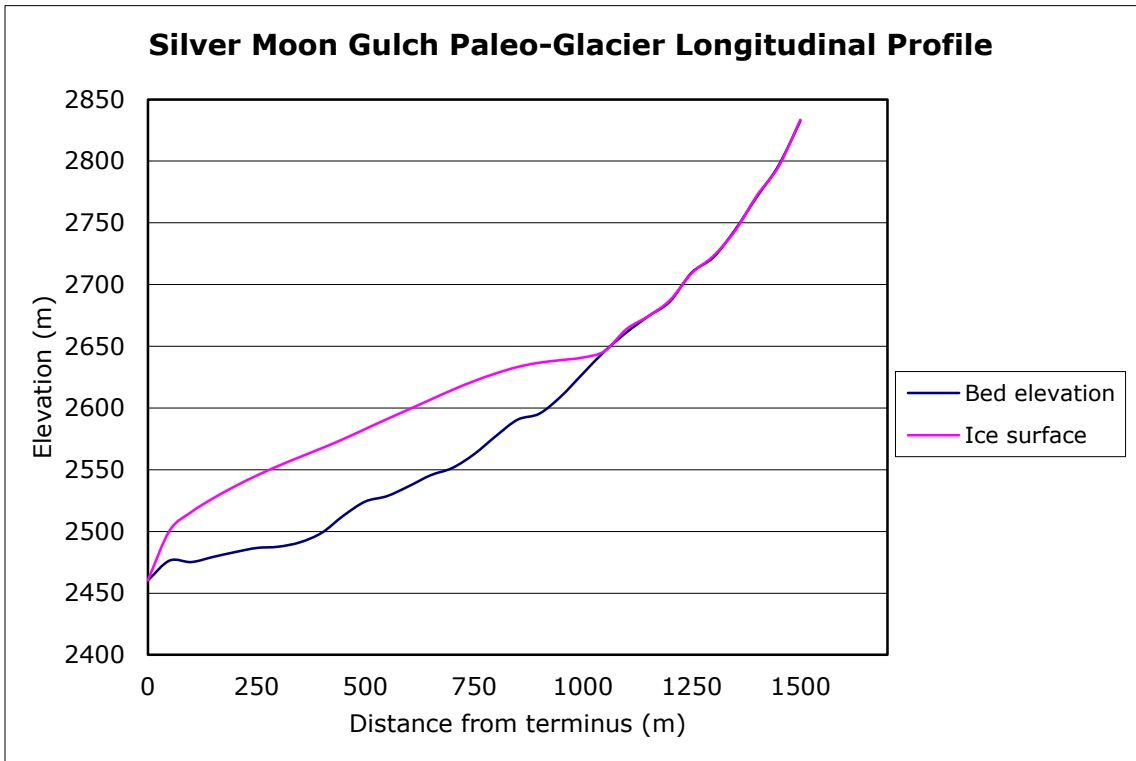
Ridgeway Mine South: $F = 0.51$



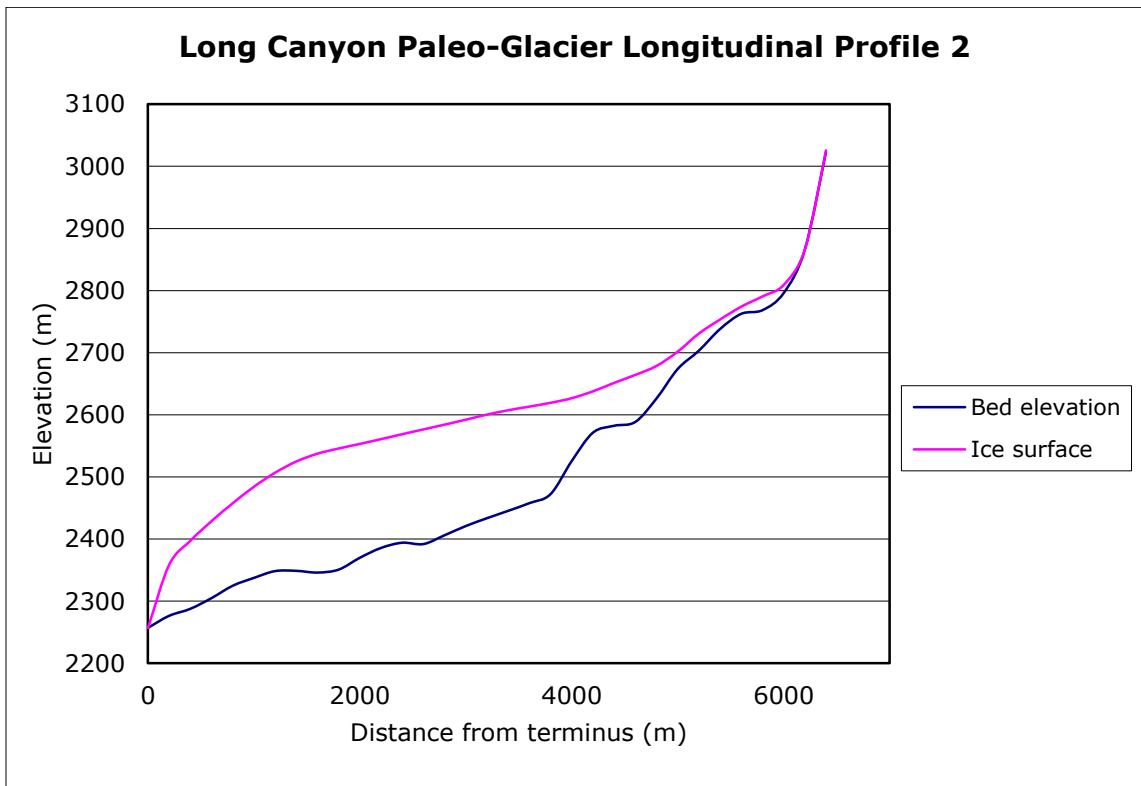
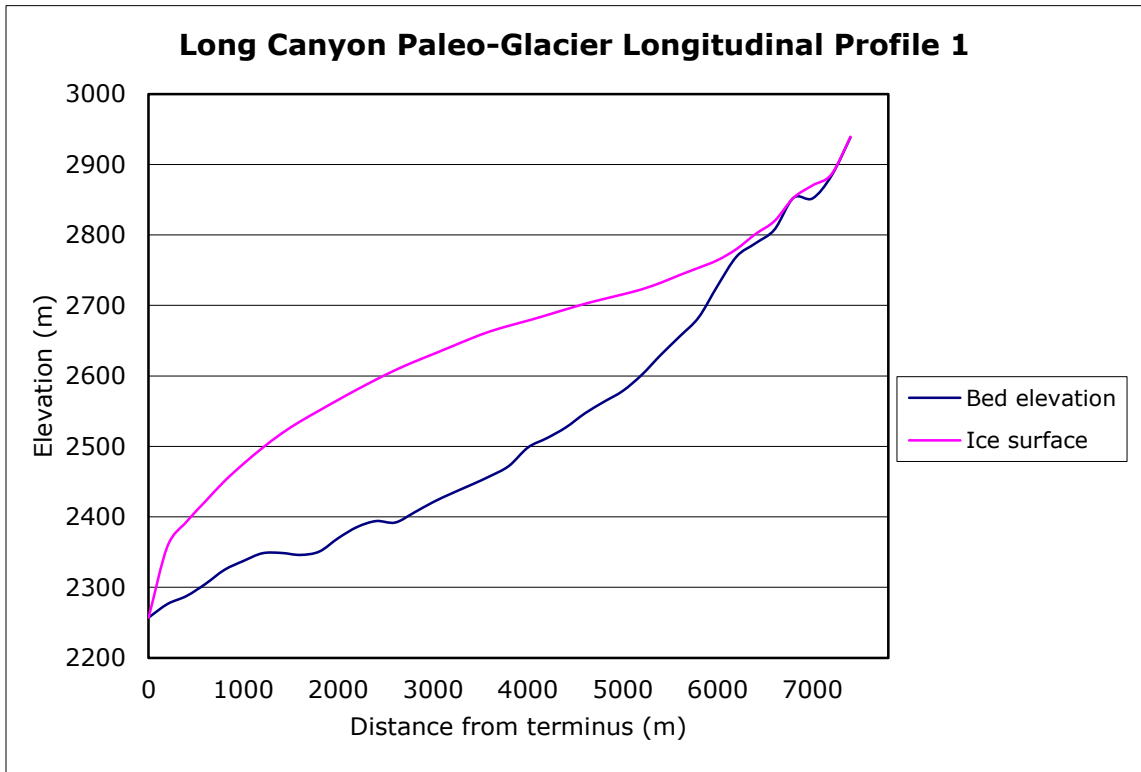
Meadow Lake Creek: $F = 0.53$

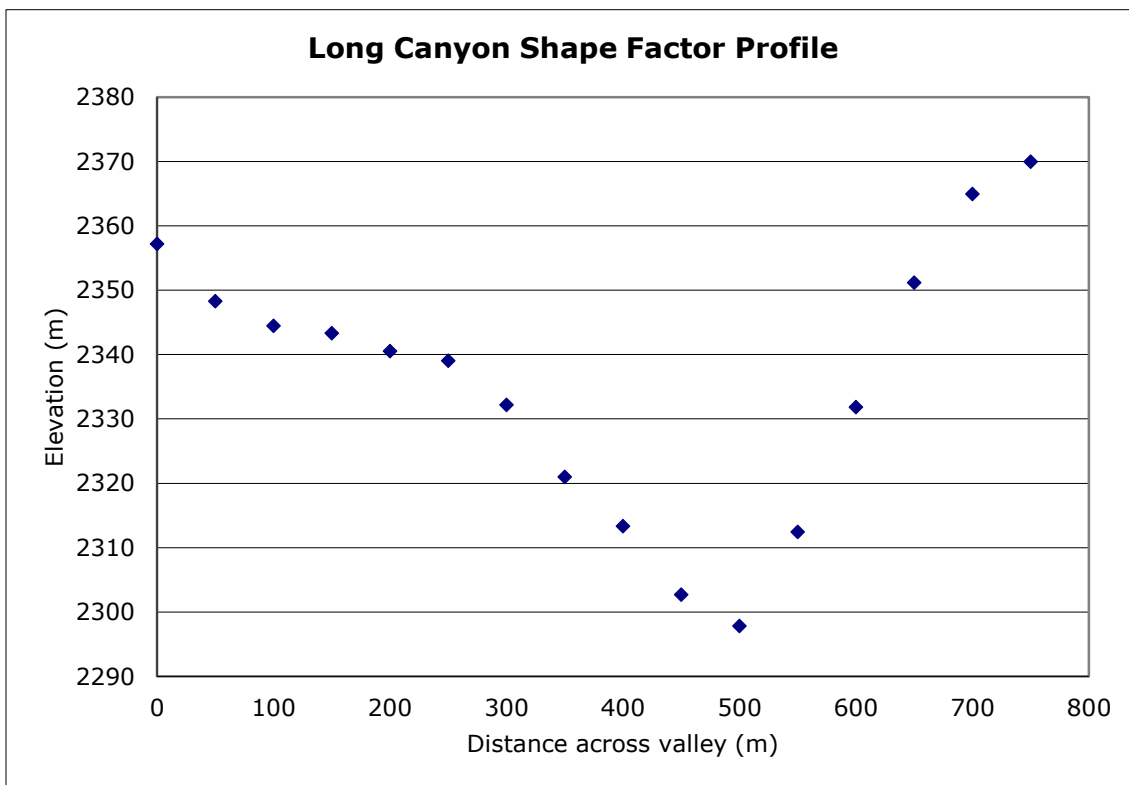
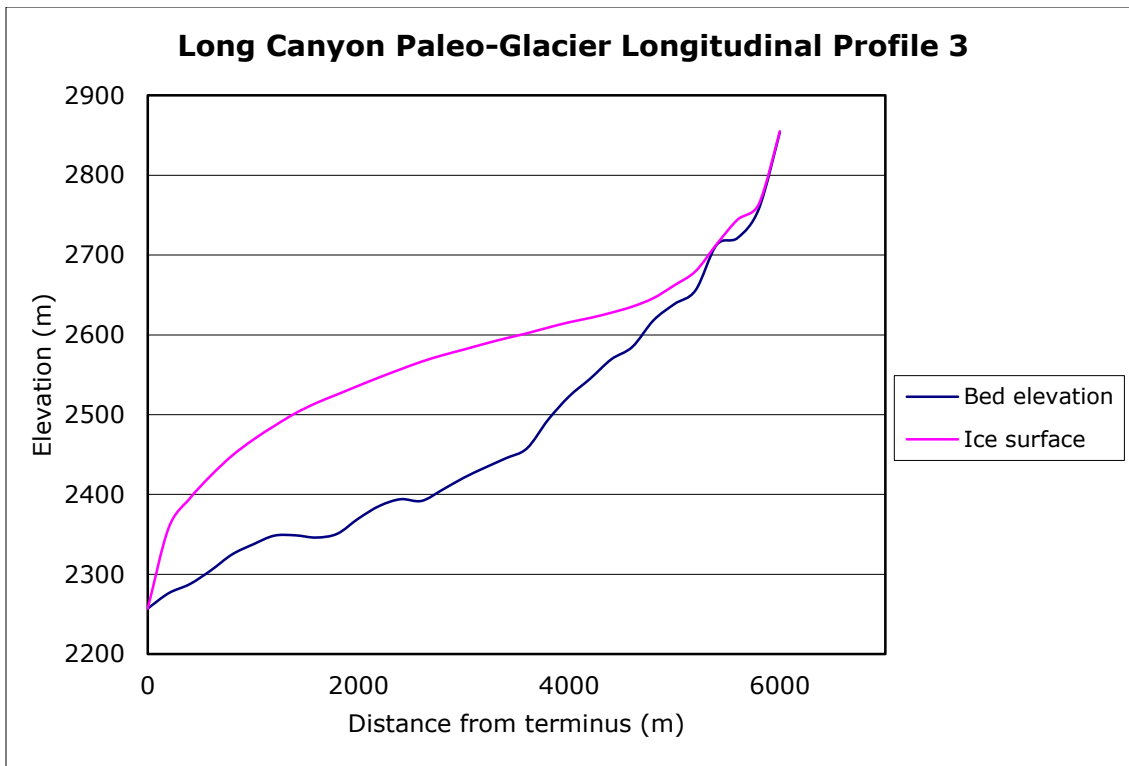


Silver Moon Gulch: $F = 0.58$

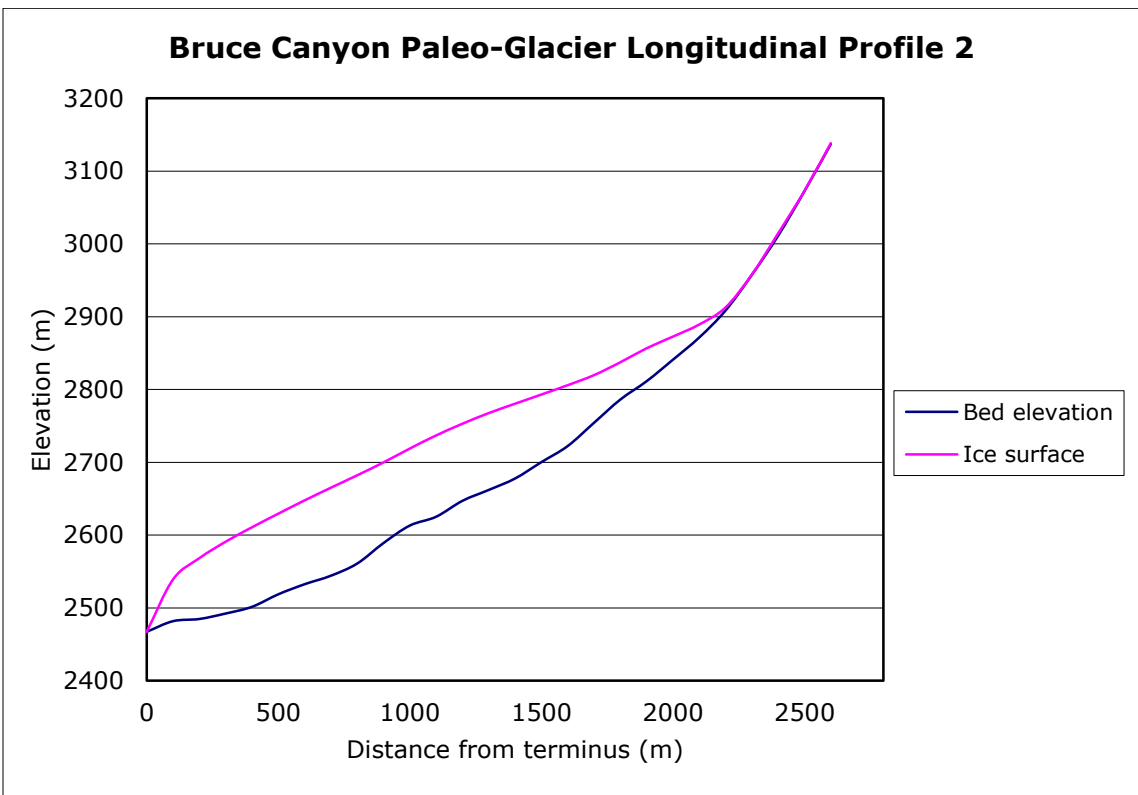
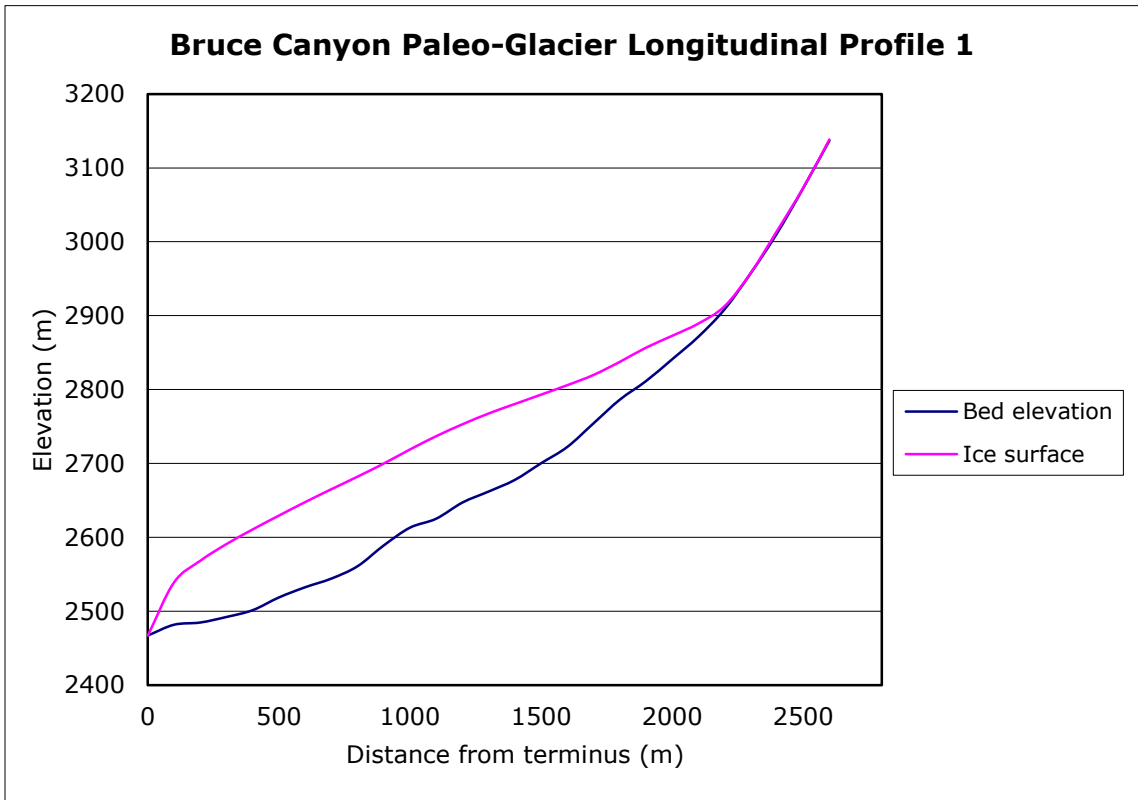


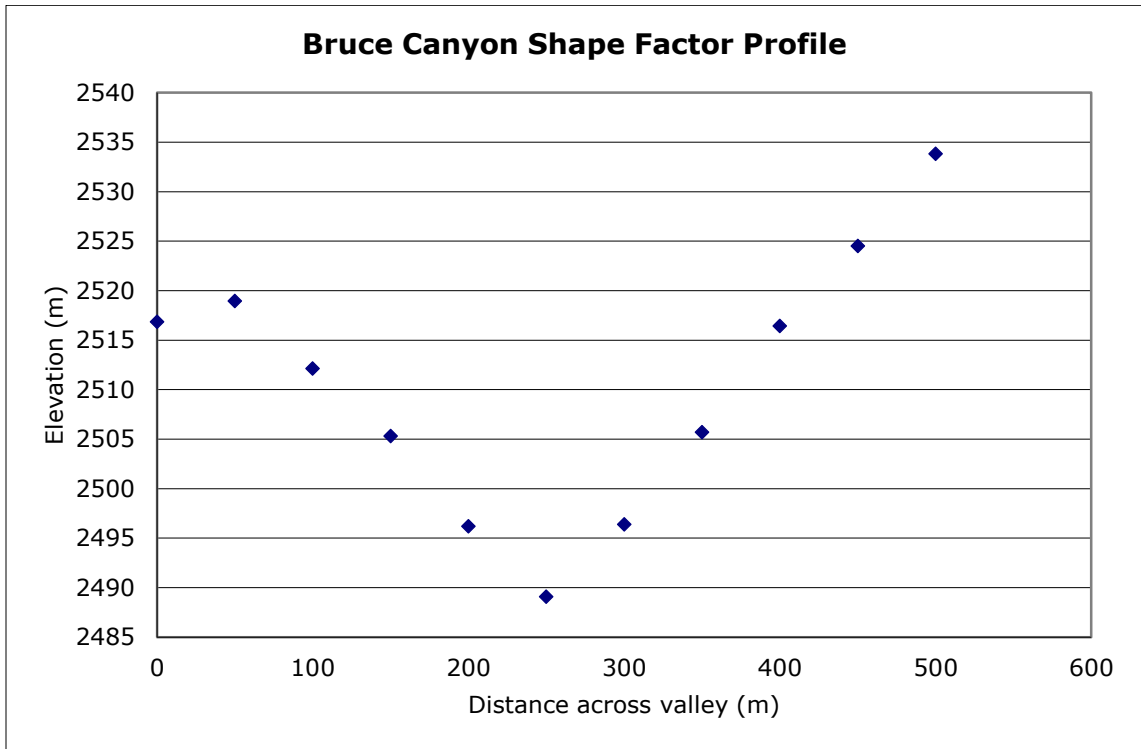
Long Canyon: F = 0.49





Bruce Canyon: $F = 0.55$

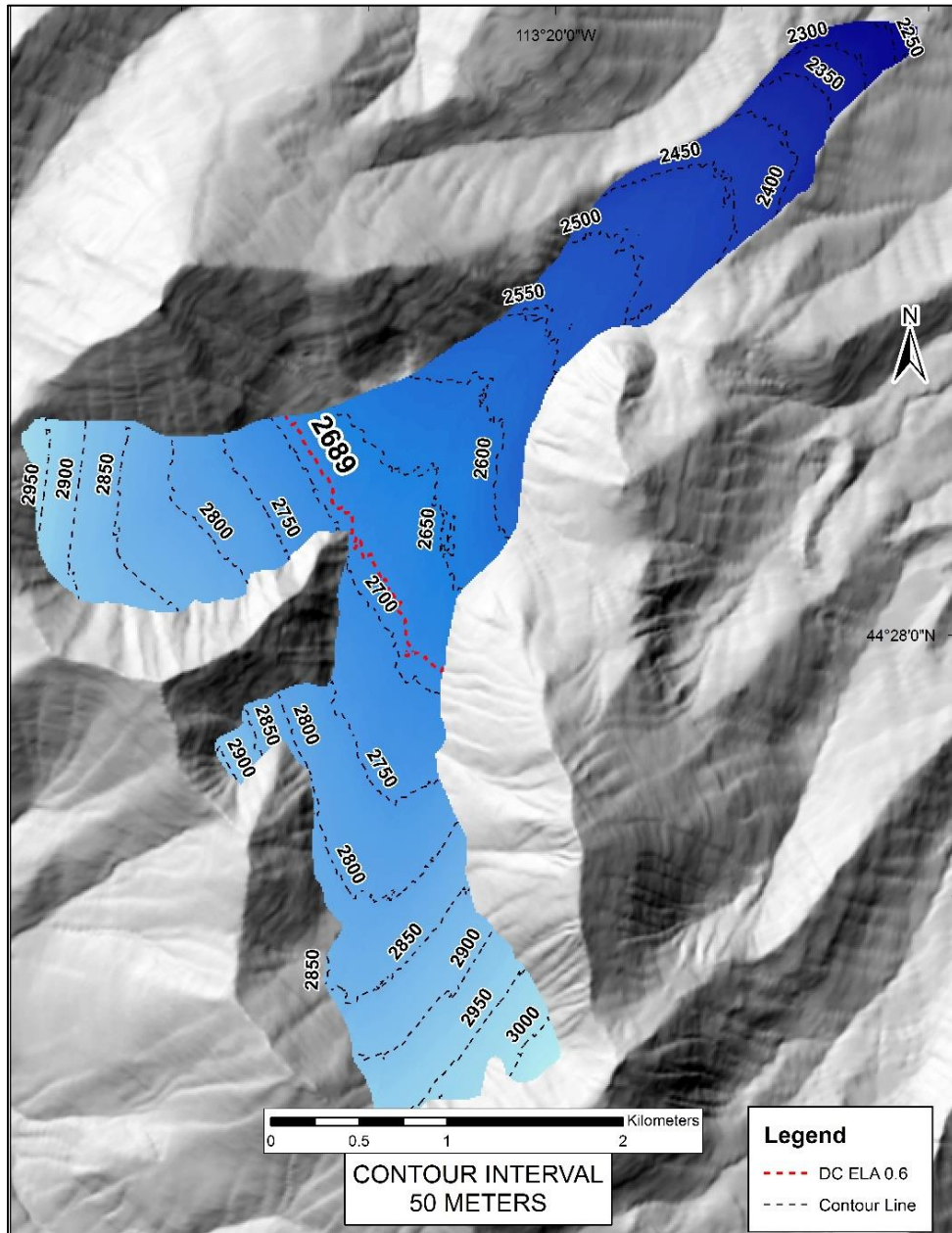




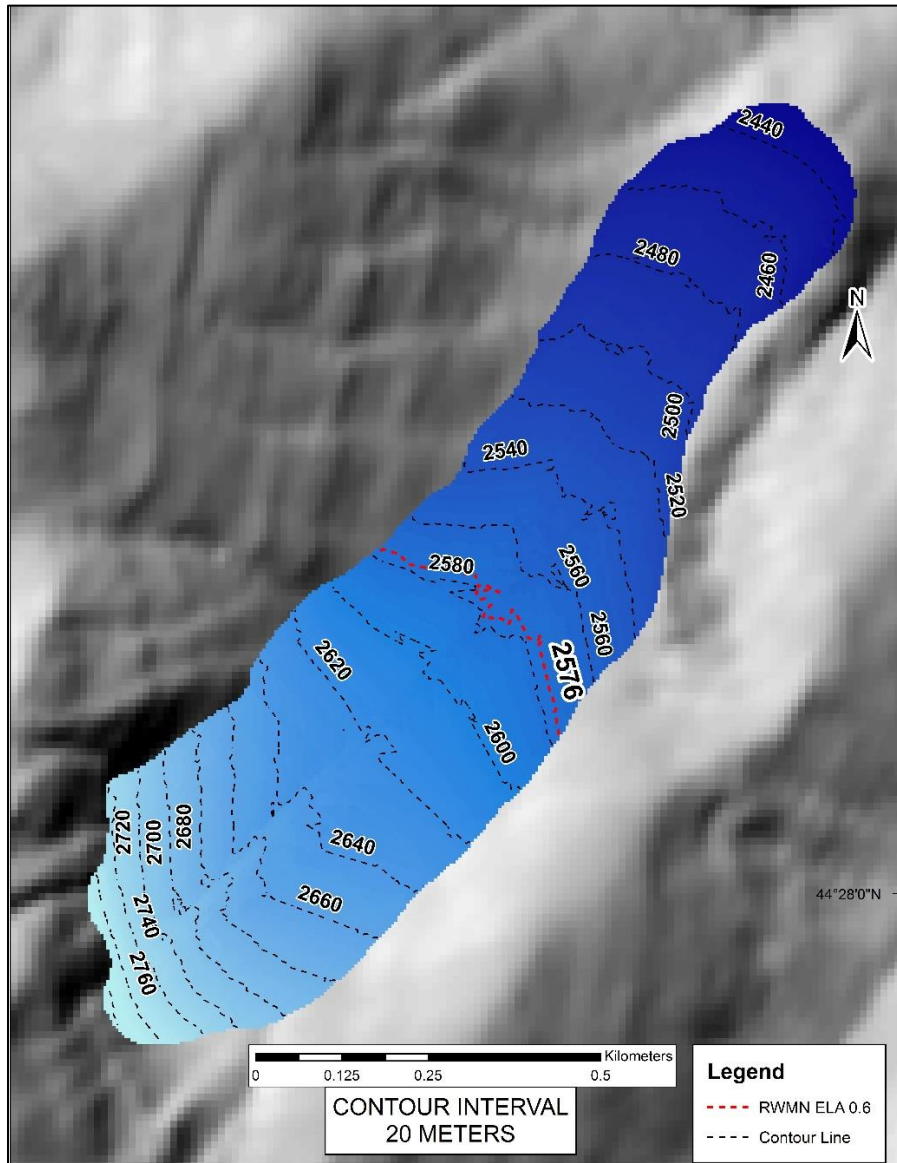
Individual Reconstructed Paleo-Glacier Surfaces

The following figures depict the individual reconstructed glacier surfaces for Qm3 end moraines for seven major valleys across the central Lemhi Range. The red dashed line reflects the equilibrium-line altitude, calculated using an AAR value of 0.6, while the black dashed lines are contour lines reflecting the ice surface elevation. Contour intervals vary between each paleo-glacier surface:

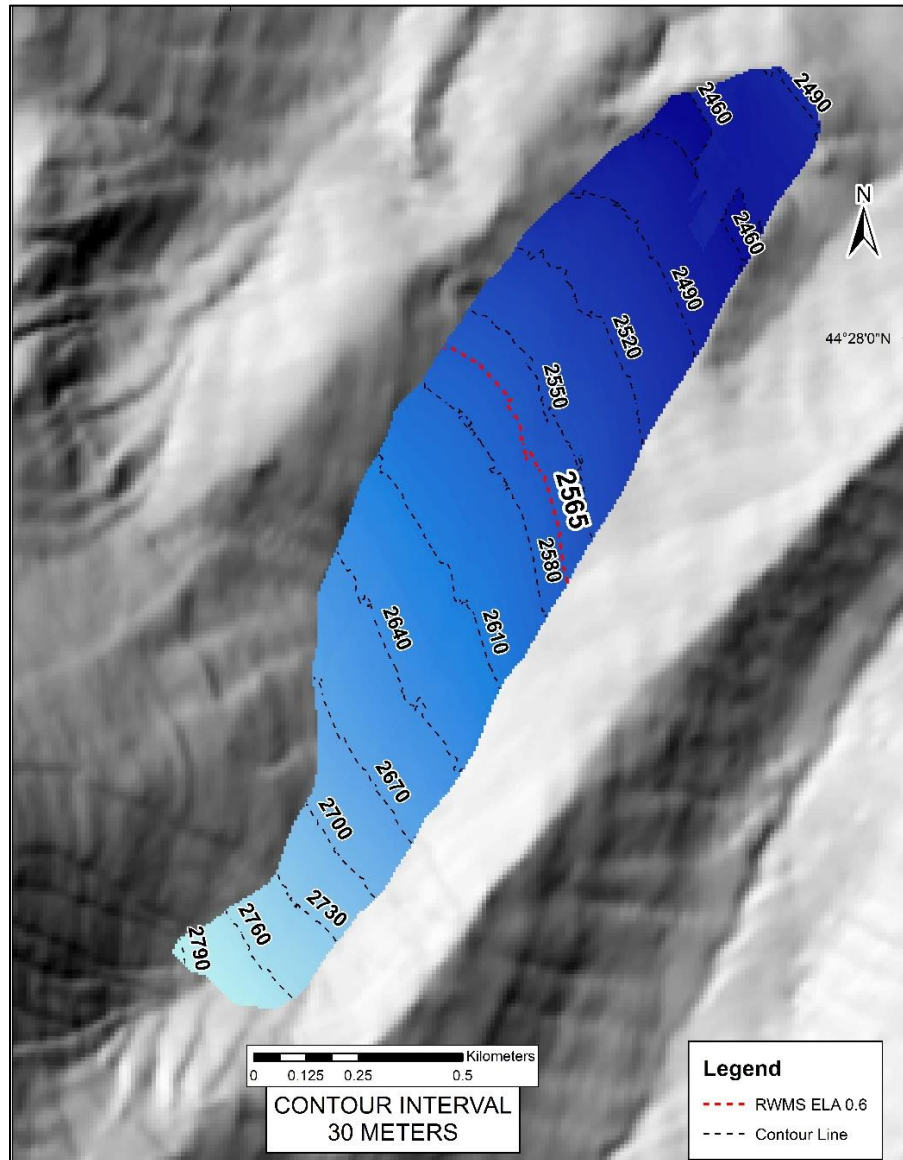
Deer Creek



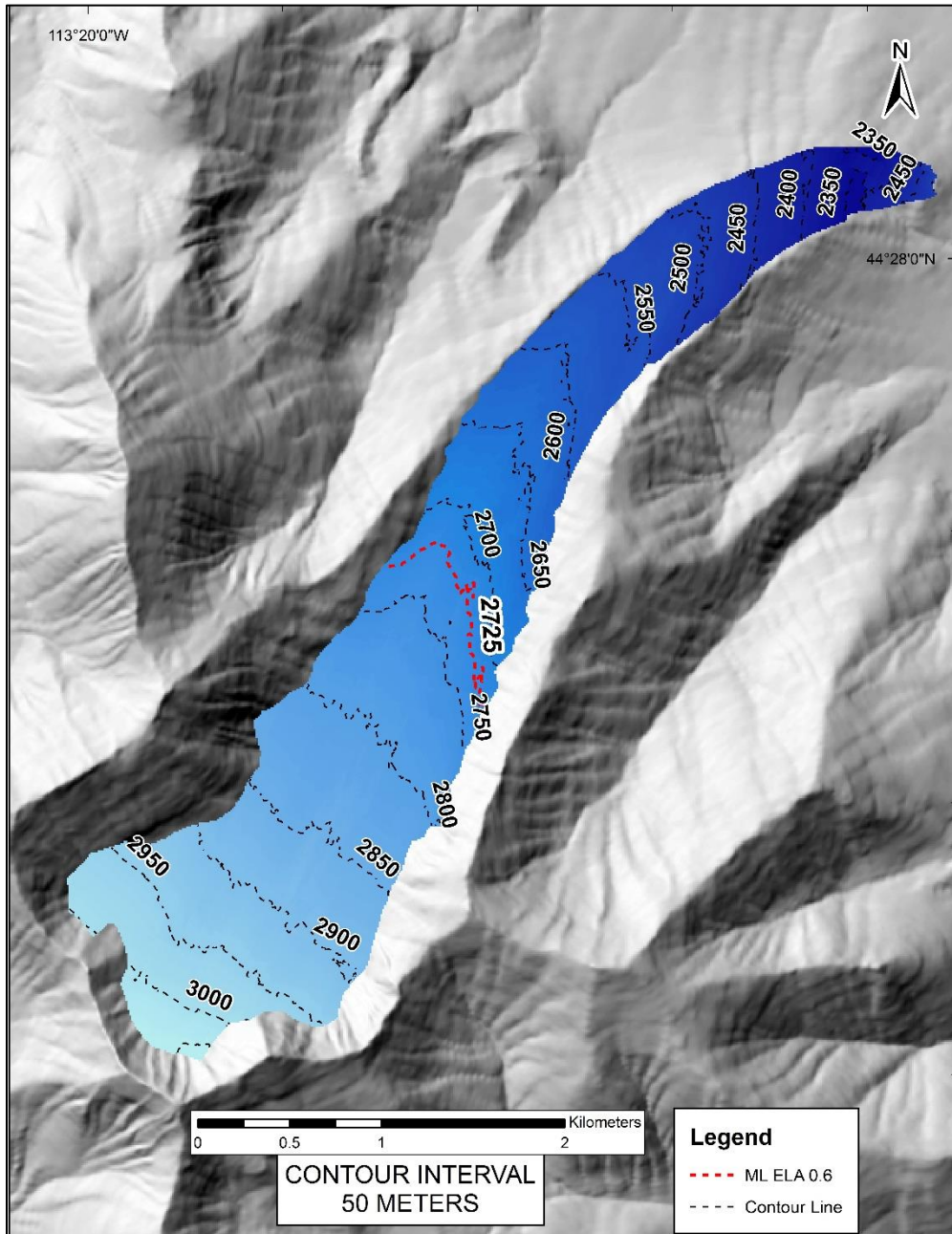
Ridgeway Mine North



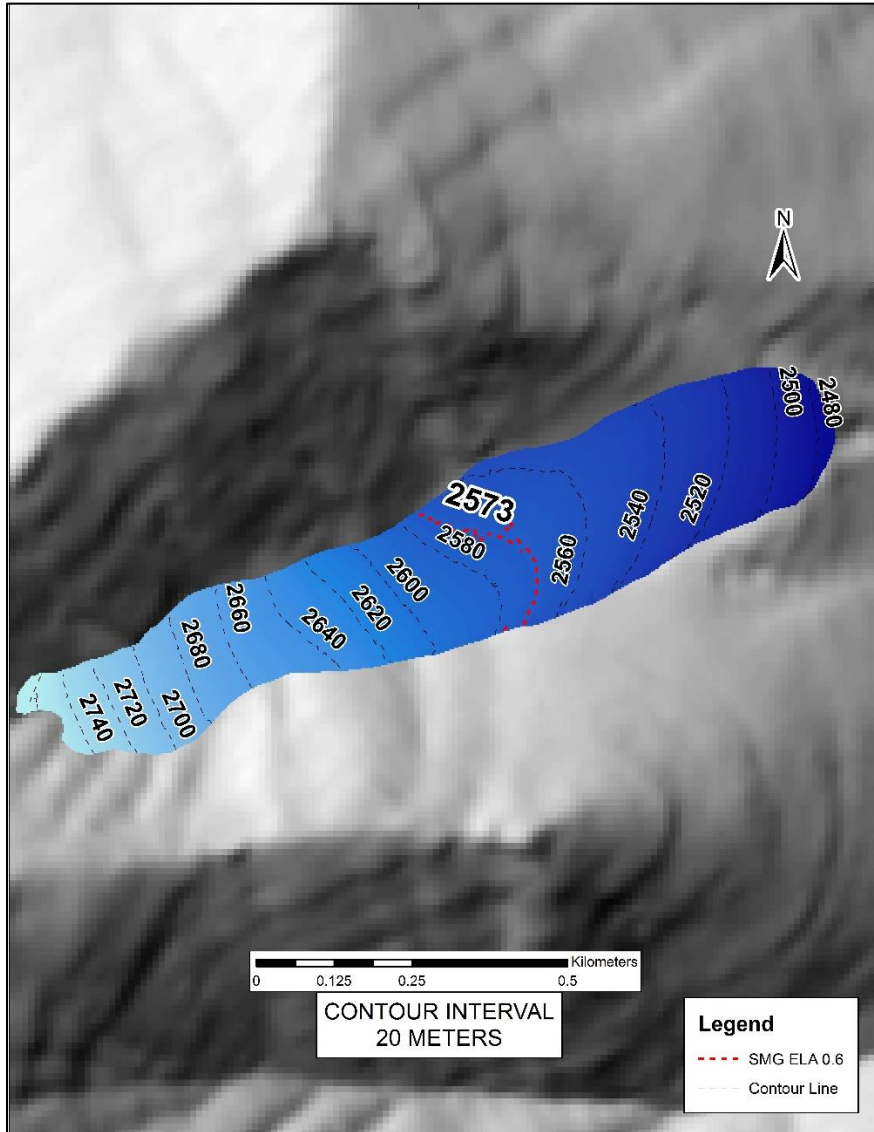
Ridgeway Mine South



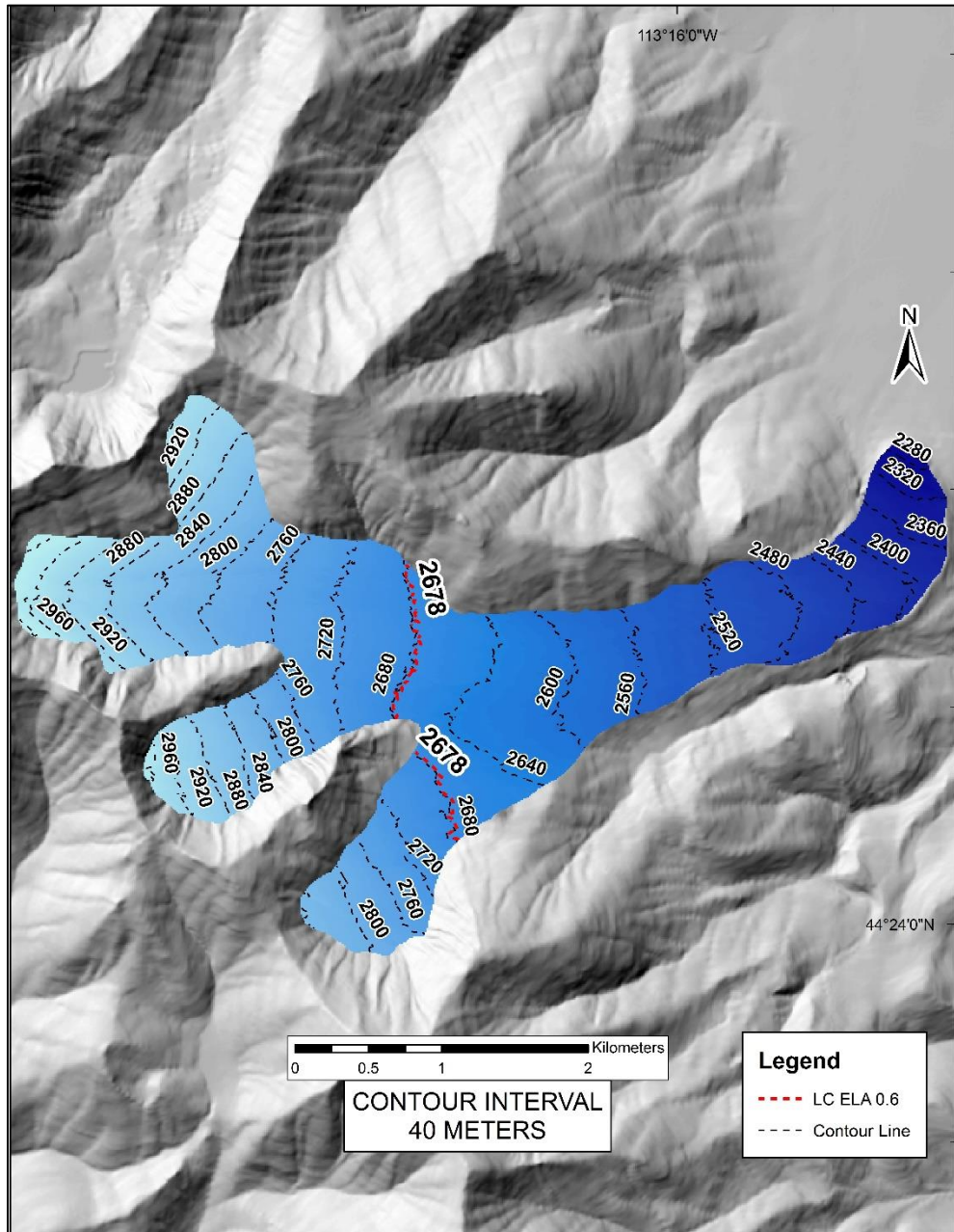
Meadow Lake Creek



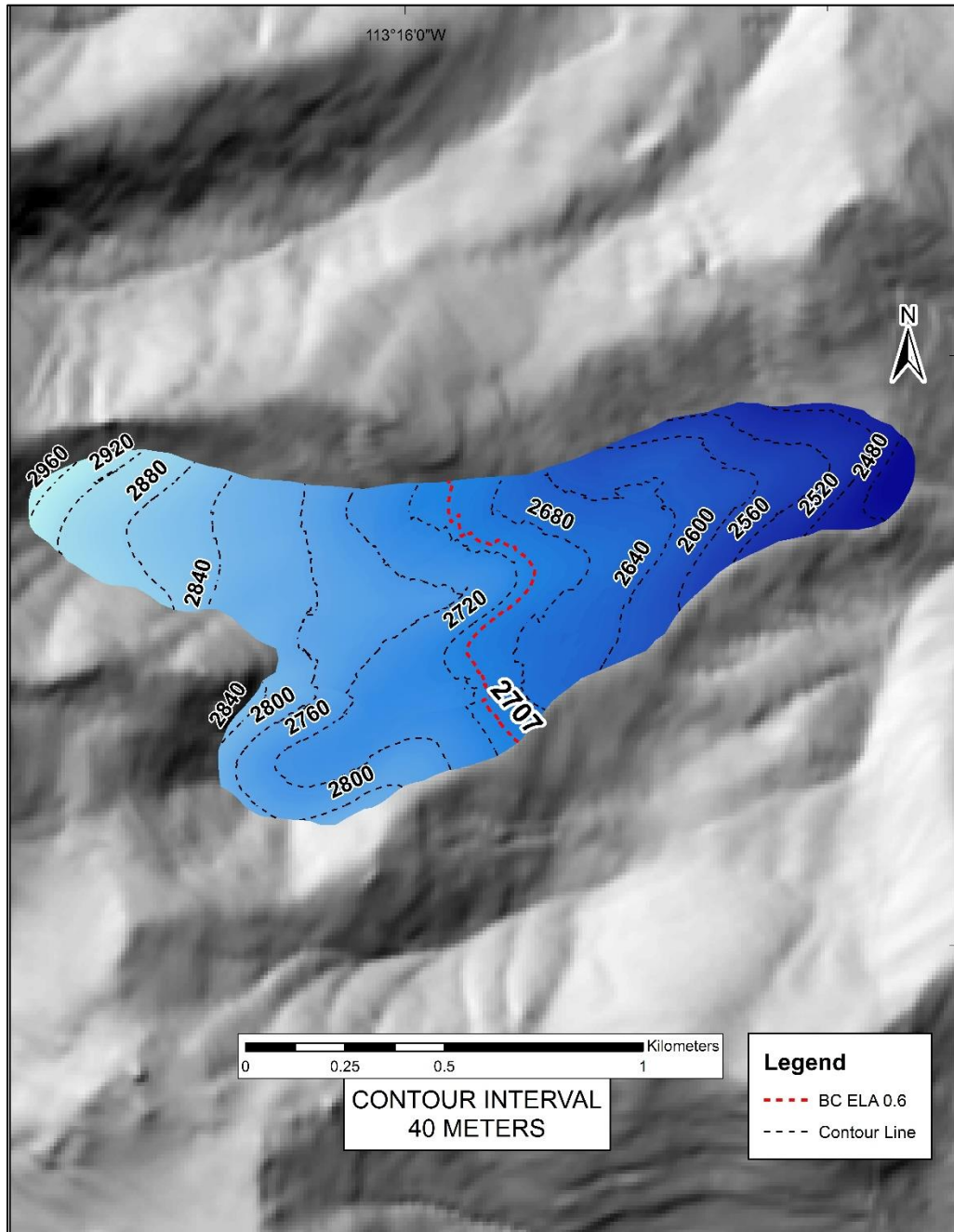
Silver Moon Gulch



Long Canyon



Bruce Canyon



Appendix C: Equilibrium-Line Altitudes and Temperature Depression – Accumulation-Area Ratio Method ELAs, Toe-to-Headwall-Altitude Ratio Method ELAs, Temperature Depression, and Regional Comparisons

Additional Accumulation-Area-Ratio Method ELAs

Table C-1 Equilibrium-line altitudes calculated for inland mountain glacier systems using the accumulation-area ratio (AAR) method using an AAR value of 0.55. Average value is rounded to nearest tenth.

Lemhi Range Paleo-Glacier ELAs (AAR of 0.55)			
Location	Valley Name	ELA (m)	Method
1	Deer Creek	2709	AAR
2	Ridgeway Mine North	2586	AAR
3	Ridgeway Mine South	2575	AAR
4	Meadow Lake Creek	2755	AAR
5	Silver Moon Gulch	2583	AAR
6	Long Canyon	2698	AAR
7	Bruce Canyon North	2727	AAR
Average		2660	

Table C-2 Equilibrium-line altitudes calculated for inland mountain glacier systems using the accumulation-area ratio (AAR) method using an AAR value of 0.65. Average value is rounded to nearest tenth.

Lemhi Range Paleo-Glacier ELAs (AAR of 0.65)			
Location	Valley Name	ELA (m)	Method
1	Deer Creek	2659	AAR
2	Ridgeway Mine North	2556	AAR
3	Ridgeway Mine South	2545	AAR
4	Meadow Lake Creek	2685	AAR
5	Silver Moon Gulch	2563	AAR
6	Long Canyon	2648	AAR
7	Bruce Canyon North	2687	AAR
Average		2620	

Toe-to-Headwall-Altitude Ratio ELAs

Table C-3 Equilibrium-line altitudes calculated for inland mountain glacier systems using the toe-to-headwall-altitude ratio (THAR) method.

Regional Paleo-ELAs (THAR Method)					
Location	Range Name	ELA (m)	Age	Source	Method
11	McCall, ID	2127	MIS 6	Staley (2015)	THAR
11	McCall, ID	2128	MIS 4	Staley (2015)	THAR
11	McCall, ID	2128	MIS 2	Staley (2015)	THAR
12	Sawtooth Mountains, ID	2606	MIS 4	Staley (2015)	THAR
12	Sawtooth Mountains, ID	2624	MIS 3	Staley (2015)	THAR
12	Sawtooth Mountains, ID	2627	MIS 2	Staley (2015)	THAR
13	Pioneer Mountains, ID	2827	MIS 6	Staley (2015)	THAR
13	Pioneer Mountains, ID	2832	MIS 4	Staley (2015)	THAR
13	Pioneer Mountains, ID	2836	MIS 3	Staley (2015)	THAR
13	Pioneer Mountains, ID	2932	MIS 2	Staley (2015)	THAR
13	Pioneer Mountains, ID	2740	MIS 3-2	Brugger (1996)	THAR
14	Lost River Range, ID	2909	MIS 4	Staley (2015)	THAR
14	Lost River Range, ID	2912	MIS 3	Staley (2015)	THAR
14	Lost River Range, ID	2914	MIS 2	Staley (2015)	THAR
15	Lemhi Range, ID	2690	Inferred MIS 2	Colandrea (2016)	THAR
16	Teton Range, WY	2900	MIS 4	Staley (2015)	THAR
16	Teton Range, WY	2900	MIS 2	Staley (2015)	THAR

Regional Comparison of THAR ELAs

Although the AAR method provides a more accurate calculation of ELAs (Meierding, 1982), the THAR method can be used to compare ELAs of the Lemhi Range to a wide array of ELAs of other inland mountain ranges. Staley (2015) calculated ELAs across a transect of the western United States, spanning maritime and inland mountain ranges, using the THAR method, revealing MIS 5-2 climatic variability across the

transect (summarized in Table C-3). Brugger (1996) used the THAR method for ELA calculation in the Idaho Pioneer Mountains, revealing an average ELA of 2740 m for the Wildhorse Advance 1 (correlative to MIS 2 or 3). Foster et al. (2008) determined an average LGM ELA of 2940 m, using the THAR and AABR methods, for the entire Lost River Range, with easterly decreases in ELAs across the Lost River Range, Lemhi Range, and Beaverhead Mountains. Inferences of the climatic conditions of the Lemhi Range can be made through the comparison of these THAR derived ELA values (Figure C.1).

Comparisons between THAR derived ELAs show minimal similarities between the Lemhi Range, McCall, and Lost River Range. McCall ELAs are ca. 600 m lower than the average Lemhi Range ELA, likely because this range is located further west and receives greater Pacific-sourced precipitation. The Lost River Range (LRR) ELAs are ca. 200 m higher than the average ELA of the Lemhi Range. One possible explanation is that the diversion of moist air masses towards the central and western border of Montana and south into the Snake River Plain (Locke, 1990; Meyer et al., 2004) dried the air masses, affecting the two ranges. Additionally, ELA estimates are derived from the western side of the LRR, which receive longer durations of solar insolation and less wind-blown snow accumulation, yielding less extensive glaciation and higher ELAs.

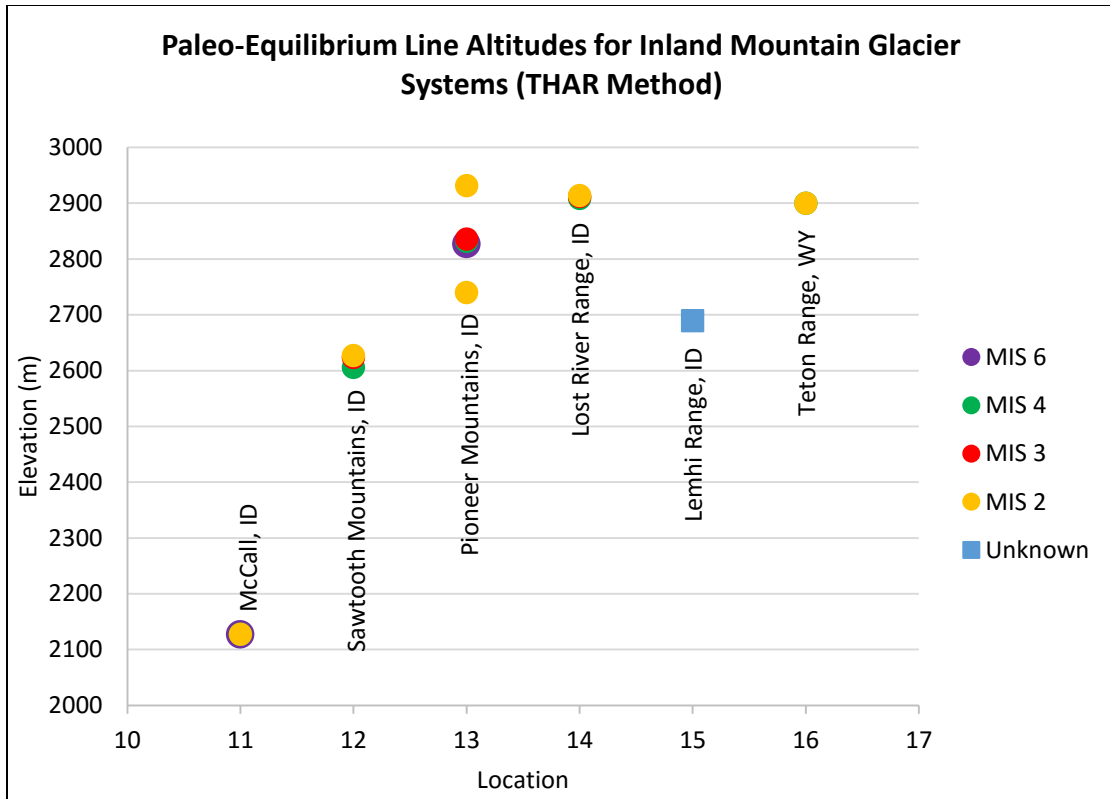


Figure C.1 Comparison of equilibrium-line altitudes (shown in Table 3-4) calculated using the Toe-to-Headwall-Altitude Ratio method across the inland mountain glacier systems of McCall, Idaho, Sawtooth Mountains, Idaho, Pioneer Mountains, Idaho, Lost River Range, Idaho, Lemhi Range, Idaho, and Teton Range, Wyoming. Data modified from Staley (2015).

Temperature Depression

A comparison of paleo-ELAs to modern ELAs of proximal inland mountain ranges allows for an estimate of minimum temperature change since the last glacial cycle. In this study, paleo-ELAs, calculated using the AAR and THAR methods generate an ELA depression of ca. 600 m when compared to the modern ELA of the Otto Glacier in the Lost River Range (Table C-2, C-3). The Otto Glacier was chosen for comparison due to its close proximity to the Lemhi Range. Using an environmental lapse rate (the change in temperature with elevation) of 6°C/km, as implemented by Locke (1990) and discussed by Benn and Evans (2014), in conjunction with the calculated ELA depression,

a temperature depression of 3.6°C is determined for both AAR and THAR derived ELAs, under the assumption that paleo-precipitation was equivalent to modern precipitation (Table 3-3) (Table C-1). This indicates that the climate was ca. 3.6°C cooler in the Lemhi Range during the glaciation associated with Qm3 moraines. Lundeen (2001) determined snowline depressions for Pettit Lake, Yellow Belly Lake, and Hell Roaring Lake valleys in the Sawtooth Range, Idaho, yielding an average temperature depression of 3.3°C during MIS 3. Borgert (1999) estimated that the climate was 3.4°C cooler in the Sawtooth Mountains during this period. An ELA depression of ca. 500 m was determined for the Sawtooths by Meyer et al. (2004). The ELA and temperature depressions determined for the Sawtooths show a strong resemblance to those determined for the Lemhi Range, indicating that uniform cooling and precipitation may have persisted across these ranges. Beiswenger (1991) analyzed pollen contained in sediment cores from Grays Lake, Idaho, which indicated cold and dry conditions from 70-30 ka (early Pinedale). From 30-11.5 ka (late Pinedale), moister conditions persisted, supporting a conifer woodland, with summer temperatures inferred to be 10°C colder than today.

The similarities in ELA and temperature depressions may not reflect uniform cooling across the inland mountainous ranges of Idaho, as ranges further inland (e.g., the Lemhi Range) likely receive less precipitation and reflect continental climate conditions. Thus, the glacier mass balances of continental interior regions are strongly influenced by summer temperatures (Meyer et al., 2004) and the regional patterns of ELAs are influenced by proximity to moisture sources and prevailing wind directions (Porter et al., 1983). In a study regarding the sub-regional distribution of ELAs and climate in intercontinental mountainous regions, Locke (1990) inferred that the paleoclimate of

Montana must have been significantly different from the present. During the last glacial cycle, the Laurentide and Cordilleran ice masses were juxtaposed with the locally glaciated mountains (Locke, 1990). Regional airflow patterns were altered by prevailing cold, continental easterly winds weakening westerlies, and thus influencing the paleoclimate of southwest Montana mountain ranges (i.e., the Beaverhead Mountains), and proximal ranges in Idaho (i.e., the Lemhi Range) (Kutzbach et al., 1993; Thompson et al., 1993).

Table C-2 Equilibrium-line altitudes for each reconstructed glacier surface using an AAR of 0.6. The change in ELA values relative to modern ELAs are rounded to the nearest whole number to avoid inferences of precision. Temperature depression is calculated using a lapse rate of 6 °C/km. Average temperature depression is indicated by red bounding box.

Location	Valley Name	ELA (m)	Method	Approximate Change in ELA (relative to Modern) (m)	Change in ELA (relative to Modern) (km)	Temperature Depression (°C)
1	Deer Creek	2689	AAR	570	0.57	3.4
2	Ridgeway Mine North	2576	AAR	680	0.68	4.1
3	Ridgeway Mine South	2565	AAR	690	0.69	4.1
4	Meadow Lake Creek	2725	AAR	530	0.53	3.2
5	Silver Moon Gulch	2573	AAR	690	0.69	4.1
6	Long Canyon	2678	AAR	580	0.58	3.5
7	Bruce Canyon North	2707	AAR	550	0.55	3.3
Average		2645		600	0.60	3.6
Modern Glacier ELAs						
Location	Range Name	ELA (m)	Notes			
28-0	Lost River Range, ID	3260	Otto Glacier			
				AAR = 0.6		Env Lapse Rate = 6 °C/km

Table C-3 Equilibrium-line altitudes for each reconstructed glacier surface using a THAR of 0.6. The change in ELA values relative to modern ELAs are rounded to the nearest whole number to avoid inferences of precision. Temperature depression is calculated using a lapse rate of 6 °C/km. Average temperature depression is indicated by red bounding box.

Location	Valley Name	ELA (m)	Method	Approximate Change in ELA (relative to Modern) (m)	Change in ELA (relative to Modern) (km)	Temperature Depression (°C)
1	Deer Creek	2686	THAR	570	0.57	3.4
2	Ridgeway Mine North	2648	THAR	610	0.61	3.7
3	Ridgeway Mine South	2634	THAR	630	0.63	3.8
4	Meadow Lake Creek	2760	THAR	500	0.50	3.0
5	Silver Moon Gulch	2651	THAR	610	0.61	3.7
6	Long Canyon	2694	THAR	570	0.57	3.4
7	Bruce Canyon North	2746	THAR	510	0.51	3.1
Average		2690		600	0.60	3.6
Modern Glacier ELAs						
Location	Range Name	ELA (m)	Notes			
8	Lost River Range, ID	3260	Otto Glacier			
				THAR = 0.6		
				Env Lapse Rate = 6 °C/km		

References

- Beiswenger, J.M., 1991, Late quaternary vegetational history of Grays Lake, Idaho. *Ecological Monographs*, 61, 165-182.
- Benn, D., & Evans, D.J., 2014, *Glaciers and glaciation*, Routledge, 43.
- Borgert, J.A., Lundeen, K.A., Thackray, G.D., 1999, Glacial geology of the southeastern Sawtooth Mountains, in Hughes, S.S., and Thackray, G.D., eds., *Guidebook to the Geology of Idaho: Pocatello, Idaho Museum of Natural History*, 205-217.
- Brugger, K.A., 1996, Implications of till-provenance studies for glaciological reconstructions or the paleoglaciers of Wildhorse Canyon, Idaho, U.S.A., *Annals of Glaciology*, 22, 93-101.
- Foster, D., Brocklehurst, S.H., Gawthorpe, R.L., 2008, Small valley glaciers and the effectiveness of the glacial buzzsaw in the northern Basin and Range, *Geomorphology*, 624-639.
- Kutzbach, J.E., Guetter, P.J., Behling, P.J., Selin, R., 1993, Simulated climatic changes: Results of the COHMAP Climate-Model Experiments, in, Wright, H.E. Jr., Kutzbach, J.E., Webb, T. III, Ruddiman, W.F., Street-Perrott, P.A., Bartlein, P.J., University of Minnesota Press, Minneapolis, MN, *Global climates since the Last Glacial Maximum*, 24-93.
- Locke, W.W., 1990, Late Pleistocene glaciers and the climate of western Montana, USA, *Arctic and Alpine Research*, 22, 1-13.
- Lundeen, K.A., 2001, Refined late Pleistocene glacial chronology for the eastern Sawtooth Mountains, Central Idaho, *M.S. Thesis Idaho State University*, 117.
- Meierding, T.C., 1982, Late Pleistocene glacial equilibrium-line altitudes in the Colorado Front Range: a comparison of methods, *Quaternary Research*, 18.3, 289-310.
- Meyer, G.A., Fawcett, P.J., Locke, W.W., 2004, Late-Pleistocene equilibrium-line altitudes, atmospheric circulation, and timing of mountain glacier advances in the interior northwestern United States, in Haller, K., Wood, S.H., eds., *Geological Field Trips in Southern Idaho, Eastern Oregon, and Northern Nevada: Geological Society of America Field Guide*, 61-66.
- Porter, S.C., Pierce, K.L., Hamilton, T.D., 1983, Late Wisconsin mountain glaciation in the western United States, in Wright, H.E., Porter, S.C., eds, 1983, *Late Quaternary Environments of the United States: The Late Pleistocene*, U of Minnesota Press, 70-111

Staley, A.E., 2015, Glacial geomorphology and chronology of the Quinault Valley, Washington, and broader evidence of marine isotope stages 4 and 3 glaciation across northwestern United States, *M.S. Thesis Idaho State University*, 188.

Thompson, R. S., Whitlock, C., Bartlein, P. J., Harrison, S. P., Spaulding, W. G., 1993, Climatic changes in the western United States since 18,000 yr BP, *in Global climates since the last glacial maximum*, H.E. Wright, Jr., J.E. Kutzbach, T. Webb III, W.F. Ruddiman, F.A. Street-Perrott, and P.J. Bartlein, eds, University of Minnesota Press, 468-513.